UNIVERSITY OF SOUTHAMPTON

FACULTY OF MEDICINE

Clinical and Experimental Sciences

The modulation of smooth muscle contractility by specialised pro-resolving mediators

by

Melanie Jannaway

Thesis for the degree of Doctor of Philosophy

September 2015

UNIVERSITY OF SOUTHAMPTON

ABSTRACT

FACULTY OF MEDICINE
Clinical and Experimental Sciences
Thesis for the degree of Doctor of Philosophy

THE MODULATION OF SMOOTH MUSCLE CONTRACTILITY BY SPECIALISED PRO-RESOLVING MEDIATORS

Melanie Jannaway

Smooth muscle contraction, tissue remodelling and chronic inflammation are features common to many lung conditions including asthma and pulmonary arterial hypertension (PAH). Three people in the UK die each day from a fatal asthma exacerbation, whilst right heart failure caused by increased resistance in the pulmonary arteries is an end-point that over half of patients with PAH can expect just five years after diagnosis. Novel relaxants to address the inappropriate smooth muscle contraction in these diseases are required.

Recently-identified families of specialised pro-resolving lipid mediators (SPMs) including resolvins (Rv), lipoxins (LX), protectins (PD) and maresins actively limit the acute inflammatory response through the activation of G-protein-coupled receptors, but their roles in smooth muscle contraction are poorly understood. The aims of this thesis were: to determine whether SPMs, in particular RvD1, RvE1, LXA_4 and PDX, can modulate spontaneous or growth factor-induced contraction of cell-populated collagen lattices; to use wire myography to define whether Rvs D1, D2 and E1 can modulate contractility in bronchiole and artery segments from rat and human donors; and finally to use immunohistology to localise expression of the pro-resolving receptors ChemR23, GPR32 and ALX in human pulmonary artery (HPA).

None of the SPMs investigated affected spontaneous contraction of collagen lattices populated with human lung fibroblasts (HLF), human bronchial smooth muscle cells (HBSMC) or human umbilical artery smooth muscle cells (HUASMC), nor did they affect TGFβ1-enhanced lattice contraction. However, RvE1 abolished the platelet-derived growth factor (PDGF)-enhanced contraction of HBSMC lattices ($p<0.05$). In addition, PDX weakly inhibited contraction of lattices populated with HLF or HBSMC, while RvD1 and LXA_4 had no effect.

Wire myography was used to investigate the ability of RvD1, RvD2 and RvE1 to prevent or reverse contraction of bronchiole segments isolated from rat and human lung. None of the resolvins tested were able to reverse carbachol (CCh)-induced pre-constriction in rat bronchioles or leukotriene D_4 (LTD_4)-induced pre-constriction in human bronchioles. Pre-treatment with resolvins D1 or E1 failed to prevent subsequent contraction of rat bronchioles induced by either CCh or the stable thromboxane mimetic U46619, compared to the same segments contracted previously without resolvin. Pre-treatment of rat and human bronchioles with RvD1 (10 nM) appeared to dampen LTD_4-induced constriction, although complications with suspected tachyphylaxis and generally low responsiveness to LTD_4 in rat bronchioles may have precluded significant outcomes.

Wire myography was used to explore Rv effects in rat and human blood vessels. Rvs D1, D2 and E1 all failed to reverse phenylephrine (PE)- or U46619-induced pre-constriction in segments of rat thoracic aorta (RTA), and HPA, these resolvins did not reverse pre-constriction induced by LTD_4. Pre-treatment of HPA with RvD1 or RvE1 had no effect on subsequent constriction by U46619, while their effects on LTD_4-induced constriction were masked by changing baseline responses to this contractile agonist, as seen in bronchiole segments. However, in naive segments of RTA pre-treated for 1 or 24 hour with or without resolvin in parallel, RvE1 (0.1-300 nM), RvD1 and RvD2 (1-100 nM) each significantly inhibited constriction to U46619 with a bell-shaped inhibition curve, when compared to the control segments constricted by U46619 without resolvin (10 nM RvE1 $p<0.0001$; 10 nM RvD1 $p<0.01$; 10 nM RvD2 $p<0.05$). The significant inhibitory effect of RvE1 (1 hour) was also seen in U46619-constricted HPA segments ($p<0.0001$ with 10 nM RvE1), but not in RTA constricted with PE, indicating a selective effect on thromboxane receptor signalling. Immunohistochemistry of paraffin wax-embedded HPA sections indicated that the pro-resolving receptors GPR32 and ChemR23 were both expressed in the vascular smooth muscle, with GPR32 also apparent in the endothelium.

This thesis provides the first evidence that acute pre-treatment with SPMs can directly impair the contractile responses of intact segments of rat aorta and human pulmonary arteries to well-known contractile agonists, and that they can also modulate the PDGF-enhanced contraction of 3D collagen matrices by human bronchial smooth muscle cells. These findings provide novel insights into SPM activity with important implications for understanding the regulation of smooth muscle contractility in chronic inflammatory diseases such as asthma, PAH and systemic hypertension.

Table of Contents

List of Tables

List of Figures

DECLARATION OF AUTHORSHIP

I, ...

declare that this thesis and the work presented in it are my own and has been generated by me as the result of my own original research.

THE MODULATION OF OF SMOOTH MUSCLE CONTRACTILITY BY SPECIALISED PRO-RESOLVING MEDIATORS.

I confirm that:

1. This work was done wholly or mainly while in candidature for a research degree at this University;
2. Where any part of this thesis has previously been submitted for a degree or any other qualification at this University or any other institution, this has been clearly stated;
3. Where I have consulted the published work of others, this is always clearly attributed;
4. Where I have quoted from the work of others, the source is always given. With the exception of such quotations, this thesis is entirely my own work;
5. I have acknowledged all main sources of help;
6. Where the thesis is based on work done by myself jointly with others, I have made clear exactly what was done by others and what I have contributed myself;
7. Parts of this work have been published as:

- '*Effect of resolvin D1 on leukotriene D_4-induced constriction of rat and human bronchioles'* was presented in the session *Asthma Drugs: new findings* at the European Respiratory Society Annual Congress (2013), and is available at http://www.ers-education.org/events/international-congress/barcelona-2013.aspx?idParent=125434.
- '*Resolvins do not vasodilate rat thoracic aorta in vitro*' was presented at the Physiological Society Annual Meeting (2014), and is published in Physiology 2014 (London, UK) (2014) Proc Physiol Soc 31, PCB199.
- '*Resolvin E1 Inhibits Thromboxane-Induced Contraction of Rat Aorta and Human Pulmonary Artery*' was presented at Atherosclerosis, Thrombosis and Vascular Biology (San Francisco, US) (2015) and is published in Arteriosclerosis, Thrombosis, and Vascular Biology. 2015; 35: Suppl 1.

Signed: .....

Date:.....

Acknowledgements

I am very grateful to my supervisors, Dr. Tony Sampson, Dr. Jane Warner and Dr. Christopher Torrens, who have provided me with great support and guidance throughout my time at Southampton. Tony in particular has taught me a lot of lessons and offered really brilliant advice, even if at the time it didn't seem like it, and I am sure that his wisdom will continue to benefit me for the rest of my career.

Thank you to my colleagues, Sam Maitland, Andy Hutton and Jess Rajaram, for their help over the years with collecting tissue, as well as their excellent guidance in tissue culture. These guys have also become my good friends and I will miss sharing an office and lab with all of them.

There are many people who have helped me with techniques, methods and materials, including Dr. Franco Conforti of the Brooke Lab, who gave me the initial lattice contraction protocol along with excellent advice on getting it set up. I am also grateful to Dr. Tim Miller and Micky Olding who kindly let me use the donated umbilical cords from the patients at the Princess Anne Hospital, to whom I am also very thankful. Thanks to Dr. David Johnston of the Biomedical Imaging Unit who helped me to obtain some really beautiful fluorescent images. Thank you very much to everyone in the Immunohistochemistry Research Unit including Jenny Norman, Jon Ward and Dr. Susan Wilson, who helped to process my tissue samples, taught me lots of skills and suffered my endless questions!

Thank you to the lab managers, including Dr. Richard Jewell, Dr. Carolann McGuire and Dr. Laurie Lau in Dermatopharmacology, as well as Richard Reynolds in the Vascular Lab, whose help, advice and patience kept the place running smoothly. Thank you also to Mike Broome from the Biomedical Research Facility who looked after the Wistar Rats.

I am extremely grateful to all of the patients who donated their lung tissue to the study, as well as all of the Surgeons (Mr Aiman Alzetani, Mr Khalid Amer, Mr Edwin Woo, Mr Martin Chamberlin, Mr ZoltanVeres), the nurses, the theatre staff, and the TARGET Lung group (Dr. Serena Chee and Benjamin Johnson) who helped us to collect this tissue.

I am very appreciative of all the support offered to me throughout my project by my family and friends especially my Mum, my Dad, Bec, Peter and my boyfriend Edoardo, without whom I couldn’t have done it. Thanks to Alastair Watson, who has been there from day one, made me laugh every day since and always been there for a tea. Thanks to my wonderful housemate, Wen Chean Lim, I will miss you a lot! Thanks to Agnieszka Janeczek and Matt Loxham for always making me see the positive in everything, and to all of the others who have made Southampton a great place to spend four years.

Finally, I would like to thank the Gerald Kerkut Charitable Trust for funding my PhD project.

Definitions and Abbreviations

5-HT – 5-hydroxytryptamine / serotonin

AA – arachidonic acid

AEC – 3-amino-9-ethylcarbazole

AHR – airway hyperresponsiveness

ALX – lipoxin A_4 receptor

ANOVA – analysis of variance

ASM – airway smooth muscle

ASMC – airway smooth muscle cell

AT-LX – aspirin triggered lipoxin

BLT1 – leukotriene B_4 receptor

BSA – bovine serum albumin

cAMP – cyclic adenosine monophosphate

CCB – calcium channel blocker

CCh – carbachol

CCRC – cumulative concentration response curve

cDNA – complementary deoxyribonucleic acid

cGMP – cyclic guanylyl monophosphate

COPD – chronic obstructive pulmonary disease

COX – cyclooxygenase enzyme

CPI-17 – C-kinase potentiated protein phosphatase-1 inhibitor

CSE – cigarette smoke extract

CysLT – cysteinyl leukotriene

DAG – diacylglycerol

DAPI – 4',6-diamidino-2-phenylindole

DHA – docosahexaenoic acid

DMEM – Dulbecco’s modified Eagle’s médium

DMT – Danish Myo Technology

EC_{80} – concentration of agonist required to evoke 50% of the maximum response

ECM – extracellular matrix

eNOS – endothelial nitric oxidfe synthase

EPA – eicosapentaenoic acid

ERK – extracellular signal-regulated kinases

ET - endothelin

FEV1 – forced expiratory volume

FP – formyl peptide

FPR – formyl peptide receptor

FVC – forced vital capacity

GF – growth factor

GINA – global initiative for asthma

GOLD – global initiative for chronic obstructive lung disease

GPCR – G-protein-coupled receptor

GTP – guanylyl triphosphate

HBSMC – human bronchial smooth muscle cell

HEK-293 – human embryonic kidney 293 cells

HeLa – Henrietta Lacks

HETE – hydroxyeicosatetraenoic acid

HLF – human lung fibroblast

HLMF – human lung myofibroblasts

HPA – human pulmonary artery

HUASMC – human umbilical artery smooth muscle cell

HUVEC – human umbilical vein endothelial cell

ICAM-1 – intercellular adhesion molecule

ICS – inhaled corticoid steriods

IgE – immunoglobulin E

IHC – immunohistochemistry

IL – interleukin

IP_3 – inositol trisphosphate

IP_3R – inositol trisphosphate receptor

IUPHAR – International Union of Pharmacology

IV – intravenous

JNK – c-Jun N-terminal kinases

KPSS – potassium physiological salt solution

LABA – long-acting beta-2 agonist

LAS-AF – leica application suite – advanced fluorescence

LL-37 – cathelicidin-related anti-microbial peptide

LO – lipoxygenase

LPS – lipopolysaccharide

LREC – local research ethical committee

LT – leukotriene

LTA_4H – leukotriene A_4 hydroxylase

mAChR – muscarinic acetylcholine receptor

MAI – million adult inhabitants

MAPK – mitogen-activated protein kinases

MaR – maresin

MLC – myosin light chain

MLCK – myosin light chain kinase

MLCP – myosin light chain phosphatase

MMP – matrix metalloprotease

MYPT – myosin binding subunit

MYPT-1 – myosin phosphatase target subunit 1

NCS – newborn calf serum

NETs – neutrophil extracellular trap

NF-κB – nuclear factor kappa-light-chain-enhancer of activated B cells

NO – nitric oxide

PAH – pulmonary arterial hypertension

PD – protectin

PDE – phosphodiesterase

PDGF – platelet-derived growth factor

PDL – periodontal ligament

PE – phenylephrine

PFA – paraformaldehyde

PG – prostaglandin

PIP_2 – phosphatidylinositol 4,5-bisphosphate

PKA – protein kinase A

PKC – protein kinase C

PKG – protein kinase G

PMN – polymorphonuclear cell

PPAR-α – peroxisome proliferator-activated receptor-α

PSS – physiological salt solution

PUFA – polyunsaturated fatty acid

REVEAL – registry to evaluate early and long-term pulmonary arterial hypertension disease management

Rv – resolvin

SAA – serum amyloid A

SABA – short-acting beta-2 agonist

SERCA – sarco/endoplasmic reticulum Ca^{2+}-ATPase

SGaw – specific airway conductance

siRNA – small interfering ribobucleic acid

SMC – smooth muscle cell

SPM – speclialised pro-resolving lipid mediator

TBS – tris-buffered saline

TCS – true confocal scanning

TGFβ1 – transforming growth factor beta-1

Th-2 – t helper cell 2

TMEM16A – transmembrane protein member 16A

TNF-α – tumour necrosis factor -α

TP – thromboxane A_2 receptor

TRITC – tetramethylrhodamine

TRPV1 – transient receptor potential V1

TxA_2 – thromboxane

V_{25} – expiratory flow rate at 25% of the vital capacity

VC – vital capacity

VCAM-1 – vascular cellular adhesion molecule-1

VIP – vasoactive intestinal peptide

VSM – vascular smooth muscle

vWF – von Willebrand factor

α-SMA – alpha smooth muscle actin

βARK/GRK2 – beta-adrenergic receptor kinase

Chapter 1: Introduction

1.1 Smooth muscle

Smooth muscle is located throughout the body, lining hollow organs and contracting involuntarily in response to a wide range of mediators. Smooth muscle plays many important physiological roles, from facilitating digestion within the gastrointestinal tract, mediating uterine contractions during childbirth, to controlling the shape of the lens for accommodation. However, smooth muscle also contributes to an array of pathological conditions particularly within the vascular system, such as systemic hypertension, atherosclerosis, coronary vasospasm (Prinzmetal's angina), peripheral artery disease, and even the vascular complications occurring in diabetes. Within the pulmonary system, smooth muscle is present on the airways and the arteries, and it is this smooth muscle that is the focus of this thesis.

1.2 Smooth muscle contraction in chronic lung diseases

Inappropriate smooth muscle contraction, that is, the contraction of smooth muscle where it is unnecessary, is central to a diverse range of chronic lung diseases including asthma and pulmonary arterial hypertension (PAH), as well as to systemic diseases such as essential hypertension. Superficially, the two pulmonary disorders produce decidedly distinct phenotypes, with asthma affecting principally the airways, and PAH the pulmonary vasculature, but they are characterised by many of the same pathological features including inflammation, tissue remodelling and smooth muscle contraction (Said et al. 2010, Wu et al. 2011).

Smooth muscle dilators including beta-2 adrenoceptor agonist salbutamol and prostacyclin analogue epoprostenol are mainstay management options for asthma and PAH. However, the high morbidity of asthma and the high mortality rates associated with PAH suggest unmet clinical needs for the development of novel smooth muscle dilators (Cazzola, Rogliani, et al. 2012). This thesis will consider both airway smooth muscle (ASM) contraction with respect to asthma, and vascular smooth muscle (VSM) contraction with respect to PAH, and their modulation by lipid mediators.

1.3 Asthma

1.3.1 Definition

Asthma is defined by the charity Asthma UK as ‘a chronic lung condition in which the airways are inflamed and narrowed, making it harder to breathe normally’. This airway narrowing is both recurrent and reversible, and is driven by inappropriate contraction of the smooth muscle around the airways in response to a wide variety of stimuli, a feature known as airway hyperresponsiveness (AHR) (Bossé 2012). There is increasing recognition that the word ‘asthma’ is an umbrella term for the many different phenotypes seen in asthmatic patients, for example, exercise-induced asthma or Th2-mediated asthma, and the acknowledgement of specific subgroups is becoming more important in a bid to tailor treatments and improve disease management (Wenzel 2013).

1.3.2 Epidemiology

Across the developed world up to 10% of people suffer from asthma (Wenzel 2012). In the UK alone, asthma affects more than 5 million people over a wide range of ages and the disease has a major impact on the economy, costing the NHS an estimated £1 billion a year (Department of Health 2012). Each year more than 1000 people die from asthma in the UK, and it is believed that around 90% of these could have been prevented. There are numerous studies highlighting the prevalence of poor patient compliance and inhaler technique. However, such studies often also show that despite improvements in inhaler technique and compliance, there are a proportion of patients who still have poorly controlled asthma (Yildiz and Group 2014), suggesting that novel treatments are required.

1.3.3 Pathophysiology of airway smooth muscle in asthma

The presence of smooth muscle around the airways has traditionally been believed to be necessary for the control of resistance to airflow through the tracheobronchial tree, thus aiding the distribution of ventilation and ultimately gas exchange (Bossé et al. 2010), although there are some who consider it a redundant feature of the lungs (Seow and Fredberg 2001, Mitzner 2004). What is clear is that an excessive increase in resistance primarily caused by abnormal ASM contraction is a fundamental feature of asthma, and the exacerbations to which it can lead are the chief reason for asthma-related patient hospitalisation. The term airway hyperresponsiveness is used to describe this characteristic of asthma and can be defined as ‘an increased sensitivity of the airways to an inhaled

constrictor agonist, a steeper slope of the dose-response curve, and a greater maximal response to the agonist' (O'Byrne and Inman 2003).

One of the first descriptions of AHR came in 1946 when the vital capacity (VC) of asthmatics was found to decrease in response to histamine administration, whilst the VC of healthy subjects did not (Curry 1946). Despite extensive research interest the mechanism behind AHR remains unknown. There is considerable disagreement on whether AHR occurs as a result of an inherent defect in the components of airway smooth muscle cells (ASMCs) (Martin et al. 2000), such as an augmented Rho-kinase response (Chiba et al. 2010), or whether inflammatory mediators and neural pathways in the microenvironment influence the responsiveness of the ASMCs (Bossé 2012).

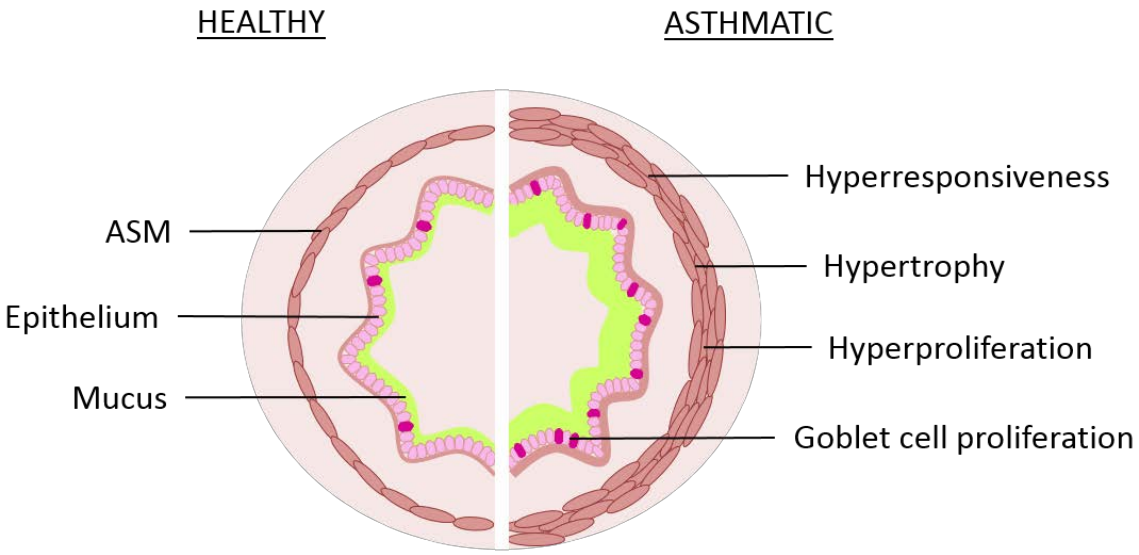

Figure 1.1: A schematic to illustrate differences between a healthy airway (left) and an asthmatic airway (right).The airway smooth muscle (ASM) not only undergoes pathological changes such as hypertrophy and hyperproliferation, but is also thought to become hyperresponsive. Mucus-secreting goblet cells proliferate, thereby increasing the presence of mucus in the asthmatic airway.

In addition to the role they may play in AHR, the ASMCs in asthmatic airways undergo hyperproliferation and hypertrophy, increasing the mass of ASM (Figure 1.1) (Berair et al. 2013). This process is thought to be a major component of airway remodelling – the term used to describe the many structural changes that occur in the asthmatic airways, also including sub-epithelial fibrosis and mucus gland hyperplasia. It has been suggested that airway remodelling may occur in the absence of inflammation, and that the increase in muscle mass may simply be the functional consequence of excessive and repeated episodes of bronchoconstriction (Davies et al. 2003, Grainge et al. 2011).

Given this, and the fact that it is the asthma exacerbations that contribute most directly to morbidity and mortality in asthmatic patients, the development of novel bronchodilators is believed critical for improving the management of asthma (Cazzola, Page, et al. 2012).

1.3.4 Existing treatments for asthma

The successful treatment of asthma requires the long-term control of the underlying inflammation, as well as dilators to relieve the patient from exacerbations. Inhaled corticosteroids (ICS) are recommended first-line treatment for long-term control of moderately-severe asthma, whilst short-acting beta-2 agonists (SABA) such as salbutamol are prescribed for relief during asthma attacks (FitzGerald 2014). In some patients, SABA and ICS provide adequate control, but many patients find these drugs do not sufficiently relieve their symptoms or they develop adverse effects.

A few studies have concluded a link between a specific polymorphism in the gene for the beta-2 adrenergic receptor and responsiveness to SABA such as salbutamol (Israel et al. 2001, 2004), but not to long acting beta-2 agonists (LABA) like salmeterol (Bleecker et al. 2007). LABAs are therefore a good alternative, but their long term use can lead to a loss of sensitivity due to receptor down-regulation (Nishikawa et al. 1996) and increased mortality (Cates and Cates 2010). ICS are capable of decreasing this beta-2-receptor desensitisation (Johnson 2004), and as a result LABAs are recommended only as an add-on therapy to ICS, often given in a combined inhaler. An ‘add-on therapy’ is the term used to describe an additional therapy prescribed for a patient whose symptoms persist on first line treatment and existing treatment thereafter. There are many stages of add-on therapy which can be progressively prescribed in order to control symptoms. ICS are one of the first offered add-on therapies. However, ICS are not without problems; in some patients with severe asthma resistance to ICS develops, meaning that even at maximum inhaled doses or with oral corticosteroids, their asthma symptoms are uncontrolled (Wenzel 2012a). Although a relatively small subset of patients, severe asthmatics represent >50% of healthcare costs (Weiss and Sullivan 2001; Van Ganse et al. 2006), and as such are often described as the single greatest unmet need in asthma (Jarjour et al. 2012).

In line with recommendations from the GINA report (FitzGerald 2014), if LABA and ICS are not adequately controlling asthma symptoms, then a number of add-on therapies can be considered. Alternative bronchodilators like anti-muscarinic drugs are one such option, including ipratropium, which has been used for many years. The longer-acting anti-

muscarinic tiotropium, which is typically used in the treatment of chronic obstructive pulmonary disease (COPD), may be useful in the treatment of asthma (Peters et al. 2010). As an add-on therapy to LABA and high dose ICS, tiotropium was found to help improve patient lung function (Kerstjens et al. 2011).

Montelukast, a cysteinyl-leukotriene (cysLT) receptor antagonist acts to prevent $CysLT_1$ receptor-mediated bronchoconstriction, and also to combat airway eosinophilic inflammation. It can be prescribed as an oral monotherapy in patients who experience adverse effects to ICS, or as an add-on therapy to ICS to help treat chronic inflammation (Joos et al. 2008). Studies investigating the potential benefit of montelukast during acute asthma exacerbations have produced mixed results (Ramsay et al. 2011; Zubairi et al. 2013). Variability in patient response to montelukast may be due to polymorphisms in genes involved in the LT biosynthetic pathway (Lima et al. 2006; Klotsman et al. 2007; Kotani et al. 2012), suggesting that montelukast may be useful only in a subset of patients.

Methylxanthines, such as the phosphodiesterase (PDE) inhibitor theophylline, were once commonly used as bronchodilators in developed countries, but their adverse effects meant that they were replaced as first-line treatment following the development of beta 2-agonists (Barnes 2013). Theophylline is now typically used as an add-on therapy when ICS and β_2-agonists are insufficiently controlling symptoms, or intravenous (IV) during acute asthma exacerbations (Travers et al. 2012). More recently, theophylline has been recognised for its anti-inflammatory effects through PDE4 inhibition, and so drugs that specifically inhibit PDE4, for example, cilomilast, could be useful in the treatment of asthma and other chronic inflammatory lung diseases, although they continue to have unpleasant side effects such as nausea, vomiting and diarrhoea (Lipworth 2005; Boswell-Smith et al. 2006).

Beyond mainstay treatment and add-on therapies, treatment choices become less generic and more targeted. Humanised antibodies such as the anti-IgE omalizumab can be effective at controlling symptoms and reducing acute exacerbations in allergic asthmatics uncontrolled by other therapies (Rodrigo et al. 2011; Norman et al. 2013), but the cost-effectiveness of humanised antibodies is questionable. The cost of omalizumab for 1 year is £15,400 (NICE 2007).

Apart from beta 2-agonists, all of the therapies above are designed to block pro-inflammatory and/or pro-constrictor pathways, most have deleterious side effects or are ineffective in subsets of patients, and a few are costly. Endogenous agonists of resolution

have the potential to 'switch on' endogenous protective and repair pathways, particularly if these endogenous pathways are under-active in patients with asthma. This is an approach used in the treatment of PAH, in which the prostacyclin analogues epoprostenol and treprostinil actively induce potent vasodilatation via GPCRs. Prostacyclin analogues have differing affinities for the prostanoid receptors. Epoprostenol is thought to achieve vasodilatation solely via the IP receptor, whilst evidence suggests that treprostinil can activate both the IP receptor and the EP_2 receptor (prostaglandin E_2 receptor) (Mubarak 2010); however, these Gαs-coupled receptors converge on the same intracellular signalling pathway, stimulating adenylyl cyclase activity thereby enhancing the production of cyclic adenosine monophosphate (cAMP) and subsequent protein kinase A (PKA) activation.

1.4 Pulmonary arterial hypertension

1.4.1 Definition

Pulmonary arterial hypertension (PAH) is described by the charity Pulmonary Hypertension UK as a 'condition where the blood pressure in pulmonary arteries is high. This causes progressive damage to the heart and lungs'. PAH is assigned as group 1 of the five phenotypes of pulmonary hypertension (Simonneau et al. 2009), as shown in Table 1-1.

Group	Classification
1	Pulmonary arterial hypertension
2	Pulmonary hypertension due to left heart disease
3	Pulmonary hypertension due to chronic lung disease and/or hypoxia
4	Chronic thromboembolic pulmonary hypertension
5	Pulmonary hypertension due to unclear multifactorial mechanisms

Table 1-1: Pulmonary arterial hypertension (PAH) is classified as group 1 of the types of pulmonary hypertension defined during the 4th World Symposium on Pulmonary Hypertension in 2008 (Simonneau et al. 2009).

Critically, it is the right ventricular heart failure caused by increased resistance in the pulmonary arteries that tends to lead to patient death, hence the development of vasodilators to treat the disease (Humbert et al. 2004).

1.4.2 Epidemiology

The annual incidence of PAH ranges from 2 per million adult inhabitants (MAI) in the US to 3.2 per million in Spain (Jiang and Jing 2013). This information is taken from national registries, and all those currently available are from developed countries. The procurement of accurate epidemiological information is hindered by difficult diagnosis and poor healthcare access in some countries. Indeed, the incidence may actually be higher in developing countries because their incidence of diseases associated with PAH, such as HIV, is typically higher (Archer et al. 2010).

Prognosis for those with PAH is unacceptably poor. The REVEAL study of 484 people with PAH showed that 81.1% of patients can expect to live for 1 year, 61.1% for 3 years, and only 47.9% for 5 years from the time of diagnosis (Kane et al. 2011). Despite the relatively recent approval of a number of vasodilators for the treatment of PAH, it is believed that <20% of PAH patients respond to conventional vasodilators (Archer et al. 2010).

1.4.3 Pathophysiology of vascular smooth muscle contraction in PAH

Whilst the normal physiological purpose of ASM remains contested, VSM is known to serve the role of establishing vasomotor tone, aiding the flow of blood through the vasculature. The mechanisms behind its regulation are somewhat less certain (Aalkjær et al. 2011). In patients with PAH, there is excessive vasoconstriction of the pulmonary arteries leading to an increase in vascular resistance, much as bronchoconstriction causes an increase in airway resistance in the lungs of asthmatics. However, whilst in airways the AHR is an inappropriate response to non-specific stimuli, the dysfunction in vascular tone is believed to be caused, at least in part, by an imbalance in the levels of vasoactive mediators (Farber and Loscalzo 2004) (Figure 1.2).

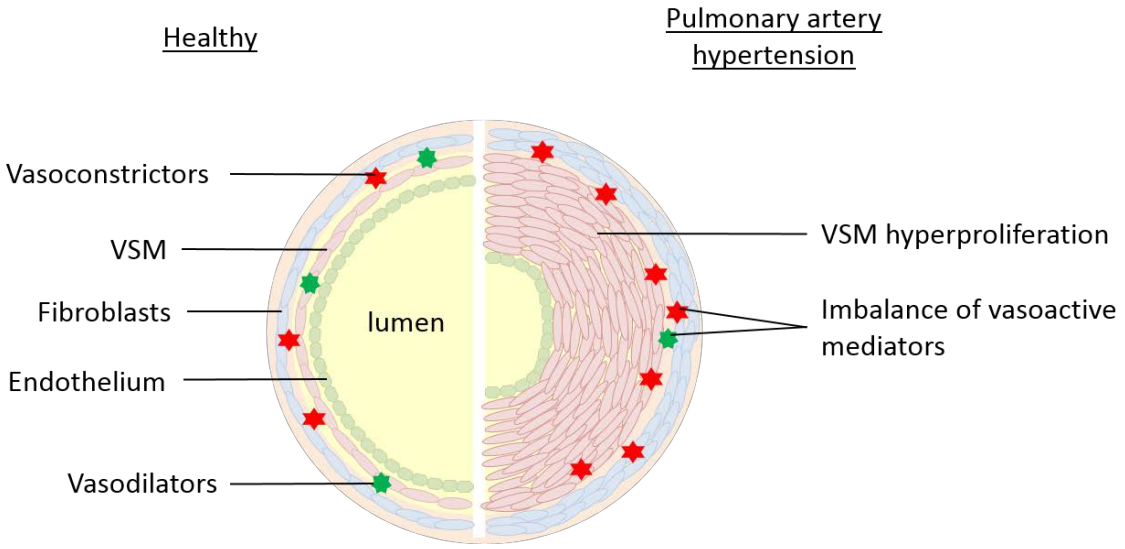

Figure 1.2: A summary of the cellular changes that occur in a pulmonary artery in patients with PAH (right) compared with healthy (left). In the healthy artery a balance of vasoactive mediators regulates vasomotor tone, whilst in PAH an overproduction of vasoconstrictors is coupled with an underproduction of vasodilators.

Patients with PAH have increased levels of potent vasoconstrictors, with two separate studies finding increased levels of thromboxane in urinary excretion of patients with PAH compared with healthy controls (Christman et al. 1992, Adatia et al. 1993), whilst the levels of endothelin (ET)-1 messenger RNA were found to be increased in lung samples from PAH patients compared to controls (Giaid et al. 1993). The impact of this increase is magnified by the fact that patients with PAH also exhibit decreased levels of vasodilators such as prostaglandin I_2 (prostacyclin) in urine (Christman et al. 1992), as well as low levels of prostacyclin synthase (Tuder et al. 1999) and nitric oxide (NO) synthase (Giaid and Saleh 1995) in lung samples from PAH patients. These studies indicate that there is a dysregulation of vasoactive mediators at both a local and systemic level.

1.4.4 Existing treatments for PAH

Following diagnosis of PAH, patients are typically tested to see if they are 'acutely vasoreactive'. This screening involves administration, usually IV, of a potent short-acting vasodilator and the positive detection of a 'fall in mean pulmonary artery pressure of >10 mmHg to a level of <40 mmHg with an unchanged or increased cardiac output and unchanged systemic pressure' (Opitz and Rubin 2009). This response is seen only in a minority of patients, and is used to identify the subset of patients who are most likely to respond to calcium channel blockers (CCB). In non-responders, there are a small number

of other approved drugs for treatment of PAH which target the dysfunctional pathways believed to lead to the development of this disease.

ET receptor antagonists are one such group of drugs. ET-1 is a potent vasoconstrictor, so antagonism of the receptor through which ET mediates vasoconstriction (ET_A) can decrease blood pressure. In contrast to the ET_A receptor, which is located on pulmonary vascular smooth muscle cells, ET_B receptors are expressed on endothelial cells and are believed to mediate vasodilatation (Rubin 2012).

A number of ET receptor antagonists have been developed. They can be dual ET receptor antagonists e.g. bosentan and macitentan, or ET_A selective e.g. ambrisentan and sitaxsentan. Although the logic behind selective ET_A antagonists is clear given the differences in receptor actions, direct comparisons between the two types of drugs are lacking (Trow and Taichman 2009). Sitaxsentan was withdrawn from the market following concerns about its safety, but ambrisentan appears safer and more tolerable in adults (McGoon et al. 2009) and children (Takatsuki et al. 2013), and thus remains approved for PAH treatment (Kingman et al. 2009). Macitentan is the more novel of the two existing dual receptor antagonists and data from clinical trials indicates a promising safety and efficacy profile (Pulido et al. 2013, Dingemanse et al. 2014).

Whilst the ET receptor antagonists act to block vasoconstriction, prostacyclin analogues are an important therapeutic option aimed at directly promoting vasodilatation. Prostacyclin derivatives, such as epoprostenol and treprostinil, can be administered as continuous IV or SC infusions and although both can improve patient quality of life, there can be issues with the method of delivery resulting in temporary interruption, infections at the delivery line site and even thrombotic complications (Barst et al. 1996). Inhaled forms of these prostacyclin analogues pose a potential way around these delivery issues (Enderby et al. 2014).

In addition to over-production of ET-1 and under-production of prostacyclin, the putative imbalance in vasoactive mediators in PAH is worsened by decreased production of the potent vasodilator nitric oxide (NO). NO is synthesised from L-arginine by endothelial NO synthase (eNOS), of which there is lower expression in the lungs of patients with PAH (Giaid and Saleh 1995). NO induces relaxation by stimulating soluble guanylyl cyclase to catalyse the conversion of guanylyl triphosphate (GTP) to cyclic guanylyl monophosphate (cGMP), leading to a decrease in $[Ca^{2+}]_i$ and thus a decrease in Ca^{2+}-dependent contractile activity. cGMP can be broken down by phosphodiesterase 5

(PDE5), so inhibitors of this enzyme have been developed to induce relaxation of the pulmonary vessels. Sildenafil was the first available PDE5 inhibitor, but since then the long-acting PDE5 inhibitor tadalafil has been developed and is proving effective in a subset of PAH patients (Arif and Poon 2011, Shapiro et al. 2013).

There are a number of potential therapies in the pipeline, including vasoactive intestinal peptide (VIP), which relaxes pulmonary arterial smooth muscle. This vasodilatory peptide was proposed as a treatment for PAH sufferers more than a decade ago, and had exciting results in the small number of patients tested in one study (Petkov et al. 2003). It also showed promise in another study in which patients inhaled VIP (also named Aviptadil) (Leuchte et al. 2008). Unfortunately progress appears to have halted following publication of an abstract with negative implications presented at an American Thoracic Society meeting, for which the full results are yet to be published some 4 years later, despite calls from the scientific community (Said et al. 2012).

1.5 Mechanisms of smooth muscle contraction

The contraction of both airway and vascular smooth muscle is dependent on intracellular calcium concentration, as well as modulation by mechanisms that alter the sensitivity of the contractile machinery. Alterations in membrane potential contribute little to smooth muscle contraction, and instead the initiation of contraction is determined either by agonist-receptor interaction or by 'stretch' activation (Webb 2003).

When a contractile agonist binds to its G-protein-coupled receptor (GPCR), for example leukotriene D_4 binding to its cysteinyl-leukotriene receptor 1 ($CysLT_1$), phospholipase C (PLC) becomes activated and cleaves the membrane component phosphatidylinositol bisphosphate (PIP_2) to generate diacylglycerol (DAG) and inositol trisphosphate (IP_3). Both these second messengers play important roles in the regulation of smooth muscle contraction. IP_3 binds to IP_3 receptors (IP_3R) on the sarcoplasmic reticulum – an internal calcium store. The IP_3R functions as a calcium channel, which once opened, releases calcium into the cytosol where it is free to bind to calmodulin. This protein requires four calcium ions to bind before it is activated and thus able to complex with myosin light chain kinase (MLCK), which then proceeds to phosphorylate the myosin light chain (MLC). It is to the phosphorylated form of the MLC that actin can bind, initiating contraction (Figure 1.3) (Webb 2003).

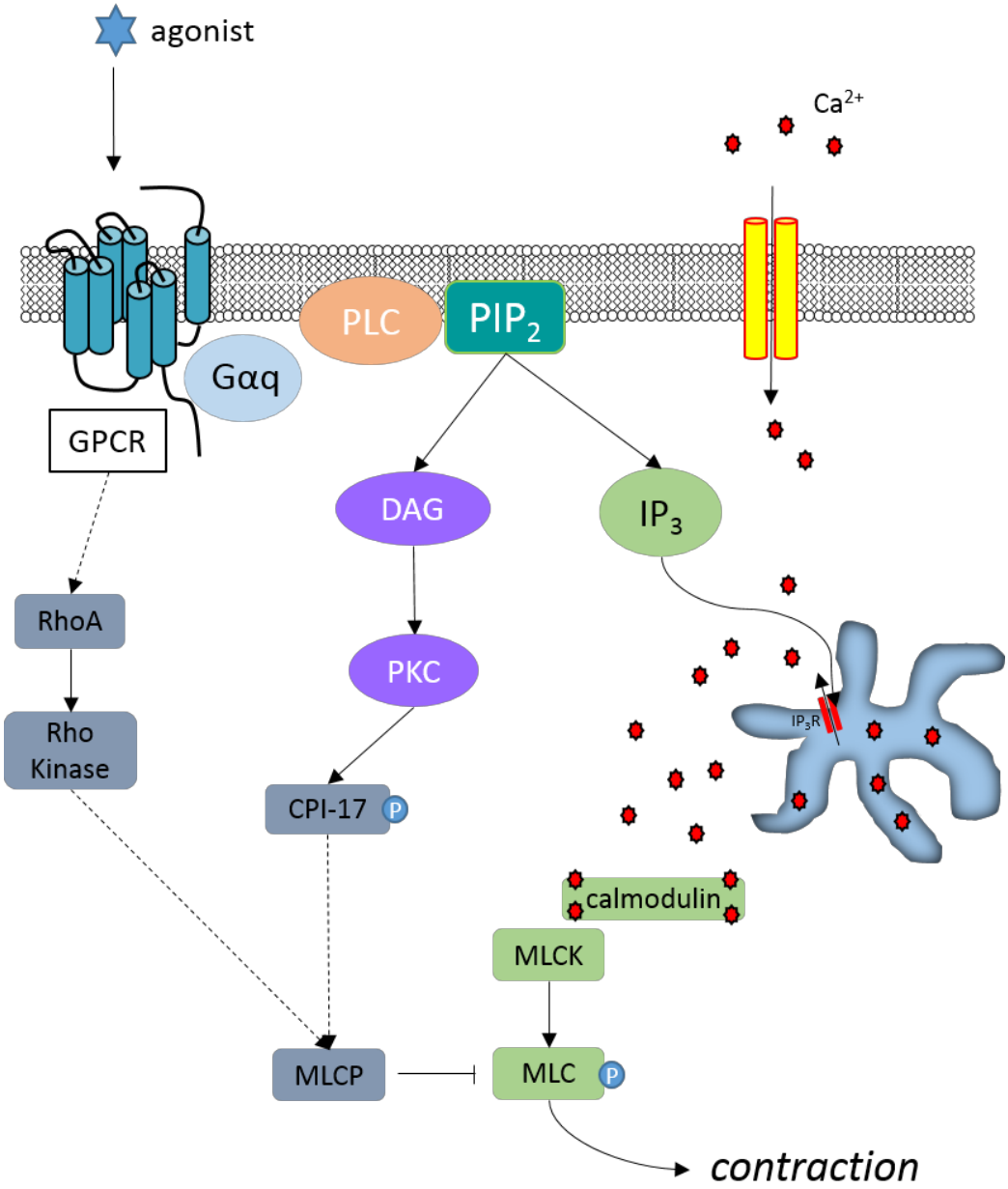

Figure 1.3: Mechanism of smooth muscle contraction. An agonist binds to its G-protein-coupled receptor initiating a second messenger cascade that results from the cleavage by phospholipase C (PLC) of phosphatidylinositol bisphosphate (PIP_2) to inositol trisphosphate (IP_3) and diacylglycerol (DAG). IP_3 binds to IP_3 receptors on the sarcoplasmic reticulum, releasing calcium ions into the cytosol, thus increasing intracellular calcium concentration. Calcium can also enter the cell from extracellular sources via calcium channels, but the contribution of this mechanism to the contractile response is believed to be minimal in terms of smooth muscle. A rise in intracellular calcium concentration results in the formation and activation of the calcium-calmodulin-myosin light chain kinase (MLCK) complex. MLCK phosphorylates the myosin light chain (MLC), permitting the formation of actin-myosin cross-bridges and thus smooth muscle cell contraction. There are also a number of calcium-independent mechanisms by which the sensitivity of the contractile machinery is manipulated. Myosin light chain phosphatase (MLCP) works in opposition of MLCK, dephosphorylating the myosin light chain and promoting relaxation. MLCP is inhibited by two main mechanisms – the Rho kinase pathway and the protein kinase C (PKC)/C-kinase potentiated protein phosphatase-1 inhibitor (CPI-17) pathway. These second messenger pathways act to maintain the tension already developed by the rise in intracellular calcium concentration. Figure redrawn from (Pelaia et al. 2008).

Whilst the increase in intracellular calcium concentration causes an initial development in tension, there are other mechanisms in play designed to sustain it (Pelaia et al. 2008). DAG, the other metabolite of PIP_2, can activate protein kinase C (PKC) which in turn phosphorylates CPI-17 (C-kinase potentiated protein phosphatase-1 inhibitor) rendering it active. CPI-17 and Rho kinase, whose activation mechanism is unknown, can inhibit myosin light chain phosphatase (MLCP), thereby inhibiting relaxation (Dimopoulos et al. 2007, Eto 2009, Puetz et al. 2009).

The relaxation of smooth muscle is simply the reverse of contraction – i.e. removal of calcium ions from the cytosol and the re-activation of MLCP. The sarcoplasmic reticulum calcium ATPase (SERCA) acts as a calcium ion pump, refilling the sarcoplasmic reticulum with calcium ions. There are other SERCA pumps and exchangers located on the plasma membrane aiding the reduction in intracellular calcium concentration. In the absence of calcium ions, calmodulin can no longer form active complexes with MLCK, and thus the MLC is not phosphorylated further. Instead a decrease in the activity of the calcium sensitivity regulators CPI-17 and Rho kinase renders MLCP active and thus able to dephosphorylate the MLC, promoting relaxation (Webb 2003).

1.6 Mediators of smooth muscle contraction

There are many mediators that regulate the tone of airways and blood vessels, some of which act directly on the SMCs and others that act upon neighbouring cells such as endothelial cells. It is thought that in normal physiology, a balance between pro-contractile and pro-dilating mediators is maintained but in disease states there is often an over- or under-production of some of these mediators which can disrupt such a balance.

The eicosanoids are a group of lipids derived from the omega-6 polyunsaturated fatty acid (PUFA) arachidonic acid (AA) (20:4ω6), and their roles as modulators of smooth muscle contraction are relatively well characterised (Table 1-2).

Molecule	Primary receptor	Physiological effect	Reference
Leukotriene D_4	$CysLT_1$	Bronchoconstriction	(Dahlén et al. 1980)
		Vasoconstriction	(Walch et al. 2002)
Leukotriene C_4	$CysLT_2$	Bronchoconstriction	(Dahlén et al. 1980)
		Vasoconstriction	(Walch et al. 2002)
Leukotriene E_4	Unknown	Bronchoconstriction	(Lee et al. 1984)
Thromboxane A_2	TP	Bronchoconstriction	(Coleman and Sheldrick 1989)
		Vasoconstriction	(Coleman et al. 1981)
Prostaglandin D_2	DP	Bronchoconstriction	(Johnston et al. 1995)
		Vasodilatation	(Johnston et al. 1995)
Prostaglandin E_2	EP_2	Bronchodilation	(Tilley et al. 2003)
	EP_1	Bronchoconstriction	
	EP_2/EP_4	Vasodilatation	(Yang and Du 2012); (Foudi et al. 2008)
Prostaglandin I_2	IP	Vasodilatation	(Norel et al. 2004)

Table 1-2: Smooth muscle activity of eicosanoids in humans.

LTD_4 is the most potent human ASM contractile agonist known (Dahlén et al. 1980), and it belongs to the cysLT family which includes the second, less potent contractile agonist LTC_4 as well as LTE_4. These omega-6 lipids are derived from the PUFA AA, and in addition to their pro-contractile roles, also mediate important pro-inflammatory events in a number of allergic inflammatory responses, including asthma. LTD_4 is also able to constrict blood vessels but with a weaker potency than it does in airways (Labat et al. 1992). LTE_4 is said to be a partial agonist in both the airways and vasculature, mediating constriction that is significantly lower than that of LTD_4 in isolated human airways, and both LTD_4 and LTC_4 in isolated human veins (Labat et al. 1992).

Thromboxane A_2 is another contractile mediator of both ASM (Coleman and Sheldrick 1989) and VSM (Coleman et al. 1981) and, like LTD_4, is derived from omega-6 PUFAs. It belongs to the prostanoid family of lipids, a subfamily of the eicosanoids, named after their original members, the prostaglandins (PGs) (Woodward et al. 2011). The vascular and airway effects of the PG are complicated, not only because each family member mediates different effects, sometimes via multiple receptors, but also because their contractile activity on ASM is not necessarily mirrored on VSM. PGI_2, commonly known

as prostacyclin, is an important vasodilator synthesised by the endothelium and mediates its potent relaxant effects via the IP receptor on smooth muscle cells (Norel et al. 1999, Mubarak 2010). This GPCR couples to Gαs, stimulating an increase in the levels of intracellular cAMP which mediates PKA activity. Prostacyclin is often referred to as a physiological antagonist of thromboxane as they work in opposition to regulate both platelet aggregation and vasoconstriction, a balance that is key to the pathogenesis of PAH (Gryglewski 2008).

The differential effect of a single mediator on the two smooth muscle types is also seen with the muscarinic receptor (mAChR) agonist acetylcholine. In ASM, the neurotransmitter acetylcholine binds to mAChRs directly on the ASM cell, causing the activation of PLC which cleaves PIP_2 into DAG and IP_3, with the latter binding to IP_3R on the sarcoplasmic reticulum to generate the release of calcium and thus contraction. In contrast, VSM cells are devoid of mAChRs, and instead acetylcholine mediates vasodilatation through the binding of mAChRs on endothelial cells to activate the calcium dependent eNOS and thus generate the potent vasodilator NO.

In human pulmonary arteries pre-constricted with serotonin (5-HT), histamine has a biphasic effect. At low concentrations up to 100 nM histamine, vessels relax before proceeding to constrict in response to higher concentrations of this mediator (Ortiz et al. 1992). The authors found that by mechanically removing the endothelium, the relaxation seen at low concentrations of histamine is abolished, indicating a role for the endothelium in this effect. Histamine is produced by mast cells in the lung in response to an antigen during an inflammatory response, mediating constriction in human bronchial tissue from asthmatic patients (SCHILD 1951). In the past, anti-histamines held great hope in the treatment of asthma but studies demonstrated a lack of effectiveness (Van Ganse et al. 1997). More recently a review of the evidence led to suggestions that anti-histamines might be useful when used alongside anti-leukotrienes (Bartho and Benko 2013).

A number of peptides are also active on smooth muscle, including angiotensin II and ET-1, both of which mediate vasoconstriction and contribute to hypertension (Davenport et al. 1995, Maguire and Davenport 1995, Touyz 2003, Maron and Leopold 2014).

The wide range of mediators capable of mediating contraction or relaxation of bronchial or vascular smooth muscle highlights the multifactorial nature of diseases characterised by inappropriate smooth muscle contraction. The contractile agonists and

vasorelaxants discussed here all function via GPCRs typically expressed either on the smooth muscle itself or, in arteries, on the endothelium.

1.7 The resolution of inflammation

The acute inflammatory response is critical to the body's defence against injury, invasion or infection, and consists of two phases – initiation and resolution (Figure 1.4). There are five cardinal signs of inflammation – *rubor* (redness), *calor* (heat), *tumour* (swelling), *dolor* (pain) and lastly *functio laesa* (loss of function), the first four of which were described in the 1st century AD. In contrast, a recent review designated distinct hallmarks as the 'cardinal signs of resolution', and these are (a) cessation of leukocytic infiltration, (b) counterregulation of pro-inflammatory mediators, and (c) the uptake of apoptotic neutrophils and cellular debris (Serhan, Chiang, Dalli, et al. 2015).

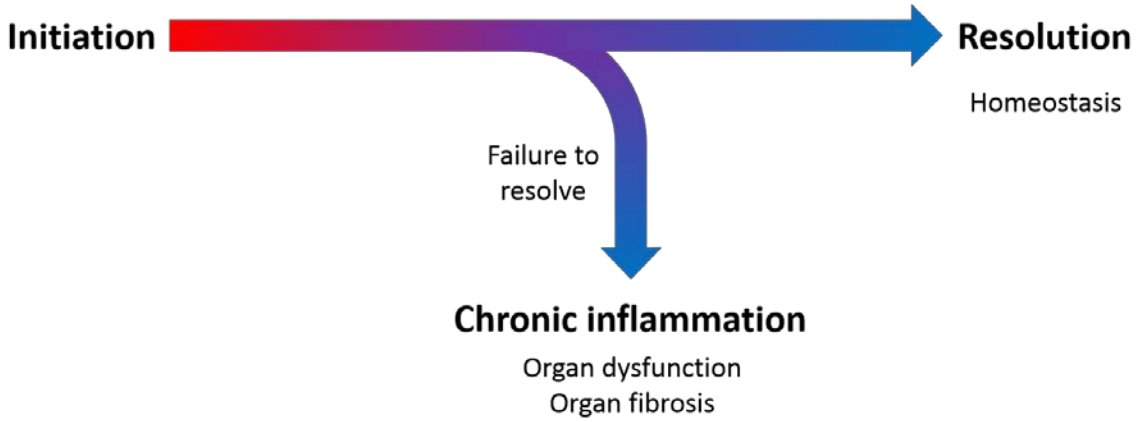

Figure 1.4: The acute inflammatory response. Both the initiation phase and the resolution phase of the acute inflammatory response are active processes, but if uncontrolled, acute inflammation can become chronic, leading to organ dysfunction and fibrosis.

During the initiation phase, neutrophils and other leukocytes are recruited from the blood stream via diapedesis into the interstitial fluid, where they are guided by chemotactic gradients to the site of insult. Upon arrival, the neutrophils protect against invading pathogens by many mechanisms, including phagocytosis, the release of anti-microbials such as LL-37 and the production of NETs (neutrophil extracellular traps) (Brinkmann et al. 2004, Tabas and Glass 2013).

Whilst the initiation phase has long been recognised as an active process, until recently the resolution phase was believed to be passive, entailing the gradual 'disappearance' of pro-inflammatory mediators. The resolution of inflammation is now

appreciated as a highly complex and biochemically active process, largely due to the identification of a diverse range of mediators found to be involved in resolution, including peptides and proteins such as annexin A1, bioactive lipids such as lipoxins, resolvins, protectins and maresins, as well as gaseous mediators such as carbon monoxide. Many of these mediators function as agonists rather than antagonists, thus actively opposing inflammation. As such, resolution differs from 'anti-inflammation' since the process acts to promote tissue repair and restore the tissues to their former state pre-insult (Nathan and Ding 2010, Serhan and Chiang 2013).

The understanding that the resolution phase of the acute inflammatory response is an active process has led to the emergence of some interesting concepts, in particular, that a failure to resolve may contribute to the development of chronic inflammation, and ultimately tissue injury and fibrosis (Figure 1.4). These concepts, including resolution deficits and resolution pharmacology, will be discussed in more detail at the end of this chapter.

1.7.1 Resolution agonists

The first resolution agonists to be identified were the lipoxins (lipoxygenase interaction products), potent lipid mediators derived from AA known as lipoxin A_4 and lipoxin B_4 (Serhan et al. 1984a, 1984b). Subsequent studies identified a plethora of endogenous bioactive lipids derived from omega-3 PUFAs which are collectively known as specialised pro-resolving lipid mediators (SPM), and include the resolvins, protectins and maresins. The term SPM was chosen to reflect the specificity of their actions and roles in the resolution of inflammation, due in part to their temporally distinct appearances throughout this active process. Importantly, many of the SPMs have recently been detected within their bioactive range (picomolar – nanomolar) in the blood of healthy volunteers (Colas et al. 2014), and in the urine of healthy volunteers (Sasaki et al. 2015).

A key characteristic of SPMs is their ability to attenuate the transmigration of neutrophils, as well as enhance the phagocytosis of apoptotic neutrophils and bacteria such as *E.coli* by macrophages (Serhan et al. 2006, Spite et al. 2009, El Kebir et al. 2012). Tumour necrosis factor-α (TNF-α) increased the expression of cell adhesion molecules, vascular cell adhesion molecule-1 (VCAM-1) and intracellular adhesion molecule-1 (ICAM-1), in vascular smooth muscle cells, and this increase was concentration-dependently inhibited in the presence of either resolvin (Rv) D1 or RvD2 (Miyahara et al. 2013). SPMs have also been found to modulate pro-inflammatory signalling, inhibiting

TNF-α-induced NF-κB (nuclear factor kappa-light-chain-enhancer of activated B cells) activity in both endothelial and saphenous vein vascular smooth muscle cells (Miyahara et al. 2013, Chatterjee et al. 2014) and in human pulmonary artery smooth muscle cells (Hiram et al. 2015), whilst NF-κB signalling induced by LTB_4 was shown to be inhibited by RvE1 using a luciferase reporter assay in HeLa cells through RvE1's ability to act as a partial agonist at BLT1 receptors (Arita et al. 2007).

SPMs do not act in isolation to mediate the resolution of inflammation, as there are many other molecules working alongside. Pro-resolving peptides and proteins, such as the calcium-dependent superfamily of annexin proteins which includes annexin A1 (Perretti et al. 1991, 2000), are thought to contribute important roles in the resolution of inflammation, including the promotion of neutrophil apoptosis (Vago et al. 2012), which is one of the 'cardinal signs of resolution' (see section 1.7).

1.7.2 The class switch – lipoxins

Unlike most SPMs, the lipoxins are derived from the omega-6 PUFA AA (Serhan et al. 1984a, 1984b) via the sequential actions of a variety of lipoxygenase (LO) enzymes. In the vasculature, when leukocytes and platelets interact, platelets are able to uptake leukocytic 5-LO product, LTA_4, and transcellularly convert it into LXA_4 or LXB_4 via 12-LO. Alternatively, interactions between leukocytes and either epithelial cells, monocytes or eosinophils allow 15-LO to convert AA to 15S-hydroxyeicosatetraenoic acid (HETE), which can then be converted to LX via 5-LO within polymorphonuclear leukocytes (PMN). This latter reaction reduces the amount of 5S-HETE produced, thus having the added benefit of decreasing LT production (Chiang et al. 2005).

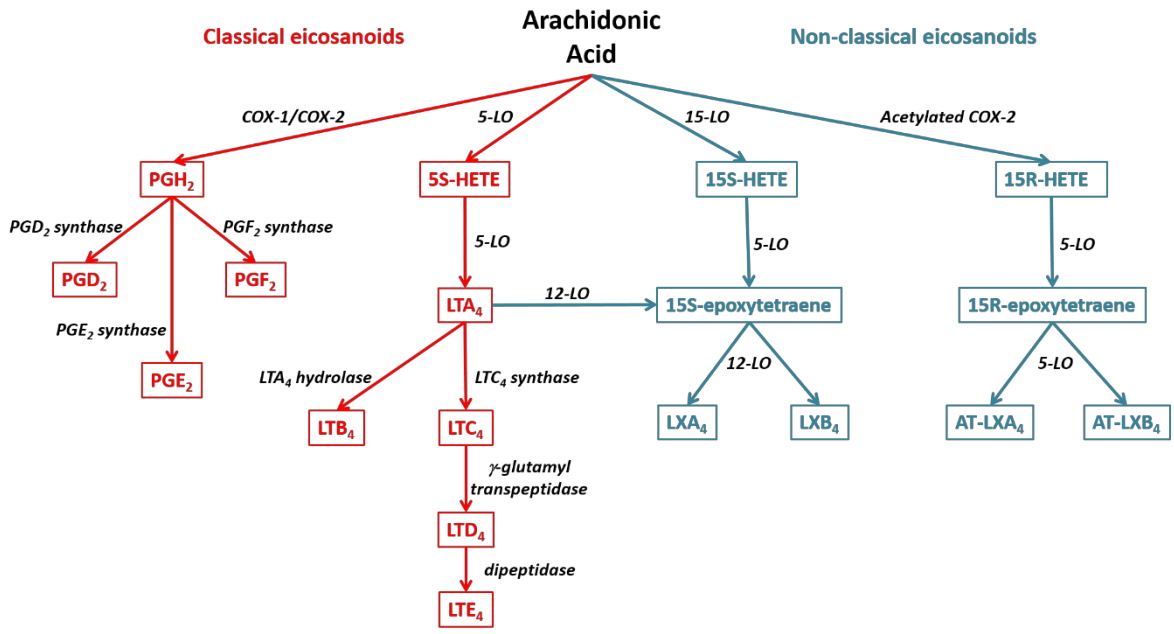

Figure 1.5: Biosynthesis of eicosanoids. The eicosanoid family of bioactive lipids is derived from the omega-6 PUFA arachidonic acid (AA). Prostaglandins are produced via COX-1 and COX-2, but when COX-2 becomes irreversibly acetylated by aspirin, 'aspirin-triggered' lipoxins are synthesised. 5-LO acts to convert AA to leukotrienes, but when platelets interact with leukocytes, the 12-LO found abundantly in platelets converts the 5-LO product LTA_4 into lipoxins with 'S' chirality. In addition, lipoxins can be synthesised from AA via the sequential actions of 15-LO and 5-LO. (COX cyclooxygenase; LO, lipoxygenase; PG prostaglandin; LT leukotriene; HETE, hydroxyeicosatetraenoic acid; LX, lipoxin; AT-LXA_4 aspirin-triggered lipoxin A_4).

In addition to being enzymatically synthesised by LO enzymes, lipoxin epimers with 'R' chirality can be produced in the presence of aspirin, hence their name of aspirin-triggered lipoxins (Clària and Serhan 1995). Aspirin inhibits the production of prostaglandins by inhibiting both cyclooxygenase-1 (COX-1) and COX-2, and it does so by irreversible acetylation of the active site. However, by acetylating COX-2, aspirin also directs the synthesis of anti-inflammatory/pro-resolving lipoxins, helping to explain the anti-inflammatory actions of aspirin.

The lipoxins are known to contract ASM, albeit in a manner that is 10,000 times less potent than the classical eicosanoid, LTD_4, in guinea pigs (Jacques et al. 1988) as well as rabbits and rats (Lefer et al. 1988). In spite of this similarity between the lipoxins and the CysLTs, whilst the CysLTs are potent pro-inflammatory mediators, the lipoxins are crucial to the resolution of inflammation in what has been termed 'class switching'. Prostaglandins (PGs) PGE_2 and PGD_2 initiate a shift in LO enzymic activity from 5-LO to 15-LO (Levy et al. 2001) resulting in decreased CysLT production and increased lipoxin production (Figure 1.5), and thus instigating a self-limiting programme. This switch from the synthesis

of a pro-inflammatory class of AA derivatives to anti-inflammatory and pro-resolution AA derivatives marks the beginning of the resolution of inflammation.

Like other resolution agonists, LXA_4 mediates its effects via a GPCR. Radiolabelled LXA_4 was used to demonstrate binding of LXA_4 to the orphan receptor pINF114, a GPCR with ~70% homology to the formyl peptide receptor (FPR) (Fiore et al. 1994) and so it was named FPR2 (Ye et al. 2009). Although the FPR2 can be bound by formyl peptide (FP), the concentrations of FP required to elicit a biological response are high, and thus IUPHAR (International Union of Pharmacology) recommended renaming it the lipoxin A_4 receptor (ALX) (Brink et al. 2003). The ALX receptor is an unusual GPCR as it was the first found to be activated by both lipids and peptides – the pro-resolving peptide annexin A1 is also a natural ligand for ALX (Perretti et al. 2002), in addition to a number of other molecules, some of which may have important implications in respiratory diseases such as serum amyloid A (SAA) (Bozinovski et al. 2008). Levels of this apolipoprotein were shown to be increased during acute exacerbations in patients with COPD, and, *in vitro*, promoted the release of pro-inflammatory mediators via the ALX receptor (Bozinovski et al. 2012).

SAA is not the only pro-inflammatory agonist of this receptor; LL-37, a cathelicidin-related anti-microbial peptide, is stored in PMN cells where its release can be triggered by LTB_4 in a BLT1 receptor-mediated manner. LL-37 then acts in a positive feedback loop (Figure 1.6), promoting the translocation of 5-LO to the nucleus where it is believed to preferentially convert AA to LTB_4, rather than LXA_4 (Wan et al. 2007). This is in contrast to RvD1, which is thought to promote the cytosolic localisation of 5-LO via GPR32 or ALX, enhancing LXA_4 synthesis and decreasing levels of LTB_4 (Fredman et al. 2014). To add further complexity, RvE1, which is known to antagonise the BLT1 receptor (Arita et al. 2007), inhibits LTB_4-induced LL-37 release from human neutrophils (Wan et al. 2011).

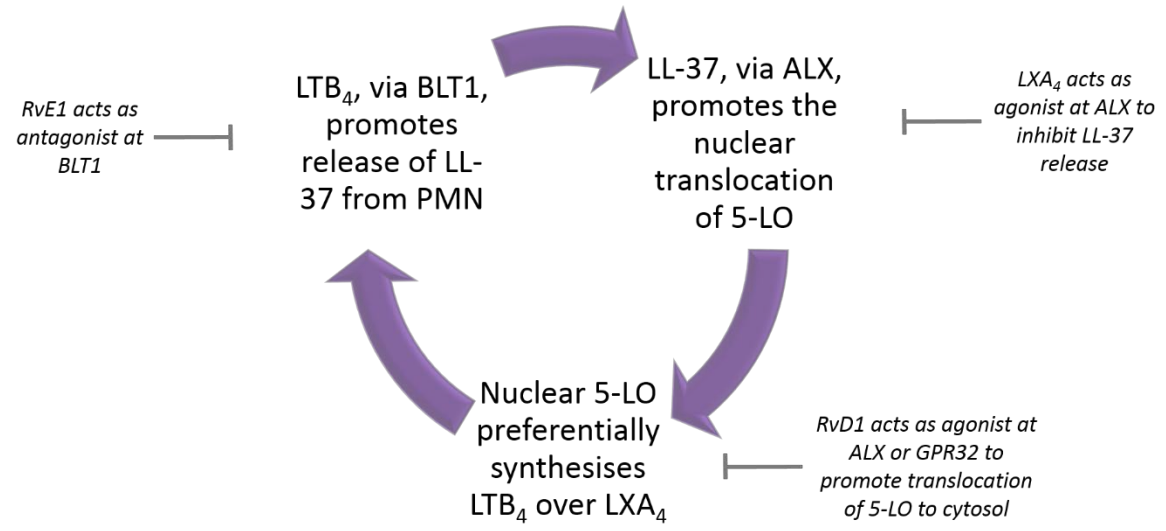

Figure 1.6: Multifactorial regulation of the balance between pro-inflammatory and pro-resolving mediators. Pro-inflammatory mediator LTB_4 is released during the initiation phase of acute inflammation and binds its G-protein-coupled receptor (GPCR), BLT1, on PMN to promote the release of anti-microbial peptide, LL-37. This peptide then acts in a positive feedback loop, binding to ALX to promote the nuclear translocation of 5-lipoxygenase – the mutual enzyme for LTB_4 and LXA_4 synthesis. Localisation of this enzyme at the nucleus is thought to result in the preferential synthesis of LTB_4 over LXA_4, thus further LTB_4 is released through LTB_4-mediated actions. Various specialised pro-resolving lipid mediators (SPMs) function to oppose the synthesis and actions of LTB_4, with resolvin (RV) E1 antagonising the BLT1 receptor, LXA_4 opposing the actions of LL-37 via ALX, and RvD1 promoting the movement of 5-LO to the cytosol.

This remarkable ability of a single GPCR to mediate the effects of such a range of ligands, some of which have opposing agonistic effects, may be explained by differential conformational changes in the ALX receptor specific to each agonist. One study found that the ALX receptor is constitutively expressed as a dimer, and that depending on whether it exists as a homodimer or as a heterodimer in conjunction with FRP1 or FRP3, it is activated by different ligands (Cooray et al. 2013). Furthermore, there is evidence for receptor activation by each ligand via different regions of the receptor (Bena et al. 2012).

LXA_4 has also been shown to compete with LTD_4 for the $cysLT_1$ receptor in rat mesangial cells (Badr et al. 1989), in human umbilical vein endothelial cells (HUVECs) (variety of LXA_4 analogues tested) (Takano et al. 1997), and in $cysLT_1$-transfected COS-7 cells (Gronert et al. 2001). The non-specific cysLT receptor antagonist SKF-104353 (pobilukast) has been used to block LXA_4-mediated activity in human mesangial cells (McMahon et al. 2000) and rat mesangial cells (Badr et al. 1989). In this latter study, pre-exposure of the cells to 100 nM LXA_4 for 10 minutes completely abolished the ability of LTD_4 to mediate IP_3 formation to the same extent as did SKF-104353, and yet alone LXA_4

(10 nM) elicited a ~50% increase in IP_3 formation, leading the authors to suggest that LXA_4 may be a partial agonist of the $cysLT_1$ receptor.

The ability of LXA_4 to act as a partial agonist at the $cysLT_1$ receptor could explain the weak pro-contractile effect of this resolution agonist. Indeed the combined inhalation of LXA_4 and LTC_4 by asthmatic patients caused a significant rightward curve shift in both specific airway conductance (sGaw) and expiratory flow rate at 25% of the vital capacity (V_{25}) when compared with the inhalation of LTC_4 alone (Christie et al. 1992). Although the mechanism by which LXA_4 antagonised the LTC_4 response was not sought, LTC_4 is known to act at the $cysLT_1$ receptor as well as the $cysLT_2$ receptor, so LXA_4 could be acting as an antagonist or partial agonist at either of these receptors. Indeed, LXA_4 was able to inhibit LTD_4-induced responses in CHOK1 cells expressing $cysLT_2$ but not $cysLT_1$ (McMahon et al. 2002). Raising the possibility of yet more complex interactions, the specific $cysLT_1$ receptor antagonist MK571 (IC_{50} 0.3 nM) was found to compete with radiolabelled LXA_4 with less than or equal affinity to unlabelled LXA_4 (Gronert et al. 2001).

Whilst the receptor-mediated actions of lipoxin A_4 and its analogues are relatively well characterised, a receptor for lipoxin B_4 is still to be identified.

1.7.3 Resolvins

Resolution-phase interaction products, lipids more commonly known as resolvins, are omega-3 derived bioactive lipids belonging to one of two branches, the ‘E series’ derived from eicosapentaenoic acid (EPA) or the ‘D series’ derived from docosahexaenoic acid (DHA). They include some of the best characterised SPMs and were initially discovered in inflammatory exudates from mice supplemented with omega-3 PUFAs. They are also produced by HUVECs (Serhan et al. 2000). Since then the existence of RvE2 (Tjonahen et al. 2006) and RvE3 (Isobe et al. 2012), as well as resolvins D1 to D6 (Serhan et al. 2002), has been proposed, although only a select few are commercially available for study.

In these initial papers identifying the novel lipids derived from EPA (Serhan et al. 2000) and DHA (Serhan et al. 2002), the authors performed experiments demonstrating that one of the most important roles of the resolvins in the resolution of inflammation is inhibition of LTB_4-mediated neutrophil migration during transepithelial migration. In

addition, this work was the first to suggest that resolvins could interact with receptors for Ω-6 fatty acid derived lipid mediators (Serhan et al. 2000).

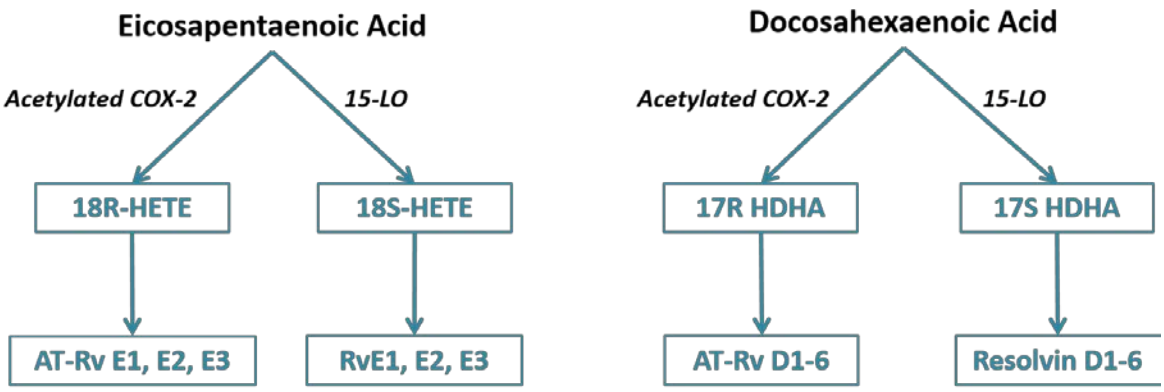

Figure 1.7: Biosynthesis of resolvins from eicosapentaenoic acid (EPA) and docosahexaenoic acid (DHA). The 'E series' resolvins are derived from the omega-3 PUFA eicosapentaenoic acid (EPA) via hydroxylated intermediates by the activity of 15-lipoxygenase (15-LO), whilst the same enzyme generates the 'D series' resolvins in two steps from docosahexaenoic acid (DHA). Cyclooxygenase-2 (COX-2) is irreversibly acetylated by aspirin to permit the conversion of EPA or DHA in two steps to 'aspirin-triggered' resolvins which have 'R' chirality rather than 'S'.

Whilst LTs are produced during the initiation phase of the acute inflammatory response, resolvins are produced later, following the PG/LXA_4-mediated class switch, although it has been suggested that RvD3 is produced slightly later on than other SPMs in the resolution process (Dalli, Winkler, et al. 2013). This temporally organised production of omega-6 and then omega-3 derived SPMs has been described as 'the beginning programmes the end' (Serhan and Savill 2005).

It was not long after the discovery of the resolvins themselves that resolvin receptors began to be identified. GPCRs closely related to ALX were expressed in human embryonic kidney (HEK)293 cells and the ability of RvE1 to inhibit TNF-α-stimulated NF-κB activation was shown to be dependent on the orphan receptor ChemR23 (Arita et al. 2005). Later RvE1 was also found to bind to the leukotriene B_4 receptor BLT1, as either LTB_4 or RvE1 were able to displace radiolabelled [^{3}H]-RvE1 binding in PMN cells. Importantly, the chemoattractant protein chemerin, which is known to bind specifically to ChemR23 (Wittamer et al. 2004), did not displace [^{3}H]-RvE1, ruling out the possibility that the displacement of [^{3}H]-RvE1 was occurring at ChemR23, rather than at BLT1 receptors (Arita et al. 2007). In addition, the authors confirmed their initial results by expressing BLT1 in HEK293 cells and demonstrating the same displacement activity. RvE2 has also been found to bind to the BLT1 receptor to a similar level as RvE1, inhibiting LTB_4-

mediated activity (Oh et al. 2012). ChemR23, which is sometimes referred to as chemokine-like receptor 1 (CMKLR1), has recently been paired with chemerin and named the chemerin receptor (Davenport et al. 2013). This GPCR is also capable of mediating the effects of RvE2 but in a manner that is less potent than RvE1 since in a β-arrestin system RvE1 achieved approximately double the level of luminescence compared with RvE2. Because of this, the authors suggest that the pro-resolving actions of RvE2, including the enhancement of phagocytosis by macrophages and the promotion of the release of anti-inflammatory cytokines such as IL-10, are likely achieved instead via another receptor yet to be identified (Oh et al. 2012).

Within the D series resolvins, RvD1 was the first to be linked to a receptor. HeLa cells were transfected with cDNA of selected GPCRs and a luciferase reporter system was used to show that RvD1 bound to the LXA_4 receptor ALX, and also to the orphan receptor GPR32 (Krishnamoorthy et al. 2010), a chemoattractant receptor related to formyl peptide receptors. Since then, both RvD3 (Dalli, Winkler, et al. 2013) and RvD5 (Chiang et al. 2012) have also been found to bind to GPR32. Very recently, the orphan GPCR GPR18 has been shown to mediate the pro-resolving actions of resolvin D2, and it is expressed in PMN, monocytes and macrophages (Chiang et al. 2015). The literature regarding the deorphanisation of this GPCR contains mixed reports on the agonistic activity of N-arachidonoyl glycine at GPR18 (Kohno et al. 2006, Yin et al. 2009). A recent study provided evidence of biased agonism at this receptor, with several agonists including N-arachidonoyl glycine inducing increases in intracellular calcium concentration and extracellular signal-regulated kinases (ERK) phosphorylation, but only one of those ligands (not N-arachidonoyl glycine) demonstrated the capability to recruit β-arrestin (Console-Bram et al. 2014). Additionally, whilst the results from the study with N-arachidonoyl glycine suggest the involvement of Gαi proteins (Kohno et al. 2006), the data characterising the activation of GPR18 by RvD2 indicates a role for Gαs proteins, and further still there is evidence for Gαq proteins coupling to this intriguing orphan receptor (Console-Bram et al. 2014).

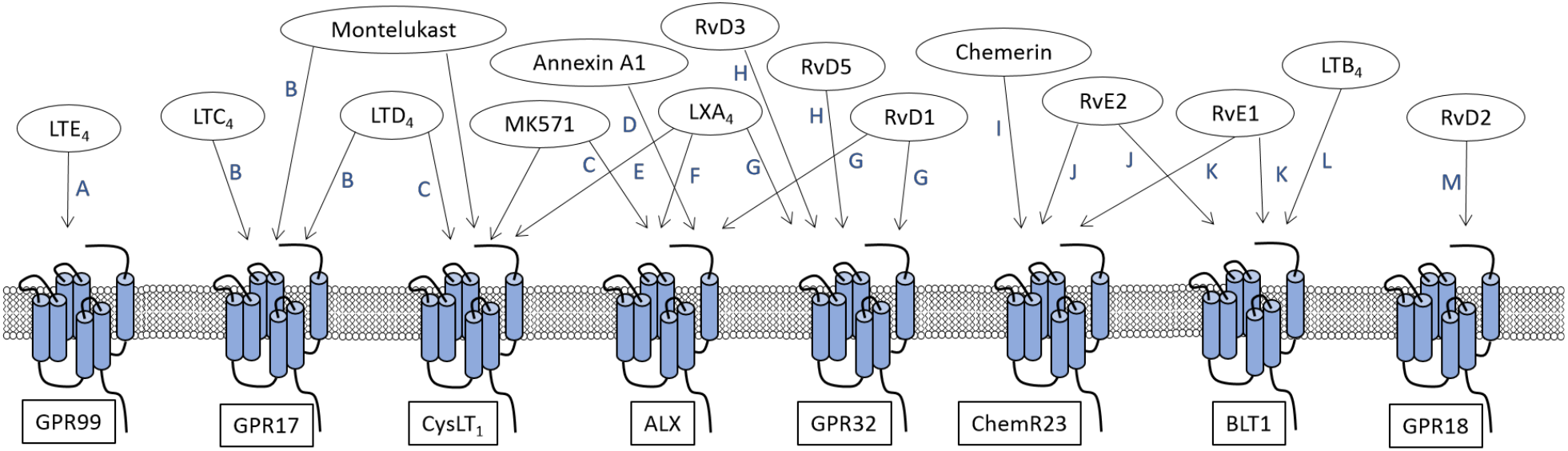

A. Kanaoka et al., 2013
B. Ciana et al., 2006
C. Gronert et al., 2001
D. Perretti et al., 2002
E. Badr et al., 1989; Takano et al., 1997; Gronert et al., 2001
F. Fiore et al., 1994
G. Krishnamoorthy et al., 2010
H. Dalli et al., 2013
I. Wittamer et al., 2004
J. Oh et al., 2012
K. Arita et al., 2007
L. Yokomizo et al., 1997
M. Chiang et al., 2015

Figure 1.8: GPCR activity of molecules including classical eicosanoids, specialised pro-resolving lipid mediators (SPMs), pro-resolving peptides and chemotactic proteins. Over the last decade, GPCR have been identified as responsible for mediating the effects of a range of molecules involved in the acute inflammatory response. A number of orphan receptors have been identified as important in mediating the actions of SPMs (GPR32 and GPR18), whilst the ALX receptor can be activated by pro-resolving lipids and peptides. As research in the field advances, more receptors are likely to be identified as important receptors in the resolution of inflammation.

It is interesting that, like the classical eicosanoids, the resolvins and lipoxins appear to be relatively promiscuous in terms of receptor binding. RvE1 and RvE2 bind to both ChemR23 and BLT1, RvD1 binds to both ALX and GPR32, whilst LXA_4 binds to both ALX and $CysLT_1$. The LTs have not been found to bind to pro-resolving receptors, but there is evidence which suggests they have activity at other receptors such as peroxisome proliferator-activated receptor (PPAR)-α (Devchand et al. 1996, Narala et al. 2010), purine receptors such as P2Y12 (Paruchuri et al. 2009), as well as the orphan receptors GPR17 (Ciana et al. 2006, Daniele et al. 2011) and GPR99, which has been suggested as a possible receptor for LTE_4 (Kanaoka et al. 2013).

The majority of evidence that has accumulated for the role of resolvins in the resolution of inflammation is *in vitro* across a wide range of cells including neutrophils and macrophages (see section 0), as well as fibroblasts (Qu et al. 2012, Hsiao et al. 2013), epithelial cells (Hsiao et al. 2014) and smooth muscle cells (Ho et al. 2010, Miyahara et al. 2013). RvE1 can enhance human corneal epithelial cell migration, enhancing closure in a wound healing assay (Zhang et al. 2010), and it has since been shown to promote tear production and corneal epithelial integrity (Li et al. 2010) as well as maintaining goblet cell population in a murine model of the disease (de Paiva et al. 2012). In addition, resolvins have been found to inhibit goblet cell secretion of mucins mediated by both LTs and the acetylcholine mimetic carbachol (Dartt et al. 2011) and histamine (Li et al. 2013) by preventing increases in $[Ca^{2+}]$ and ERK activation, which could have implications for chronic inflammatory diseases such as allergic conjunctivitis and dry eye disease since these feature an overproduction of mucins. In addition, these findings could have wider implications in inflammatory diseases outside of the eye in which mucins are overproduced, for example, in asthma.

Resolvins have been shown to alter ERK signalling in other situations. For example, RvD1 and RvE1 can inhibit platelet-derived growth factor (PDGF) induced proliferation of primary renal fibroblasts via inhibition of the second, prolonged phase of ERK activation.

This effect of RvE1 was abolished when the resolvin receptor ChemR23 (chemerin receptor), but not the LTB_4 receptor BLT1 (Yokomizo et al. 1997), was knocked down with siRNA (Qu et al. 2012). In a separate study, AT-RvD1 exhibited protective effects against lipopolysaccharide (LPS)-induced acute kidney injury, including inhibiting ERK phosphorylation and preventing the increase in ICAM-1 and VCAM-1 expression (Chen et al. 2014).

Adhesion molecule expression is also concentration-dependently decreased by D series resolvins in VSMCs, the overall phenotype of which was found to be altered. The proliferation, migration, and expression of pro-inflammatory genes of human saphenous vein-derived VSMCs were all shown to be reduced by resolvins D1 and D2 (Miyahara et al. 2013). Similar findings were published for RvE1 and AT-LXA_4 (Ho et al. 2010). These two studies also confirm the expression of resolvin receptors in these human saphenous vein cells, including ALX and ChemR23 (Ho et al. 2010), as well as GPR32 (Miyahara et al. 2013).

A number of recent studies have been published by the same research group presenting work that throws light on the work presented in this thesis. In the first of these studies, the authors pre-treated isolated segments of human pulmonary artery (HPA) with a range of different 'pro-inflammatory' mediators such as ET-1, TNF-α and IL-6 for 24 or 12 hours, resulting in segments of HPA that were 'hyperreactive' to the stable thromboxane mimetic, U46619. When these segments were simultaneously incubated with RvD1 (300 nM), the increased response to U46619 was abolished, and RvD1 also increased the expression of GPR32 (Hiram et al. 2014). The authors uncover CPI-17 (c-kinase potentiated protein phosphatase-1 inhibitor), TMEM16A (transmembrane protein member 16A) and MYPT-1 (myosin phosphatase target subunit 1), which have the ability to either manipulate the sensitivity of contractile machinery or modulate membrane potential, as effectors of this novel RvD1 effect on pre-treated HPA. Interestingly, they also demonstrated that the response of a segment to a single concentration of U46619 (30 nM) was unaffected in segments treated with RvD1 (300 nM), suggesting that, at this high nanomolar concentration, RvD1 can act to prevent the enhanced contractility caused by pro-inflammatory mediators and not to simply prevent contraction induced by an agonist in HPA that have not been co-treated with pro-inflammatory mediators.

The same authors then conducted a similar study with isolated human bronchial rings, this time pre-treating the segments with the cytokine IL-13 (10 ng/ml) for 48 hours to induce enhanced contraction to methacholine (Khaddaj-Mallat et al. 2015).

Simultaneous treatment with RvD1 (300 nM) inhibited the enhanced methacholine responsiveness by approximately 60%. Western blot analysis indicated that phosphorylation of CPI-17 was increased following treatment with IL-13, whilst the expression of the RvD1 receptor GPR32 was increased in the presence of RvD1. These studies provide interesting evidence for the ability of RvD1 to counteract the hyperreactivity to contractile agonists induced by pro-inflammatory mediators in isolated segments of human pulmonary artery and bronchi.

1.7.4 Docosapentaenoic acid-derived resolvins

In 2013, the Serhan laboratory identified novel resolvins derived not from EPA or DHA, but from docosapentaenoic acid (n-3 DPA) (Dalli, Colas, et al. 2013). DPA is an intermediate in the conversion of EPA to DHA, and its breakdown to novel SPMs would suggest the existence of an additional series. These molecules were reportedly produced from human leukocytes that had been incubated with DPA, and were found to demonstrate pro-resolutory roles such as dampening neutrophil recruitment to levels comparable with DHA (Dalli, Colas, et al. 2013). More recently, work by this group has demonstrated the existence of additional DPA metabolites coined RvTs and carrying an alcohol at carbon 13 (Dalli et al. 2015), rather than at carbon 17 as is the case with the previously identified 'n-3 DPA' metabolites. These RvTs were detected in healthy volunteers following exercise, as well as in sepsis patients, and their synthesis *in vitro* by the sequential actions of endothelial cells and neutrophils was inhibited by the selective COX-2 inhibitor celecoxib, suggesting a key role for this enzyme. Interestingly, they detected the production of RvTs very early on in the resolution phase of the acute inflammatory response, peaking at 4 hours, whilst other SPMs such as RvD2 and LXB_4 did not reach maximum levels until 12 hours into resolution.

1.7.5 Protectins and maresins

Like the D series resolvins, both the protectins and the maresins are enzymatically derived from DHA. Initially protectin D1 (10,17S-docosatriene) was termed neuroprotectin D1 (Mukherjee et al. 2004) owing to its abundance in the brain and neuronal cells, as well as its actions in brain ischaemia-reperfusion (Hong et al. 2003, Marcheselli et al. 2003). However, it was later renamed protectin D1 (PD1) following the realisation of the molecule's more widespread actions (Ariel et al. 2005). Whilst PD1 is not yet commercially available, its isomer protectin DX (PDX) is available (Chen et al. 2009).

Although no receptors have been formally proposed for either PD1 or PDX, that part of the ability of PDX to inhibit thromboxane-mediated platelet aggregation may be achieved directly at the thromboxane (TP) receptor (Chen et al. 2011). However, the authors used high concentrations of PDX (1 µM) to inhibit platelet aggregation, supporting the suggestion that PDX is not responsible for the reported pro-resolving actions of PD1 (Serhan, Dalli, et al. 2015). In 2010, a study investigated the binding of PD1 in a human retinal pigment cell line as well as human neutrophils, and whilst they did not identify a specific receptor responsible for the pro-resolving actions of PD1, they noted that RvE1 and LXA_4 were unable to compete with PD1 in binding assays (Marcheselli et al. 2010). This would suggest that PD1 is unable to function via either the chemerin receptor, the ALX receptor or GPR32.

The maresins (MaR or macrophage mediators in resolving inflammation) (Serhan et al. 2009, Dalli, Zhu, et al. 2013, Deng et al. 2014), are also DHA-derived and were originally believed to be exclusively biosynthesised by macrophages, since macrophages possess both of the necessary enzymes (Figure 1.9). However, in accordance with the increasing recognition of the importance of transcellular biosynthesis of lipid metabolites, MaR1 has been proposed to be synthesised from DHA through the sequential actions of platelets and neutrophils (Abdulnour et al. 2014).

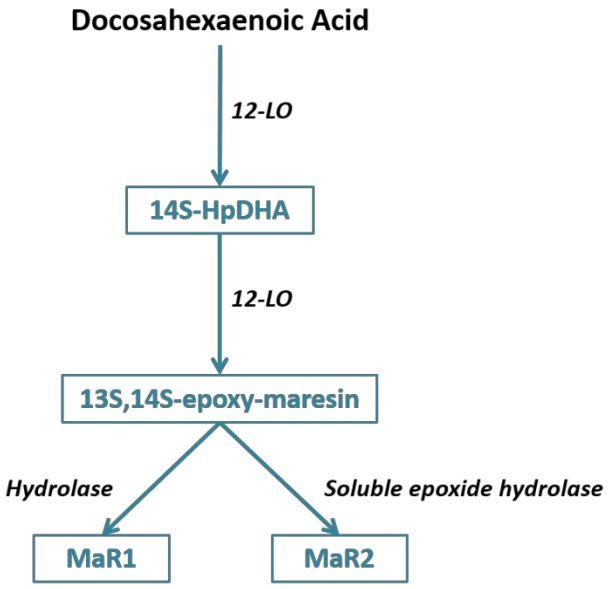

Figure 1.9: Biosynthesis of maresins. Maresins (MaR or macrophage mediators in resolving inflammation) are synthesised by macrophages through the consecutive actions of 12-lipoxygenase (12-LO) and either hydrolase to generate MaR1, or soluble epoxide hydrolase to give MaR2.

A recent study found that MaR1 is able to stimulate tissue regeneration in planaria following surgical head resection more efficiently than RvE1 at the same concentration, whilst the capsaicin-induced current of nociceptor transient receptor potential V1 (TRPV1) was inhibited by MaR1 in a concentration dependent manner (Serhan et al. 2012). Interestingly, this inhibitory activity was approximately 1000 times more potent than an existing TRPV1 antagonist, and it was blocked by the addition of pertussis toxin (PTX), which inhibits Gαi-mediated activity.

The Conte group, who have previously published studies investigating the effects of resolvins on vascular smooth muscle cells (as discussed above), recently found that MaR1 reduces monocyte adhesion to VSMC induced by the pro-inflammatory mediator TNF-α (Chatterjee et al. 2014). Treatment with MaR1 (100 nM) also mediated time-dependent increases in intracellular cAMP concentration in VSMC during the initial 30 minutes post-treatment, whilst it took 120 minutes to see similar increases in endothelial cells. Considering that PTX inhibited the effects of MaR1 in murine dorsal root ganglion cells (Serhan et al. 2012), these findings in VSMC suggest that MaR1 may act at different receptors to promote or inhibit the production of cAMP depending on the cell type. However, as yet no receptors for MaR1 or MaR2 have been proposed.

The precursor for maresin 1, termed 13S,14S-epoxy-DHA, has been found to have interesting pro-resolving roles of its own (Dalli, Zhu, et al. 2013). When leukotriene A_4 hydrolase (LTA_4H), the enzyme that converts epoxy-LTA_4 to LTB_4, was incubated with 13S,14S-epoxy-DHA, LTB_4 synthesis was inhibited by approximately 40%. Similar inhibitory effects were seen when the maresin 1 precursor was incubated with 12-LO and AA - the conversion of arachidonate to the hydroxylated intermediate 12-HETE was reduced. Interestingly, the conversion of DHA to its own hydroxylated intermediate was unaffected, indicating a selective inhibition of AA breakdown by the MaR1 precursor.

1.7.6 SPMs in tissue repair and remodelling

Wound healing and tissue repair following injury are normal processes that aid the restoration of tissues to their pre-insult state. As described in section 1.2, chronic pulmonary diseases such as asthma and PAH exhibit uncontrolled tissue repair which contributes to irreversible tissue remodelling, a key feature of these diseases (Said et al. 2010). In fact, a failure to actively resolve the acute inflammatory response, and the subsequent development of chronic inflammation, are believed to lead to organ fibrosis and loss of function, as indicated in Figure 1.4.

Tissue remodelling refers to structural and functional changes in tissue organisation. It is seen in the airways and arteries of patients with chronic pulmonary diseases including asthma and PAH (Al-Muhsen et al. 2011), and involves the combined actions of a range of cells including fibroblasts and SMCs, as well as endothelial cells and platelets in the vasculature and epithelial cells in the airways. In asthma, SMC proliferation and hypertrophy result in increased muscle mass (Figure 1.1), epithelial cells proliferate and transition into mesenchymal cells, and there is an increased number of mucin-secreting goblet cells (Pascual and Peters 2005). In addition, fibroblasts become activated, acquiring the contractile phenotype of myofibroblasts and so obtaining an increased capacity to migrate, contract and deposit extracellular matrix components including collagen (Westergren-Thorsson et al. 2010). Similar changes manifest in PAH; SMCs undergo hyperplasia and hypertrophy, fibroblasts become activated and, as the endothelium becomes dysfunctional, endothelial cells become resistant to apoptosis and proliferative (Sakao et al. 2009).

The over-activation of growth factor (GF) signalling pathways contributes significantly to tissue remodelling, and chronic lung diseases are no exception. GFs including transforming growth factor β (TGFβ) and platelet derived growth factor (PDGF) are produced by many of the cell types within the airway and vasculature and act via receptor tyrosine kinases. In both normal repair processes and chronic lung diseases, the deposition of ECM is a dynamic process, regulated in part by GFs which are thought to promote deposition, as well as matrix metalloproteases (MMP), which are able to degrade ECM (Boxall et al. 2006, Eickelberg and Morty 2007). TGFβ, which is arguably the most studied GF involved in wound repair and fibrosis, exists as three isoforms (1, 2, 3) and is secreted into the ECM in a non-active form and must be dissociated from the latent associated protein for activation. Once dissociated, the active form can act at TGFβ receptors to trigger intracellular signal transduction pathways which ultimately activate transcription factors (Hyytiäinen et al. 2004). PDGF also exists as different isoforms (PDGF-A, PDGF-B) and these are known to form homo- and heterodimers (PDGF-AA, PDGF-AB and PDGF-BB). The isoforms PDGF-C and PDGF-D have also been recognised recently; much less is known about the C and D isoforms, but they are believed to form homodimers (Heldin et al. 2002).

Given their importance in remodelling and repair, the ability of growth factors to modulate cell-mediated contraction and matrix remodelling has been studied extensively using an *in vitro* model first developed for investigating wound healing and fibroblast

function more than 35 years ago (Bell et al. 1979). The collagen lattice contraction assay has since been developed to study the behaviour of SMC and fibroblasts derived from many tissues and to study how their behaviour might be manipulated in the presence of growth factors. Dermal fibroblasts contract lattices in the absence of growth factor (Moulin et al. 1996). Myofibroblasts from patients with and without lung fibrosis and embedded in collagen lattices demonstrate constitutive contraction but the rate is increased with presence of TGFβ1 (Roach et al. 2015), whilst ASMC derived from patients with asthma were found to contract lattices significantly more effectively than ASMC from healthy volunteers, suggesting that disease status can influence the contractility of SMC (Matsumoto et al. 2007).

The intertwined contributions to wound healing and fibrosis of chronic inflammation and overactive GF signalling (Stramer et al. 2007) have led to studies of the ability of resolution agonists to modulate these processes, largely due to the discovery of the SPMs. Most recently, a 24 hour pre-treatment with LXA_4 (10 nM) was found to inhibit both constitutive contraction and TGFβ1-induced contraction of collagen lattices populated with human lung myofibroblasts (HLMF), whilst collagen secretion, α-SMA expression and serum-induced proliferation were also decreased (Roach et al. 2015). In addition, treatment with either RvD2 or LXA_4 (10-100 nM) inhibited TGFβ1-induced scratch closure in the scratch assay with mouse fibroblasts at 24 hours of the assay, but not 48 or 72 hours (Herrera et al. 2015). However, RvD1, which shares ALX and GPR32 receptors with LXA_4, was previously shown to increase the proliferation and migration rate of human periodontal ligament (PDL) fibroblasts in the scratch assay at 24 hours (Mustafa et al. 2013). The authors explain that this may initially seem counterintuitive since the enhanced migration and proliferation of cells such as fibroblasts is characteristic of fibrosis and scarring, but in the context of periodontal treatment, PDL fibroblasts are unique in that they deposit hard tissue, which aids regeneration. Given the significant contribution of remodelling to the pathogenesis of chronic lung diseases such as asthma and PAH, it is of great interest to better understand the actions that SPMs may have beyond their well-documented actions on leukocytes and to focus also on structural cells such as fibroblasts and smooth muscle cells.

1.7.7 A resolution deficit?

Many diseases previously thought to have no element of inflammation are increasingly being associated with an underlying component of uncontrolled inflammation,

including atherosclerosis (Merched et al. 2008, Viola and Soehnlein 2015) and Alzheimer's disease (Wang et al. 2014). Concomitantly, it has been suggested that chronic inflammatory diseases may arise from situations in which there is a resolution *deficit*; that is, situations in which there is inadequate availability of pro-resolving mediators. For example, the levels of PD1 in the exhaled breath condensates (EBC) of asthmatic patients experiencing an asthma attack were significantly lower in comparison to healthy individuals (Levy et al. 2007). Similarly, a study identified high levels of LXA_4 in the bronchoalveolar lavage fluid (BALF) of non-severe asthmatics compared to both healthy volunteers and severe asthmatics (Planagumà et al. 2008), whilst the severe asthmatics had significantly increased levels of CysLTs compared with healthy individuals. This could suggest that those patients who develop severe asthma have an impaired ability to produce LXA_4, which coupled with their high levels of pro-inflammatory LTD_4, indicates an overall imbalance in lipid mediators in the more severe stages of this chronic inflammatory lung disease.

The study described above by Planaguma et al (2008) supported previous findings that severe asthmatics have decreased levels of LXA_4 compared to mild asthmatics, whilst having increased levels of the inflammatory cytokine IL-8, identifying an imbalance of mediators (Vachier et al. 2005). Similar findings of a LXA_4 deficit in severe asthmatics have been reported elsewhere (Levy et al. 2005, Kazani et al. 2013). As mentioned previously, a study found that the simultaneous inhalation of LXA_4 and LTB_4 offered mild asthmatics protection from LTC_4-induced effects on airway conductance (SGaw) and expiratory flow rate at 25% of the vital capacity (V_{25}) when compared with the inhalation of LTC_4 alone (Christie et al. 1992).

The levels of SPMs in patients with COPD, a chronic lung disease characterised by chronic inflammation and irreversible airway narrowing, were recently quantified in the EBC, the BALF and the serum and compared with those of healthy volunteers (Croasdell et al. 2015). Whilst there were no significant differences in RvD1 in EBC, COPD patients have significantly lower levels of RvD1 in both BALF and serum, which is indicative of an impaired ability to produce this SPM. LXB_4 levels were also significantly decreased in the EBC from COPD patients compared with healthy volunteers. The detection of other SPMs was hindered by low levels which fell under the detection limit in this study.

In patients with peripheral artery disease (claudication or critical limb ischaemia), the circulating levels of AT-LXA_4 were significantly decreased compared to healthy controls (Ho et al. 2010). Levels of LXA_4 were also impaired in the blood of patients with localised

aggressive periodontitis, and this was coupled with an increased capacity to generate the pro-inflammatory mediator LTB_4 (Fredman et al. 2011).

There are instances of altered resolutory pathways in other chronic inflammatory diseases; for example, in Alzheimer's disease patients, increased levels of the ALX receptor were detected in glial cells (Wang et al. 2014). Somewhat surprisingly, decreased levels of its anti-inflammatory ligand LXA_4 were also detected, but the authors explain that there are pro-inflammatory ligands for the ALX receptor, which could imply an imbalance of mediators. In fact in one study analysing the levels of RvD1 and PD1 in patients with multiple sclerosis, the levels of these two mediators were actually increased in patients with a more active form of the disease compared with those whose disease was considered less active (Prüss et al. 2013). Similarly, compared to healthy volunteers, patients with sepsis were found to have higher plasma levels of resolvin and lipoxins, as well as the novel RvT 13-series resolvins (Dalli et al. 2015).

As interest in this research field grows, it is likely that more studies will be published to present the physiological levels of the various SPMs discussed in many different chronic inflammatory diseases, including asthma and PAH. Such studies would prove invaluable for identifying how 'resolution pharmacology' might be used to enhance endogenous processes that limit inflammation (Recchiuti 2013, Buckley et al. 2014). Given that this project is considering these SPMs as more than pro-resolution mediators, but also as modulators of smooth muscle contraction much like their omega-6 relatives, it is possible that inappropriate smooth muscle contraction in disease can also be targeted with agonists of resolution.

1.8 Hypothesis

The overall hypothesis of this PhD project is that specialised pro-resolving lipid mediators (SPM) may modulate the contractility of smooth muscle in rat and human airways and blood vessels, either directly or by modulating responses to known contractile agonists and growth factors.

1.9 Aims

The three specific aims of the project were:

1) To investigate whether SPM including resolvin D1, resolvin E1, lipoxin A_4 and protectin DX can alter the contraction of collagen lattices populated by human lung fibroblasts (HLF), human bronchial smooth muscle cells (HBSMC) or human umbilical artery smooth muscle cells (HUASMC), or modulate lattice contractions induced by the growth factors TGFβ1 or PDGF-AB.

2) To investigate using wire myography whether SPM including resolvin D1, resolvin D2 and resolvin E1 can modulate the constriction of intact bronchiole segments dissected from rat and human lungs and constricted with the stable acetylcholine mimetic carbachol (CCh), the stable thromboxane A_2 mimetic U46619 or the cysteinyl-leukotriene (LT)D_4.

3) To investigate (a) whether SPM including resolvin D1, resolvin D2 and resolvin E1 can modulate the constriction of intact segments of rat thoracic aorta or human pulmonary artery constricted by the alpha-1 adrenoceptor agonist phenylephrine, the thromboxane mimetic U46619 or LTD_4, using wire myography, and (b) the expression of the putative SPM receptors ChemR23, GPR32 and ALX in human pulmonary arteries and their localisation with markers of smooth muscle and other cell-types, using immunofluorescent confocal microscopy and immunohistochemistry.

Chapter 2: Materials and Methods

2.1 Human lung samples

Ethical permission exists for the use of human lung tissue resected with informed consent from patients undergoing thoracic surgery at Southampton General Hospital (Southampton & SW Hants LREC 08/H0502/32). Later in the project, tissue was also donated from patients consented under alternative ethical permission (REC Reference Number 14/SC/0186). A summary of the characteristics of the patient samples used in this thesis are shown in Table 2-1.

Functional viability	Category	No. of patients	M / F / U	Average Age (years)	Average FEV1/FVC
Unviable	Bronchiole	28	13 / 15 / 0	65.4	0.64
	Artery	1	1 / 0 / 0	58	0.78
Viable	Bronchiole	18	10 / 8 / 0	62.5	0.73*
	Artery	38	20 / 17 / 1	65.3	0.69

Table 2-1: Summary of patient sample characteristics. Human lung tissue samples were collected from the operating theatre and, if the sample was large enough to have a high probabiliy of containing artery or bronchiole segments, it was taken immediately for microdissection. Approximately equal numbers of male (m) and females (f) were donated in this project, although the notes for one patient was unavailable so their gender is unknown (U). Lung function data for recruited patients is also available, including forced expiratory volume (FEV1) and forced vital capacity (FVC). On 28 occasions, the bronchiole segments isolated were mounted but completely failed to respond to potassium-physiological salt solution (KPSS), and these were deemed functionally-unviable. These patients had an average age of 65.4 years and an average FEV1/FVC ratio of 0.64. On 18 occasions, bronchiole segments isolated from human lung samples were found to be functionally-viable. These bronchioles were isolated from samples donated by patients who were 62.5 years on average and had a FEV1/FVC ratio of 0.73. A Student's t test suggests that there is a significant difference between the FEV1/FVC ratio of the patients from which functionally-unviable bronchiole segments were isolated and the ratio of patients from which the functionally-viable bronchiole segments originated ($p<0.05$). On one occasion, an artery isolated from a patient with an FEV1/FVC ratio of 0.78 failed to constrict in response to KPSS, whilst on 38 occasions, the arteries isolated responded positively to KPSS. These 38 patients had an average age of 65.2 years and an FEV1/FVC ratio of 0.69.*

Information on patient age, gender, lung function, smoking status and medications is also available. Lung function data includes forced expiratory volume in 1 second (FEV1) which is the volume of air that can be expelled from maximum inspiration in 1 second, as well as forced vital capacity (FVC), which is the volume of air that can be expelled during

a forced breath. Lung tissue samples from consented patients undergoing thoracic surgery were collected from the surgical theatre in PBS at room temperature once removed from the patient.

2.2 Human pulmonary artery and bronchiole isolation

Samples of human lung lobe were received and pinned out on a dissection dish. Bronchioles and vessels were located and cut free of surrounding parenchyma in preparation for mounting on the wire myograph.

2.3 Rat bronchiole isolation

Wistar rats (Charles River, UK or in-house stock) weighing 200–300 g were culled according to the Home Office Schedule One procedure, that is, by a rising concentration of carbon dioxide and cervical dislocation, after which their lungs were removed. The lungs were then pinned out on a dissection dish containing calcium-free physiological salt solution (PSS) and, under a light microscope, forceps and scissors were used to cut away the surrounding tissue starting at the trachea to expose the bronchioles in the left lung. The same bronchiole segments were removed from each rat and placed into a smaller dissection dish containing calcium-free PSS. Any remaining parenchyma was removed from the segments in preparation for mounting. Each segment was approximately 1.5 mm in length and 350-400 μm in width.

2.4 Rat thoracic aorta isolation

Wistar rats (Charles River, UK, or in-house stock) weighing 200-300 g were culled according to the Home Office Schedule One procedure and their thoracic aorta removed. The aorta was carefully cleaned of any surrounding tissue and cut into 2 mm segments, with a lumen diameter of approximately 800 μM.

2.5 Wire myography

The basis of this experimental technique is to isolate and mount bronchiole and vessel segments so that reagents can be tested under physiological conditions for their relative potency, efficacy and time-course to induce constriction or dilation directly, or to modulate responses to other agents.

Ideally wire myography should be carried out as soon as possible after tissue arrival from the Pathology department in the case of human tissue or, in the case of rat lungs, immediately after removal from the animal.

2.5.1 The wire myograph system

A Danish Myo Technology (DMT) multi wire myograph system 610 was used to carry out all experiments (Figure 2.1). The system has four chambers, permitting the study of four bronchiolar or vascular segments simultaneously. There are two types of chamber, one type with two jaws and the other with two pins. In each type of chamber one jaw/pin is static and attached to a force transducer and the other jaw/pin is attached to a mobile micrometer.

Figure 2.1: The wire myograph system. A Danish Myo Technology (DMT) multi-wire myograph was used to generate contractile data from vessels and segments throughout this project. Image taken with permission from DMT.

The chambers are heated, allowing the mounted segments to be submersed in PSS at a physiological temperature of 37°C. A thermometer probe was used to check the temperature of the buffer in the chambers before beginning any experiments. Chambers were gassed with 95% O_2 and 5% CO_2 via tubing that is integrated within the wire myograph machine itself. A chamber cover was placed over the bath to aid draining, refilling and gassing, and to reduce heat loss. Chamber volume reducers were used to

reduce the chamber volume from 5 ml to 3 ml, thus reducing the amount of reagents being required for each experiment.

2.5.2 Segment mounting on jaws

Bronchiolar segments were mounted on jaws (Figure 2.2), while segments of aorta and human pulmonary artery, which have a wider diameter, were mounted on pins (Figure 2.3). Each of the four chambers can be separated from the main equipment and placed under a microscope to allow the bronchiolar segments to be mounted using wires (Figure 2.2). The wires are 40 µm thick and approximately 3 cm long.

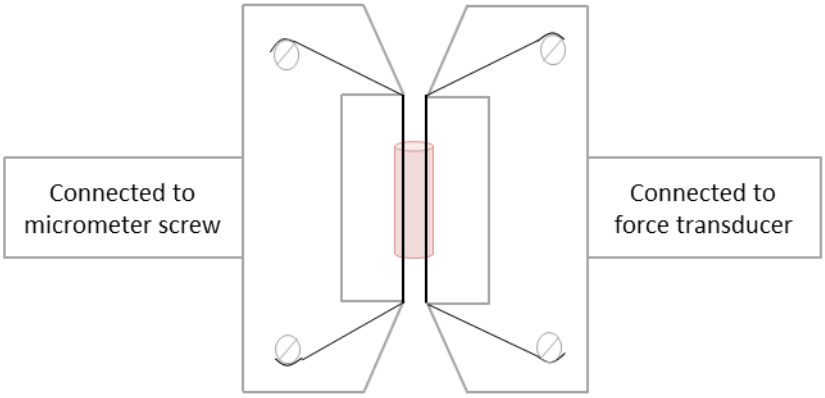

Figure 2.2: Bronchiolar segments were mounted on jaws on the wire myograph using wires (approx. 3 cm x 40 µm) as shown. The first piece of wire was secured to the jaw inside the myography chamber containing physiological salt solution, and the wire carefully passed through the lumen of the bronchiolar segment before being secured. The second piece of wire was then passed through the lumen of the segment and both ends secured to the jaw.

The first piece of wire was secured underneath the top screw of the static jaw. The chamber was then filled with PSS, the segment placed into the chamber and the wire passed through the lumen of the segment (Figure 2.2). The wire was pulled taut and the free end secured beneath the bottom screw of the static jaw. The second wire was then passed through the lumen of the segment and secured underneath the top screw of the mobile jaw, pulled taut and secured underneath the bottom screw of the mobile jaw. Each chamber was individually connected to feed information to the Powerlab system (ADInstruments), which converts the data so that it is readable on LabChart (version 5) and LabChart Reader (version 8) (ADInstruments) software on the computer.

2.5.3 Mounting of vascular segments on pins

Segments of rat thoracic aorta and human pulmonary artery were mounted onto pins by simply sliding them on (Figure 2.3).

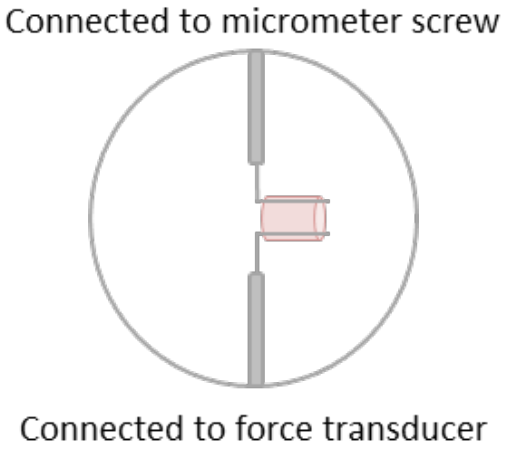

Figure 2.3: Segments of rat thoracic aorta or human pulmonary artery were mounted onto pins inside the myograph chamber. The chamber was filled with physiological salt solution and the segment simply slid on to the pins.

2.5.4 Baseline tension

A baseline tension was set by increasing tension incrementally from 0 g to 1.5 g. The elastic properties of the vessels and bronchioles meant that the tension required 'topping up' back to 1.5 g periodically until the tension stabilised. The purpose of the baseline tension was to ensure that the segments were held taut on the jaws/pins so that the addition of a contractile agonist could be measured as a change in tension. If the segments were loose on the jaws/pins then any contraction might not be picked up by the transducer, thus giving inaccurate measurements of changes in tension.

2.5.5 Functional integrity

Given that the dissection of the segments and their mounting was a complex process taking at least 1 hour, the segments did not always function well once mounted. Their response to 125 mM potassium physiological salt solution (KPSS) was therefore used as an indicator of whether a segment was functional and likely to respond to the addition of a lipid agent or drug (as described previously in Pike et al. 2014). At this concentration of KPSS, there is an equimolar substitution of the sodium ions with the potassium ions which

maintains osmolarity. KPSS can elicit an increase in tension because the potassium ions depolarise the smooth muscle cell (SMC) membrane, which opens voltage-gated calcium channels. This results in an influx of calcium ions into the SMC, which induces constriction of the vessels or airway.

The PSS was drained from the four chambers simultaneously by the vacuum pump connected in parallel to each chamber. Three ml of 125 mM KPSS that had been warmed in a water bath to 37°C were then added to each chamber with a 20 ml syringe. The LabChart software permitted information such as reagent concentration to be recorded on the chart. A stopwatch was used to time a 2 minute period. Any change in tension induced by the KPSS was measured by the force transducer and outputted onto the Lab Chart software as an upward change in tension. Agonist-induced constrictions were subsequently calculated as percentages of the maximum contraction induced by 125 mM of KPSS to normalise the response from each segment.

2.5.6 Experimental designs

To fully investigate the ability of resolvins to modulate the contractility of intact bronchioles and vessels using the wire myograph, a number of experimental designs were implemented and they differ for each chapter. A full description of the experimental designs is provided in the protocol section at the beginning of each chapter, but the general methods are described below.

2.5.7 Constructing cumulative concentration-response curves

Cumulative concentration-response curves (CCRC) have been used extensively throughout this thesis. To a chamber containing PSS a volume of the stock concentration of agonist was added using a Gilson pipette to produce the desired final concentration bathing the bronchiole or artery in the chamber. The response was recorded by LabChart for two minutes, after which the next volume of agonist was added to cumulatively increase the concentration of agonist inside the chamber. Note that some agonists, particularly lipid mediators like thromboxane, are slow acting and therefore can take longer than two minutes to exert their full effect. In this case, the next concentration of agonist was not introduced to the chamber before a plateau had been achieved. The addition of each concentration of agonist was recorded on the LabChart trace so that the resulting tension after each agonist incubation could be recorded in an Excel spreadsheet.

2.5.8 Determining EC_{80} for pre-constriction

To determine whether resolvins could relax airway or blood vessel segments, pre-constriction experiments were carried out in which segments were submaximally constricted and then incubated with resolvin. Submaximal constriction was achieved by constricting the segments to 80% of the maximum constriction (EC_{80}), which meant that if the segment were to relax visualisation would be possible but also that there is scope for any increase in tension to be seen.

The EC_{80} is calculated by first constructing a whole CCRC and then interpolating the concentration of agonist required to constrict the segment by 80% of the maximum. After the segments were washed with PSS to restore baseline tension, the calculated EC_{80} concentration of agonist is added to the chamber to produce a submaximal response and allowed 10 minutes to reach a plateau.

2.6 3D collagen lattice contraction assay

Wound healing involves re-epithelialisation by the proliferation of epithelial cells, deposition of collagen by fibroblasts, and contraction by myofibroblasts and other contractile cells to close the wound site (Martin 1997). Collagen lattice contraction assays have been used extensively to study the factors that regulate the contractile aspects of wound healing (Bell et al. 1979). In this thesis, 3D collagen lattice contraction assays were used to explore the effects of resolvins on growth factor-induced contraction in three cell types – human lung fibroblasts, human bronchial smooth muscle cells, and human umbilical artery smooth muscle cells, details of which are given below.

The protocol used for the collagen lattice contraction assay is similar to the methods used in published studies (Matsumoto et al. 2007, Horie et al. 2014), but was then further developed by a colleague. To optimise the efficiency of the protocol, a number of optimisation experiments were carried out and are discussed further in Chapter 3. Below a basic description of the steps to create the cell-populated collagen lattices is given.

Cells were detached from the flask and counted using a haemocytometer. To create the collagen lattices, a ratio of 7 parts rat tail collagen type 1 (Millipore, UK), 1 part newborn calf serum (NCS) (Life Technologies, UK), 1 part 10X Dulbecco's modified Eagle's medium (DMEM) (Sigma Aldrich, UK) and 1 part cell suspension in complete DMEM (GE Healthcare Life Sciences, UK) were carefully mixed so as to avoid the

introduction of bubbles. The mixture was neutralised with 0.2 M NaOH. The rat tail collagen type 1, the 10X DMEM and the NCS were all kept cool on ice. Once thoroughly mixed, 0.5 ml of the suspension was pipetted into each well of a 24-well plate, which was then placed immediately into an incubator (37°C, 95% air/5% CO_2) for 1 hour to allow the collagen lattices to set. The lattices were lifted from the plate using a sterile needle and floated into 60 mm petri dishes (Greiner Bio One, UK) containing media ± treatment.

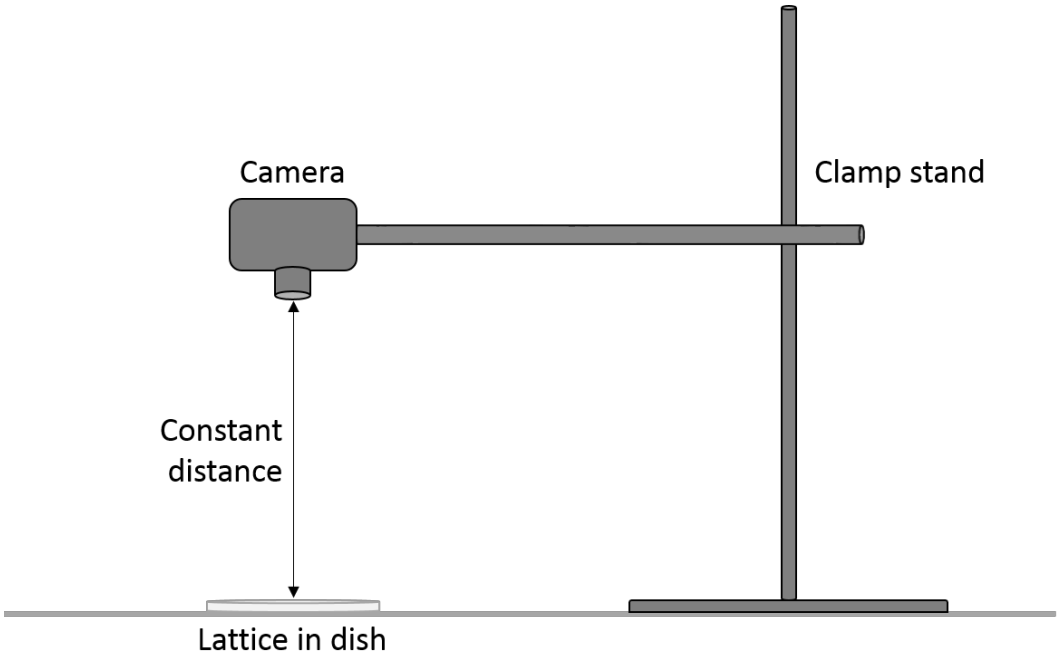

Figure 2.4: Images of cell-populated lattices were captured with a Canon PowerShot A480 digital camera. By securing the camera to a clamp stand, the distance between the camera lens and the lattice remained constant through the 24 hour time points, allowing accurate recording of the area of the lattice.

Images of the lattices floating in the petri dishes were taken at time 0, and then at given time points, using a Canon PowerShot A480 digital camera attached to a clamp stand so as to maintain a consistent distance between the camera lens and the dish (Figure 2.4). The size of the area of the floating collagen lattice was measured using the 'region of interest' tool on Image J software (National Institute of Health, USA).

2.6.1 Growth factor-induced contraction of collagen lattices

Collagen lattices populated with cells contract at a quicker rate in the presence of some growth factors. Transforming growth factor β1 (TGFβ1) (Peprotech, UK) or platelet-derived growth factor-AB (Millipore, UK) was added to the medium in which the collagen lattices were floating in the petri dish to induce contraction of the cell-populated collagen

lattices. The PDGF protein used was comprised of one PDGF-A peptide and one PDGF-B peptide dimerised *in vitro*.

2.7 Cell culture

Three types of primary human cells were grown and used in the 3D collagen lattice contraction assay. Human lung fibroblasts (HLF) and human umbilical artery smooth muscle cells (HUASMC) were grown in-house from human donor tissue samples, whilst the human bronchial smooth muscle cells (HBSMC) were purchased from PromoCell.

2.7.1 Human lung fibroblasts

Human lung fibroblasts were grown from human lung samples obtained from consented patients undergoing thoracic surgery at Southampton General Hospital. Fragments of parenchyma were cut and placed in a 6-well plate, washed with Hanks balanced salt solution (HBSS) (Life Technologies, UK) and then cultured in DMEM supplemented with L-glutamine, penicillin, streptomycin, sodium pyruvate and non-essential amino acids (all GE Healthcare Life Sciences, UK) at 37°C with 95% air and 5% CO_2. HLF were allowed to migrate out from the tissue fragments, and upon 90% confluency were upgraded from 6-well plates to T25 flasks, and then to T75 flasks. HLFs were used between passages 3-6. For the purpose of the collagen lattice contraction assay, only HLF obtained from patients with a GOLD (Global Initiative for Chronic Obstructive Lung Disease) status of 0 as determined by spirometry, or from patients undergoing bullous repair surgery predicted to have healthy lung function were used.

2.7.2 Human bronchial smooth muscle cells

Cryopreserved human bronchial smooth muscle cells (HBSMC) which had been isolated from the bronchi of a single normal human donor were purchased from PromoCell and revived according to PromoCell's instructions using PromoCell smooth muscle cell growth medium 2. Cells were expanded before being resuspended in 90% human serum/10% DMSO and aliquoted for cryopreservation in liquid nitrogen. When required, an aliquot was removed from storage in liquid nitrogen and rapidly defrosted using warm (37°C) PromoCell smooth muscle cell growth medium 2. The cells were grown in a T75 flask until near confluent at which point they were used in the collagen lattice contraction

assay. Experiments by PromoCell suggested that these HBSMC stained positive for α-smooth muscle actin and negative for CD90.

2.7.3 Human umbilical artery smooth muscle cells

Human umbilical artery smooth muscle cells (HUASMC) were grown as described in (Churchman and Siow 2009). Human umbilical cords were obtained from the Broadland ward, Princess Anne Hospital, Southampton, UK, from non-complicated vaginal births according to ethics approved by the Local Research Ethical Committee (LREC) Ref: 07/H0502/83. Human umbilical cords contain one vein and two arteries.

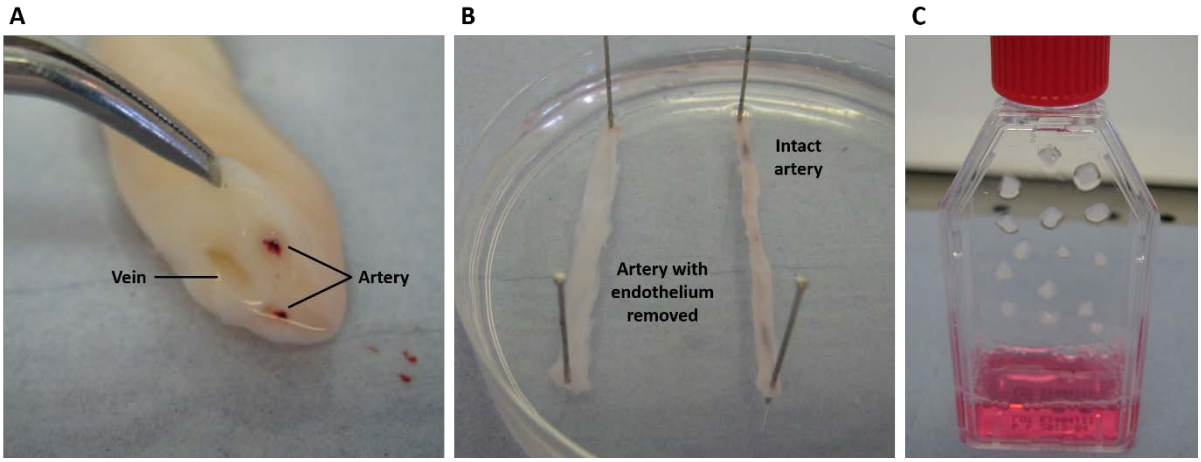

Figure 2.5: Isolation and culture of human umbilical artery smooth muscle cells. (A) The human umbilical artery was isolated from the cord and cleaned of surrounding Wharton's jelly. (B) The intact artery was cut open longitudinally and the endothelium removed using a sterile razor blade. (C) Fragments of the artery were then placed lumen-side down on a collagen-coated T25 flask. The fragments were coated in DMEM-F12 and the flask kept upright in an incubator for 2-4 hours, after which it was lowered to the horizontal to submerge the fragments in medium.

For the purpose of growing human umbilical artery smooth muscle cells, one of the arteries was isolated and cleaned of surrounding Wharton's jelly and connective tissue. The artery was the pinned out on a dissection dish and cut open longitudinally so that the endothelium could be carefully scraped away using a sterile razor blade. The artery was then cut into fragments approximately 1 cm^2 and placed lumen-side down on a collagen-coated (1%) (Millipore, UK) T25 flask. Using a Pasteur pipette, the fragments were coated with DMEM-F12 (Life Technologies, UK) supplemented with L-glutamine, penicillin, streptomycin and non-essential amino acids. The 1:1 combination of DMEM and Ham's F-12 nutrient mixture is routinely used for culturing smooth muscle cells. The flask was

placed upright in the incubator (37°C, 5% CO_2) for 2-4 hours, permitting the fragments to adhere to the flask.

The flask was then carefully lowered onto its side so that the fragments would be covered in DMEM-F12, and were checked every two days for infections or tissue fragments which had become loose. Two T25 flasks were set up for each artery and then pooled to ensure enough cells were obtained.

After approximately three weeks, once enough cells had migrated out of the tissue fragments, the fragments were removed from the two T25 flasks and the cells detached from the flask using Tryple express (Life Technologies, UK). Cells were pooled and then centrifuged at 5000 rpm for 5 minutes at 4°C, before resuspending the pellet in PromoCell smooth muscle cell growth medium 2. The HUASMC were seeded into three new T25 flasks and grown in PromoCell smooth muscle cell growth medium 2 until near confluency. The cells in the three T25 flasks were pooled and re-seeded into two T75 flasks. HUASMC were used in the collagen lattice contraction assay up to passage 6. The HUASMC grew much better when grown in PromoCell smooth muscle cell growth medium 2, but this medium does not contain antibiotics so was not used during the explant stages.

2.8 Immunohistological staining

2.8.1 Fixing and embedding tissue samples

Tissue was fixed in 10% neutralised buffered formalin (Leica Microsystems, UK) for 24 hours at room temperature. The fixed samples were processed and embedded in paraffin by staff in the Immunohistochemistry (IHC) Unit at the University of Southampton.

2.8.2 Sectioning paraffin-embedded human tissue samples

The paraffin-embedded human tissue samples were sectioned on a microtome at 4 μm thickness and mounted on glass slides. The slides were then placed into an oven for 24 hours.

2.8.3 Deparaffinisation of tissue sections

Slides were placed into a rack and into clearene for 2 x 5 minutes, and then rehydrated through graded alcohol solutions for 5 minutes.

At this point, the sections could be used in the protocol for staining with immunofluorescence or with an AEC chromogen, which are described below.

2.8.4 Immunofluorescent staining of human pulmonary artery sections for Von Willebrand factor, α-smooth muscle actin and nuclei

Sections were permeabilised with 0.1% triton X (Santa Cruz Biotechnology, USA), 1% bovine serum albumin (BSA) (GE Healthcare Life Sciences, UK) diluted in PBS for 15 minutes.

Sections were washed and covered with a primary antibody (rabbit host) against Von Willebrand factor (Dako, UK) diluted in 0.1% triton X, 1% BSA in PBS (1:200) for 60 minutes at room temperature. This primary antibody was then stained with a $F(ab')_2$ fragment of goat anti-rabbit IgG tagged with CF488A secondary antibody (Biotium, USA) diluted in 0.1% triton X, 1% BSA in PBS (1:500) for 60 minutes at room temperature.

Sections were washed and covered with a primary antibody (mouse host) against α-smooth muscle actin (Abcam, UK) diluted in 0.1% triton X, 1% BSA in PBS (1:100) for 60 minutes at room temperature. This primary antibody was then stained with an AlexaFluor 555 secondary antibody (donkey anti-mouse) (Abcam, UK) diluted in 0.1% triton X, 1% BSA in PBS (1:500) for 60 minutes at room temperature.

Sections were washed and covered with DAPI (1:500) (Sigma Aldrich, UK) diluted in 0.1% triton X, 1% BSA in PBS for 15 minutes at room temperature.

A small volume of mounting solution was place on a coverslip and the slide lowered on to the solution. The mounting solution consists of Mowiol 4-88 powder (Harco Chemical Company, Belgium), glycerol and antifade (Citifluor Ltd, UK) in PBS. The slides were left to dry overnight at 4◦C.

2.8.5 AEC chromogen staining of human pulmonary artery sections for pro-resolving mediator receptors

Endogenous peroxidase activity was inhibited with 0.5% hydrogen peroxide in methanol for 10 minutes. Following washes with tris-buffered saline (TBS), heat-mediated antigen retrieval was performed in order to break the bonds formed across the antigenic sites during tissue fixation. The sections were heat-treated by microwaving in citrate buffer (0.01 M, pH 6.0) for 25 minutes.

The sections were covered in avidin solution (part of a kit from Vector Laboratories, USA) for 20 minutes at room temperature, washed with TBS, and then covered in biotin solution (Vector Laboratories, USA) for a further 20 minutes at room temperature. The sections were washed with TBS and then blocked with in-house culture blocking medium (containing DMEM, NCS and BSA) for 20 minutes at room temperature, which blocks epitopes on the sample and minimise non-specific binding.

The slides were drained of culture blocking medium and the sections covered with either the primary antibody diluted in TBS, the rabbit IgG polyclonal isotype control antibody (Abcam, UK) diluted in TBS, or TBS only. The primary antibodies used here against the chemerin receptor (1:100), GPR32 receptor (1:400) and the ALX receptor (1:500) were all from a rabbit host (all Abcam, UK). The sections were incubated overnight at 4◦C. Note that the antibody for the ALX receptor is stored in whole serum so an isotype control was not carried out when staining for this receptor.

The slides were washed with TBS before the biotinylated secondary antibody (swine anti-rabbit) was applied for 30 minutes at room temperature. The sections were washed again with TBS and the avidin-biotin peroxidase complex applied for 30 minutes at room temperature.

The slides were washed with TBS and the AEC chromogen applied to the sections for 10 minutes at room temperature. After further TBS washes, the sections were counterstained with Mayer's haematoxylin (Acros organics, UK) for 1 minute at room temperature. The slides were placed under running water for 5 minutes to turn the haemotoxylin stain blue in colour.

Aqueous mounting medium (Bio-Rad, UK) was applied evenly to the sections and they were baked at 80◦C for 20 minutes. Once cooled, the sections were mounted with coverslips. To do this, a small volume of Pertex mounting solution (Histolab, Germany)

was placed on a coverslip, and the slide carefully lowered onto the coverslip. The slides were then left overnight to dry at room temperature.

2.8.6 Staining 3D collagen lattices

The 3D collagen lattice gels were stained to image the interaction between collagen fibres in the lattice and the cells. The lattices were fixed in 4% paraformaldehyde (PFA) (Sigma Aldrich, UK) for 24 hours at room temperature before being stored at 4°C in PBS. Prior to staining, the lattices were permeabilised in 0.1% triton X, 1% BSA in PBS for 30 minutes at room temperature.

2.8.7 Staining lattices with TRITC-phalloidin

Tetramethylrhodamine (TRITC)-phalloidin (Sigma, UK) is a fluorescently labelled toxin that binds to filamentous actin. Square sections of the lattices were placed in the well of a 48-well plate and submersed in TRITC-phalloidin (1 μM) diluted in 0.1% triton X, 1% BSA in PBS for 30 minutes at room temperature. Plates were placed on a shaker for the duration of the incubation period to ensure the lattice was evenly stained.

2.8.8 Staining lattices for collagen type I

Lattices were placed in the well of a 24-well plate and submersed in a primary antibody (host rabbit) for collagen type I (1:500) diluted in 0.1% triton X, 1% BSA in PBS for 60 minutes at room temperature. Plates were placed on a shaker for the duration of the incubation period to ensure the lattice was evenly stained. This primary antibody was then stained with a $F(ab')_2$ fragment of goat anti-rabbit IgG tagged with CF488A secondary antibody diluted in 0.1% triton X, 1% BSA in PBS (1:500) for 60 minutes at room temperature. Plates were placed on a shaker for the duration of these incubation periods to ensure the lattice was evenly stained.

2.8.9 Staining lattices with DAPI

Lattices were placed in the well of a 24-well plate and submersed in DAPI diluted in 0.1% triton X, 1% BSA in PBS for 15 minutes at room temperature. Plates were placed on a shaker for the duration of the incubation period to ensure the lattice was evenly stained.

2.8.10 Growing cells on coverslips

To confirm that the cells isolated from human umbilical cords were arterial smooth muscle cells, cells were grown on coverslips ready to be stained for α smooth muscle actin.

Coverslips were sterilised with 70% ethanol and then washed in PBS. The coverslips were then coated in 1% BSA in PBS for 60 minutes. Cells were seeded into the plate at the desired density in complete DMEM with 10% NCS and left overnight in the incubator (37°C, 95% air/5% CO_2) to adhere to the coverslip.

2.8.11 Fixing and permeabilising cells on coverslips

The cells were washed with PBS and then fixed with 4% PFA for 30 minutes. The cells were then permeabilised with 0.1% triton X, 1% BSA in PBS for 30 minutes.

2.8.12 Staining cells for α-smooth muscle actin

Fixed cells on coverslips in the plate were covered with a primary antibody for α smooth muscle actin (mouse host) diluted in 0.1% triton X, 1% BSA in PBS for 60 minutes (1:100) at room temperature. Following washes with PBS, the primary antibody was then stained with an AlexaFluor 555 secondary antibody (donkey anti-mouse) (Abcam, UK) diluted in 0.1% triton X, 1% BSA in PBS (1:500) for 60 minutes at room temperature.

2.8.13 Staining cells for DAPI

Coverslips were stained with DAPI (1:500) diluted in 0.1% triton X, 1% BSA in PBS for 15 minutes at room temperature.

2.8.14 Mounting the coverslips on to slides

A small volume of mounting solution was placed on a slide and the coverslip lowered on to the solution, being careful to make sure the side with cells was face down on the slide. The mounting solution consists of Mowiol 4-88 powder (Harco Chemical Company, Belgium), glycerol and antifade (Citifluor Ltd, UK) in PBS. The coverslips were left to dry overnight at 4◦C.

2.9 Microscopy

2.9.1 Confocal laser scanning microscopy

Cells and tissue sections fluorescently labelled were imaged on a Leica TCS (true confocal scanning) SP5 confocal laser scanning microscope with the kind expertise of David Johnston (Biomedical Imaging Unit, University of Southampton). This microscope can scan the samples in single slices, or scan several slices in sequence and stack them in the Z plane to generate 3D image stacks, with both methods producing high resolution images with up to five channels simultaneously. A number of different fluorophores (Table 2-2) were used in the various fluorescent staining protocols (see section 2.8).

Name	**Laser line**	**Excitation max (λ)**	**Emission max (λ)**
AlexaFluor 488	488	480	525
AlexaFluor 555	488/532	555	580
TRITC	532	557	576
DAPI	405	350	470

Table 2-2: Fluorophores used in fluorescent staining protocols. A number of different fluorophores were used for confocal microscopy enabling the simultaneous imaging of several cell markers.

Leica application suite-advanced fluorescence (LAS-AF) (version 2.5.1) software was used to capture and view confocal images. When generating images of the cell-populated collagen lattices the number of slices taken varied to ensure a similar number of cells were present in the image for each treatment and time point. On average of 88 slices were taken and stacked to create images that illustrated the interaction between cells and their environment. Images of cells grown on coverslips were generated from just a single slice.

2.9.2 dotSlide microscopy

Tissue sections stained with an AEC chromogen were imaged on an Olympus dotSlide system which generates an overview (X20) of the entire slide so as to create a virtual slide. From the overview, the tissue section could be selectively outlined and

scanned at the higher magnification of X200 so as to generate a high quality magnified version of the tissue section.

2.9.3 Phase contrast microscopy

Cells in culture were imaged using an Olympus CKX41 inverted phase contrast microscope equipped with a JVC camera attachment at X40 initial magnification.

2.10 Chemicals and reagents

2.10.1 Physiological salt solution

Physiological salt solution (PSS) consisted of the following (mM) dissolved in distilled water: NaCl, 119; KCl, 4.7; $CaCl_2$, 2.5; $MgSO_4$, 1.17; $NaHCO_3$, 25; KH_2PO_4, 1.18; EDTA, 0.026; and D-glucose, 5.5 (all Sigma Aldrich). PSS was used throughout once the bronchioles were mounted on the wires.

2.10.2 Calcium-free physiological salt solution

Calcium-free PSS was used during bronchiole dissection and mounting. It consisted of the same components as PSS with the exception of $CaCl_2$.

2.10.3 Potassium physiological salt solution

The composition of the potassium PSS (KPSS) used was PSS (section 2.10.1) with an equimolar substitution of KCl for NaCl.

2.10.4 Tris-buffered saline

Tris-buffered saline (TBS) was made by the technical staff in the immunohistochemistry unit (see acknowledgements).

2.10.5 Phosphate-buffered saline

Phosphate-buffered saline (PBS) (Oxoid) was made by dissolving 10 tablets in 1 litre of reverse osmosis water.

2.10.6 Specialised pro-resolving mediators

All specialised pro-resolving mediators (SPM), including resolvin E1, resolvin D1, resolvin D2, lipoxin A_4 and protectin DX were supplied by Cayman Chemicals (Ann Arbor, USA), and distributed via Cambridge Bioscience, UK. Initially DMSO (Sigma Aldrich) was used for the long term storage of the omega-3 lipids listed below. However, the supplier, Cayman Chemicals, changed their recommendations in 2014, suggesting that the omega-3 lipids be 'stored and handled in ethanol solution'. As a result, new resolvins and LTs were purchased and diluted in ethanol rather than DMSO. Throughout the experiments, no difference in activity has been seen between those lipids dissolved in DMSO and those lipids dissolved in ethanol.

All SPMs were stored in aliquots in a -80◦C freezer. On the day of use, SPMs were futher diluted in aqueous solutions (PSS or media depending on the experiment) and discarded after use.

Table 2-3: The common and chemical names of the specialised pro-resolving mediators used within this thesis.

Common name	Chemical name
Resolvin D1	7(S),8(R),18(S)-trihydroxy-4Z,9E,11E,13Z,15E,19Z,-DHA
Resolvin D2	7(S),16(R),17(S)-trihydroxy-4Z,8E,10Z,12E,14E,19Z-DHA
Resolvin E1	5(S),12(R),18(R)-trihydroxy-6Z,8E,10E,14Z,16E-EPA
Lipoxin A_4	5(S),6(R) lipoxin A_4 methyl ester
Protectin DX	10(S),17(S)-DiDHA

2.10.7 Leukotriene D_4

Leukotriene D_4 (LTD_4) (5)S-hydroxy-6(R)-(S-cysteinylglycinyl)-7E,9E,11Z,14Z-eicosatetraenoic acid) (Cambridge Bioscience, UK) was diluted in ethanol and stored in aliquots in a -80◦C freezer. On the day of use, LTD_4 was futher diluted in aqueous solution (PSS) and discarded after use.

2.10.8 U46619

U46619 (9,11-dideoxy-9α,11 α-methaoepoxy-prosta-5Z,13E-dien-1-oic acid) (Cambridge Bioscience, UK) is a stable thromboxane mimetic and was delivered diluted in methyl acetate. To change the solvent, the methyl acetate was evapourated off under nitrogen and then rediluted in DMSO.

2.10.9 Carbachol

Carbachol (CCh) (Sigma-Aldrich) was supplied as a white powder that was dissolved in PSS to produce a stock concentration of 100 mM which was stored in a -20◦C freezer. Immediately prior to performing biological experiments the CCh was removed from the freezer to thaw and then used immediately. Any unused CCh from a given aliquot was discarded once thawed.

2.10.10 Phenylephrine hydrochloride

The alpha-1 adrenoceptor agonist, phenylephrine hydrochloride (PE), was used to constricted rat aorta segments. PE (Sigma-Aldrich) was supplied as a white to off-white powder that was dissolved in PSS to produce a stock concentration of 100 mM, which was stored in a -20◦C freezer. Immediately prior to performing biological experiments the PE was removed from the freezer to thaw and then used immediately. Any unused PE from a given aliquot was discarded once thawed.

2.10.11 Acetylcholine chloride

The muscarinic acetylcholine receptor agonist, acetylcholine chloride (ACh), was used to relax rat aorta segments. ACh (Sigma-Aldrich) was supplied as white to white with a faint yellow cast powder that was dissolved in PSS to produce a stock concentration of 100 mM, which was stored in a -20◦C freezer. Immediately prior to performing biological experiments the ACh was removed from the freezer to thaw and then used immediately. Any unused ACh from a given aliquot was discarded once thawed.

2.10.12 Atropine

Atropine (Sigma Aldrich) was supplied as a white powder that was dissolved in PSS to produce a stock concentration of 100 mM which was stored in a -20◦C freezer. Immediately prior to performing biological experiments the atropine was removed from

the freezer to thaw and then used immediately. Any unused atropine from a given aliquot was discarded once thawed.

2.10.13 Salbutamol

Salbutamol (Sigma Aldrich) was supplied as a white/yellow powder that was dissolved in PSS to produce a stock concentration of 100 mM, which was stored in a -20◦C freezer. Immediately prior to performing biological experiments the salbutamol was removed from the freezer to thaw and then used immediately. Any unused salbutamol from a given aliquot was discarded once thawed.

2.10.14 Montelukast

Montelukast (sodium salt) (Cayman Chemicals, Ann Arbor) was supplied as a crystalline solid which, upon arrival, was diluted in DMSO to give a stock concentration of 100 mM. This stock was then stored in a -20◦C freezer. Immediately prior to performing biological experiments, the required volume of montelukast (sodium salt) was diluted in PSS. Such aqueous solutions were used on the day of preparation.

2.10.15 Cytochalasin D

Cytochalasin D (Sigma-Aldrich) was diluted in DMSO and stored in a -20◦C freezer.

2.11 Statistical analyses

Where there are two concentration-response curves on the same graph, or two or more time-response curves on the same graph, a two-way repeated measures analysis of variance (ANOVA) has been performed. In a small number of cases where there are missing data points or the data are unpaired, a two-way ANOVA without repeated measures has been performed and this is stated in the applicable places. There is no recognised non-parametric equivalent of a two-way ANOVA.

Data that are shown grouped in columns have been assumed to be non-parametric and thus analysed using a Friedman test with Dunn’s multiple comparisons, or where the data is not paired, a Kruskal-Wallis test with Dunn’s multiple comparisons.

Where there are only two groups to compare, the data have been assumed to be non-parametric and a Wilcoxon matched-pairs signed rank test has been performed.

All statistical analyses have been carried out on GraphPad Prism version 6.

Chapter 3: Effect of specialised pro-resolving mediators on spontaneous and growth factor-induced contraction of collagen lattices

3.1 Background

Wound healing requires epithelial proliferation, collagen deposition, and contraction of the wound site by myofibroblasts and other contractile cells. These processes are regulated by complex interactions between growth factors and other mediators. The ability of resolvin E1 to promote re-epithelialisation in a corneal wound healing model (Li et al. 2010, Zhang et al. 2010) was described in section 1.7.3 but little is known about the effects of resolvins and other SPM families in other aspects of wound healing, in other cell types or in other models. That said, two very recent papers have identified potential roles for both LXA_4 and RvD2 in wound healing and attenuating fibrosis using both a scratch assay and the collagen lattice contraction assay to investigate fibroblasts (Herrera et al. 2015, Roach et al. 2015).

Collagen lattice contraction assays were first described in 1979 as a model of the contraction phase of wound healing. The study used human foreskin fibroblasts to demonstrate that the rate at which the lattices contract is dependent upon many variables, including collagen concentration, cell number and the presence of inhibitors of filament polymerisation (cytochalasin) (Bell et al. 1979). In this thesis, collagen lattices were constructed using three different cell types – human lung fibroblasts (HLF), human bronchial smooth muscle cells (HBSMC) and human umbilical artery smooth muscle cells (HUASMC).

The aim of these experiments was to determine whether the rate of contraction and remodelling of 3D collagen lattices could be modulated by resolvins and related SPMs acting alone, or whether SPMs can modulate the contraction of lattices induced by growth factors including TGFβ1 and PDGF-AB. Existing evidence indicates that the presence of growth factors and contractile agonists can increase the rate at which cell-populated collagen lattices can contract (Tingström, Heldin, and Rubin 1992, Kobayashi et al. 2005, Kitamura et al. 2008, 2009). In addition, previous studies have demonstrated that cells derived from patients with chronic diseases such as asthma mediate an enhanced rate of contraction when compared with cells pertaining from healthy volunteers (Matsumoto et al. 2007, Cheng 2012).

Given that a large number of collagen lattices can be set up from a single flask of cultured cells, the method enables examination of many treatment permutations at one time, allowing simultaneous study of the effects of up to four different SPMs on the actions of PDGF-AB and TGFβ1. The EPA-derived resolvin E1, as well as resolvin D1, lipoxin A_4

and protectin DX, all derived from DHA, were investigated. In addition, as previous studies found that cell-populated lattices continue to contract for up to 10 days (Arora et al. 1999), it was possible to explore the long-term effects of SPM in this model. Initial experiments focussed on optimising experimental variables including cell concentration.

3.2 Protocol

3.2.1 Optimisation of the lattice contraction assay

The original protocol, based on previous studies but developed by a colleague (see section 2.6), suggested using 150,000 cells per lattice. To ascertain whether this was optimal for the current studies, lattices were constructed with zero, 50,000, 100,000, 150,000, 200,000 or 250,000 cells.

The rat tail collagen type 1 was supplied by Millipore dissolved in 0.02 N acetic acid at concentrations of 4.0 mg/ml, 3.35 mg/ml, 3.31 mg/ml or 2.92 mg/ml, depending on the batch. It was decided to improve the original protocol by normalising the collagen concentration to a standard concentration determined by titration, in order to produce truly uniform lattices. Lattices were therefore set up with a range of final collagen concentrations (1.4 mg/ml, 1.75 mg/ml, 2.1 mg/ml or 2.3 mg/ml), using 0.02N acetic acid for all dilutions to avoid differences in pH.

To moderate the rate at which lattices contracted and thus permit treatment-induced changes to be detectable, the concentration of newborn calf serum (NCS) in the floating DMEM was reduced from 10% to 0.5%. In addition, because the lattices are pink in colour as they contain 10X DMEM, DMEM without phenol red pH indicator (supplemented with L-glutamine, penicillin, streptomycin, sodium pyruvate and non-essential amino acids) (Life Technologies, UK) was used to permit clear visualisation of the lattices.

3.2.2 Treatment of lattices with specialised pro-resolving mediators and growth factors

To investigate whether pre-treating the cell-populated collagen lattices with an SPM would affect their subsequent contraction in response to the addition of a growth factor, lattices set in 24-well plates for 1 hour in the incubator were transferred (at a point defined as ‘Time 0’) into Petri dishes and floated in a DMEM containing the SPM and incubated for 60 minutes. The lattices were then further incubated for up 96 hours in the presence of

a growth factor (Figure 3.1). Parallel control experiments included incubations performed with an SPM alone ('no GF' control), and others in which neither an SPM nor a growth factor were included ('no treatment' control).

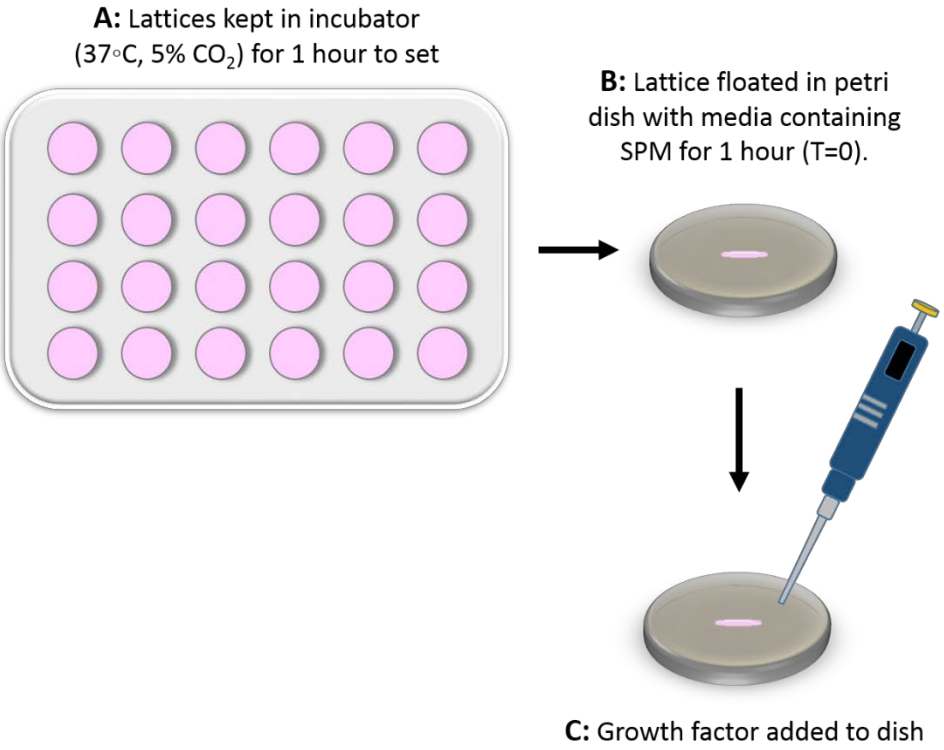

Figure 3.1: Treatment of lattices with a specialised pro-resolving mediator (SPM) and growth factor (GF). (A) The cell-populated collagen lattices were set in a 24-well plate for 1 hour in an incubator (37◦C, 5% CO_2). (B) At 'Time 0', the lattices were transferred into a Petri dish where they were floated in DMEM containing an SPM for a further hour. (C) The lattices were then further incubated with or without added GF.

For each graph with data from either HLF or HUASMC, the value of '*n*' represents an individual experiment with cells derived from different patient tissues, cultured up to passage 6. For HBSMC data, a single vial was purchased from PromoCell and expanded before being frozen and stored in liquid nitrogen, so '*n*' represents an individual experiment with a different frozen vial. HBSMC were used up to passage 7.

3.3 Results – characterising human lung fibroblasts, human bronchial smooth muscle cells and human umbilical artery smooth muscle cells in culture

Figure 3.2 shows micrographs of HLF, HBSMC and HUASMC in culture at nearly full confluency. The three cell types look similar, forming spindles and extending projections to create cell-to-cell contacts.

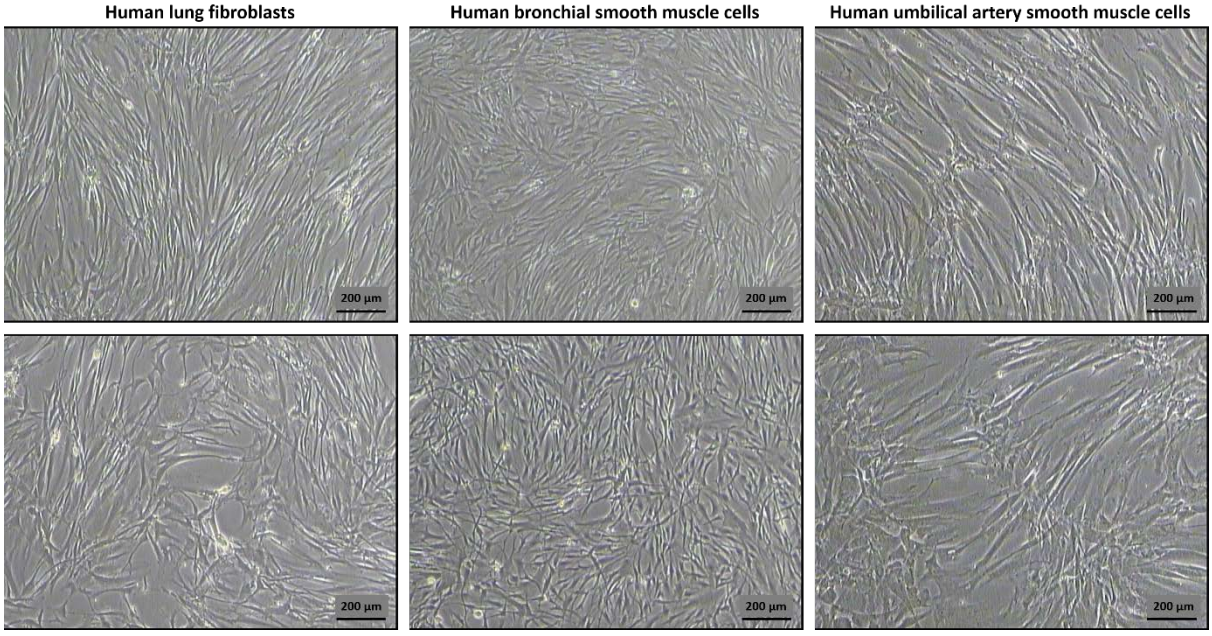

Figure 3.2: Representative images captured by inverted phase-contrast microscopy of primary human cells in culture. HLF, HBSMC and HUASMC were grown in T75 flasks.

Figure 3.3 shows representative images from immunostaining of HLF, HBSMC and HUASMC with a primary antibody for α-smooth muscle actin (α-SMA). When compared to immunostaining in the absence of the primary antibody, the results show the expected gradation of α-SMA immunoexpression with very low or absent expression in HLF, moderate, poorly-organised expression in HBSMC, and the highest expression in well-organised filaments in HUASMC.

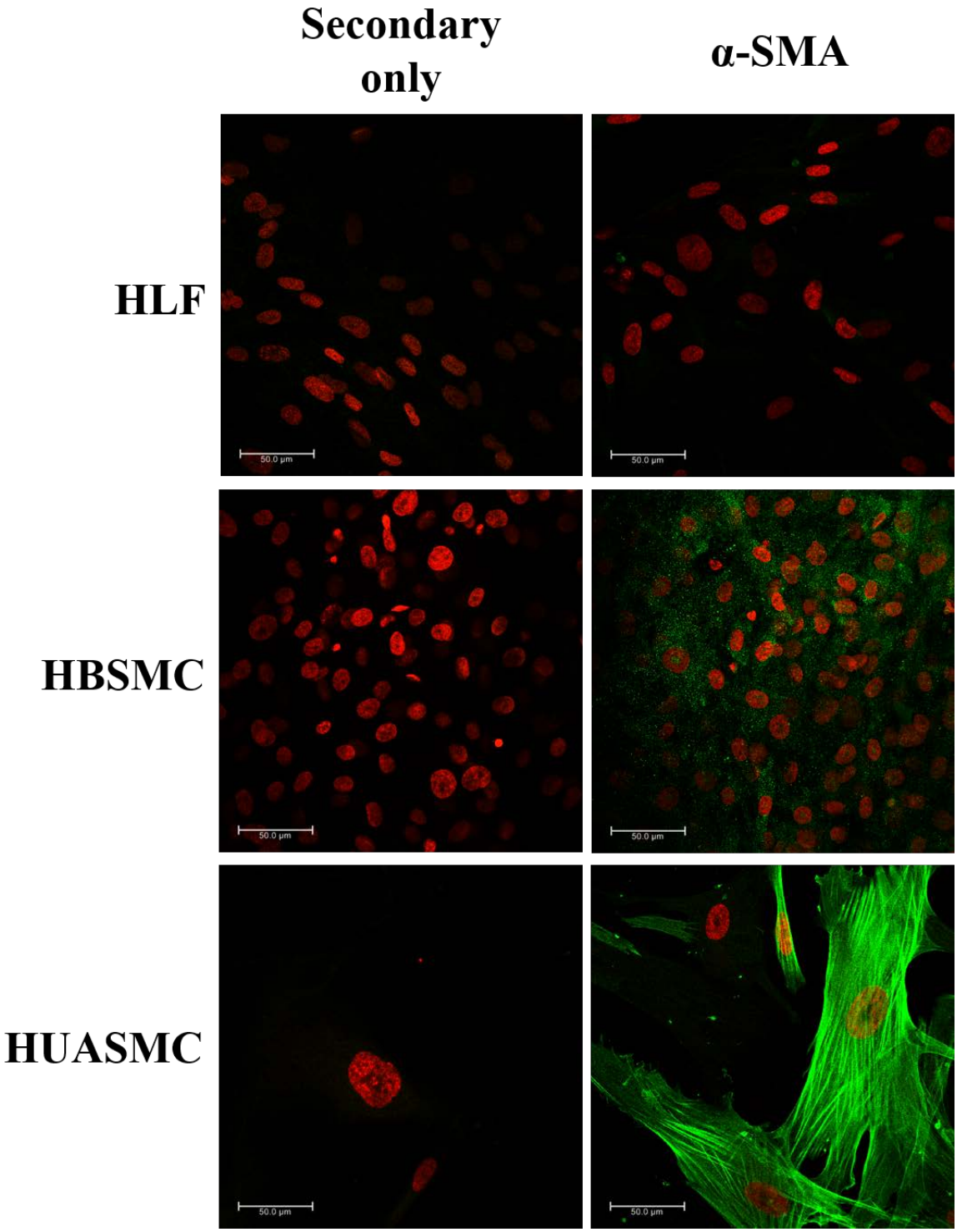

Figure 3.3: Immunostaining for α-smooth muscle actin (α-SMA) in human lung fibroblasts (HLF), human bronchial smooth muscle cells (HBSMC) and human umbilical artery smooth muscle cells (HUASMC). Cells grown on coverslips in a 24-well plate overnight were fixed with 4% PFA for 60 minutes then stained for α-SMA (green) in the right-hand panels or in the absence of primary antibody (i.e. secondary antibody only) in the left-hand panels. DAPI staining (red) shows cell nuclei in all images. HUASMC strongly express α-SMA in organised filaments, whilst the α-SMA in HBSMC is less well-organised. A small number of HLF appear to express very low levels of α-SMA. Scale bar = 50µm.

3.4 Results – human lung fibroblast-populated collagen lattices

3.4.1 Effect of cell number on rate of contraction of HLF-populated collagen lattices

HLF were embedded in a 3D collagen lattice at densities of zero, 50,000, 100,000, 150,000, 200,000 or 250,000 cells per lattice and with collagen concentration at an initial concentration of 3.31 mg/ml. Following the addition of the other components of the lattice, the final collagen concentration was 2.32 mg/ml, although this was varied in some experiments described below.

Figure 3.4 illustrates how lattice contraction is a cell-mediated process, since lattices containing no cells did not contract at any point over the 72 hours of culture. In addition, the data indicate that the recommended number of 150,000 cells per lattice is optimal for inducing maximal lattice contraction, as populating lattices with more cells (either 200,000 or 250,000) did not further increase the rate of contraction, while using fewer than 150,000 cells per lattice (either 50,000 or 100,000) significantly reduced the rate of contraction over 72 hours.

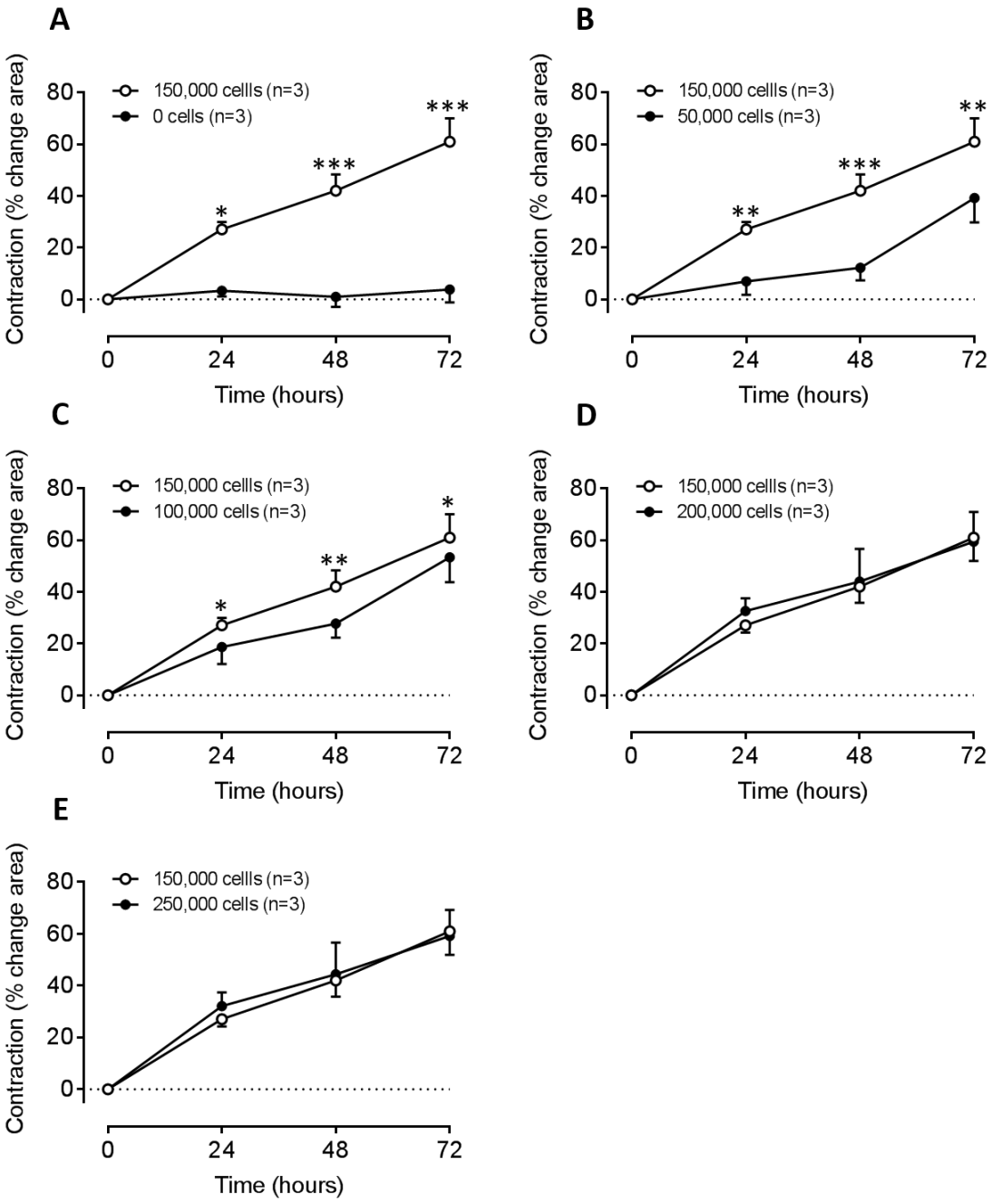

*Figure 3.4: Lattice contraction is mediated by the presence of relevant cells and depends both on cell number (per lattice) and time. Human lung fibroblasts were embedded into collagen lattices and floated in a petri dish with DMEM containing 10% serum. To optimise rate of contraction over 72 hours, the number of cells was varied from the recommended value of 150,000 per lattice. (A) Lattices with zero cells do not contract over the 72 hours (n=3) indicating that the contraction of lattices is cell-mediated. Lattices populated with (B) 50,000 cells or (C) 100,000 cells contracted significantly more slowly at 24, 48 and 72 hours (n=3, mean ± SEM) compared with those lattices populated with 150,000 cells. Contraction of lattices populated with either (D) 200,000 cells or (E) 250,000 cells was not significantly different from lattices populated with 150,000 cells, confirming that that 150,000 cells per lattice is optimal for maximal contraction of collagen lattices. Multiple comparisons: *p<0.05 vs 150,000 cells,** p<0.01 vs 150,000 cells, ***p<0.001 vs 150,000 cells.*

3.4.2 Effect of collagen concentration on rate of contraction of human lung fibroblast populated-collagen lattices

To determine the effect of final collagen concentration on lattice contraction, 150,000 HLF were embedded in lattices with final collagen concentrations of 1.4, 1.75, 2.1 and 2.32 mg/ml.

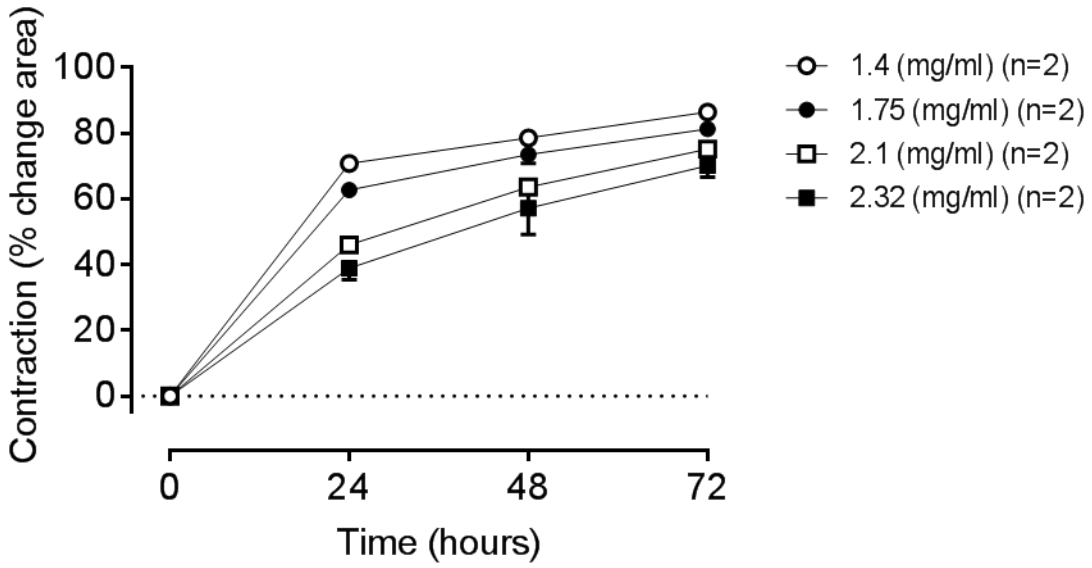

Figure 3.5: Effect of collagen varying concentrations on human lung fibroblast (HLF)-induced contraction of collagen lattices (n=2, mean ± SEM). HLF (150,000 per lattice) were embedded with the indicated collagen concentrations and lattice contraction was measured at 24 hour intervals over 72 hours. The data suggest that decreasing collagen concentration from 2.32 mg/ml to 1.4 mg/ml increases the rate of lattice contraction, particularly at earlier time-points.

It is important that the collagen lattice is sufficiently robust to permit its manual transfer from the 24-well plate to the Petri dish for experiments, and also that it does not contract so rapidly that it masks any further acceleration of contraction induced by the growth factor or SPM. Based on the data in Figure 3.5 a final collagen concentration of 2.0 mg/ml was therefore chosen as optimal for all further experiments described below.

3.4.3 Effect of a stimulus on rate of contraction of human lung fibroblast populated-collagen lattice

TGFβ1 is an effective and reproducible stimulus of collagen lattice contraction, mimicking its putative role in wound healing *in vivo*. To define the time-course of TGFβ1-induced contraction in our model and its relationship to the concentration of newborn calf

serum (NCS) in the DMEM in the current experiments, HLF-populated lattices were first floated into DMEM containing 10% NCS in the presence or absence of 2 ng/ml TGFβ1 and lattice contraction was recorded at 24-hour intervals up to 72 hours. A concentration of 10% NCS was chosen initially as this is the same as the NCS concentration in the DMEM used during the formation and setting of lattices in 24-well plates, before their transfer to Petri dishes for experiments.

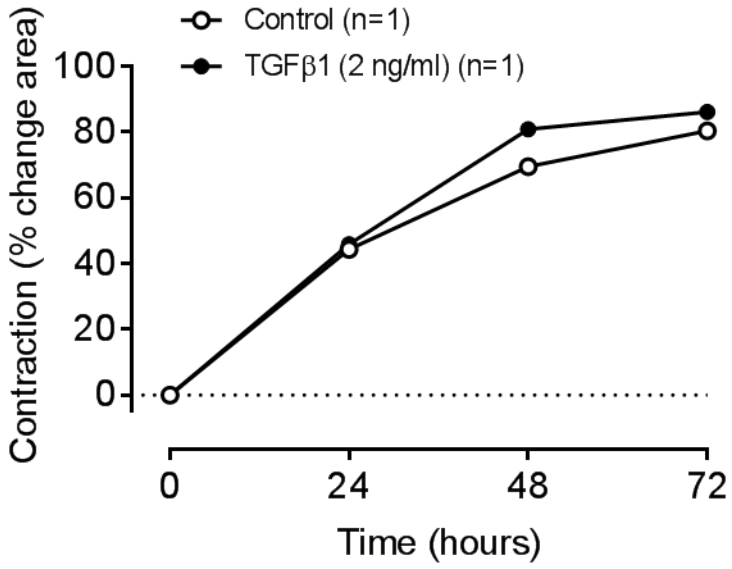

Figure 3.6: Effect of TGFβ1 on human lung fibroblast (HLF)-populated lattice contraction with 10% newborn calf serum (NCS). Collagen lattices populated with 150,000 HLF were floated in petri dishes with DMEM containing 10% NCS with or without TGFβ1 (2 ng/ml) and their contraction was measured up to 72 hours (n=1). TGFβ1 appeared to have no effect on lattice contraction at this concentration of NCS.

With 10% NCS, the lattices contracted by approximately 80% even in the absence of TGFβ1, and the growth factor had little effect on the rate of contraction compared to control dishes without TGFβ1. To slow down the basal rate of lattice contraction, the concentration of NCS present in the incubation DMEM in the Petri dishes during experiments was lowered from 10% to 0.5%, although the concentration of NCS used during the formation and setting of the lattices in 24-well plates before the experiments was unchanged at 10%.

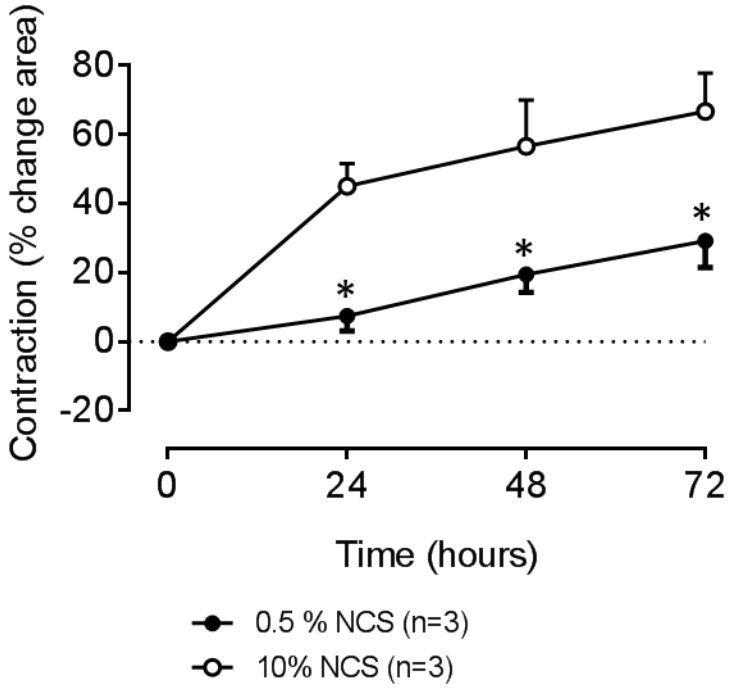

*Figure 3.7: Effect of newborn calf serum (NCS) concentration on spontaneous lattice contraction. Lattices formed in 24-well plates with 10% NCS and 150,000 human lung fibroblasts were floated in Petri dishes in DMEM containing either 10% NCS or 0.5% NCS. Lattices in 10% NCS DMEM contracted rapidly, reducing in size by 45% in 24 hours (n=3, mean ± SEM), putatively stimulated by endogenous growth factors present within 10% NCS. In contrast, lattices floated in 0.5% NCS-containing DMEM contracted by only 7.5% in 24 hours and failed to contract by more than 30% over 72 hours (n=3, mean ± SEM). At all time points after 0 hours, contraction of lattices in 0.5% NCS was significantly lower than in 10% NCS (n=3, mean ± SEM, $p<0.05$ (two-way ANOVA repeated measures in rows)). Multiple comparisons: * $p<0.05$.*

Lowering the concentration of NCS from 10% during lattice formation to 0.5% during contraction in the Petri dishes significantly reduced both the rate and extent of lattice contraction (n=3, mean ± SEM, $p<0.05$) (Figure 3.7). Reducing the concentration of NCS to 0.5% therefore allowed the expected enhancement of contraction by growth factors to be more readily detectable, so a concentration of 0.5% NCS was used during the contraction phase of subsequent experiments.

3.4.4 Effect of growth factors on rate of contraction of human lung fibroblast-embedded lattice contraction

Having established optimum conditions of a cell density of 150,000 HLF cells per lattice, with a collagen concentration of 2 mg/ml and 0.5% NCS in the contraction DMEM, experiments were performed to determine the effect of TGFβ1 (1 ng/ml) or PDGF-AB (10 ng/ml) on lattice contraction over 72 hours. Both TGFβ1 (1 ng/ml) and PDGF-AB (10

ng/ml) significantly enhanced the rate and extent of contraction of HLF-populated collagen lattices compared with controls (p=0.0006 vs TGFβ1; p=0.0009 vs PDGF-AB) (Figure 3.8).

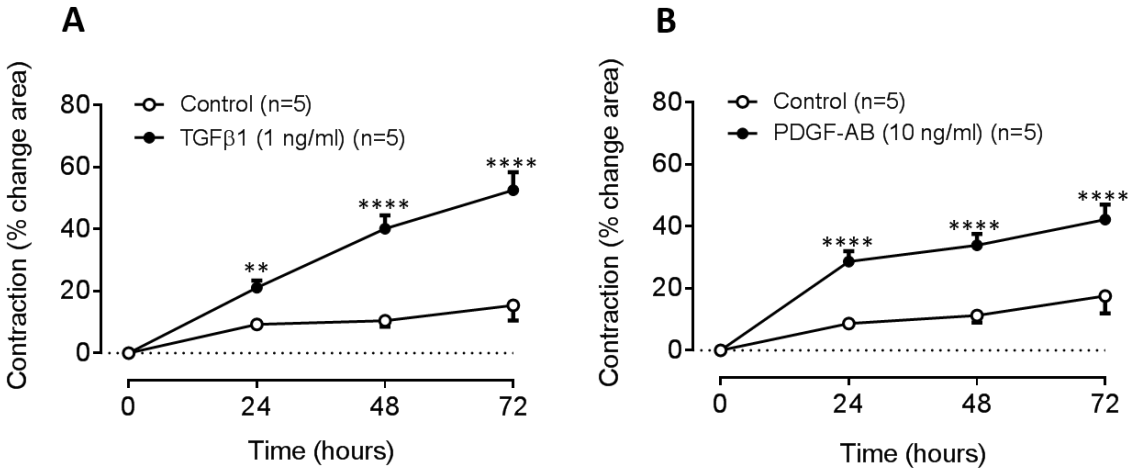

*Figure 3.8: Effect of TGFβ1 and PDGF-AB on human lung fibroblast (HLF)-populated collagen lattice contraction. The addition of either (A) TGFβ1 (1 ng/ml) (n=5, mean ± SEM, p=0.0006 vs control) or (B) PDGF-AB (10 ng/ml (n=4, mean ± SEM, p=0.0009 vs control) caused significantly enhanced rate and extent of contraction of the lattices. Multiple comparisons: ** p<0.01 vs control, **** p<0.0001 vs control.*

The effect of the growth factors tested can be visualised by eye and representative photos for TGFβ1 are shown below in Figure 3.9. At the 72 hour time point, the HLF-populated lattices exposed to TGFβ1 have contracted considerably and appear to be approximately half of their original size (0 hours). In contrast, the control lattices appear to have contracted only slightly. These changes in size are in agreement with the mean calculated changes as displayed in Figure 3.8.

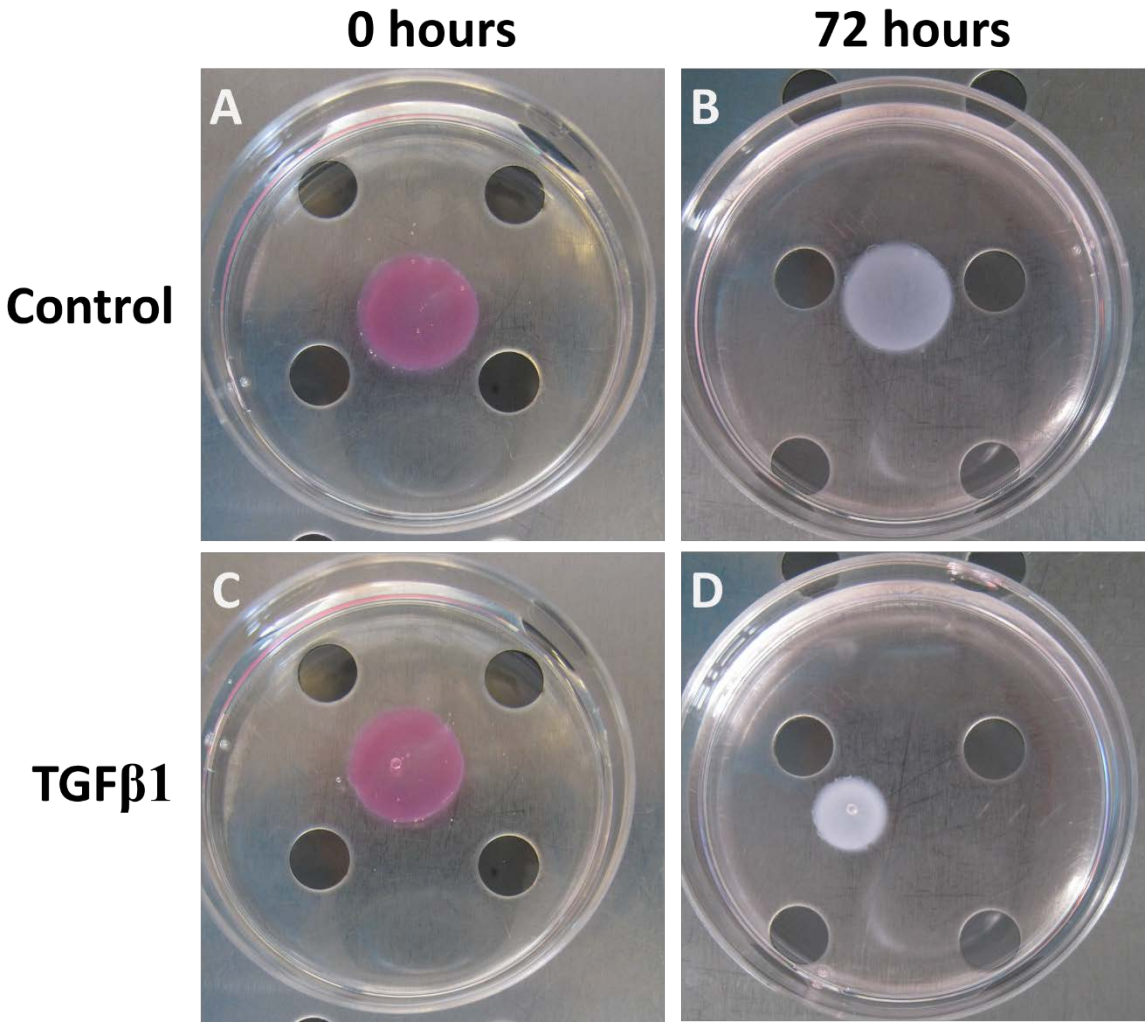

Figure 3.9: Representative photos of human lung fibroblast-populated collagen lattices, either control or TGFβ1 (1 ng/ml)-treated, and at both 0 and 72 hours. The control lattices undergo very little change in diameter between (A) 0 and (B) 72 hours. In contrast, The TGFβ1-exposed lattices contract considerably from (C) 0 to (D) 72 hours and appear to be approximately half their original size. By 72 hours both the control and TGFβ1-treated lattices have lost their pink colour conferred on them by the concentrated medium (10X DMEM) and appear white in colour. In conjunction, the floating medium in the Petri dish has acquired a light pink colour following the exit of the medium from the lattice.

3.4.6 Effect of specialised pro-resolving mediators on contraction of human lung fibroblast-populated collagen lattices

To determine whether SPMs (RvD1, RvE1, LXA_4 or PDX) acting alone can modulate contraction of HLF-populated collagen lattices, lattices containing 150,000 HLF were floated in Petri dishes containing DMEM with 0.5% NCS and each SPM at a concentration of 10 nM for 72 hours (Figure 3.10). In these experiments no exogenous growth factor (TGFβ1 or PDGF-AB) was added.

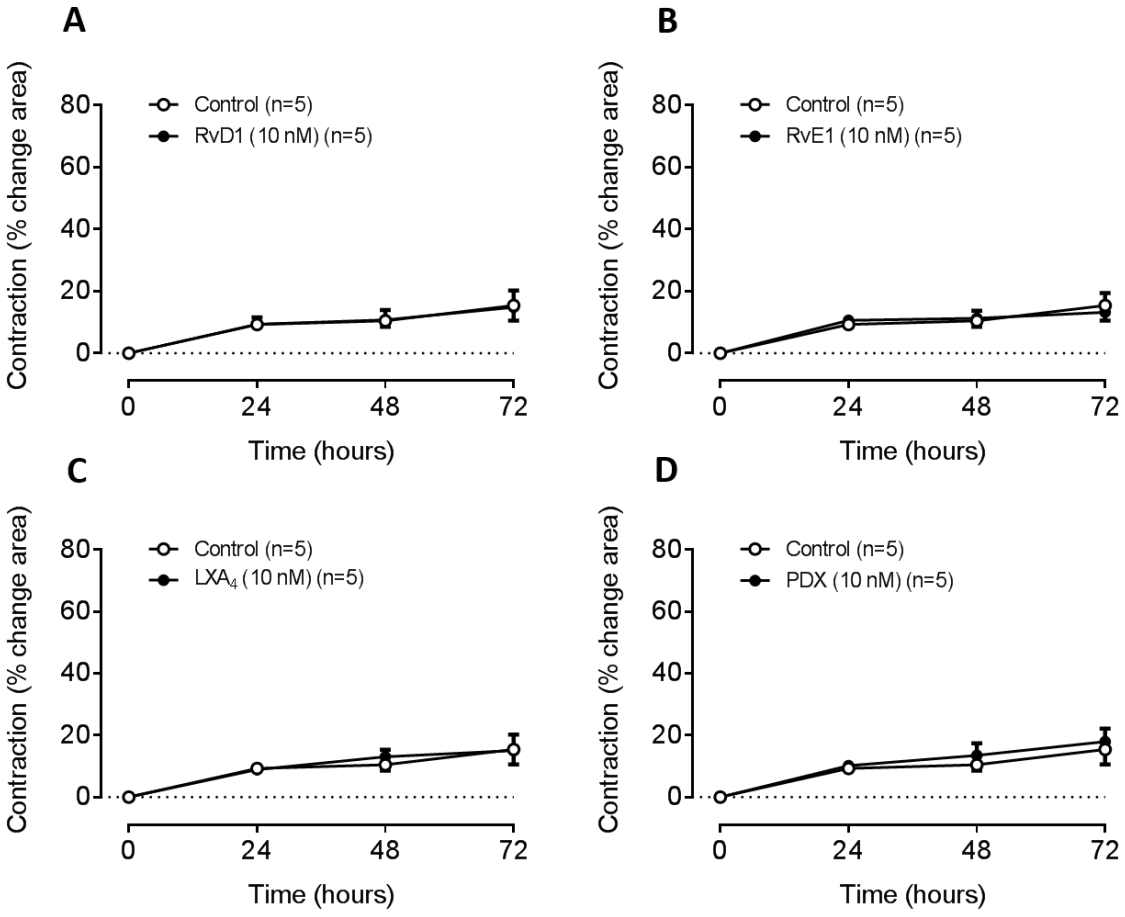

Figure 3.10: Effect of specialised pro-resolving mediators (SPM) on contractions of human lung fibroblast (HLF)-populated collagen lattices, in the absence of an exogenous growth factor, over 72 hours. Collagen lattices populated with HLF were floated in DMEM containing 10 nM resolvin D1 (RvD1), 10 nM resolvin E1 (RvE1), 10 nM lipoxin A_4 (LXA_4) or 10 nM protectin DX (PDX). No significant effect of (A) RvD1, (B) RvE1, (C) LXA_4 or (D) PDX was seen on the rate or extent of lattice contraction (p=ns vs control).

The ability of HLF to contract collagen lattices was unaffected by the presence of RvD1, RvE1, LXA_4 or PDX (10 nM) (n=5, mean ± SEM, p=ns) in the absence of an exogenous growth factor (Figure 3.10).

3.4.7 Effect of specialised pro-resolving mediators on growth factor-induced contraction of human lung fibroblast-populated collagen lattices

As the SPM alone did not appear to affect HLF-mediated collagen lattice contraction in the absence of an exogenous growth factor, experiments were performed to determine whether SPM may modify the effects of growth factors on HLF-populated collagen lattices. Firstly, the effect of resolvin D1 (RvD1) on lattice contraction was assessed by floating HLF-populated collagen lattices in DMEM (with 0.5% NCS) containing RvD1 (10 nM) for 1 hour, before the addition of TGFβ1 (1 ng/ml) or PDGF-AB (10 ng/ml) to the appropriate dishes (Figure 3.11).

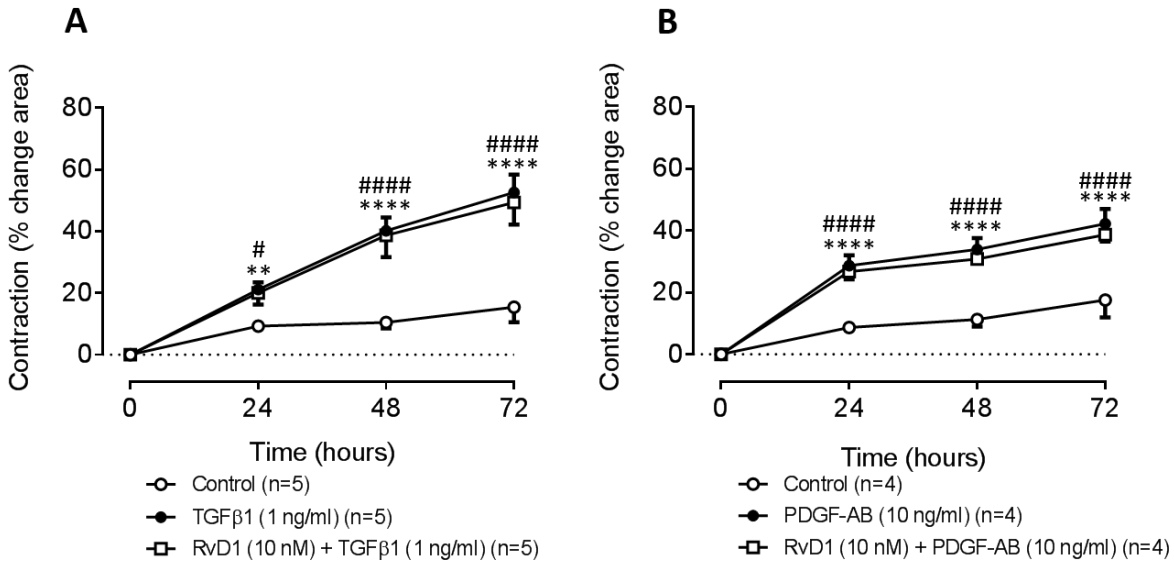

*Figure 3.11: Effect of resolvin D1 (RvD1) on growth factor-induced human lung fibroblast (HLF)-populated lattice contraction. (A) TGFβ1 (1 ng/ml) significantly enhanced the rate of contraction of lattices at all time points compared to controls (n=5, mean ± SEM, p=0.0006), but the addition of RvD1 (10 nM) had no effect on TGFβ1-induced contractions (n=5, mean ± SEM, p=ns vs GF alone). (B) Similarly, PDGF-AB (10 ng/ml) enhanced contractions of HLF-populated lattices compared with control (n=4, mean ± SEM, p=0.0009), but RvD1(10 nM) had no effect on PDGF-AB-induced contractions (n=4, mean ± SEM, p=ns vs GF alone). Multiple comparisons: ** p<0.01 GF vs control. **** p<0.0001 GF vs control, # p<0.05 RvD1 and GF vs control, #### p<0.0001 RvD1 and GF vs control.*

The contraction of collagen lattices by HLF was significantly increased by the presence of either TGFβ1 or PDGF-AB, but these responses were not altered by the addition of 10 nM RvD1 (p=ns, n=4-5) (Figure 3.11).

Similar experiments were performed using resolvin E1 (RvE1). HLF-populated collagen lattices were floated in dishes containing DMEM (with 0.5% NCS) with and

without RvE1 (10 nM) for 1 hour, before the addition of TGFβ1 (1 ng/ml) or PDGF-AB (10 ng/ml) (Figure 3.12). RvE1 (10 nM) did not significantly affect growth factor-induced contraction of HLF-populated collagen lattices over 72 hours compared with either of the growth factors alone (n=4/5, mean ± SEM, p=ns).

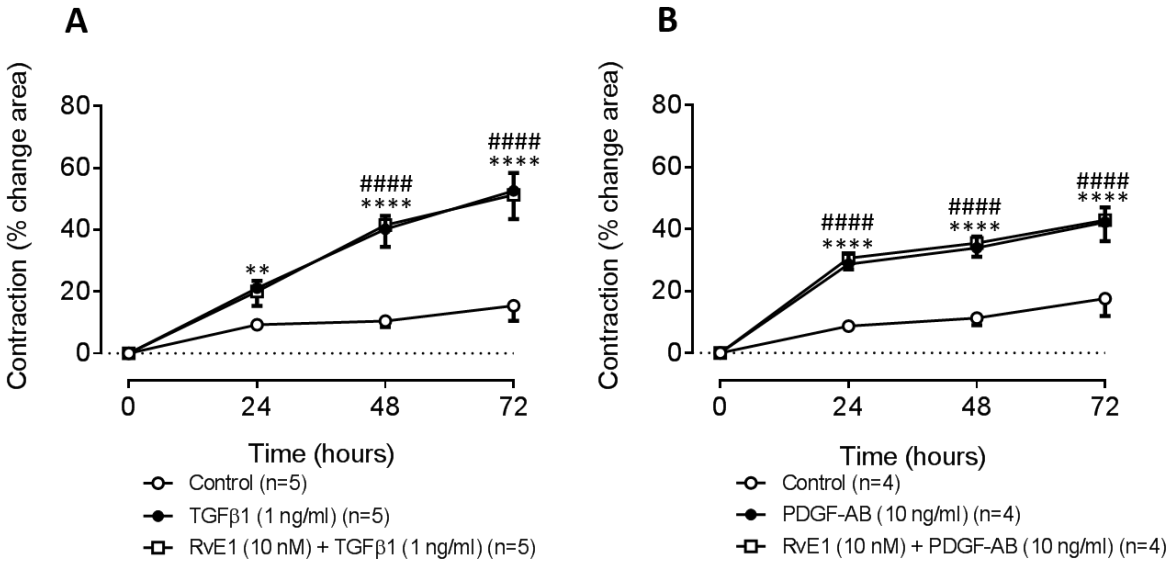

*Figure 3.12: Effect of resolvin E1 (RvE1) on growth factor-induced lattice contraction. Human lung fibroblast (HLF)-populated collagen lattices in the presence of (A) RvE1 and TGFβ1 (1 ng/ml) (n=5, mean ± SEM) or (B) RvE1 and PDGF-AB (10 ng/ml) (n=4, mean ± SEM) contracted at the same rates as those in the presence of each growth factor alone (p=ns). Multiple comparison: ** p<0.01 vs GF vs control, **** p<0.0001 GF vs control, #### p<0.0001 RvE1 and GF vs control.*

The effect of lipoxin A_4 (LXA_4) on lattice contraction induced by the growth factors (TGFβ1 and PDGF-AB) was next assessed in the same way. HLF-populated collagen lattices were floated in DMEM (with 0.5% NCS) in the absence or presence of LXA_4 (10 nM) for 1 hour, before the addition of TGFβ1 (1 ng/ml) or PDGF-AB (10 ng/ml) to the appropriate dishes. As observed with both RvD1 (Figure 3.11) and RvE1 (Figure 3.12), LXA_4 did not significantly modulate TGFβ1 or PDGF-AB-induced contraction of HLF-populated collagen lattices (Figure 3.13).

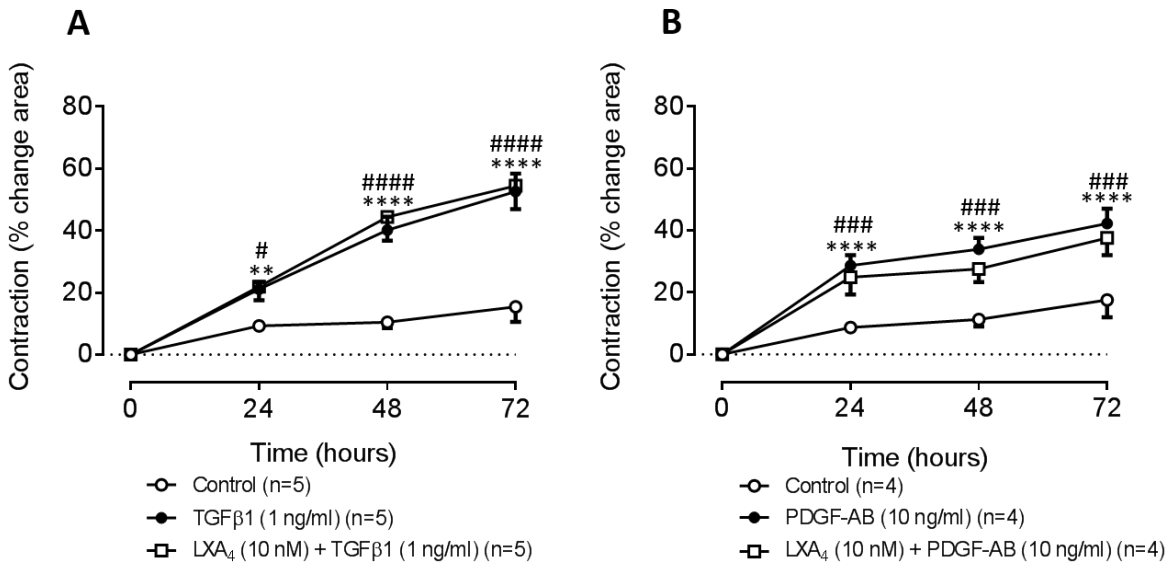

*Figure 3.13: Effect of lipoxin A_4 (LXA_4) on growth factor-induced lattice contraction. Treatment of human lung fibroblast (HLF)-populated lattices with LXA_4 did not significantly affect the ability of (A) TGFβ1 (1 ng/ml) (n=5, mean ± SEM, p=ns) or (B) PDGF-AB (10 ng/ml) (n=4, mean ± SEM, p=ns) to increase the rate of contraction of HLF-populated collagen lattices when compared with growth factor alone. Multiple comparison: ** p<0.01 vs GF vs control, **** p<0.0001 GF vs control, # p<0.05 RvE1 and GF vs control, ### p<0.001 RvE1 and GF vs control, #### p<0.0001 RvE1 and GF vs control.*

The effect of protectin DX (PDX) on lattice contraction induced by the growth factors TGFβ and PDGF was assessed by floating collagen lattices in DMEM (with 0.5% NCS) in the absence or presence of PDX (10 nM) for 1 hour, before the addition of TGFβ1 (1 ng/ml) or PDGF-AB (10 ng/ml) to the appropriate dishes (Figure 3.14). In contrast to the other SPMs, the PDX results show that, although over the entire curve PDX does not modulate PDGF-AB-induced contraction (p=0.06), at 24 and 48 hours PDX does demonstrate an inhibitory effect (p<0.05 GF vs PDX and GF). However, the magnitude of the inhibition by PDX was weak and this is visible in the graph. In addition, the overall difference between PDX + PDGF-AB treated lattices and control lattices is significant (p<0.05), further suggesting that any inhibitory effect is negligible. Contractions to TGFβ1 were completely unaffected by PDX.

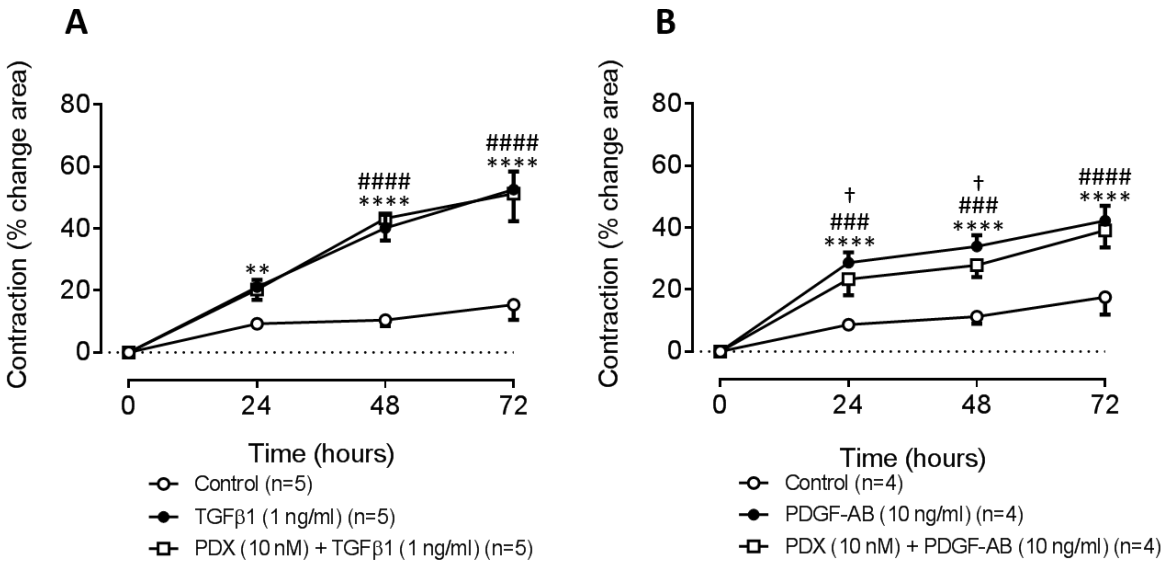

*Figure 3.14: Effect of protectin DX (PDX) on growth factor (GF)-induced contraction of human lung fibroblast (HLF)-populated lattices. (A) PDX (10 nM) did not affect the ability of TGFβ1 (1 ng/ml) to contract lattices (n=5, mean ± SEM, p=ns vs TGFβ1 only). (B) In contrast, two-way ANOVA suggests that there is a trend for PDX-mediated inhibition of PDGF-AB-induced contraction (p=0.06), and Sidak's multiple comparisons analysis suggests that this effect is most prominent at 24 and 48 hours (n=4, mean ± SEM, p<0.05 vs PDGF-AB only), but not at 72 hours (p=ns). Multiple comparisons: * p<0.05 GF vs control, ### p<0.001 PDX and GF vs control, #### p<0.0001 PDX and GF vs control, † p<0.05 GF vs PDX and GF.*

3.4.8 Effect of inhibiting f-actin filament polymerisation on contraction of human lung fibroblast-populated collagen lattices

Cytochalasin D inhibits the polymerisation of f-actin filaments, which are cytoskeletal elements believed to be important in contractions of cell-populated collagen lattices (Redden and Doolin 2006). To confirm this in the present model, HLF-populated collagen lattices were floated in dishes containing DMEM (with 0.5% NCS) with or without cytochalasin D (100 nM). In parallel, the ability of cytochalasin D to inhibit contraction of lattices induced by TGFβ1 (1 ng/ml) was also investigated (Figure 3.15).

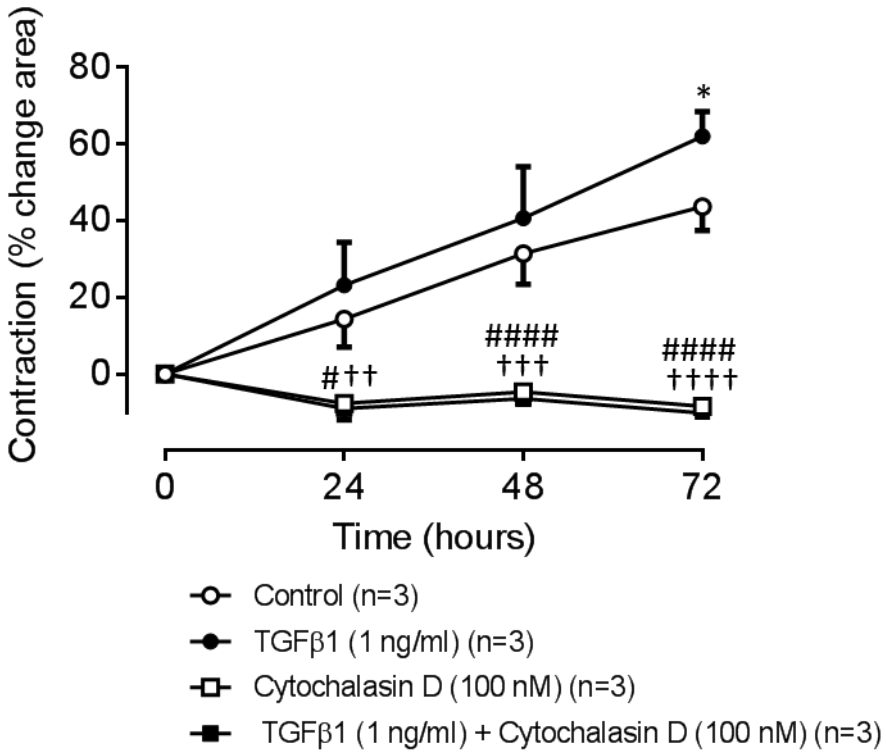

*Figure 3.15: Effect of cytochalasin D on spontaneous and TGFβ1-induced contractions of human lung fibroblast (HLF)-populated collagen lattices. Cytochalasin D inhibited HLF-induced contractions of collagen lattices, both in the absence (n=3, mean ± SEM, p<0.05) and presence of TGFβ1 (1 ng/ml) (n=3, mean ± SEM, p<0.05). Multiple comparisons: * p<0.05 TGFβ1 vs control, # p<0.05 cytochalasin D vs control, #### p<0.0001 cytochalasin D vs control, †† p<0.01 TGFβ1 and cytochalasin D vs control, ††† p<0.001 TGFβ1 and cytochalasin D vs control, †††† p<0.0001 TGFβ1 and cytochalasin D vs control.*

The data indicate that cytochalasin D, an inhibitor of f-actin polymerisation, completely abolishes the ability of HLF to contract collagen lattices ($p<0.0001$), including the enhanced contractions observed in the presence of TGFβ1 ($p<0.0001$) (Figure 3.15). To visualise the morphology of HLF-populated collagen lattices and to investigate how this

might change in the presence of cytochalasin D and/or TGFβ1, images of the lattices were captured on a confocal microscope. In these images, f-actin is labelled with TRITC-conjugated phalloidin (red) and the nuclei are labelled with DAPI (blue) (Figure 3.16).

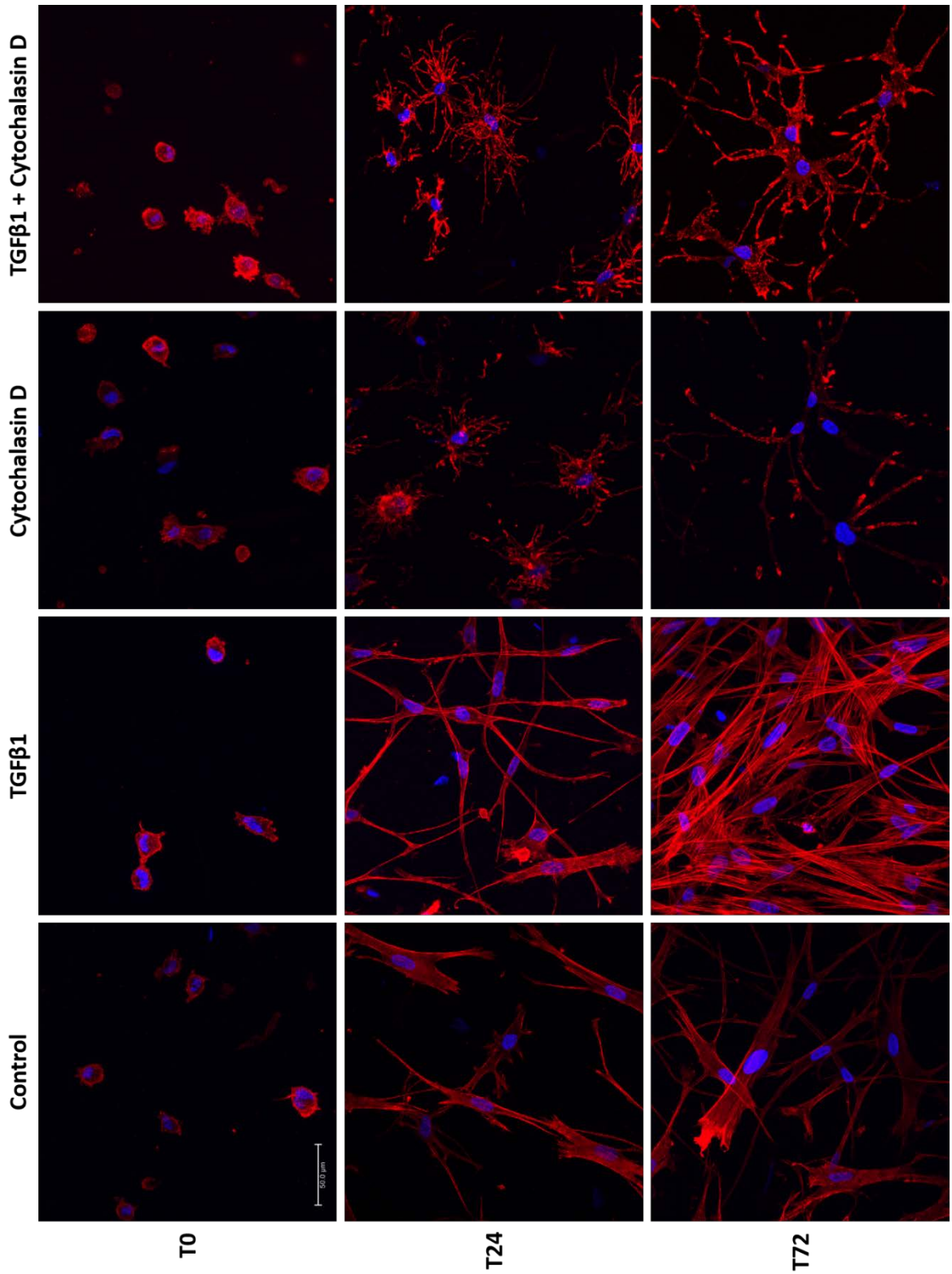

Figure 3.16: The morphology of human lung fibroblasts (HLF) populating a 3D collagen lattice. HLF in collagen lattices extend projections and cause lattice contraction both in the absence (control) and presence of TGFβ1. Cytochalasin D, an inhibitor of f-actin polymerisation, prevents the HLF from extending projections, thus inhibiting lattice contractions. Scale bar = 50µm.

The images in Figure 3.16 indicate that at time 0 (T0), the cells appear rounded regardless of treatment. At the 24 hour time-point (T24), those cells in lattices with no treatment (NT) have extended projections and appear to be interacting with one another. These features are enhanced in cells treated with TGFβ1. In contrast, cells in lattices treated with cytochalasin D (with or without TGFβ1) have largely failed to establish long filamentous projections and there are far fewer cells within the field of view.

3.5 Results – human bronchial smooth muscle cell-populated collagen lattices

3.5.1 Effect of TGFβ1 and PDGF-AB on contraction of human bronchial smooth muscle cell-populated collagen lattices.

Human bronchial smooth muscle cells (HBSMC) purchased from PromoCell were used to investigate their ability to contract collagen lattices, and their propensity to be modulated by growth factors (GF) and specialised pro-resolving mediators (SPM). Collagen lattices populated with 150,000 HBSMC were floated in petri dishes containing DMEM (with 0.5% NCS) with or without TGFβ1 (1 ng/ml) or PDGF-AB (10 ng/ml). Contraction of these lattices was measured at 24 hour intervals by calculating changes in lattice surface areas (Figure 3.17).

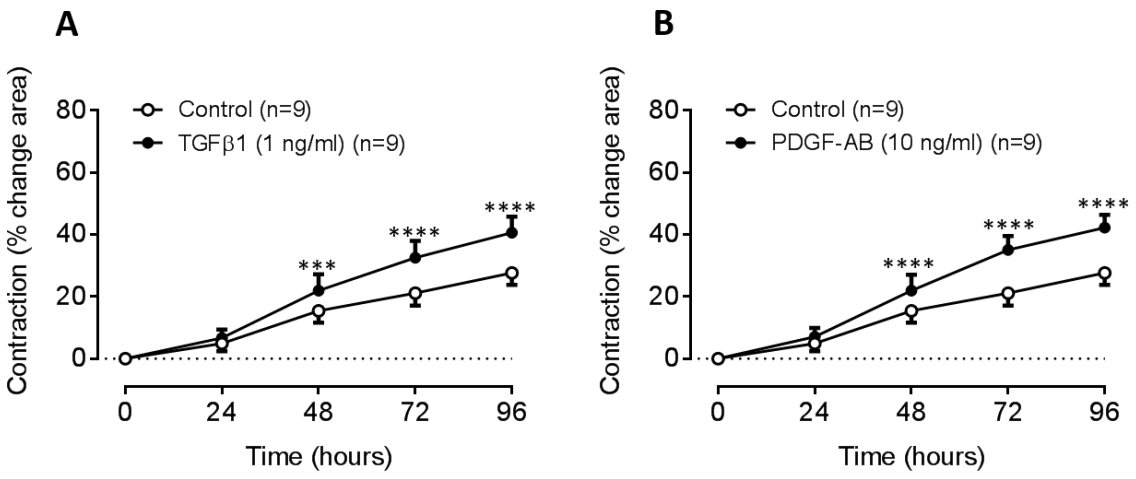

*Figure 3.17: Effect of TGFβ1 and PDGF-AB on contraction of human bronchial smooth muscle cell (HBSMC)-populated collagen lattices (n=9). (A) TGFβ1 (1 ng/ml) significantly increased the rate and extent of contraction of lattices populated with HBSMC (n=9, mean ± SEM, p<0.05). (B) PDGF-AB (10 ng/ml) also significantly increased the rate and extent to which HBSMC-populated collagen lattices contract (n=7, mean ± SEM, p<0.0001). Multiple comparisons: *** p<0.001 GF vs control, **** p<0.0001 GF vs control.*

In the presence of either TGFβ1 (1 ng/ml) or PDGF-AB (10 ng/ml), HBSMC-populated collagen lattices contracted at a significantly quicker rate and to a greater extent when compared with control (n=9, p<0.05) (Figure 3.17). HBMSC–populated lattices appeared to contract more slowly than HLF lattices in previous experiments, so the HBSMC assay was continued for a further 24 hours up to 96 hours in total.

3.5.2 Effect of specialised pro-resolving mediators on contraction of human bronchial smooth muscle cell-populated collagen lattices.

As described previously with HLF-populated lattices (section 3.4.5), the purpose of this experiment was to determine whether incubation with SPM on their own can modulate spontaneous contractions of HBSMC-populated collagen lattices. Lattices populated with HBSMC were floated in petri dishes containing DMEM (with 0.5% NCS) with or without either RvD1, RvE1, LXA_4 or PDX (10 nM), and the contraction of the lattices determined at 24 hour intervals by measuring changes in area. The contraction of HBSMC-populated collagen lattices was not significantly different in the presence of any of the four SPM investigated when compared with controls (Figure 3.18).

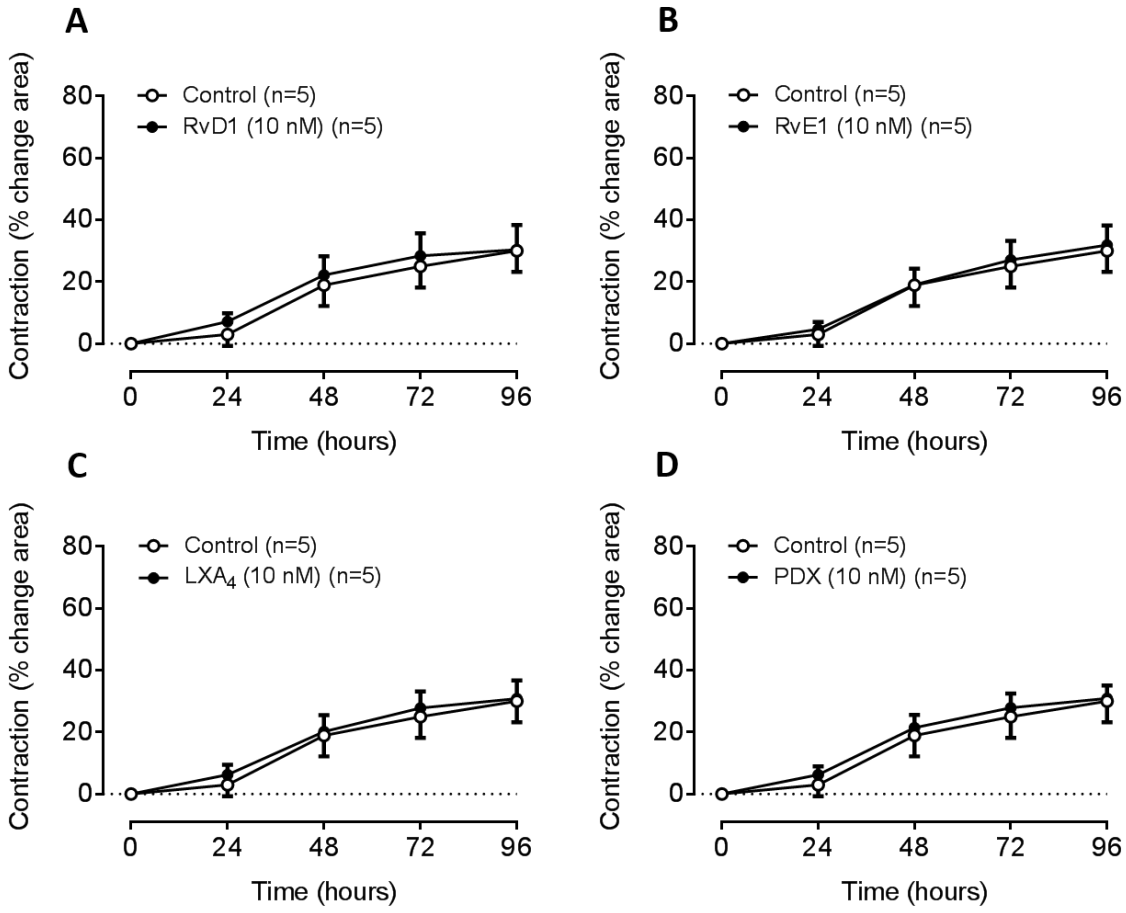

Figure 3.18: The effects of specialised pro-resolving mediators acting alone on contractions of human bronchial smooth muscle cell (HBSMC)-populated collagen lattices. No growth factors were added in these experiments. Incubation of lattices with (A) resolvin D1 (RvD1) (10 nM) (B) resolvin D1 (RvE1) (10 nM) (C) lipoxin A_4 (LXA_4) (10 nM) or (D) protectin DX (PDX) (10 nM) had no significant effect on lattice contraction compared with controls (n=5, mean ± SEM, p=ns).

3.5.3 Effects of specialised pro-resolving mediators on growth factor-induced contraction of human bronchial smooth cell-populated collagen lattices

SPM were also investigated for their ability to modulate HBSMC-populated lattice contractions induced by growth factors, as described previously for HLF-populated lattices (section 3.4.7). Having shown that both TGFβ1 and PDGF-AB increase the rate and extent of contraction of HBSMC-populated lattices (Figure 3.17), the ability of four SPMs to modulate GF-induced contraction was investigated. Lattices were floated in DMEM (with 0.5% NCS) containing either TGFβ1 (1 ng/ml) or PDGF-AB (10 ng/ml) with or without the SPM and contractions were measured over 72 hours at 24-hour intervals. The first SPM investigated was **RvD1** (10 nM) (Figure 3.19).

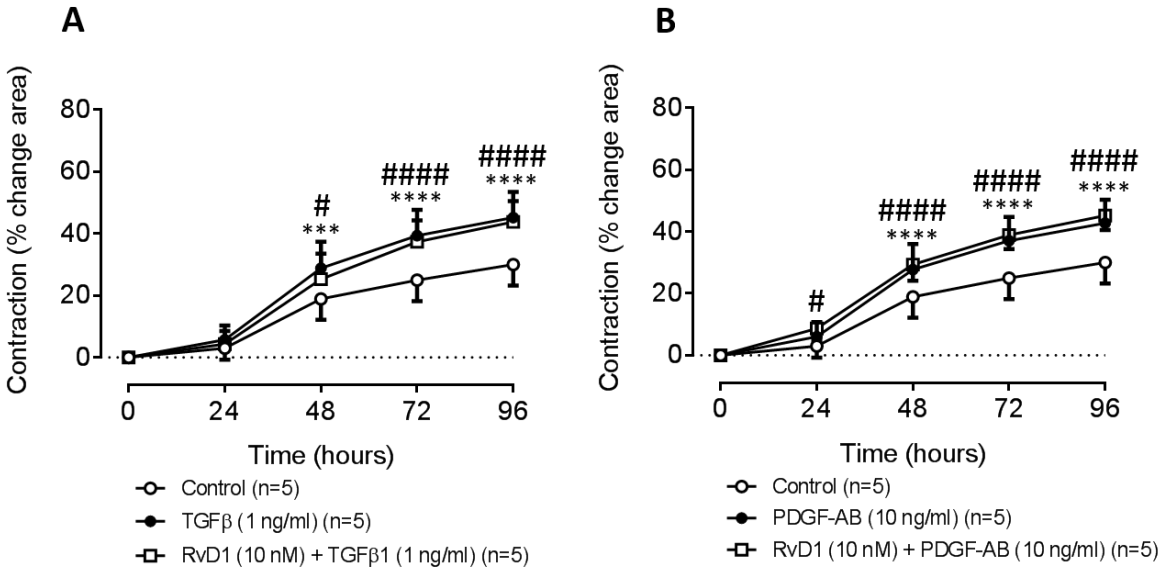

*Figure 3.19: The effect of resolvin D1 (RvD1) on growth factor (GF)-induced contraction of human bronchial smooth muscle cell (HBSMC)-populated collagen lattices. Lattices were floated in petri dishes containing DMEM (with 0.5% NCS) with RvD1 (10 nM) for 60 minutes before either TGFβ1 or PDGF-AB was added to the same dish. (A) RvD1 mediated no significant effect on TGFβ1-induced contraction (1 ng/ml) (B) RvD1 did not modulate PDGF-AB-induced (10 ng/ml) contraction of HBSMC-populated lattices (n=5, mean ± SEM). Multiple comparisons: *** p<0.001 GF vs control, **** p<0.0001 GF vs control, # p<0.05 RvD1 and GF vs control, #### p<0.0001 RvD1 and GF vs control.*

RvD1 had no significant effect overall on the contraction of HBSMC-populated collagen lattices induced by either TGFβ1 or PDGF-AB when compared with the contraction induced by either growth factor alone (n=5, mean ± SEM, p=ns).

RvE1 was investigated next. To determine whether it can modulate contractions of HBSMC-populated collagen lattices, the lattices were floated in DMEM (with 0.5% NCS)

with RvE1 (10 nM) for 60 minutes. Following this, either TGFβ1 (1 ng/ml) or PDGF-AB (10 ng/ml) was added to the dish and contraction of the lattices measured at 24 hour intervals for a total of 96 hours (Figure 3.20).

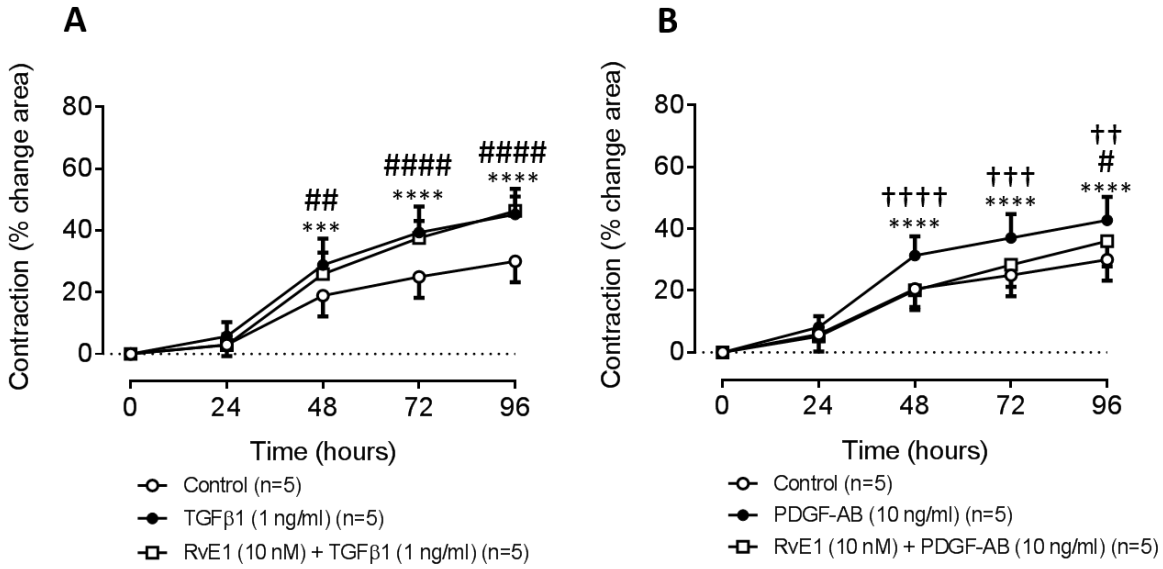

*Figure 3.20: The effect of resolvin E1 (RvE1) on TGFβ1 and PDGF-AB induced contractions of human bronchial smooth muscle cell (HBSMC)-populated collagen lattices. (A) HBSMC-populated collagen lattices contracted in the presence of TGFβ1 (1 ng/ml) (n=5, mean ± SEM, p<0.05) and this contraction was not affected by the additional presence of RvE1 (10 nM) (n=5, mean ± SEM, p=ns). (B) The pre-treatment of HBSMC-populated lattices with RvE1 (10 nM) significantly inhibited PDGF-AB induced contraction at 48 (p<0.0001), 72 (p<0.001) and 96 hours (p<0.01). In addition, no significant difference in contraction was seen overall between control lattices and those treated with both RvE1 and PDGF-AB (p=ns) suggesting that RvE1 can inhibition PDFG-AB-induced contraction back to control levels. Multiple comparisons: *** p<0.001 GF vs control, **** p<0.0001 GF vs control, # RvE1 and GF vs control, ## p<0.01 RvE1 and GF vs control, #### p<0.0001 RvE1 and GF vs control, †† p<0.01 GF vs RvE1 and GF, ††† p<0.001 GF vs RvE1 and GF, †††† p<0.0001 GF vs RvE1 and GF.*

Pre-treatment with RvE1 (10 nM) had no effect on TGFβ1-induced contraction of HBSMC-populated lattices, but Figure 3.20B shows that it significantly inhibited the ability of PDGF-AB to contract these lattices at 48 ($p<0.0001$), 72 ($p<0.001$) and 96 ($p<0.01$) hours when compared with PDGF-AB alone (n=5, mean ± SEM, $p<0.05$). The extent of inhibition of PDGF was complete, such that lattice contraction with both PDGF and RvE1 together was no different from control values.

Lipoxin A_4 (LXA_4) was investigated for its ability to modulate growth factor-induced contraction of HBSMC-populated collagen lattices. Lattices were floated in dishes containing DMEM (with 0.5% NCS) and LXA_4 for 60 minutes, before either TGFβ1 (1

ng/ml) or PDGF-AB (10 ng/ml) was added to the dish and contractions were measured over 96 hours.

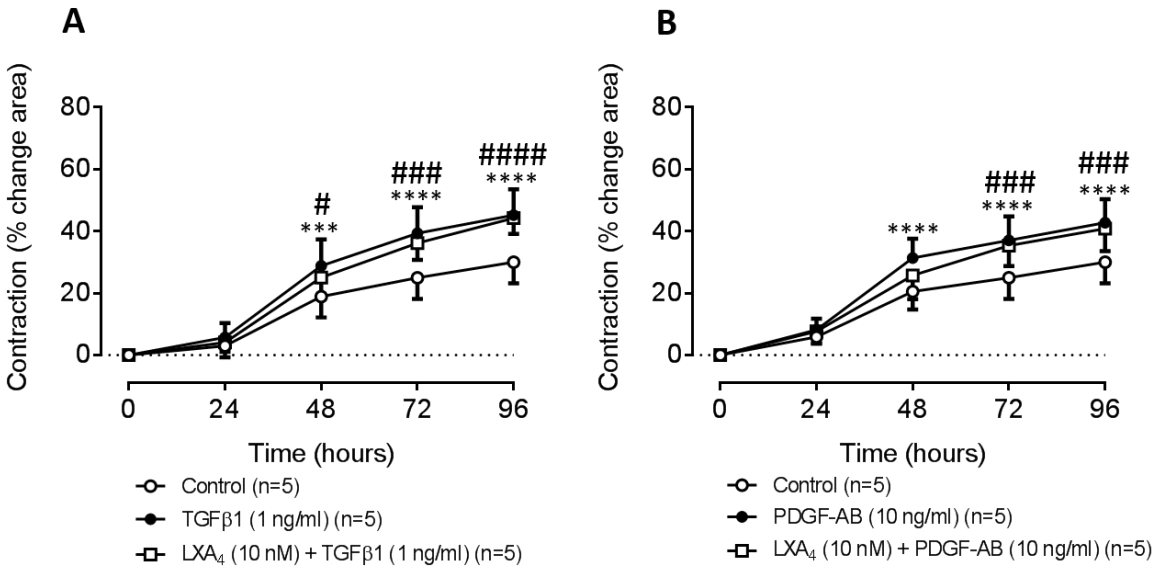

*Figure 3.21: The effect of lipoxin A_4 (LXA_4) on TGFβ1- and PDGF-AB-induced contraction of human bronchial smooth muscle cell (HBSMC)-populated collagen lattices. HBSMC-populated lattices were floated for 60 minutes in dishes containing LXA_4 (10 nM), before either TGFβ1 (1 ng/ml) or PDGF-AB (10 ng/ml) was added to the dish. Contraction of the lattices was calculated by measuring the area of the lattices at 24 hour intervals over 96 hours in total. (A) Compared to control, TGFβ1 significantly increased contraction of lattices at 48, 72 and 96 hours, but the addition of LXA_4 had no significant effect (n=5, mean ± SEM). (B) PDGF-AB mediated a significantly increased rate of lattice contraction at 48, 72 and 96 hours compared with control (n=5, mean ± SEM). Contraction in the presence of both LXA_4 and PDGF-AB was not significantly different to contraction of lattices in the presence of PDGF-AB alone. Multiple comparisons: *** $p<0.001$ GF vs control, **** $p<0.001$ GF vs control, # $p<0.05$ LXA_4 and GF vs control, ### $p<0.001$ LXA_4 and GF vs control, #### $p<0.0001$ LXA_4 and GF vs control.*

The data indicate that LXA_4 does not significantly modulate contraction of HBSMC-populated collagen lattices induced by either TGFβ1 or PDGF-AB (n=5, p=ns) (Figure 3.21).

Finally in this section, the ability of **protectin DX (PDX)** to modulate the rate of either TGFβ1- or PDGF-AB-induced contractions of HBSMC-populated collagen lattices was assessed by floating lattices in dishes with the PDX for 60 minutes and then adding the growth factors to the same dishes. Contraction of the lattices was recorded by capturing images of the lattices in their dishes at 24 hour intervals over a total of 96 hours.

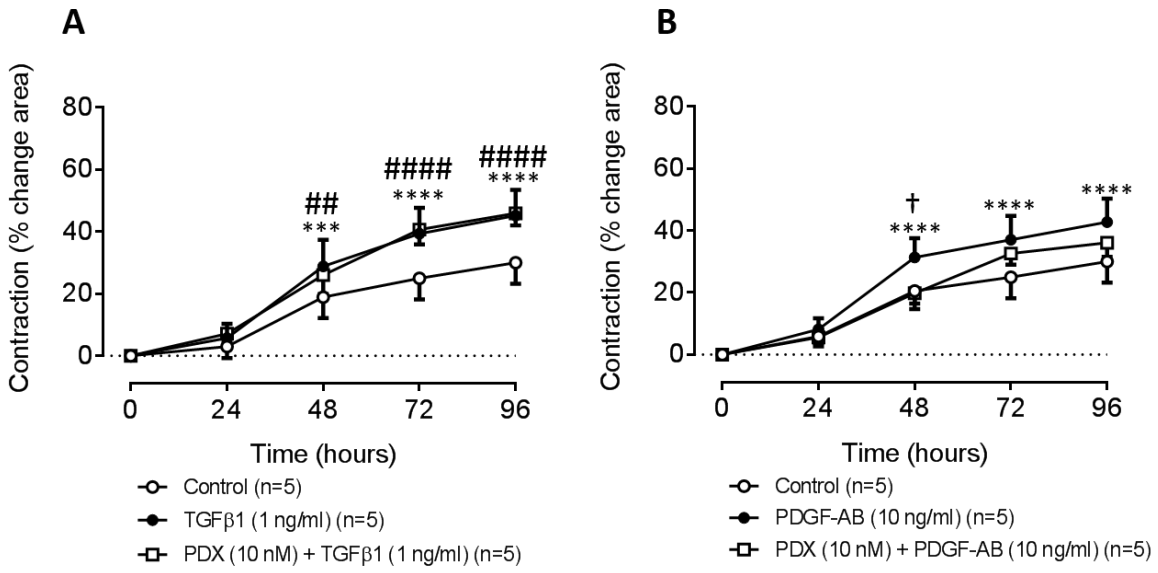

*Figure 3.22: Effect of protectin DX (PDX) on the contraction of human bronchial smooth muscle cell (HBSMC)-populated collagen lattices induced by either TGFβ1 or PDGF-AB. (A) PDX did not significantly affect the ability of TGFβ1 to induce contraction of HBSMC-populated collagen lattices (n=5, mean ± SEM, p=ns). (B) PDX did not affect PDGF-AB-induced contraction of lattices overall (p=ns), but multiple comparison testing suggests that at 48 hours PDX is able to significantly inhibit PDGF-AB-induced contraction, and this is visible on the graph (p<0.05). Multiple comparison: *** p<0.001 GF vs control, **** p<0.0001 GF vs control, ## p<0.01 PDX and GF vs control, #### p<0.0001 PDX and GF vs control, † p<0.05 GF vs PDX and GF.*

Previous work in this chapter suggested PDX (10 nM) may modestly modulate PDGF-AB-induced contraction of HLF-populated collagen lattices at both 48 and 72 hours (Figure 3.14). Here, a similar effect was seen with HBSMC-populated collagen lattices, in which PDX (10 nM) inhibited PDGF-AB-induced contraction significantly at 48 hours, but not at other time-points (Figure 3.22B). PDX was unable to significantly affect TGFβ1-induced contraction of collagen lattices (Figure 3.22A).

3.6 Results – human umbilical artery smooth muscle cell-populated collagen lattices

3.6.1 Effect of TGFβ1 and PDGF-AB on contraction of human umbilical artery smooth muscle cell-populated collagen lattices

To determine firstly whether the growth factors TGFβ1 and PDGF-AB can modulate the contraction of collagen lattices populated by HUASMC, the lattices were floated in a Petri dish with DMEM (with 0.5% NCS) with or without TGFβ1 (1 ng/ml) or PDGF-AB (10 ng/ml).

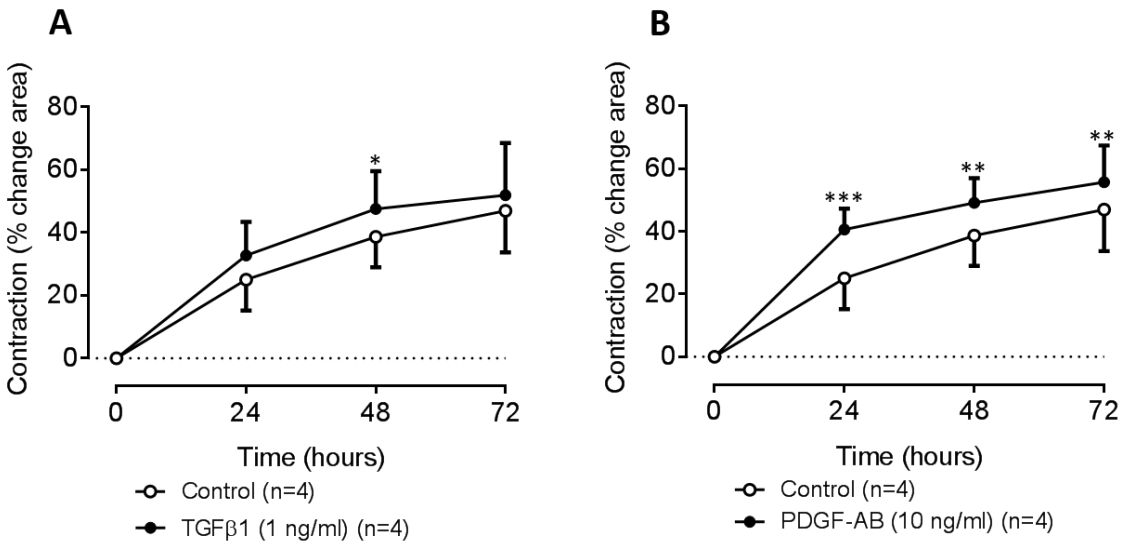

*Figure 3.23: Effect of growth factors on human umbilical artery smooth muscle cell (HUASMC)-populated lattice contraction. (A) Treatment of lattices with TGFβ1 (1 ng/ml) did not significantly increase contraction of the lattices overall (n=4, mean ± SEM, p=ns), but a multiple comparisons test suggested that the curves are significantly different at 48 hours (p<0.05). (B) Treatment of lattices with PDGF-AB (10 ng/ml) significantly increased contraction of lattices at 24, 48 & 72 hours (n=4, mean ± SEM, p<0.05). Multiple comparisons: *p<0.05 GF vs control, ** p<0.01 GF vs control, *** p<0.001 GF vs control.*

HUASMC contracted collagen lattices in the absence of growth factors (control), but the rate of contraction was significantly enhanced by treatment with TGFβ1 (1 ng/ml) at 48 hours (n=4, mean ± SEM, p<0.05) (Figure 3.23A) and by PDGF-AB (10 ng/ml) at 24, 48 and 72 hours (n=4, mean ± SEM, p<0.05) (Figure 3.23B).

3.6.2 Effect of specialised pro-resolving mediators on contraction of human umbilical artery smooth muscle cell-populated collagen lattices

The ability of specialised pro-resolving mediators applied alone to modulate contraction of HUASMC-populated collagen lattices was firstly investigated without the addition of growth factors. Here, HUASMC-populated collagen lattices were floated in 0.5% DMEM with and without RvD1, RvE1 or LXA_4 (all 10 nM) and the changes in lattice area measured at 24 hour intervals over 72 hours. The three SPM at 10 nM had no significant effect on contraction of HUASMC-populated collagen lattices over 72 hours (n=4, mean ± SEM, p=ns) (Figure 3.24).

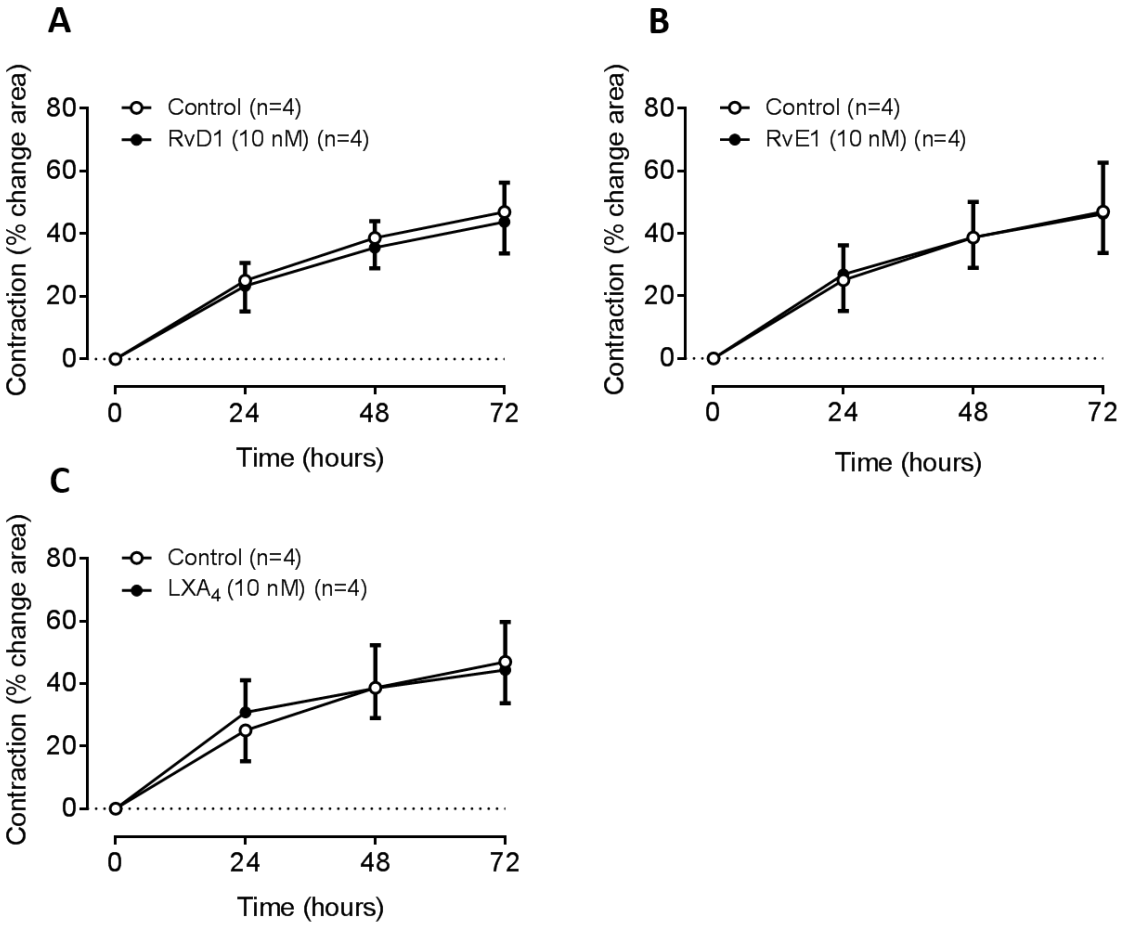

Figure 3.24: Effect of specialised pro-resolving mediators on contraction of collagen lattices populated by human umbilical artery smooth muscle cells (HUASMC). Lattices were floated in DMEM (with 0.5% NCS) ± RvD1, RvE1 or LXA_4 (10 nM) and their rate of contraction measured every 24 hours. The SPM administered alone did not significantly affect the ability of HUASMC to contract collagen lattices.

3.6.3 Effect of specialised pro-resolving mediators on growth factor-induced contraction of human umbilical artery smooth muscle cell-populated collagen lattice

Alone the SPM alone had no effect on HUASMC-populated collagen lattice contraction (Figure 3.24), the possibility that they may modulate the enhanced contraction

induced by the growth factors TGFβ1 and PDGF-AB was next explored. **RvD1** (10 nM) was investigated first (Figure 3.23).

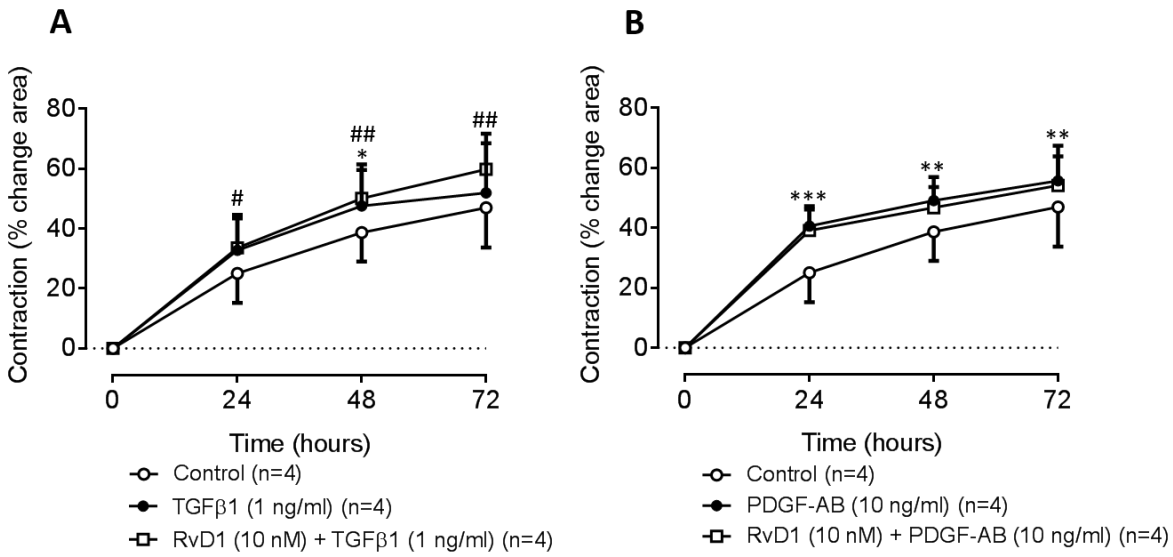

*Figure 3.25: Effect of resolvin D1 (RvD1) on growth factor (GF)-induced contraction of human umbilical artery smooth muscle cell (HUASMC)-populated collagen lattices. (A) RvD1 (10 nM) did not modulate TGFβ1-induced (1 ng/ml) contraction of HUASMC-populated collagen lattices (n=4, mean ± SEM, p=ns). (B) There is no significant difference between the contraction of those lattices treated with PDGF-AB alone and those treated with RvD1 (10 nM) and PDGF -AB (n=4, mean ± SEM, p=ns). Multiple comparisons: * p<0.05 GF vs control, ** p<0.01 GF vs control, *** p<0.001 GF vs control, # p<0.05 control vs GF and RvD1, ## p<0.01 control vs GF and RvD1.*

RvD1 is unable to modulate TGFβ1- or PDGF-AB-induced contraction of HUASMC-populated collagen lattices (Figure 3.25) (n=4, mean ± SEM, p=ns).

To determine next whether **RvE1** is capable of modulating TGFβ1- or PDGF-AB-induced contraction, HUASMC-populated collagen lattices were floated in dishes containing DMEM (with 0.5% NCS) and the GF with and without RvE1 (10 nM).

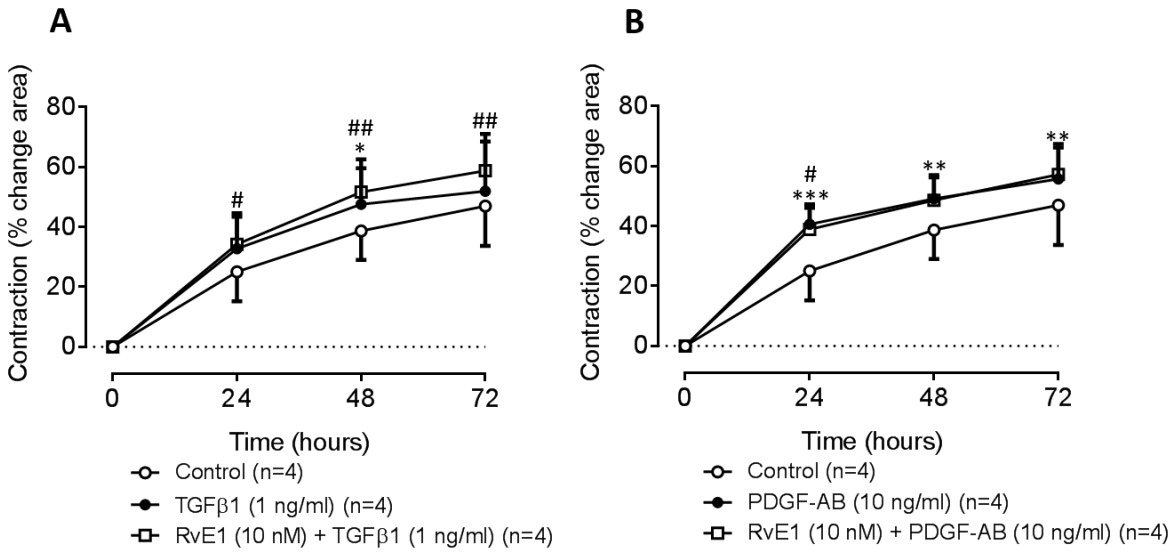

*Figure 3.26: The effect of resolvin E1 (RvE1) on growth factor-induced contraction of human umbilical artery smooth muscle cell (HUASMC)-populated collagen lattices. Lattices were floated in Petri dishes in DMEM with GF alone, with GF plus the SPM, or with neither treatment (control), and contraction measured every 24 hours. (A) There is no significant difference between lattices treated with TGFβ1 alone and lattices treated with TGFβ1 and RvE1 (n=4, mean ± SEM, p=ns). (B) RvE1 mediated no significant effect on PDGF-AB-induced contraction of HUASMC-populated collagen lattices (n=4, mean ± SEM). Multiple comparisons: * p<0.05 GF vs control, ** p<0.01 GF vs control, *** p<0.001 GF vs control, # p<0.05 GF and RvE1 vs control, ## p<0.01 GF and RvE1 vs control.*

RvE1 had no significant effect on the contraction of HUASMC-populated collagen lattices induced by either TGFβ1 or PDGF-AB (n=4, mean ± SEM, p<0.05).

To investigate whether GF-induced contraction of HUASMC-populated collagen lattices is modulated by **LXA_4** lattices were floated in dishes containing DMEM (with 0.5% NCS) with either GF alone or with GF together with LXA_4. Control lattices had neither treatment.

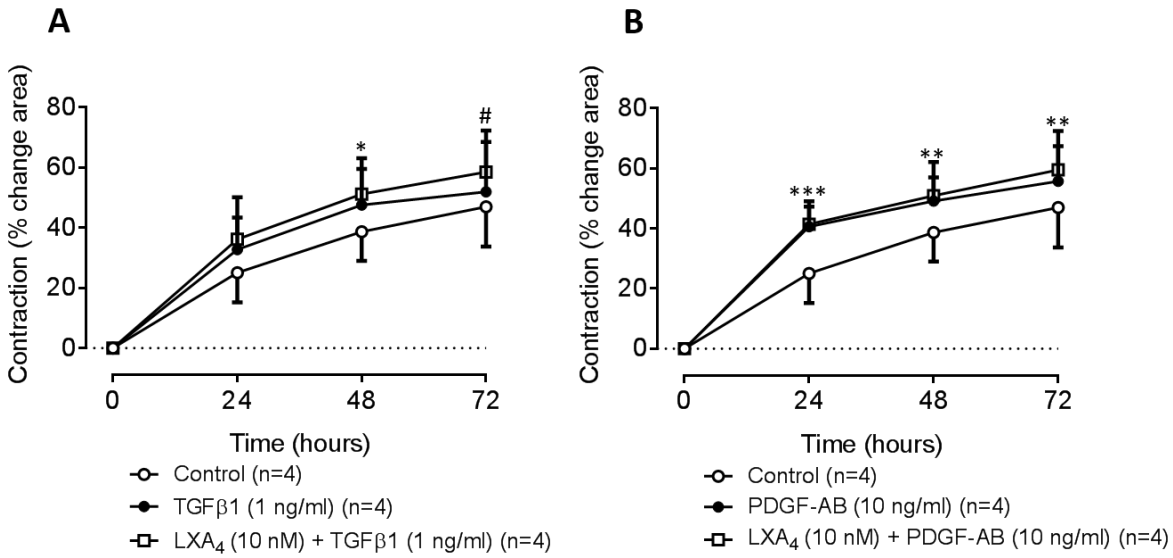

*Figure 3.27: The effect of lipoxin A₄ (LXA₄) on GF-induced contraction of human umbilical artery smooth muscle cell (HUASMC)-collagen lattices. (A) TGFβ1-induced contraction of lattices was unaffected by LXA₄ (10 nM) (n=4, mean ± SEM, p=ns). (B) LXA₄ did not modulate PDGF-AB-induced contraction of HUASMC-populated collagen lattices (n=4, mean ± SEM, p=ns). Multiple comparisons: * p<0.05 GF vs control, ** p<0.01 GF vs control, *** p<0.001 GF vs control, # p<0.05 GF and LXA₄ vs control.*

LXA_4 did not modulate contraction of lattices induced by either TGFβ1 (1 ng/ml) or PDGF-AB (n=4, mean ± SEM, p<0.05).

3.7 Summary of results

The work in this chapter investigated the ability of specialised pro-resolving lipid mediators (SPMs) to modulate the contractility of human lung fibroblasts (HLF), human bronchial smooth muscle cells (HBSMC) and human umbilical artery smooth muscle cells (HUASMC) embedded within collagen lattice matrices (Aim 1 – see section 1.9). The main findings of this chapter are given below:

- Collagen lattice contraction mediated by HLF was dependent on cell number (reaching a maximum at 150,000 cells per lattice) and inversely related to collagen concentration (over the range 1.4 to 2.32 mg/ml).
- The concentration of newborn calf serum (NCS) used in the culture medium during contraction experiments was optimised at 0.5% to produce a submaximal rate of spontaneous lattice contraction in the absence of growth factors.
- Inhibition of actin polymerisation by cytochalasin D prevented contraction of HLF-populated collagen lattices. When imaged by confocal microscopy, cells within cytochalasin D-treated lattices failed to form spindles and proper projections, even in the presence of TGFβ1.
- The SPMs RvD1, RvE1, LXA_4 and PDX administered alone were each unable to directly modulate the contraction of collagen lattices populated by HLF, HBSMC, or HUASMC.
- TGFβ1 and PDGF-AB significantly enhanced contraction of collagen lattices populated by HLF, HBSMC and HUASMC.
- The SPMs tested had no effect on TGFβ1-enhanced contraction of any of the lattices.
- RvE1 significantly inhibited PDGF-AB-induced contraction of collagen lattices populated by HBSMC.
- PDX weakly inhibited PDGF-AB-induced contraction of collagen lattices populated by either HLF or HBSMC.
- Neither RvD1 or LXA_4 had any effect on PDGF-AB-enhanced contraction of any of the lattices.

3.8 Discussion

Deposition of collagen is a hallmark of tissue remodelling in chronic inflammatory disease and its contraction is a key element of normal wound healing and scar formation in vascular and other soft tissues. These processes are regulated in part by growth factors including TGFβ1 and PDGF-AB, which have been extensively investigated using collagen lattice models. Although SPMs are putative mediators of the normal resolution of inflammation, they have not been thoroughly investigated in collagen lattice models, so this study defined the effects of RvD1, RvE1, LXA_4 and PDX in an optimised model, including their potential effects on constitutive lattice contraction and also their effects on contraction promoted by TGFβ1 and PDGF-AB.

The collagen lattice model (Figure 3.1) was initially optimised using HLF, which have a key role in sub-epithelial collagen deposition in bronchial asthma and in fibrotic processes in other chronic lung diseases. HLF-populated lattices were then investigated in parallel with lattices populated with HBSMC or HUASMC, as representatives of airway and vascular smooth muscle cells respectively. These experiments on isolated primary cells therefore throw further light on the spectrum of actions of SPMs on bronchial and vascular smooth muscle, as studied in the context of intact airway and blood vessel segments in Chapters 4 and 5 respectively.

The three cell types investigated (HLF, HBSMC and HUASMC) appear morphologically similar in culture, as they all form spindles and extend projections to maintain cell-to-cell contacts (Figure 3.2). As these were primary cells isolated from donor human lungs and umbilical arteries (section 2.8), it was important to verify the cellular phenotypes by staining for distinctive cell markers. α-Smooth muscle actin (α-SMA) is commonly used to confirm the phenotype of smooth muscle cells, since their expression of this contractile protein is typically much higher than in fibroblasts. The results in Figure 3.3 confirmed that the HLF used in the current experiments had exceptionally low levels of α-SMA expression, compared with both the HBSMC and HUASMC cultures. There were in addition differences between the HBSMC and HUASMC cultures in α-SMA expression; both cell types were fixed 24 hours after seeding (sections 2.8.2 and 2.8.3), yet α-SMA expression in HBSMC appears much less well-organised than in HUASMC. The lower level of α-SMA organisation in HBSMC may offer an explanation for the relatively low contractility of HBSMC-populated lattices (approximately 5% at 24 hours) compared to HUASMC (approx. 25% at the same time-point) (Figure 3.17 and Figure 3.23).

Validation experiments were then performed to define the optimal parameters for cell number, collagen concentration and serum concentration to produce consistent sub-maximal contraction in the absence of exogenous growth factors or SPMs. This was to ensure that changes induced by growth factors or SPMs in the spontaneous rate of contraction (either an increased rate or a decreased rate) could be readily observed. Figure 3.4 shows that spontaneous contraction was broadly proportional to HLF cell number, reaching a maximum at 150,000 cells per lattice and not increasing further with 200,000 or 250,000 cells per lattice. A cell number of 150,000 per lattice was therefore fixed for subsequent experiments. The second parameter was collagen concentration, which varies widely in different lattice models, with published studies reporting the use of 0.75 mg/ml (Kohyama et al. 2002, Kobayashi et al. 2005, Fang et al. 2013), 1 mg/ml (Cheng 2012), 1.25 mg/ml (Dallon and Ehrlich 2010), 1.5 mg/ml (Matsumoto et al. 2007) or 1.75 mg/ml (Horie et al. 2014). To determine the optimal collagen concentration in the current experiments, HLF-populated lattices were formed with collagen concentrations ranging from 1.4 to 2.3 mg/ml. A final collagen concentration of 2.0 mg/ml generated robust lattices which contracted at a submaximal rate (Figure 3.5). The third parameter was the concentration of newborn calf serum (NCS) in the DMEM used during culture with growth factors and SPMs. An NCS concentration of 0.5% produced a slower rate of contraction compared to 10% NCS (Figure 3.7), a result that is in accord with published studies (Kobayashi et al. 2005); therefore collagen lattices formed in the incubator with 10% NCS were transferred to DMEM with 0.5% NCS for subsequent culture with growth factors and SPMs (Figure 3.1).

The optimal conditions of cell number (150,000 cells per lattice), collagen concentration (2 mg/ml) and NCS concentration (0.5%) were then used for experiments to determine the effect of TGFβ1 (1 ng/ml) or PDGF-AB (10 ng/ml) on the rate of contraction of collagen lattices populated with HLF, HBSMC or HUASMC. Published studies use a range of collagen concentrations which are all optimised for each specific study depending on a number of other assay conditions such as serum concentration, assay duration, and timing and length of GF exposure. Human dental fibroblasts displayed concentration-dependent increasing levels of contraction when stimulated with 0.2, 0.6 or 3 ng/ml TGFβ1, with 0.6 and 3 ng/ml mediating very similar levels of contraction (Chan et al. 2005). Human renal fibroblast-populated lattices also contracted to similar levels in response to either 1 or 10 ng/ml TGFβ1 (Kondo et al. 2004). PDGF has also been shown to contract fibroblast embedded lattices in a concentration-dependent manner (Clark et al.

1989, Tingström, Heldin, Rubin, et al. 1992). In this latter study, both 10 and 30 ng/ml of PDGF induced high levels of contraction over just 24 hours. Various types of smooth muscle cells have been used previously in collagen lattice contraction assays but are typically stimulated with known smooth muscle contractile agonists such as histamine, methacholine (Kitamura et al. 2008) and LTD_4 (Kitamura et al. 2009). PDGF at 10 ng/ml was found to mediate contraction of collagen lattices populated with calf aortic SMC over 24 hours suggesting that this concentration may be capable of enhancing contraction in VSMC in general (Masafumi Kuzuya et al. 2004). HUASMC have been used previously in the collagen lattice contraction assay where they mediated time-dependent contraction of the lattices (Xu et al. 2013); however, no studies have investigated the ability of GFs to modulate contraction of HUASMC-populated collagen lattices.

In this chapter, 1 ng/ml TGFβ1 and 10 ng/ml PDGF-AB were chosen as submaximal concentrations known to mediate contraction of fibroblast-populated lattices. At these concentrations, the two growth factors were equally effective in significantly increasing the contraction of HLF lattices at all time points up to (and possibly beyond) 72 hours (Figure 3.8). Both growth factors also significantly increased the rate of contraction of HBSMC-populated lattices at every time-point up to 96 hours, although HBSMC (Figure 3.17) appeared somewhat less responsive to each growth factor than HLF lattices (Figure 3.8). HUASMC-populated lattice contractions (Figure 3.23) were also less responsive to the growth factors than were the HLF lattices, although they were still significantly enhanced by TGFβ1 at 48 hours and by PDGF-AB at all time-points up to 72 hours. These data provide robust growth factor-dependent responses for examination of the modulatory effect of SPMs.

Having established both the spontaneous rate of HLF-populated lattice contraction and the accelerated rates of contraction induced by the two growth factors, experiments were then performed to define the effects of SPMs, either positive or negative, on both the spontaneous and the growth factor-enhanced contractions. There is relatively little published information on the effects of SPMs on the diverse activities of fibroblasts or smooth muscle cells activity, although they have been shown to inhibit cigarette smoke extract (CSE)-induced release of pro-inflammatory mediators (IL-6, IL-8) (Hsiao et al. 2013), inhibit PDGF-induced chemotaxis of VSMC (Ho et al. 2010, Miyahara et al. 2013), inhibit TNF-α-induced expression of adhesion molecules and pro-inflammatory cytokines (IL-1β, IL-1α, IL-6) in VSMC (Miyahara et al. 2013), inhibit TGF-β1-induced proliferation and migration of fibroblasts (Herrera et al. 2015). Additionally, a recent study

found that LXA_4 concentration-dependently inhibits spontaneous contraction of human lung myofibroblasts (HLMF)-populated collagen lattices (Roach et al. 2015). In the experiments reported in this chapter, no significant effect of any of the four SPMs (RvD1, RvE1, LXA_4 and PDX) was observed on contraction of lattices populated with HLF (Figure 3.10), HBSMC (Figure 3.18) or HUASMC (Figure 3.24), when compared with those lattices in the absence of an SPM. Myofibroblasts have a more contractile phenotype than fibroblasts thus the lack of effect of LXA_4 or any of the other SPMs in this chapter may be due to a difference in the extent of spontaneous contraction induced by these two cells types, but, since only fold changes from spontaneous contraction in the absence of LXA_4 are provided in the study by Roach and colleagues, it is impossible to determine whether or not such differences exist. However, the authors also showed that treatment of HLMF with LXA_4 promoted their transition to a more fibroblast phenotype, reducing constitutive α-SMA expression and limiting the ability of the cells to construct stress fibres. The HLF used in this thesis were derived from patients with healthy lung function (GOLD 0 status) and staining revealed they have very low levels of α-SMA expression, particularly when compared to HBSMC or HUASMC (Figure 3.3). The authors of the Roach study do not specify the COPD status of the patients from whom their HMLF are derived, only that the patients are undergoing lung resection for carcinoma, but the lack of effect of LXA_4 on lattice contraction in this thesis may also reflect the basal low levels of α-SMA expression in HLF used here or differences in disease severity.

The ability of SPMs to modulate collagen lattice contraction in response to either TGFβ1 or PDGF-AB was investigated next. **RvD1** did not demonstrate any ability to modulate TGFβ1- or PDGF-induced contraction of lattices populated by any cell-type (Figure 3.11, Figure 3.19, Figure 3.25). There is little directly comparable relevant literature on the effect of SPMs on growth factor-induced contractions of collagen lattices populated by HLF, HBSMC or HUASMC. However, in epithelial cells from human small airways, RvD1 can inhibit poly(I:C)-induced pro-inflammatory signalling, with an inhibitor of TAK1, a TGFβ-activated kinase, being used to identify TAK1 as the key signalling molecule (Hsiao et al. 2014). Pre-treatment of the epithelial cells with RvD1 reduced TAK1 phosphorylation and therefore inhibited its subsequent ability to form a signalling complex. RvD1 was used at concentrations of 0.1 and 1 μM to induce such inhibitory effects, and similar micromolar concentrations were used in an earlier study from the same group (Hsiao et al. 2013). Although the inhibitory effect of RvD1 was abrogated by an ALX receptor antagonist, these RvD1 concentrations used in the study by

Hsiao and colleagues were 10- to 100-fold higher than the low nanomolar levels of RvD1 found in human blood samples from healthy volunteers (Colas et al. 2014). The nanomolar concentrations of RvD1 and other SPMs used in the studies in this thesis are therefore more likely to approach the physiological concentrations found *in vivo*. TGFβ1 is also capable of activating TAK1 (Kim et al. 2009, Choi et al. 2012), but it may not be required for cell-mediated contraction of collagen lattices induced by TGFβ1. Inhibition of actin polymerisation following treatment with cytochalasin D completely prevented cell-mediated lattice contraction even in the presence of TGFβ1 (Figure 3.15), and when imaged with a confocal microscope the cells appeared incapable of forming spindles and extending projections (Figure 3.16), indicating that lattice contraction is likely achieved through cell-mediated movement.

While 1-hour pre-treatment with **RvE1** did not modulate GF-induced contraction of collagen lattices populated by either HLF or HUASMC, it significantly inhibited PDGF-induced contraction of HBSMC-populated lattices ($p<0.05$, Figure 3.20). RvE1 reduced PDGF-induced contraction back to the basal (spontaneous) rates at 48 and 72 hours, but at 96 hours the inhibitory effect was smaller, suggesting that RvE1 delays contraction rather than suppressing it completely. RvE1 inhibits chemotaxis of vascular smooth muscle cells derived from human saphenous veins towards PDGF-BB; this was mediated by decreased phosphorylation of PDGF receptors but not by inhibition of actin polymerisation (Ho et al. 2010).

LXA_4, which shares the pro-resolving receptors ALX and GPR32 with RvD1, failed to modulate the contraction of cell-populated lattices induced by either TGFβ1 or PDGF-AB. A recent study investigated the effect of LXA_4 pre-treatment on TGFβ1-induced contraction of collagen lattices populated by human lung myofibroblasts (HLMF) (Roach et al. 2015). The HLMF were serum-starved for 24 hours then treated while still in a monolayer with LXA_4 (100 pM or 10 nM) in serum-free medium for a further 24 hours before being detached, embedded into lattices and exposed to a higher concentration of TGFβ1 (10 ng/ml) than in our experiments (1 ng/ml) for 24 hours. The longer pre-treatment of cells with LXA_4 inhibited TGFβ1-induced lattice contraction, and might explain the different outcomes compared to the 1-hour treatments that were used in this chapter. Hsiao et al. (2013) pre-treat HLF for 24 hours prior to their stimulation with CSE and the subsequent measurement of cytokine production, whilst in a similar study, blood derived macrophages and alveolar marcophages were treated with SPM for 24 hours before CSE exposure and cytokine measurement (Croasdell et al. 2015). Thus, it is possible that

more prolonged or repeated exposures to SPMs may achieve modulatory effects on collagen lattices.

Protectin X (PDX) is an isomer of protectin D1 (PD1) and both are products of DHA, but only PDX is commercially available for experiments (Balas et al. 2014). At high concentrations, PDX inhibits platelet aggregation (Chen et al. 2011), an action shared by PD1 and RvE1 (Dona et al. 2008). The latter authors postulated that PD1 and RvE1 may inhibit platelet aggregation by inhibiting actin polymerisation (Fredman and Serhan 2011). Neither PDX nor PD1 have been assessed previously for their ability to influence the behaviour of fibroblasts or smooth muscle cells. In the present experiments, there was a weak overall trend for PDX to inhibit of PDGF-AB-induced contraction of HLF-populated lattices ($p=0.06$), and multiple comparison testing suggests that at 24 and 48 hours inhibition is indeed significant. However, contraction of HLF-populated lattices in the presence of PDX and PDGF-AB remains significantly higher than control, suggesting that any inhibitory effect is negligible and unlikely to be physiological, particularly since the visual difference on the graph is small (Figure 3.14). Similar results were seen with HBSMC-populated lattices (Figure 3.22). It was recently suggested that PD1 is the major protectin product of DHA and that PDX is not responsible for the reported pro-resolving actions of protectins (Serhan, Dalli, et al. 2015). It would therefore be interesting to assess PD1 when it becomes available for modulatory activity in collagen lattices and to compare it with the PDX findings described here. Due to limitation in cell numbers, PDX was not assessed in HUASMC-populated lattices, so it would be useful to extend comparative study of PDX and PD1 in these or other types of vascular smooth muscle cells.

In summary, the collagen lattice contraction assay was successfully optimised and used to assess the ability of four SPMs from three different families to alter lattice contraction mediated by HLF, HBSMC and HUASMC, or to modulate their contraction enhanced by treatment with two different growth factors – TGFβ1 and PDGF-AB. While no SPM affected basal (cell-mediated) contraction of lattices, this may be an indication that longer pre-treatments with the SPMs are required to effect changes in the signalling pathway changes required for lattice contraction. While the same may apply to modulation of growth factor-induced enhancement of contraction, the fact that PDGF-enhanced contractions of HBSMC were inhibited strongly by RvE1 and weakly by PDX, and that PDX also weakly inhibited similar enhancement of contraction in HLF, indicates that the SPMs can exert modulatory effects after only relatively short-term exposure. RvE1 has previously been shown to inhibit chemotaxis of vascular smooth muscle cells towards

PDGF (Ho et al. 2010), suggesting that VSMC express relevant receptors and that the RvE1 and PDGF signalling pathways intersect.

Chapter 4: Effect of resolvins on contractility of bronchiolar smooth muscle

4.1 Background

This chapter covers work investigating the effects of resolvins D1, D2 and E1 on the contractions induced by carbachol, U46619 and leukotriene D_4 in bronchiolar smooth muscle from Wistar rats and patients undergoing surgery at Southampton General Hospital, as outlined in aim 2 (section 1.9). Many members of the eicosanoid family can cause bronchoconstriction (e.g. LTD_4, PGD_2, TxA_2) or bronchodilation (e.g. PGE_2, PGI_2), and some have been implicated in the excessive or inappropriate smooth muscle contraction in chronic inflammatory diseases such as asthma. Many of the same and other eicosanoids are vasoactive, with effects on blood pressure and vascular permeability, and some may be implicated in PAH and perhaps in essential systemic hypertension. In contrast, the SPMs derived from DHA or EPA are relatively novel and perhaps surprisingly their ability to contract or relax bronchial or vascular smooth muscle has not been investigated. A recent publication found that pre-treatment (every 24 hours for 2 days) of isolated human bronchial rings with RvD1 abolishes hyperreactivity to contractile agonists induced by the pro-inflammatory cytokine IL-13 (Khaddaj-Mallat et al. 2015). The aim of the experiments here is simpler; to determine any inherent ability of resolvins to modulate smooth muscle contraction, without the added complexity of a pro-inflammatory treatment as in the study by Khaddaj-Mallat et al.

The technique used in this chapter is wire myography, which measures changes in isometric tension in response to the addition of an agonist or inhibitor. In the experiments performed here, three different smooth muscle contractile agonists were used – carbachol, U46619 and leukotriene D_4. Carbachol is a stable acetylcholine (ACh) mimetic, and is a non-selective agonist of both the nicotinic and muscarinic ACh (mACh) receptors. However, it is thought to be the Gαq-linked M_3 mACh receptor present on bronchial smooth muscle cells that is responsible for bronchoconstriction in response to carbachol.

The second agonist used in this chapter, U46619, is a stable thromboxane A_2 receptor (TP) agonist. Thromboxane is derived from the omega-6 PUFA, arachidonic acid, and has both pro-contractile and pro-inflammatory properties. Leukotriene D_4 (LTD_4) is the most potent bronchoconstrictor of human airways currently known, acting as an agonist at the $cysLT_1$ receptor present on bronchial smooth muscle cells. Like thromboxane, this classical eicosanoid is synthesised from arachidonic acid and in addition to its pro-contractile activity, it also mediates potent pro-inflammatory effects. The often opposing actions between omega-6 lipid mediators such as LTD_4 and thromboxane and the omega-3-

derived resolvins during acute inflammation is an important reason for choosing to look at the effect of resolvins on contraction induced by these two eicosanoids.

Although there are 6 known resolvins derived from docosahexaenoic acid (DHA), only two are commercially available – resolvin D1 (RvD1) and resolvin D2 (RvD2). RvD1 acts via the orphan receptor GPR32 and the ALX/FPR2 receptor (Krishnamoorthy et al. 2010), whilst RvD2 has recently been shown to activate a different orphan receptor – GPR18 (Chiang et al. 2015). The E-series resolvins, derived from the omega-3 PUFA eicosapentaenoic acid (EPA), are a smaller family of lipids, consisting of just RvE1, RvE2 and RvE3, of which only RvE1 is readily available. Therefore the three commercially-available resolvins, RvD1, RvD2 and RvE1, were investigated for their effects on the contractility of rat and human bronchiolar tissue.

4.2 Protocol

The technique used in this chapter is wire myography, an organ bath apparatus traditionally used to study the reactivity and contractility of live tissue in response to reagents in the surrounding medium. Three experimental designs (A,B,C) were used in this chapter as described below.

4.2.1 Experimental design A – pre-constriction/reversal

Pre-constriction/reversal experiments were performed with rat and human bronchioles to determine whether resolvins can *reverse* constrictions previously induced by known airway smooth muscle agonists – i.e. to mediate active relaxation of a pre-constricted tissue. Rat bronchioles reliably constrict in response to carbachol (CCh) and so it was ideal to begin exploring the ability of resolvins to relax rat airways.

A sub-maximal concentration of each contractile agonist is determined as this will be more sensitive to inhibition by a relaxant substance than a concentration producing a maximal (plateau) response. To determine the submaximal concentration of carbachol, an EC_{80} (concentration required to evoke 80% of the maximum response) was calculated from a full CCh cumulative concentration-response curve for each individual bronchiole segment. Segments were then contracted to 80% of maximal using carbachol at its EC_{80}, and once a stable response was achieved, cumulative concentrations of each resolvin, or a single concentration of the muscarinic receptor antagonist atropine, or of the beta-2 adrenoceptor agonist salbutamol, were added to the myography bath to investigate their

ability to relax the pre-constricted tissue (Figure 4.1). Ten minutes was allowed for these agents to begin to relax the pre-constricted bronchioles.

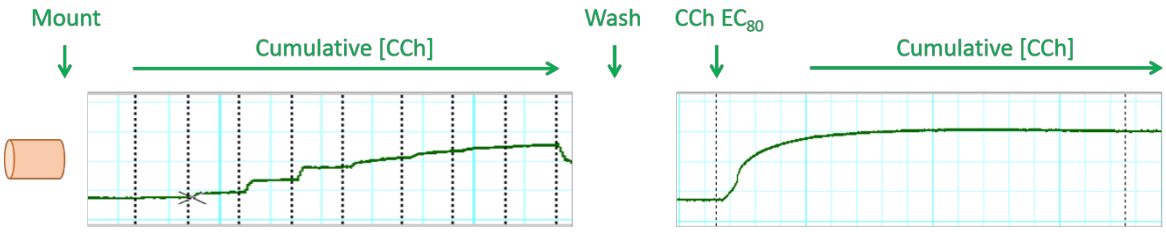

Figure 4.1: Experimental design A – reversal of a pre-constriction. Functional viable segments of rat bronchiole were constriction with cumulative concentrations of carbachol (CCh) to determine the EC_{80} for each individual segment. Following PSS washes, the segment was constricted with the CCh EC_{80} and left to plateau. The segment was then exposed to a resolvin to determine whether the resolvin can reverse a pre-constriction and thus relax a bronchiole segment. As negative controls, some segments were left untreated instead, whilst others were exposed to atropine or salbutamol to provide positive controls.

Leukotriene D_4 (LTD_4) was used to investigate the ability of resolvins to reverse pre-constriction of human bronchioles to a potent constrictor mediator implicated in human bronchial asthma. Because work described later in this chapter suggests that human bronchioles undergo tachyphylaxis to repeated LTD_4 exposures, even after washing, a single LTD_4 concentration of 100 nM was chosen to submaximally constrict human bronchioles. This concentration was defined as submaximal based on separate LTD_4 cumulative concentration-response curves on other human bronchioles, so it cannot be confirmed as an EC_{80} value in the exact same segments used in the present experiments. This procedure therefore avoided the risk of tachyphylaxis to LTD_4 by exposing the segments in the present experiments to only one LTD_4 exposure before applying the resolvin. Upon stabilisation of the sub-maximal LTD_4 response, the bronchiole was then exposed to a single concentration of resolvin (100 nM) to determine whether it could reverse the LTD_4-induced pre-constriction (Figure 4.2). It was decided that the use of a single concentration resolvin would be preferable to cumulative concentrations of resolvin since any modulation may take time to mediate its effect and thus the incorrect concentration of resolvin might be attributed to any effect seen.

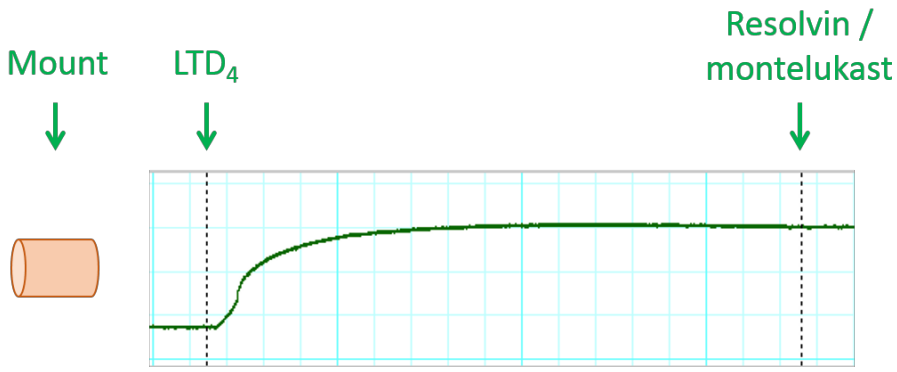

Figure 4.2: Experimental design A - human bronchioles are constricted with LTD_4 (100 nM) and then exposed to resolvin E1, D1 or D2 (100 nM), or the $CysLT_1$ receptor antagonist, montelukast (10 µM). Any change in tension is recorded and expressed as % relaxation.

In separate experiments, montelukast was used to investigate whether or not human bronchioles pre-constricted with LTD_4 could be relaxed with a known $CysLT_1$ receptor antagonist.

4.2.2 Experimental design B – cumulative concentration-response curves in series

In some experiments described in this chapter, the ability of resolvins to modulate agonist-induced constriction of rat and human bronchioles was investigated by comparing cumulative concentration-response curves for the agonist in the absence and then in the presence of (one or more) fixed concentrations of the resolvin. Functional viability of tissues was first confirmed as a positive response to KPSS (then washed with PSS to return to baseline tension). The first cumulative agonist concentration-response curve is completed, then the tissues are washed again with PSS to restore baseline tension, then incubated with the resolvin for 1 hour before performing the second cumulative concentration-response curve in the continued presence of the resolvin. Comparison between the first curve (the agonist on its own) and the second curve (the agonist in the presence of resolvin) allows any activity of the resolvin to be defined (Figure 4.3). In addition, in control experiments the resolvin treatment was omitted – in this case the two cumulative concentration-response curves should be similar if the segments remain viable and no tachyphylaxis occurs to the agonist. The advantage of this model is that responses to resolvins are compared to a control in the same tissue segments so they can be analysed statistically by paired tests.

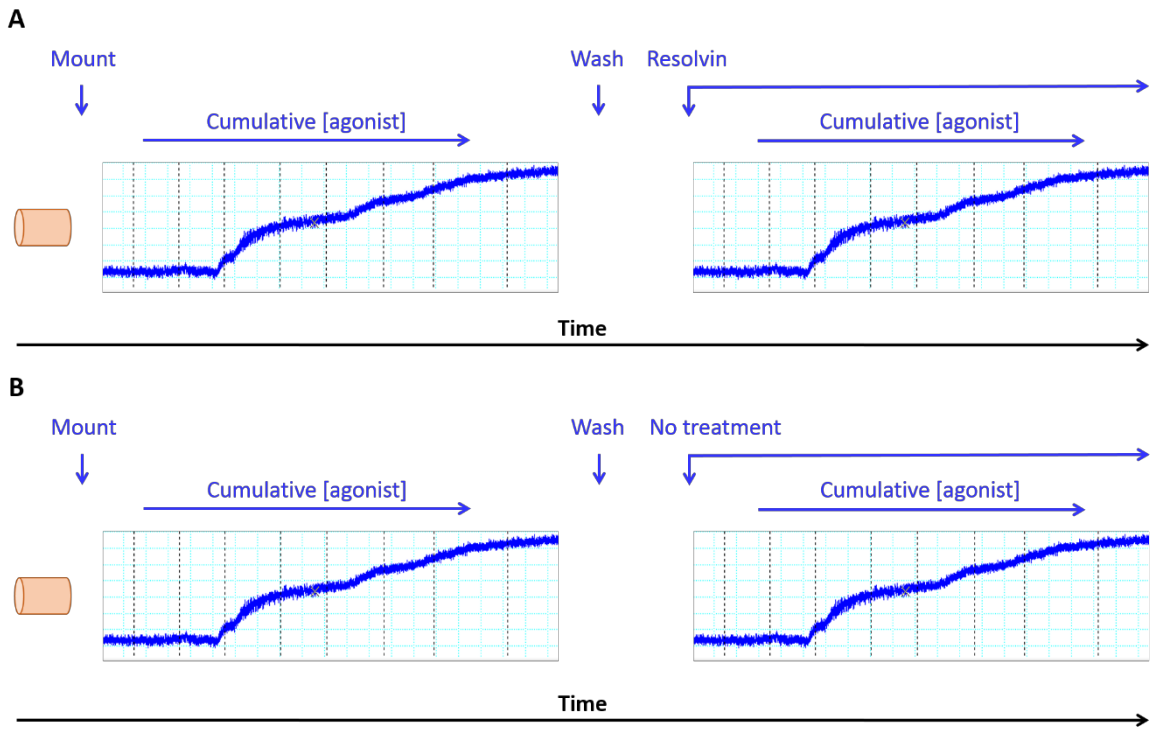

Figure 4.3: Experimental design B – cumulative concentration-response curves in series. Viable tissue segments on the wire myograph were first treated with cumulative concentrations of agonist (left). Baseline tension was restored with PSS and the segments were incubated with resolvin (A) or without resolvin (B) for 1 hour. Subsequently, the segments were constricted still in the presence/absence of resolvin with the same agonist as before.

4.2.3 Experimental design C – adjacent segments in parallel

To further ensure that differences in tissue segment responses to agonists are not affected by unstable baseline tension, loss of functional viability, or tachyphylaxis to the agonist, a third experimental model was employed that compared responses using adjacent segments in parallel chambers, with one tissue treated with a resolvin and the other tissue untreated, before measuring the response of each tissue to the contractile agonist. Segments were taken from adjacent sites in the bronchiole to reduce variation in responses between segments at different bronchiolar sites. For example, Figure 4.4 shows adjacent bronchiole segments either left untreated for 1 hour (NT) or treated for 1 hour with RvD1 (10nM), before being constricted with a single concentration of LTD_4 (100 nM).

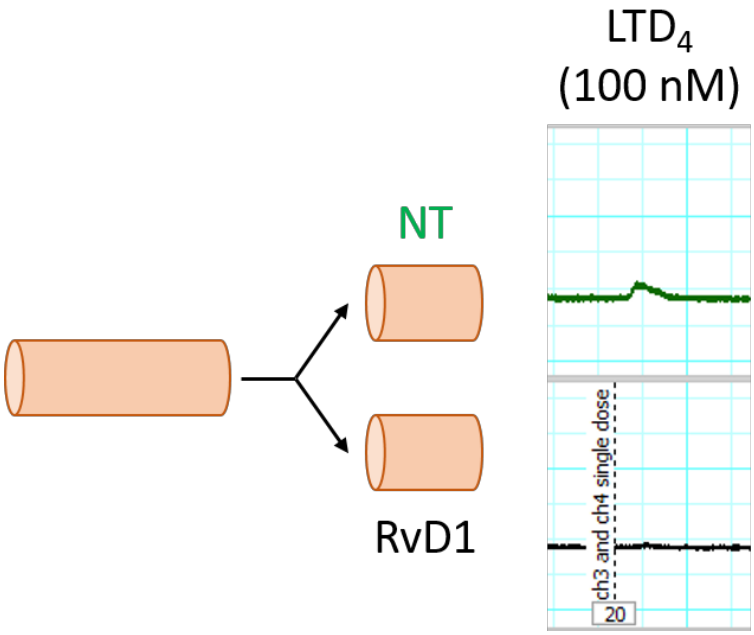

Figure 4.4: Experimental design C – pre-treatment of adjacent rat bronchiole segments with or without RvD1 on LTD4-induced constriction. One rat bronchiole was divided into two adjacent segments mounted in parallel in separate wire myograph chambers. After confirming their functional viability with KPSS (then washed with PSS), one segment was incubated without treatment for 1 hour and the other incubated with RvD1 (10 nM) for 1 hour, before both segments were exposed to LTD4 (100 nM).

4.3 Results – effect of resolvins on the contractility of rat bronchioles

4.3.1 Contraction of rat bronchioles by carbachol and the effects of atropine and salbutamol

The ability of isolated rat bronchioles to constrict in response to the stable acetylcholine mimetic carbachol was assessed using a cumulative concentration-response curve (Figure 4.5).

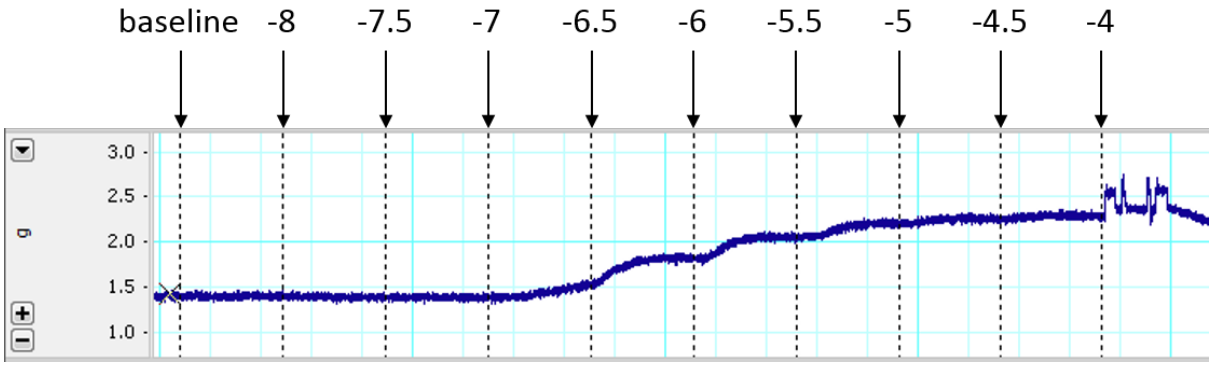

Figure 4.5: A raw Chart Lab trace to illustrate the response of rat bronchioles to a carbachol cumulative concentration-response curve (10^{-8} M to 10^{-4} M).

As described in chapter 2, the response of bronchioles to an agonist is expressed as a percentage of the response to KPSS to ensure functional viability and to correct for variations in segment size (Figure 4.6).

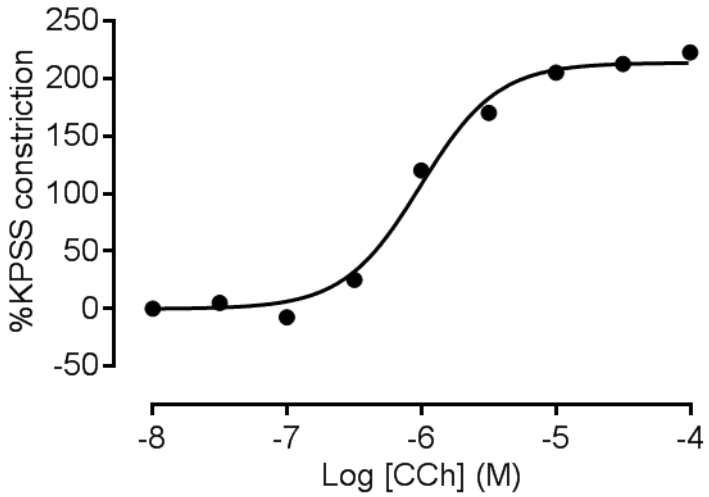

Figure 4.6: Converting a carbachol (CCh) cumulative concentration-response curve to one that is normalised to the KPSS constriction and expressed as a percentage of the KPSS constriction. This figure shows how the raw trace in Figure 4.5 looks following normalisation to the KPSS response.

Carbachol generates a concentration-dependent contractile response with a sigmoidal curve. Since both calcium-dependent and calcium-independent pathways contribute to agonist-induced constriction of intact tissue segments, and that smooth muscle contraction is primarily dependent upon agonist-induced release from intracellular calcium stores rather than changes in membrane potential and voltage gated channels (see section 1.5), it is unsurprising that constriction is >200% of the KPSS response in this example.

With the knowledge that rat bronchioles respond well to CCh, two bronchodilator drugs, namely, the muscarinic receptor antagonist atropine, and the beta-2 adrenoceptor agonist salbutamol and they were tested for their ability to reverse constriction induced by CCh. To do this, the concentration of carbachol required to evoke 80% of the maximum response (EC_{80}) was calculated individually for each bronchiole segment (Figure 4.7).

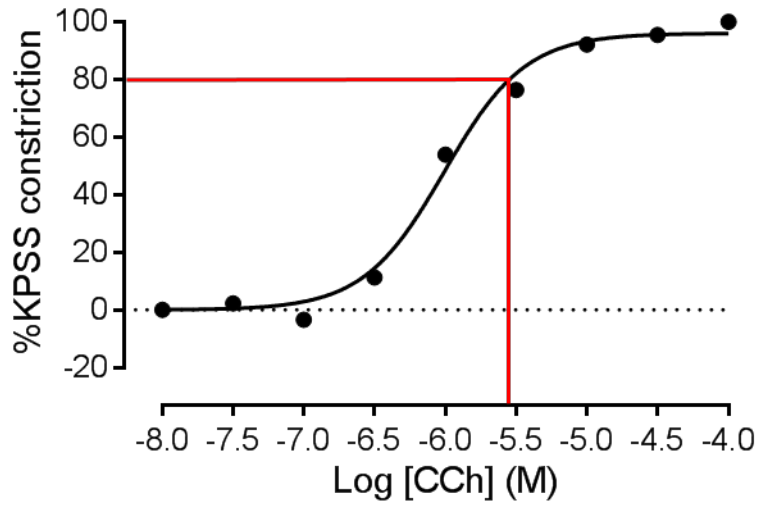

Figure 4.7: Calculating the concentration of carbachol required to elicit a submaximal response (EC_{80}) from a concentration-response curve. Expressing carbachol responses, which is measured as tension (in grams), as percentages of the maximum response to KPSS normalises the responses in segments of varying size, and allows the calculation of the concentration of carbachol required to generate 80% of the maximum KPSS constriction (the carbachol EC_{80}). The bronchiole segment is constricted submaximally with the carbachol EC_{80} and when a stable response is reached the bronchodilator drug (atropine or salbutamol) is added.

The bronchiole segments were submaximally constricted with the carbachol EC_{80} and left to generate a stable contraction before the addition of atropine (10 µM) or salbutamol (10 µM) to the myograph chamber (experimental design A). Some chambers received no

additional drug and these provided the baseline carbachol response as a control. The effects of atropine and salbutamol are shown in Figure 4.8.

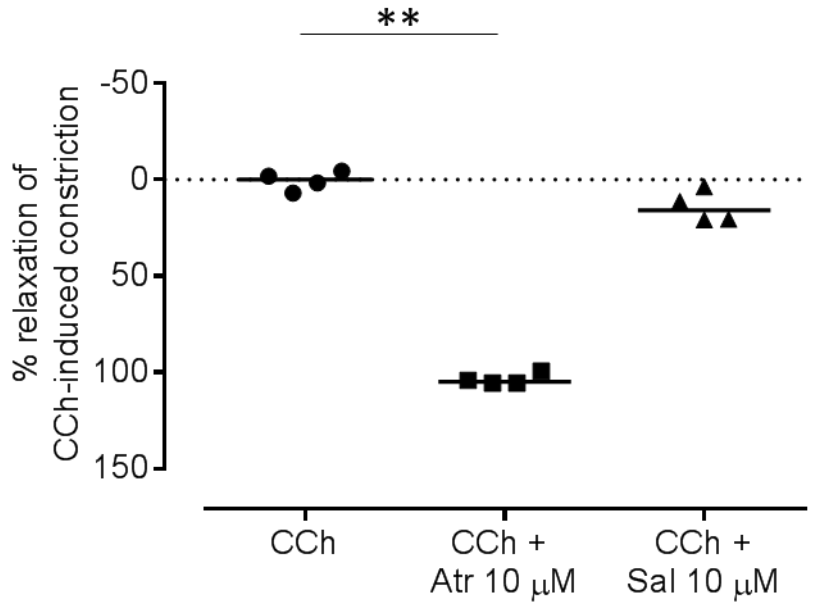

Figure 4.8: Relaxation of carbachol (CCh)-preconstricted rat bronchioles. Rat bronchioles constricted with the stable acetylcholine mimetic carbachol (CCh EC_{80}) were exposed to either the anti-muscarinic atropine (Atr) (10 μM) or the beta-1 adrenoceptor agonist salbutamol (Sal) (10 μM) (experimental design A). In the absence of bronchodilator drug, the carbachol constrictions of were stable,but those treated with atropine completely relaxed (n=4, line at median, p<0.01, Kruskal-Wallis with Dunn's multiple comparisons). Salbutamol did not significantly relax carbachol-constricted rat bronchioles (n=4, line at median, p=ns, Kruskal-Wallis with Dunn's multiple comparisons).

The purpose of the above experiment was to determine whether, under the *in vitro* setting of a wire myograph, bronchioles constricted with a muscarinic contractile agonist (carbachol) could be relaxed pharmacologically by atropine acting directly as a competitive antagonist at the muscarinic (M3) receptor, and/or physiologically by salbutamol acting as a relaxant agonist at the beta-2 adrenoceptor. This point becomes important later in the thesis in relation to the evidence that resolvins may act either as pharmacological antagonists at the receptors of contractile lipids, and/or as physiological relaxants by acting as agonists at their own resolvin receptors. In this experiment, atropine (10 μM) fully relaxed the CCh-constricted rat bronchioles (n=4, p<0.0001) in comparison to those CCh-constricted bronchioles which received no additional treatment (Figure 4.8). This result confirms that bronchioles in the wire myography module can be used effectively to detect relaxation caused by competitive antagonism of a contractile agonist.

In contrast, salbutamol, the potent beta-2 adrenergic receptor agonist, failed to relax the CCh-constricted bronchioles (n=4, p=ns), suggesting physiological antagonism of an established contractile response may be more difficult to achieve in wire myography, possibly based on the differential expression and signalling activity of relevant receptor types in animal and human bronchioles.

4.3.2 The effect of resolvins on rat bronchioles constricted submaximally with carbachol.

The ability of resolvins to relax rat bronchioles was assessed in the same manner above (experimental design A; see section 4.2.1). Bronchioles were pre-constricted with a submaximal concentration (EC_{80}) of carbachol and cumulative concentrations of resolvins D1, D2 or E1 (1 pM – 1 µM) were added to the chamber. The results are shown in Figure 4.9.

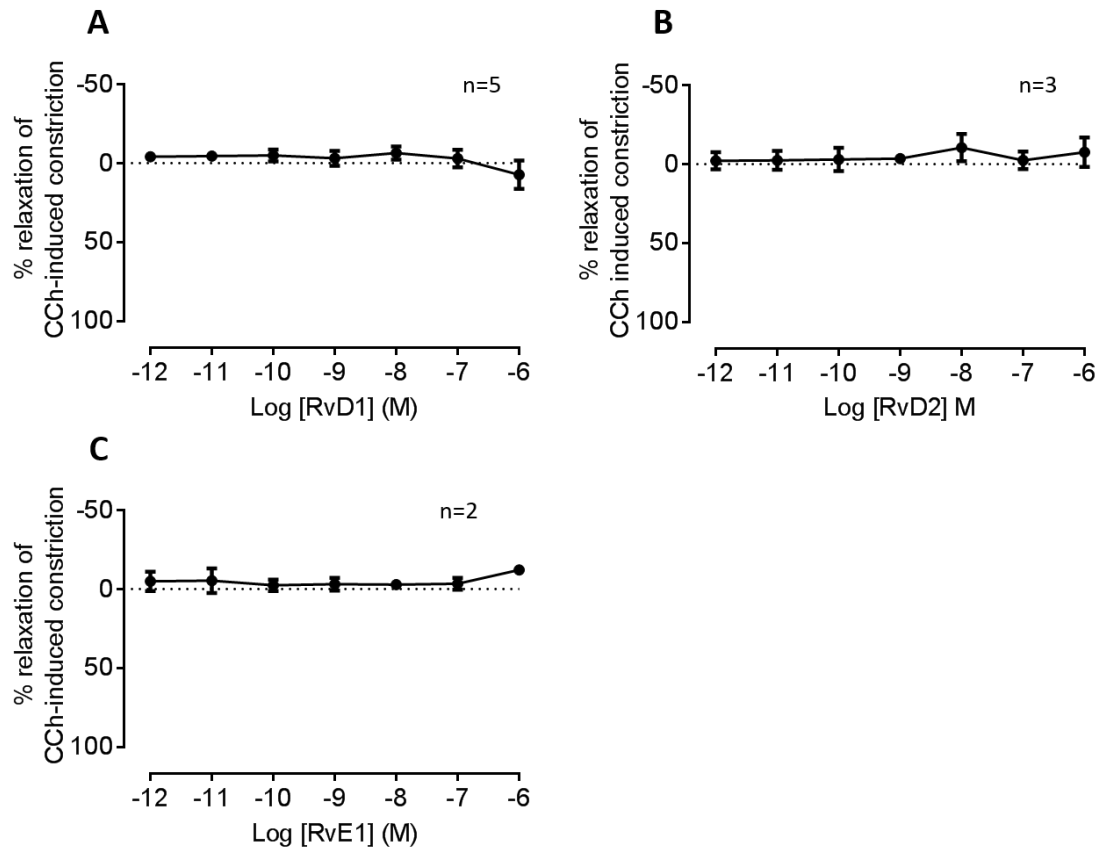

Figure 4.9: Effects of resolvins (Rv) D1, D2 and E1 on carbachol (CCh)-constricted rat bronchioles. Rat bronchioles were stably pre-constricted with a submaximal concentration (EC_{80}) of CCh, cumulative concentrations of each Rv were added (experimental design A – see section 4.3.1). (A) RvD1 did not significantly modulate CCh-induced pre-constriction of the rat bronchioles (n=5, mean ± SEM, p=ns, Friedman non-parametric test). (B) Similarly, cumulative concentrations of RvD2 had no significant effect (n=3, mean ± SEM, p=ns, Friedman non-parametric test). (C) RvE1 also showed no apparent effect on CCh pre-constricted rat bronchioles (n=2, mean ± SEM).

The data in Figure 4.9 indicate that over a concentration range from picomolar to micromolar, RvD1, RvD2 and RvE1 did not relax rat bronchiole segments pre-constricted with carbachol in this wire myography model, despite their functional viability demonstrated with KPSS and carbachol and the profound relaxation induced by a muscarinic antagonist.

4.3.3 The ability of resolvins D1 and E1 to modulate carbachol concentration-response curves in rat bronchioles

In addition to determining whether resolvins can relax pre-constricted bronchioles (experimental design A), experiments were also performed to determine whether pre-treatment with resolvins can modulate the subsequent constriction of bronchioles by known smooth muscle agonists (experimental design B; see section 4.2.2) when carried out as a pre-treatment. Functionally-viable rat bronchioles mounted on a wire myograph were constricted with cumulative concentrations of CCh and then washed to restore baseline tension. The bronchioles were then incubated with (or without) resolvins D1 or E1 (10 nM) for 1 hour before a second CCh cumulative concentration-response curve was performed in the continued presence (or absence) of the resolvin.

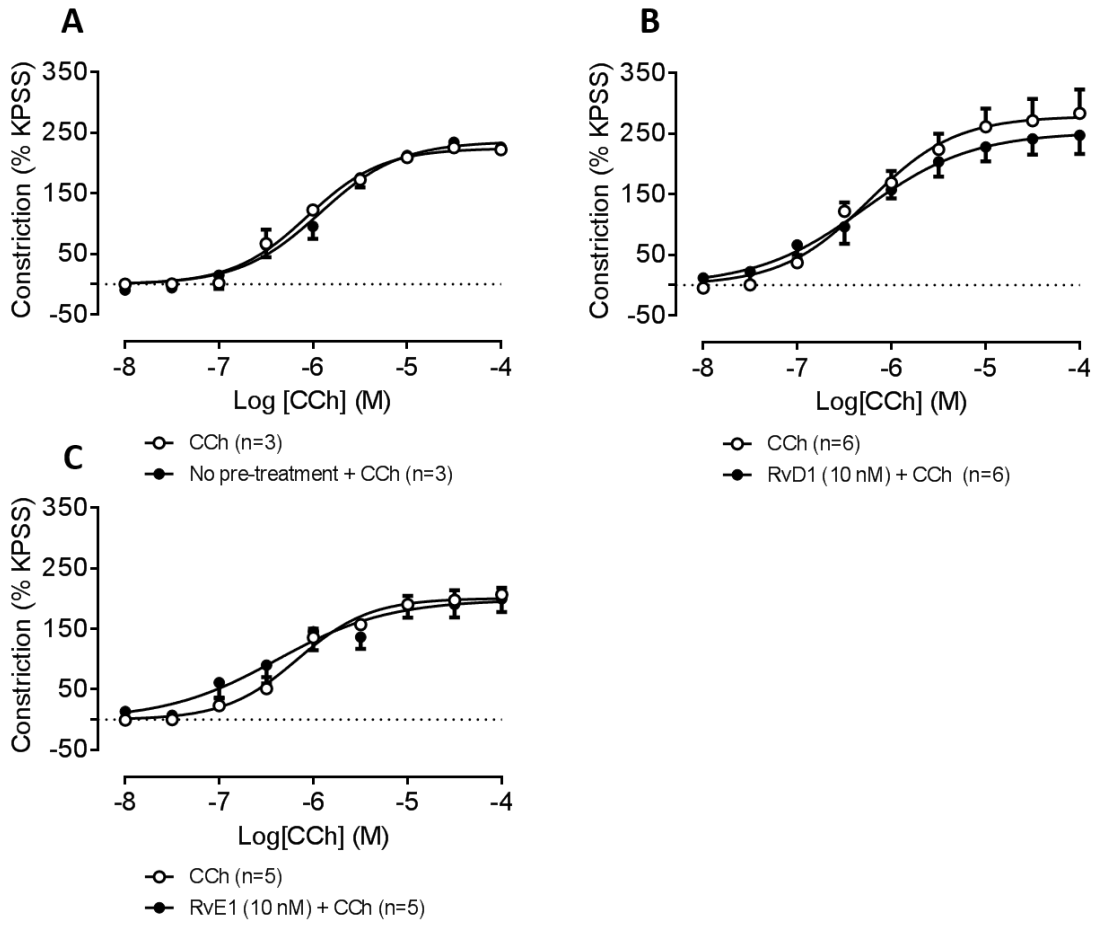

Figure 4.10: The ability of resolvins D1 and E1 pre-treatment to modulate carbachol (CCh)-induced constriction of rat bronchioles. (A) In those bronchioles constricted by carbachol in the absence of resolvin (no pre-treatment), the second CCh cumulative concentration response curve did not differ significantly from the first (n=3, p=ns, two-way ANOVA), confirming that carbachol responses are consistent over the timescale of the experiment. Incubation with either (B) RvD1 (n=6) or (C) RvE1 (n=5) at 10 nM each for 1 hour had no significant effect on the second CCh cumulative concentration response curve (mean ± SEM, p=ns vs first CCh curve).

In the experiment shown in Figure 4.10, carrying out a cumulative concentration-response curve prior to, and then again following a 1 hour incubation with a resolvin, it is possible to compare the response to a contractile agonist before and after the addition of resolvin (experimental design B). In this case, there was no significant effect on CCh-induced constriction of rat bronchioles of RvD1 (10 nM, n=6, p=ns) or RvE1 (10 nM, n=5, p=ns). Experiments carried out without the resolvin treatment confirmed that rat bronchioles produce reproducible carbachol concentration-response curves over the timescale of the experiment, with no difference observed between the first and second CCh curves (n=3, p=ns, Figure 4.10A).

4.3.4 The ability of resolvins D1 and E1 to modulate U46619 concentration-response curves in rat bronchioles

To investigate whether resolvins can modulate the constriction of rat bronchioles by the stable thromboxane mimetic U46619, segments were constricted with cumulative concentrations of U46619 (1 nM – 1 µM), then washed to restore baseline tension before incubating with (or without) resolvin D1 or E1 (10 nM) for 1 hour. A second U46619 cumulative concentration-response curve was then carried out in the presence (or absence) of RvD1 or RvE1 (experiment design B).

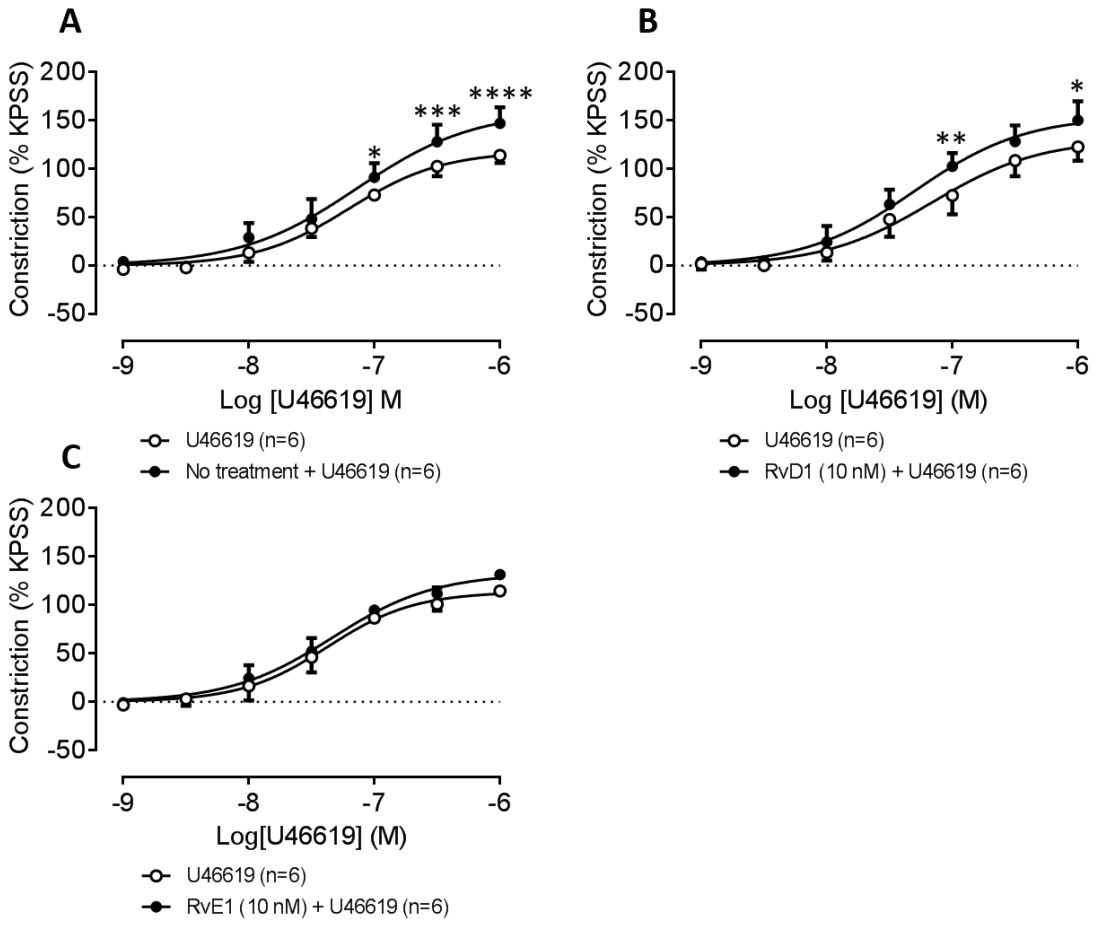

Figure 4.11: Ability of resolvin (Rv) D1 or E1 to modulate U46619-induced constriction of rat bronchioles. Using experimental design B, the ability of RvD1 or RvE1 (10 nM) to modulate U46619-induced constriction of rat bronchioles was assessed. (A) Two cumulative concentration response curves to U46619, which were separated by a washout and a 1 hour no pre-treatment incubation, suggest an increased response to U46619 in the second curve compared with the first at the higher U46619 concentrations, but this was not significant over the whole concentration range when analysed by two-way ANOVA (n=6, p=0.14). (B) In bronchioles where the second U46619 cumulative concentration-response curve was carried out in the presence of RvD1 (10 nM), there also appears to be an increased response compared with the initial U46619 curve at some higher U46619 concentrations, but again this did not reach significance overall by two-way ANOVA (n=6, p=0.16). (C) Bronchioles incubated with RvE1 (10 nM) for 1 hour showed no significant difference between the first and second U46619 cumulative concentration response curves at any single

*U46619 concentration or overall (n=6, p=0.31, two-way ANOVA). Multiple comparisons: * p<0.05 U46619 vs NT/Rv + U46619, ** p<0.01 U46619 vs NT/Rv + U46619, *** p<0.001 U46619 vs NT/Rv + U46619, **** p<0.0001 U46619 vs NT/Rv + U46619.*

The data in Figure 4.11 suggest that there is a trend for increased responses to higher concentrations of U46619 after the 1 hour incubation in the complete absence of resolvin (Fig 4.10A), although this is not apparent at lower U46619 concentrations, or overall when analysed by ANOVA. The change seems to be an increase in the magnitude of contractile response (vertical shift upwards) rather than an increased sensitivity to U46619 (no horizontal shift to right). This tendency for increased responsiveness of rat bronchioles to U46619 over the course of the experiment probably underlies the similar shift observed at high U46619 concentration following RvD1 incubation (Fig 4.10B). The lack of a similar shift in responsiveness after RvE1 incubation (Fig 4.10C) might suggest that RvE1 prevents the spontaneous increase in U46619 responsiveness over time, but a more cautious interpretation would be that the magnitude of the effect is modest and that there is no clear evidence of either resolvin affecting it significantly. It does nevertheless illustrate the value of including the 'no treatment' arm in the experimental protocol.

4.3.5 The ability of resolvin D1 to modulate leukotriene D_4 concentration-response curves in rat bronchioles

The importance of using experimental design B (as illustrated in section 4.3.4 above) lies in its ability to control for variations in tissue responsiveness or sensitivity arising over the course of the experiment in which bronchiole segments receive a series of treatments and incubations. Such changes could arise from tachyphylaxis or other changes in sensitivity to the contractile agonist, or to spontaneous metabolic changes in tissue viability over time in the myograph chambers. The potential for such changes was demonstrated in the early experiment described below, using leukotriene (LT) D_4 as the contractile agonist in rat bronchioles, and it was compounded by the relatively small proportion of rat bronchioles that generated a successful concentration-response curve to this mediator. The experiments explored the ability of RvD1 to modulate the constriction of rat bronchioles by LTD_4, with the first LTD_4 cumulative concentration-response curve being followed by a 1 hour incubation with RvD1 (10 nM). The second LTD_4 concentration-response curve in the presence of RvD1 was then compared with the first curve, but without the benefit of a 'no resolvin treatment' arm to control for changes in tissue responsiveness. The results are

shown in Figure 4.12, which suggested forcefully that RvD1 (10 nM, 1 hour) can completely inhibit the ability of LTD_4 to constrict rat bronchioles *in vitro*.

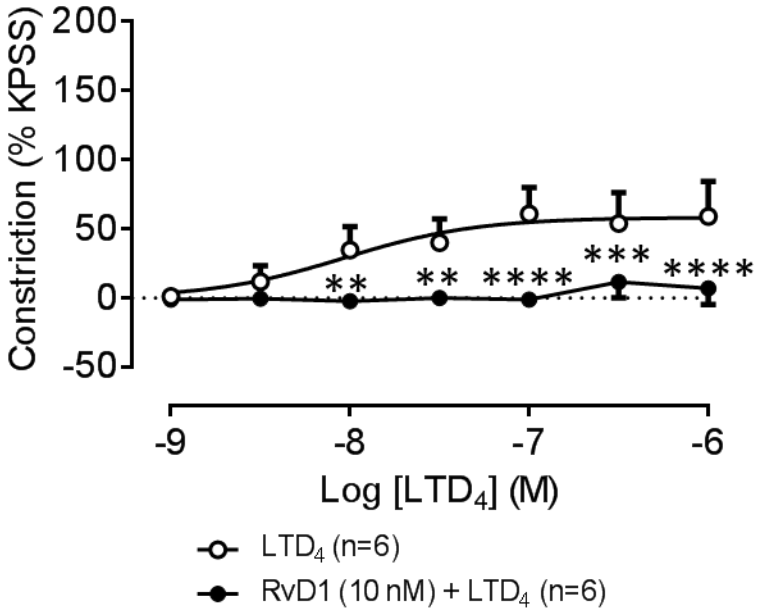

*Figure 4.12: Effect of RvD1 (10 nM) on leukotriene D_4-induced constriction of rat airway. The data, obtained using experimental design B, suggest that following incubation with RvD1, the contractile response to LTD_4 is completely abolished (n=6, $p<0.05$, two-way ANOVA) when compared with the LTD_4 curve carried out prior to the incubation. Multiple comparisons: ** $p<0.01$ LTD_4 vs RvD1 and LTD_4, *** $p<0.001$ LTD_4 vs RvD1 and LTD_4, **** $p<0.0001$ LTD_4 vs RvD1 and LTD_4.*

At a similar time to performing these experiments on LTD_4-constricted rat bronchioles, analogous experiments performed in human bronchioles using experimental design B clearly demonstrated a problem with tachyphylaxis to LTD_4, giving a false impression that LTD_4 constriction was abrogated by resolvin treatment (see section 4.4.1 below). LTD_4 produces markedly greater constriction of human airway than rat airways, and the relatively low proportion of rat bronchiole segments that generated a measurable response made it unrewarding to continue investigating rat bronchioles using the early experimental approach. The effect of RvD1 on LTD_4-induced rat bronchiolar constriction was therefore examined using a parallel design on adjacent segments (experimental design C; see section 4.2.3), which eliminates the need for repeated LTD_4 exposures and hence eliminates the possibility of tachyphylaxis confounding the resolvin results.

In this new experiment, the two adjacent segments of rat bronchiole were mounted in separate chambers in the wire myograph, tested for functional viability with KPSS then immediately incubated for 1 hour with or without RvD1 (10 nM). Subsequently, without

any washout, a single concentration of LTD_4 (100 nM) was tested on each of the adjacent bronchiole segments and their contractile responses measured (Figure 4.13).

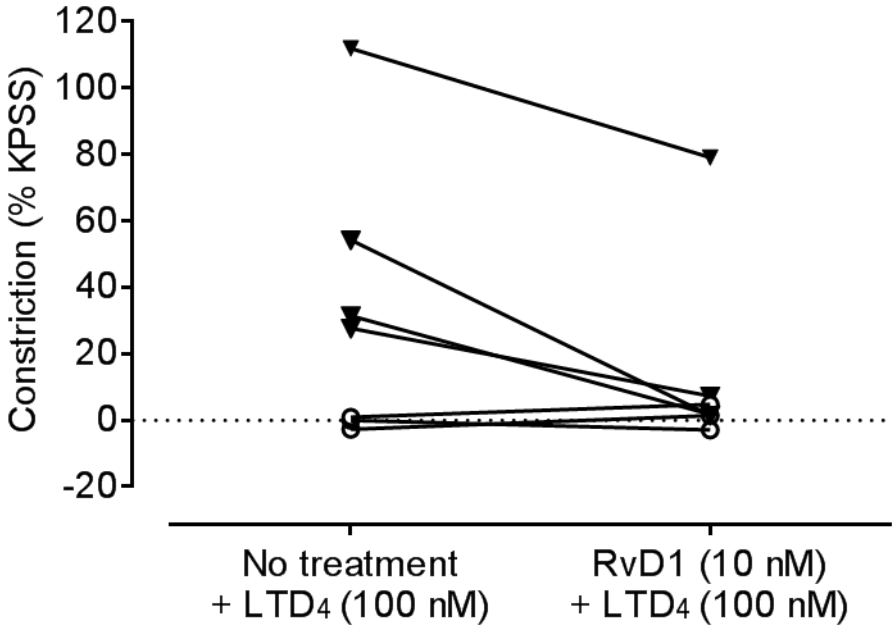

Figure 4.13: Effect of absence or presence of resolvin D1 (RvD1) on constriction of adjacent segments of rat bronchiole to leukotriene D_4. Adjacent segments were isolated and mounted in separate chambers on a wire myograph, and incubated with or without RvD1 (10 nM) for 1 hour, before the ability of LTD_4 (100 nM) to constrict each segment was tested (experimental design C). Three adjacent pairs of segments (open circles) did not respond to LTD_4 regardless of the presence or absence of RvD1 (n=3). In contrast, the other four pairs of adjacent segments (closed triangles) responded differently, contracting in response to LTD_4 100 nM by 56.38% (n=4, mean ± SEM), but the corresponding segment in each pair contracting by only 22.43% when pre-treated for 1 hour with RvD1 (10 nM). Despite this evidence that RvD1 may inhibit LTD_4-induced constriction of rat bronchiole segments, the small proportion of rat bronchioles showing an initial constriction to LTD_4 alone precluded statistical significance in this experiment (n=4, p=ns, Wilcoxon matched-pairs test).

Figure 4.13 shows firstly that not all rat bronchioles are responsive to LTD_4 (100 nM), with neither segment in three of the six pairs contracting when treated, but in the three LTD_4-responsive bronchioles, pre-treatment with RvD1 (10 nM) for 1 hour tended to reduce LTD_4-induced constriction from 56.38% to 22.43%, when compared to the adjacent untreated segments. Non-parametric statistical analysis of this data suggests that this difference is not significant, but a paired Student's t-test found that the RvD1-treated bronchioles constricted significantly less in response to a single concentration of LTD_4 ($p<0.05$). The low proportion of LTD_4-responsive rat bronchioles caused greater attention towards the experiments on human bronchioles outlined below.

4.4 Results – effect of resolvins on the contractility of human bronchioles

4.4.1 Constriction of human bronchioles by leukotriene D_4

This section focuses on experiments on human bronchioles isolated from lung tissue samples donated by patients undergoing lung resection surgery.

The most promising initial finding in rat bronchioles was the apparent abrogation of LTD_4-induced constriction by RvD1 (see previous section). This possibility was explored in human bronchioles using experimental design B, including a 'no resolvin' treatment' arm to control for any spontaneous drift or LTD_4–induced tachyphylaxis occurring over the timescale of each day of experiment.

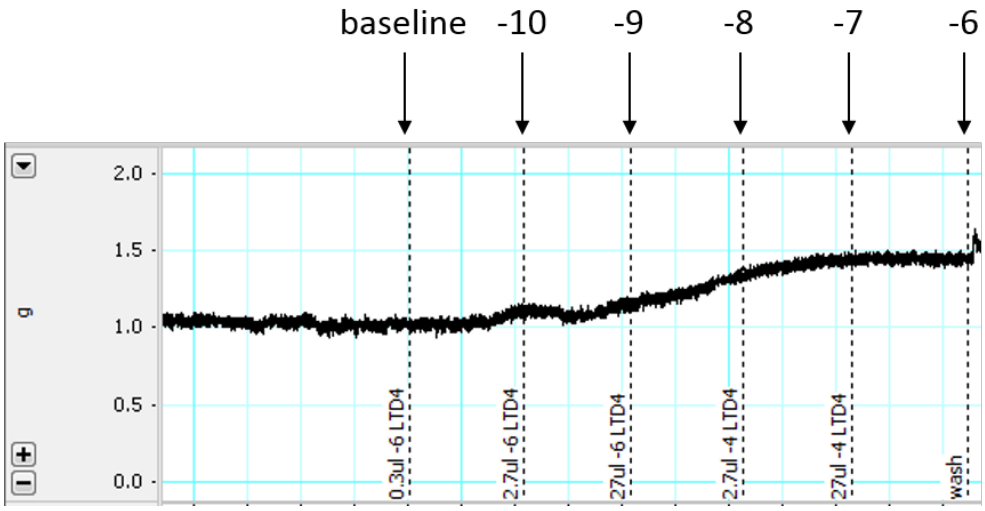

Figure 4.14: Real Chart Lab trace to illustrate the response of human bronchioles to a leukotriene D_4 cumulative concentration-response curve (10^{-10} M to 10^{-6} M).

Figure 4.14 shows that LTD_4 concentration-dependently constricts human bronchioles, and as with the rat bronchiole data, this raw trace can be expressed as a percentage of the constriction induced by KPSS used to check functional viability.

To investigate the effect of RvD1 on LTD_4-induced constriction, segments of human bronchiole were mounted on the wire myograph, their functional integrity was confirmed, and a cumulative concentration-response curve to LTD_4 (100 pM – 1 µM) was constructed. The segments were washed to restore the baseline tension, and then incubated for 1 hour with (or without) RvD1 (10 nM). A second LTD_4 cumulative concentration response curve

was then performed in the presence (or absence) of RvD1, as shown in Figure 4.15 in accordance with experimental design B.

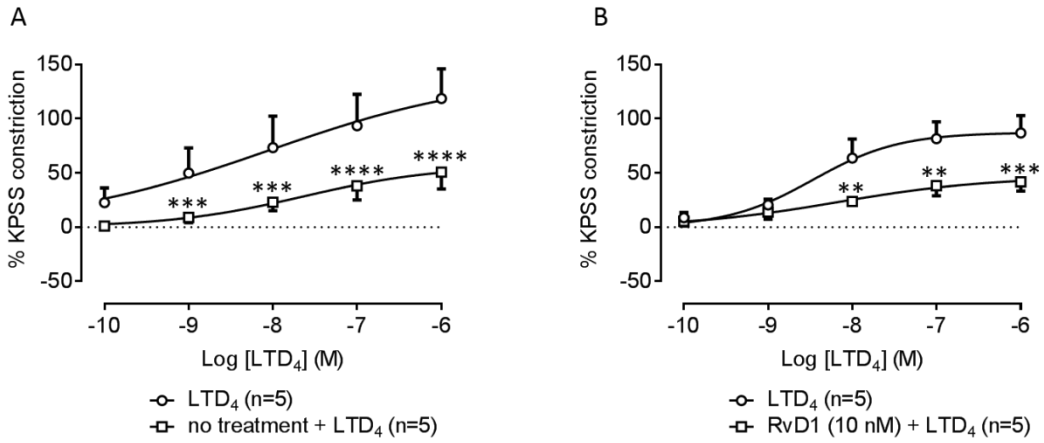

*Figure 4.15: The effect of resolvin D1 (RvD1) on leukotriene D_4 (LTD_4)-induced constriction of human bronchioles. RvD1 (10 nM) was investigated for its ability to modulate LTD_4-induced constriction of human bronchiole segments using experimental design B. (A) Following a washout and a 1 hour incubation in the absence of RvD1, human bronchioles responded significantly less to the second LTD_4 cumulative concentration-response curve compared with the first curve ($n=5$, $p<0.05$, two-way ANOVA). (B) Incubation with RvD1 (10 nM, 1 hour) appeared to significantly inhibit the ability of LTD_4 to constrict human bronchiole segments ($n=5$, $p<0.05$, two-way ANOVA), but not when compared to the post-incubation (second) curve for segments not incubated with RvD1, suggesting that the second (lower) curves in both panels are the result of tachyphylaxis to LTD_4 or to a spontaneous reduction in tissue responsiveness over the timescale of each experimental day. Multiple comparisons: ** $p<0.01$ LTD_4 vs no treatment/RvD1 + LTD_4, *** $p<0.001$ LTD_4 vs no treatment/RvD1 + LTD_4, **** $p<0.0001$ LTD_4 vs no treatment/RvD1 + LTD_4.*

Figure 4.15 suggests that the response to the second LTD_4 cumulative concentration-response curve was significantly reduced when compared to the first curve when RvD1 was either absent or present during the incubation. These data confirmed that this experimental design (experimental design B) is not suitable for the investigation of LTD_4-induced constriction as human bronchioles appear to undergo tachyphylaxis to LTD_4.

4.4.2 The effect of resolvins on human bronchioles constricted submaximally with leukotriene D_4

Human bronchioles were isolated and mounted on a wire myograph, and the ability of resolvins to relax bronchioles pre-constricted with leukotriene D_4 was determined (experimental design A). Since previous experiments in this project (Figure 4.15) suggest that the response of bronchioles to LTD_4 is significantly decreased by prior exposure to LTD_4 combined with a washout, a single, submaximal concentration of 100 nM LTD_4 was

used to establish a pre-constricted plateau response. To explore whether LTD_4-induced constrictions of human bronchiole segments can be relaxed by pharmacological antagonism of the $CysLT_1$ receptor, the $CysLT_1$ receptor antagonist montelukast (10 µM) was used, and in parallel chambers, single concentrations of resolvins D1, D2 or E1 (each at 100 nM) were also examined for their ability to relax the bronchiolar constrictions to LTD_4.

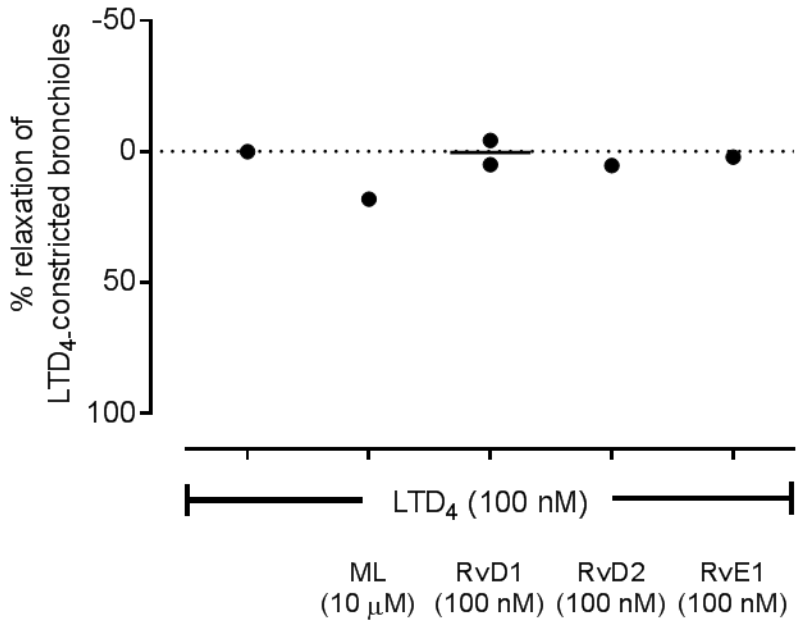

Figure 4.16: The effect of the $CysLT_1$ antagonist montelukast and resolvins (Rv) D1, D2 and E1 on LTD_4-constricted human bronchioles. Human bronchioles were pre-constricted with 100 nM LTD_4 and the effect of montelukast, RvD1, RvD2 or RvE1 determined according to experimental design A. Any changes in tension were expressed as a percent relaxation of the LTD_4 response. Preliminary evidence suggests that resolvins (n=1-2) are unable to reverse LTD_4-induced pre-constriction in human bronchioles, whilst montelukast (10 µM) induces relaxation of approximately 18% (n=1).

Preliminary experiments suggest that resolvins cannot reverse pre-constriction in human bronchiole segments constricted with LTD_4, whilst $CysLT_1$ receptor antagonist, montelukast, induced modest relaxation of the tissue segment of 18% (Figure 4.16).

4.5 Summary of results

The studies described in this chapter investigated the ability of resolvins D1, D2 and E1 to modulate the contractility of rat and human bronchiole segments, as defined in Aim 2 (see section 1.9). The main findings were:

- Resolvins D1, D2 and E1 did not relax rat bronchiole segments pre-constricted with carbachol (CCh), although constriction was completely abolished by atropine.
- Resolvins D1 and E1 produced ambiguous results on constriction induced by the thromboxane mimetic U46619, due to increases in baseline responsiveness of rat bronchioles.
- Resolvin D1 (10 nM) initially appeared to markedly inhibit constriction of human bronchioles induced by leukotriene D_4, although this was complicated by a fall in baseline responsiveness.
- Preliminary results with a modified (parallel) design to prevent changes in baseline responsiveness being caused by repeated exposure to agonists suggested that resolvin D1 (10 nM) may have an inhibitory effect on LTD_4-induced constriction of rat bronchioles.

4.6 Discussion

Bronchoconstriction in response to inhaled irritants and other inflammatory stimuli is putatively a survival mechanism to reduce airway and systemic exposure to inhaled insults, while bronchodilation is required for optimal airflow and gas exchange. Airway diameter is regulated by neural mechanisms (such as bronchoconstriction induced by parasympathetic nervous system activity at muscarinic cholinergic receptors, and bronchodilation induced by sympathetic activity at beta-2 adrenoceptors), by endocrine mechanisms (such as adrenaline circulating from the adrenal glands), and by local humoral mechanisms (such as histamine, eicosanoids and other inflammatory mediators released by mast cells, infiltrating leukocytes and other cell-types).

The ability to cause bronchoconstriction or bronchodilation *via* specific GPCRs expressed directly on bronchial smooth muscle is a characteristic of many of the classical eicosanoid mediators; for example, the cysteinyl-leukotriene LTD_4 is the most potent known bronchoconstrictor of human airways and its release from mast cells and eosinophils is implicated in bronchial asthma, while the prostanoid family includes both bronchoconstrictors (e.g. TxA_2, PGD_2) and bronchodilators (e.g. PGE_2). Some eicosanoids may also cause secondary release of bronchoactive mediators from resident mast cells, infiltrating leukocytes or structural cell-types.

In contrast, there are no published studies investigating whether SPMs including resolvins can directly contract or relax bronchiolar smooth muscle, or modulate contractions induced by other humoral or neural stimuli. The studies in this chapter explored whether resolvins D1, D2 and E1 can modulate contractions induced in rat bronchioles by carbachol (a stable mimetic of acetylcholine at parasympathetic muscarinic receptors) and U46619 (a stable mimetic of thromboxane A_2 at thromboxane TP receptors), and whether they can modulate contractions of human bronchioles induced by leukotriene D_4 (acting at $CysLT_1$ receptors).

The resolvins can be hypothesised to exert modulatory effects either by direct pharmacological interference at eicosanoid receptors shared with one or more contractile agonists (for example, perhaps by acting as antagonists or partial agonists at $CysLT_1$ or TP receptors) and/or by physiological effects exerted *via* distinct resolvin receptors (such as ChemR23 or GPR32). In the absence of specific antagonists for some of these resolvin receptors (and because other resolvin receptors probably yet remain to be identified), it is not always possible to distinguish between resolvin effects depending on shared eicosanoid

receptors and those depending on distinct resolvin receptors. However, in some experiments pharmacological antagonists of muscarinic receptors (atropine) and $CysLT_1$ receptors (montelukast) were used as controls, and the beta-2 adrenoceptor agonist salbutamol was used as a physiological (sympathomimetic) bronchodilator.

Three important points need to be made about the utility and originality of the experiments described here. Firstly, the use of wire myography meant that the experiments explored the integrated functional outcome most relevant to airway physiology and pathophysiology, namely airway contractility, rather than surrogate cellular markers of inflammation or muscular activation. Secondly, as intact small airways from rat and human lung were used, rather than strips of smooth muscle dissected from larger airways, the results of these studies take into account the many complex interactions that might occur between different cellular components within the airway segments, such as secondary release of bronchoactive mediators from resident mast cells, infiltrating leukocytes (most relevant in the human lung from COPD donors), intact bronchial epithelium or other structural cell types. This is ideal for an initial programme of research to screen resolvins for functional activity, with follow-up studies to dissect the cellular and molecular mechanisms involved in more detail. Thirdly, wire myography allowed contractility to be quantified in very small airways, typically of diameter around 400 μm; this not only enables extensive work in the airways of small laboratory animals (such as rats, in this case) but also in small airways from human lung. It is these small airways that contribute most of the unwanted airway resistance in asthma and other obstructive lung diseases, and they also represent the site of inflammatory damage and airway remodelling in chronic inflammatory conditions. If resolvins play a role in dampening inflammation and promoting resolution in airway disease, it is in the small airways that they are most likely to act.

The myography experiments followed three broad experimental designs (A, B and C). In **experimental design A** (section 4.2.1, Figure 4.1 and Figure 4.2), a single concentration of resolvin was added to airways pre-constricted with a known contractile agonist to determine whether the resolvin can reverse (or indeed enhance) the constriction. This design is a sensitive way to detect resolvin activity as any effect is readily visible (in either direction) against the stable plateau of constriction, but its disadvantage is that such an effect has to occur within the time-scale of the constriction; typically 10 minutes was allowed for a resolvin effect to become apparent. In **experimental design B** (section 4.3.2, Figure 4.3) a cumulative contractile response was established to the agonist followed by a

washout, then the cumulative agonist response was repeated following a longer pre-treatment with resolvin (or none) for 1 hour, and in its continued presence during the second agonist exposure. This 'in series' design allows for resolvin activity with a slower onset to be explored, and also enables paired statistical comparison of responses with and without the resolvin in the same vessel segments separated only in time. However, the possibility of a 'hangover' effect (such as tachyphylaxis or hyperreactivity) from the first exposure to the contractile agonist persisting into the second exposure, despite the washout in between, led to the adoption of **experimental design C** (section 4.3.3, Figure 4.4) in which the control and resolvin treatments were applied simultaneously to different airway segments 'in parallel' in separate myograph chambers. Inherent variability between the segments in parallel was minimised by rigorously using pairs of adjacent segments from exactly the same location along the airway.

Turning to the first section of results (section 4.4.1), the stable acetylcholine mimetic carbachol (CCh) reliably and concentration-dependently constricted segments of rat bronchioles (Figure 4.5 and 4.6). CCh is likely to be exerting its bronchoconstrictor action via muscarinic receptors. Resolvins have lipid chemical structures dissimilar to the amphipathic structure of acetylcholine, so it is unlikely that they would interfere directly with carbachol at muscarinic receptors; carbachol therefore provides a useful model to explore whether resolvins can relax bronchioles physiologically *via* other receptors. The muscarinic receptor antagonist atropine (10 µM) completely reversed the CCh-induced pre-constriction of rat bronchioles (Figure 4.8), but resolvins D1, D2 and E1 investigated over a million-fold concentration range (from 1 pM to 1 µM) had no such relaxant effect (Figure 4.9). Curiously, the beta-2 adrenoceptor agonist salbutamol (10 µM) also failed to significantly relax CCh-constricted rat bronchiole segments *in vitro* (Figure 4.8). This is difficult to explain in view of the reliable ability of beta-2 bronchodilators to reverse bronchoconstriction triggered *in vivo* by a range of inflammatory and other stimuli in asthmatic patients, but it may reflect the potency of each agonist (at 10 µM) relative to their affinities for their respective receptors and also the relative levels of expression and signalling efficiency of each receptor in normal rat airways compared to asthmatic human airways. Nevertheless, this control experiment does not undermine the clear result that while a muscarinic antagonist can completely inhibit CCh-induced constriction of rat bronchioles, the resolvins were ineffective.

The result above (using experimental design A) can be criticised in that a positive result would require the resolvin to act acutely (within minutes) to reverse a pre-existing

constriction to carbachol. Recently published work in conjunctival goblet cells showed that the simultaneous addition of RvD1 or AT-RvD1 and histamine (a GPCR-dependent bronchoconstrictor and mucus secretagogue) reduced intracellular calcium influx compared to histamine alone, but a delayed addition of the resolvin after the administration of histamine produced no inhibitory effect (Li et al. 2013). Thus it is possible that the lack of effect of resolvins seen here on carbachol pre-constricted rat bronchioles reflects a similar time-dependent requirement for resolvin activity i.e. resolvins may be able to *prevent* bronchiolar constriction but not to *reverse* pre-established constriction.

Given this possibility, the ability of resolvins to modulate agonist-induced constriction of rat bronchioles was next assessed using experimental design B (see section 4.2.2). This involves establishing a cumulative concentration-response curve to carbachol in the absence of resolvin, followed by a washout, then by pre-treatment for 1 hour with a resolvin (or none) before repetition of the carbachol concentration-response curve in the continued presence (or absence) of the resolvin. However, the results indicated again that neither RvD1 nor RvE1 was able to modulate CCh-induced constriction of rat bronchiole segments, when compared with the first CCh cumulative concentration response curve performed in the absence of resolvin (Figure 4.10). In a study similar to the one by Li and colleagues (described above) RvD1 and RvE1 were shown to inhibit CCh-induced mucin secretion from rat conjunctival goblet cells (Dartt et al. 2011). However, an inhibitory effect on CCh-induced constriction was not seen in these experiments, which probably reflects differences in mechanisms between constriction and mucin secretion. Indeed, the authors went on to show that the resolvins inhibited ERK1/2 activation which is an important mechanism in the stimulation of mucin secretion but probably not important in smooth muscle contractility.

The same approach (design B) showed that RvD1 and RvE1 also failed to modulate rat bronchiolar constriction induced by the TxA_2 mimetic U46619, which acts via TP receptors (Figure 4.11). In the U46619 experiments, however, the initial concentration-response curve to U46619 appeared to enhance the basal reactivity of the rat bronchioles, as the second concentration-response curve to U46619 performed as a control in the absence of resolvin was higher than the first curve (Figure 4.11A). Indeed, a changing responsiveness to U46619 has been observed previously in rat bronchioles studied immediately after isolation and also after culture for 12, 24 or 48 hours; this study suggested that the responsiveness to U46619 increases the longer the segment is in culture (Lei et al. 2011). In our experiments, such a gradually increasing responsiveness over the

time-course of the experiment undermines the value of measuring baseline responsiveness to U46619 in experimental design B and it would potentially mask any changes in responsiveness induced by resolvins. In particular it might account for the modestly increased responsiveness observed at some time-points with the 'no treatment' control (Figure 4.11A) or with RvD1 (Figure 4.11B), or it might simply have masked a possible change in responsiveness to RvE1 (Figure 4.11C). This variable baseline in responsiveness therefore creates a problem in interpreting results from experimental design B, although it is a strength of this design that it can detect such changes in baseline responsiveness by virtue of the repeated concentration-response curves performed both in the presence and absence of the resolvin.

The problem of variable baseline responsiveness also appeared (in the opposite direction) in experiments using design B to investigate whether resolvins can modulate constriction of bronchioles induced by the pro-inflammatory lipid LTD_4, which predominantly mediates its actions via $CysLT_1$ receptors. Resolvins D1 and E1 can both inhibit LTD_4-mediated mucin secretion and calcium signalling in conjunctival goblet cells (Dartt et al. 2011), although the resolvins appeared to act at an intracellular signalling site in these cells rather than by directly interfering at $CysLT_1$ receptors. In contrast, lipoxin A_4 is a partial agonist at $CysLT_1$ receptors (Badr et al. 1989), so it could also act as a partial (weak) antagonist of $CysLT_1$ receptors in the presence of a full $CysLT_1$ agonist such as LTD_4. Together, these two studies left open the possibility that resolvins D1 and E1 might modulate LTD_4-induced bronchiolar constriction by either a direct ($CysLT_1$-dependent) mechanism or indirectly by signalling *via* distinct resolvin receptors. Initially, experimental design B (Figure 4.3) was used to investigate the ability of RvD1 (10 nM) to modulate LTD_4-induced constriction in rat bronchioles. The results suggested remarkably that RvD1 (10 nM) completely prevented LTD_4-induced constriction of rat bronchioles (Figure 4.12). However, concurrent experiments in *human* bronchiole segments demonstrated problems with *decreased* responsiveness to LTD_4 (possibly tachyphylaxis) emerging over the time-course of the experiments (Figure 4.15). In conjunction with the similar problems with U46619 (the *increasing* baseline responsiveness discussed above), this prompted a change from experimental design B to experimental design C. This design (Figure 4.4) uses adjacent bronchiole segments treated with and without resolvin in separate myograph chambers simultaneously, so it eliminates the problem of basal responsiveness varying over time.

The preliminary results using design C highlighted an additional and ongoing problem with LTD_4 as a contractile agonist in rat bronchioles, namely that rat bronchioles are poorly responsive to LTD_4 compared to their responsiveness to other mediators, and also when compared to the LTD_4 responsiveness of bronchioles from other species. In this experiment, 4 of the 7 bronchiole pairs tested were responsive to LTD_4 (~57%, Figure 4.13, experimental design C), whilst in the earlier experiments performed using experimental design B, only 7 of 44 segments tested responded to LTD_4 (~16%). In a publication by Seehase and colleagues, the authors compile data from their own work and the work of others to compare the response to a range of contractile mediators (methacholine, histamine, serotonin, LTD_4, U46619, endothelin-1) in different species, showing intriguing interspecies differences (Seehase et al. 2011). The data for the LTD_4 comparison is in fact obtained from a study by Sirois and colleagues who investigated the ability of the cysLTs to constrict guinea pig, rat, rabbit and human lung tissue, demonstrating that rat lung responds exceptionally poorly to LTD_4 whilst humans and guinea pigs constrict the most of all species studied (Sirois et al. 1981). This problem entailed the screening of large numbers of rat bronchioles and the rejection of those that showed no initial response to LTD_4 after their isolation and mounting in the myograph chambers, delaying progress markedly with these experiments. Nevertheless, in the subset of bronchioles that showed a contractile response to LTD_4, there was a trend for inhibition of LTD_4 constriction in segments pre-treated with RvD1 (10 nM) compared to those not treated with RvD1 (Figure 4.13). The difficulty of finding rat bronchioles responsive to LTD_4 meant that this experiment has low n-values (n=3-4) and this may have precluded statistical significance.

Human bronchioles are more responsiveness to LTD_4 than are rat bronchioles (Sirois et al. 1981), commensurate with the recognised role of cysteinyl-LTs in human bronchial asthma. However, human airway tissue is fragile, particularly tissue from patients with chronic lung diseases like the COPD donors in this study (see *Table 2-1* for comparison of lung function in functionally-viable vs non-viable tissue segments). This means that functionally-viable human bronchiole segments are a scarce resource. The scarcity of functionally-viable human bronchioles meant that experiments using design A, with segments pre-constricted with LTD_4, were very limited (n=1-2), but the result suggested little effect of RvD1, RvD2 or RVE1 on LTD_4-induced constriction in this model (Figure 4.16). In the same experiment, treatment with montelukast (n=1) had only a small reversal effect on the LTD_4-induced constriction (Figure 4.16). It is not immediately

apparent why montelukast was not more effective at reversing pre-constriction in the experiment, as it is a potent and selective $CysLT_1$ antagonist *in vivo.* It is theoretically possible that other cysteinyl-leukotriene (or purinergic) receptors that are not blocked by montelukast (such as $CysLT_2$) may partly mediate the LTD_4 contractions, but this is highly unlikely in human airways. It may reflect poor availability of montelukast in this *in vitro* model, but a clearer answer will require further experiments, possibly including studies with the dual $CysLT_1$/$CysLT_2$ antagonist BAYu9773.

The studies in this chapter had to adapt to, and overcome, a number of unforeseen difficulties in experimental design, tissue availability and tissue responsive in order to investigate the ability of resolvins to modulate the contractility of bronchioles from rat and human lung. There remain some promising preliminary results that warrant further investigation, particularly using experimental design C to control for changes in tissue responsiveness. This parallel design was adopted increasingly in the experiments on rat and human arteries reported in chapter 5. Nevertheless, it is possible to conclude that resolvins D1, D2 and E1 are probably unable to relax bronchiole segments pre-constricted with carbachol, U46619 or LTD_4, at least under the conditions used in these experiments. Longer-term treatment with resolvins may generate different outcomes. Indeed, a recent study suggests that long-term treatment (every 24 hours for 2 days) with interleukin (IL-)13 induces hyperreactivity of human bronchial segments to U46619, histamine and methacholine (an analogue of carbachol), and that this hyperreactivity is inhibited by RvD1, although a rather high RvD1 concentration (300 nM) was required and it only partially reversed the hyperreactivity (Khaddaj-Mallat et al. 2015). *In vivo*, ovalbumin-sensitised mice injected i.v. with RvD1 (10 ng) demonstrated little protection against methacholine-induced changes in lung resistance, with any difference between RvD1-treated and control mice only reaching statistical significance at the highest dose (100 mg/ml) of methacholine, whilst mice receiving AT-RvD1 saw slightly more protection with differences between resolvin-treated and control mice apparent at the two highest doses (30 and 100 mg/ml) of methacholine (Rogerio et al. 2012). RvE1 gave similar levels of protection, significantly inhibiting increases in lung resistance to the highest two doses (30 and 100 mg/ml) of methacholine (Haworth et al. 2008). Intriguingly, in a similar study the treatment of ovalbumin-sensitised mice with PD1 (2, 20 or 200 ng) significantly reduced methacholine-dependent increases in lung resistance when compared with control, and this protective effect was bell-shaped in that the lower doses provided better protection (Levy et al. 2007). Thus, while resolvins do not appear to contract or relax airways

directly, further studies are required to determine whether there may be scope for further studies of their interactions with cytokines and growth factors in regulating the underlying responsiveness of airways to contractile agonists.

Chapter 5: Effect of resolvins on contractility, and immunohistology of pro-resolving mediator receptors, in rat and human blood vessels

5.1 Background

The work in this chapter is an investigation of the ability of resolvins D1, D2 and E1 to modulate vascular contractility induced by phenylephrine, U46619 and leukotriene D_4. The investigations were performed in thoracic aorta tissue from Wistar rats, and in pulmonary arteries isolated from lung tissue samples donated by patients undergoing surgery at Southampton General Hospital. As in chapter 4, smooth muscle contractility was quantified by wire myography. This chapter also presents data on the immunohistological expression of the pro-resolving receptors ChemR23, GPR32 and ALX in human pulmonary arteries.

In the vascular contractility experiments, three direct agonists of vascular smooth muscle were used – phenylephrine (PE), U46619 and leukotriene D_4 (LTD_4). PE is a synthetic small molecule pharmacologically related to adrenaline, but with specificity for alpha-1 adrenergic receptors. Activation of alpha-1 adrenergic receptors on vascular smooth muscle by PE mediates vasoconstriction. LTD_4 is a potent constrictor of both rat and human arteries, acting directly via $CysLT_1$ receptors on vascular smooth muscle cells, while its ability to increase vascular permeability is mediated through $CysLT_2$ receptors on vascular endothelium (Moos et al. 2008). U46619 is a stable mimetic of the short-lived vasoconstrictor thromboxane A_2 (TxA_2), and like TxA_2 it is an agonist at the thromboxane receptor TP on vascular smooth muscle cells.

Both LTD_4 and TxA_2 belong to the classical eicosanoid family of omega-6 lipids. Understanding the ways in which classical eicosanoids and specialised pro-resolving mediators (SPM) initiate, sustain or limit inflammation has been of great importance over the past decade, given the recognised role of uncontrolled inflammation a wide range of diseases, including vascular disease. A number of studies suggest that SPMs oppose the actions of classical eicosanoids in a number of inflammatory models, and one aim of this thesis is to determine whether the same is true in the regulation of smooth muscle contraction.

PE does not mimic a lipid and does not exert its actions via a lipid receptor. It is therefore a useful tool to understand whether any modulatory activity on vascular contractility depends on SPMs acting as pharmacological antagonists at receptors for the contractile lipids (such as $CysLT_1$ or TP) or whether they can exert physiological antagonism independently via their own receptors.

The vascular experiments in this chapter explored the same three resolvins that were investigated in bronchial airways in chapter 4 – resolvin D1, resolvin D2 and resolvin E1. Their ability to induce direct relaxation of isolated, intact rat and human arteries, as well as to modulate agonist-induced constriction of these vessels, was investigated using the experimental designs outlined below.

5.2 Protocols for myography experiments

A range of different experimental designs was used for the myography experiments because of limitations identified when using certain approaches, and these limitations and reasonings are explained as the chapter progresses.

5.2.1 Experimental design A – pre-constriction/reversal

To determine whether resolvins can relax rat thoracic aorta or human pulmonary artery segments pre-constricted with a known vascular smooth muscle agonist, vessel segments were first constricted with a submaximal concentration of the agonist. Because there was evidence for changing responses to consecutive cumulative concentration-response curves (CCRC) for both U46619 or LTD_4 when separated by washes in rat bronchioles, it was decided that a CCRC would not be used to calculate an EC_{80}, and instead a known standard submaximal concentration (100 nM) was used.

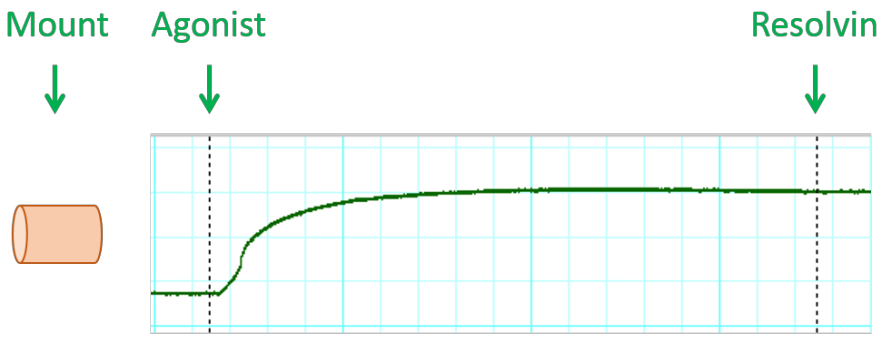

Figure 5.1: Pre-constricting rat aorta or human pulmonary artery (HPA) segments with a single, submaximal concentration of agonist. Segments of rat aorta or HPA were mounted on a wire myograph, assessed for functional viability, constricted with 100 nM of U46619 or LTD_4 and allowed to obtain a stable plateau. Segments were then incubated with or without resolvin and any change in tension over 10 minutes recorded. In some experiments with segments pre-constricted with LTD_4, the $CysLT_1$ antagonist montelukast was added to the chamber instead of a resolvin.

Unlike LTD_4 and U46619, PE is not thought to alter vascular responsiveness so an EC_{80} concentration of PE was used in pre-constriction/reversal experiments. Functionally-

viable rat aorta segments were constricted with cumulative concentrations of PE, and the concentration required to evoke 80% of the maximum response was calculated. This concentration was then used to constrict each segment again to obtain a stable response before the addition of resolvin or other reagents (Figure 5.2).

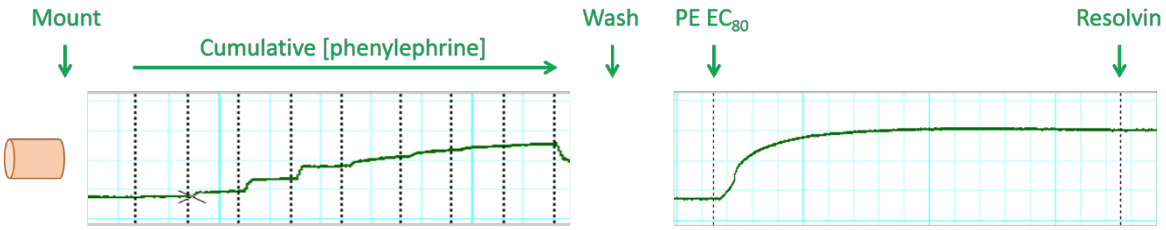

Figure 5.2: Experimental design A – pre-constricting rat aorta segments with a submaximal concentration of phenylephrine (PE). Segments of rat aorta were mounted on a wire myograph, assessed for functional viability, and constricted with cumulative concentrations of PE. Segments were then washed to restore baseline tension and constricted with the PE concentration required to evoke 80% of the maximum constriction (the EC_{80}). Upon reaching a stable response to the EC_{80} concentration, segments were incubated with or without resolvin and changes in tension were recorded.

Irrespective of whether the segment was pre-constricted with PE, LTD_4 or U46619, once the plateau had stabilised, a single concentration of resolvin D1, D2 or E1 was added to the bath and any effect on tension was recorded over 10 minutes.

5.2.2 Experimental design B – cumulative concentration-response curves in series

Analogous to experimental design B used for airway studies in chapter 4, isolated segments of HPA were mounted on a wire myograph and their functional viability confirmed with KPSS. The segments were then constricted with cumulative concentrations of a contractile agonist before being washed to restore baseline tension. Whilst still mounted on the myograph, the segments were incubated with (or without) a resolvin for 1 hour before being immediately constricted with the same cumulative concentrations of agonist, in the presence (or absence) of resolvin (Figure 5.3).

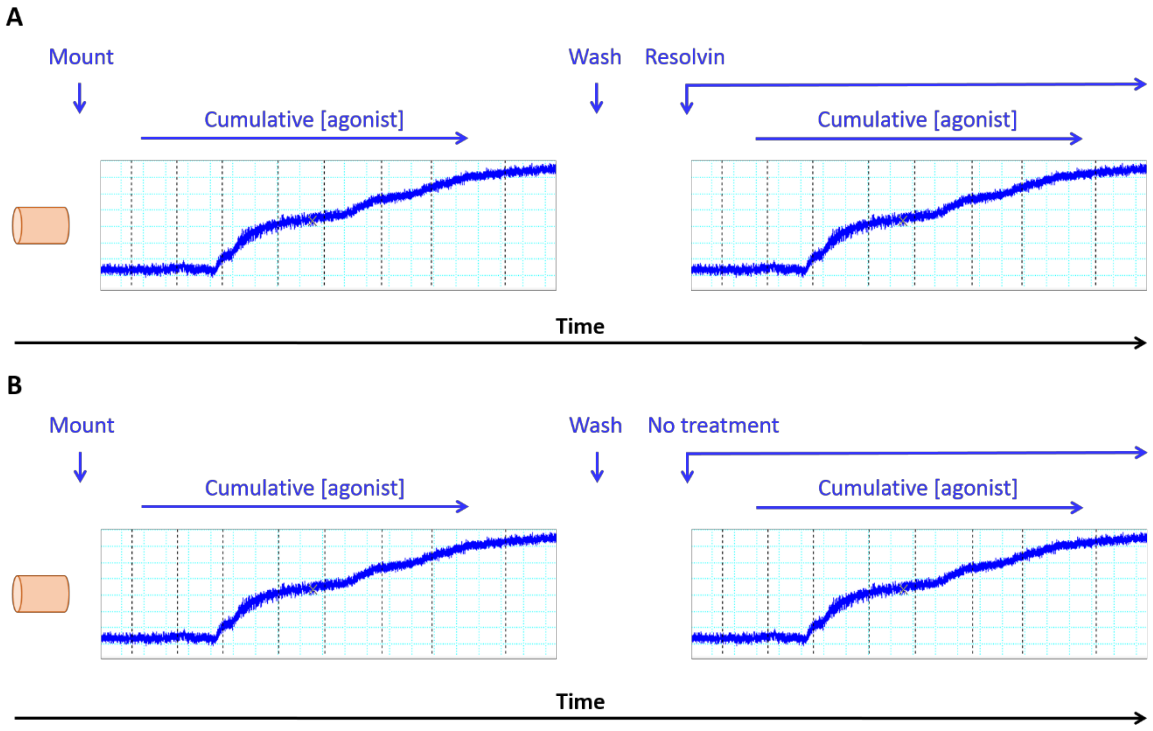

Figure 5.3: Experimental design B – constriction of segments with consecutive cumulative concentration-response curves (CCRC) separated by a washout. Segments of human pulmonary artery were mounted on a wire myograph, a baseline tension of 1.5g set and segments assessed for functional viability. The segments were constricted with cumulative concentrations of agonist, washed to restore baseline tension and then incubated with resolvin (A) or without resolvin (B) for 1 hour, before being constricted with a second cumulative concentration-response curve to the same agonist.

5.2.3 Experimental design C – cumulative concentration-response curves in parallel

Analogous to experimental design C in the airway experiments in chapter 4, cumulative concentration-responses of blood vessels to known contractile agonists were examined following pre-incubation for 1 hour with resolvin or with a control. This was done in parallel with adjacent segments in separate myograph chambers, so that segments are not pre-exposed to the agonist before the resolvin incubation. The parallel design was chosen to eliminate any tachyphylaxis or other changes in responsiveness that might be induced by the first cumulative concentration-response curve in experimental design B (the 'in series' design).

To explore the time-course of resolvin action, the resolvin pre-incubation time in these experiments was extended to include both 1 hour and 24 hour pre-incubation times. Over such extended incubation times as 24 hours, evaporative loss of water from the PSS

in the myograph chamber would present a problem, in that the active reagent (resolvin) and the physiological salts would become more concentrated in the diminished fluid volume in the chamber. This would likely lead to non-physiological behaviour or loss of viability in the segment. Therefore, segments were incubated with resolvin in a culture plate kept in an incubator (37ºC) before being mounted on the wire myograph. Here, segments (rat aorta or HPA) were incubated in a culture plate in DMEM-F12 (10% NCS) with/without resolvin for either 1 hour or 24 hours. Following this, the segments were mounted on the wire myograph, assessed for functional viability with KPSS, and then constricted with cumulative concentrations of agonist (Figure 5.4).

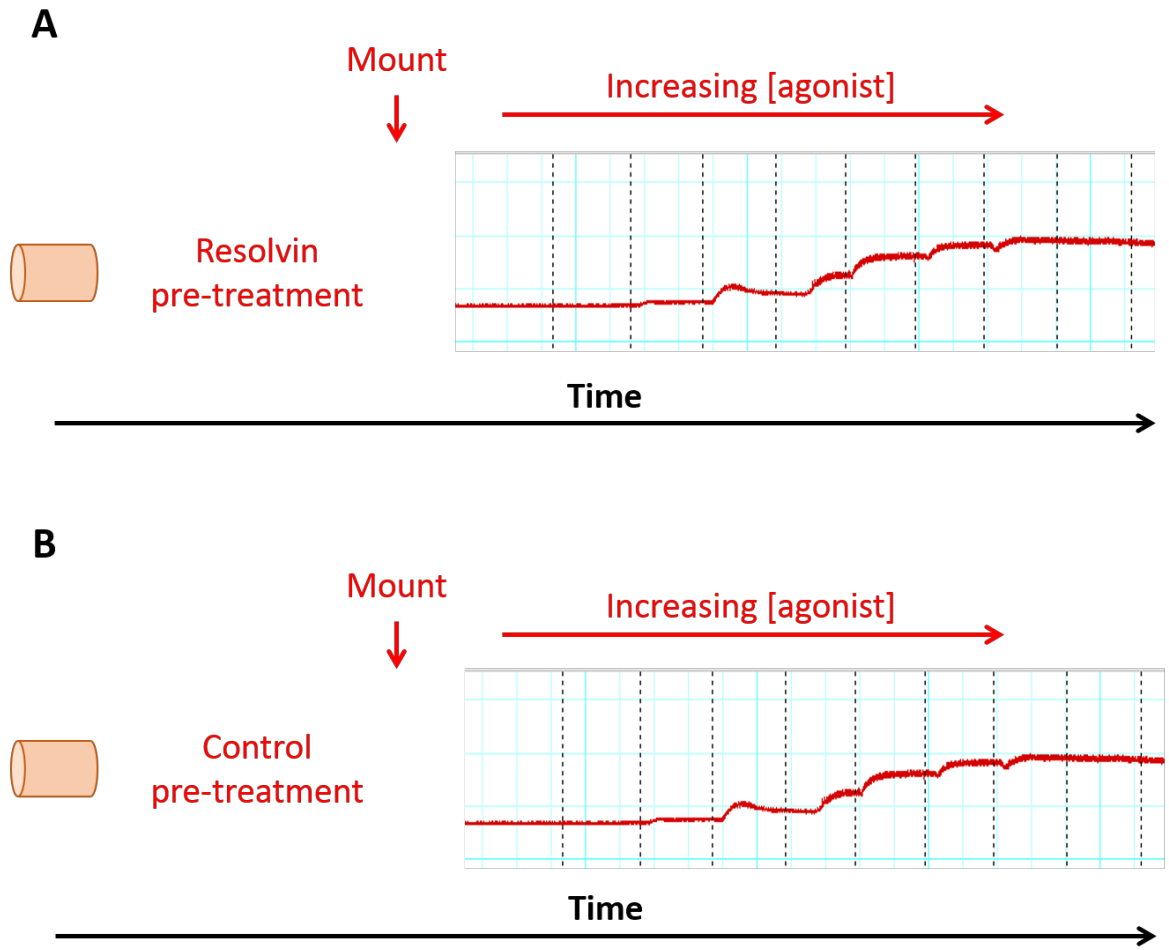

Figure 5.4: Experimental design C – pre-treatment of rat aorta or human pulmonary artery (HPA) segments with or without resolvin and constriction with cumulative concentrations of agonist. Segments of either rat aorta or HPA were incubated with (A) without resolvin (B) for 1 or 24 hours in a culture plate kept in the incubator (37◦C, 5% CO_2). The segments were mounted on a wire myograph, assessed for functional viability and then constricted with cumulative concentrations of agonist.

5.3 Results – effect of resolvins on contractility of rat and human arteries

5.3.1 Contraction of rat thoracic aorta by phenylephrine and the effect of acetylcholine

The ability of the alpha-1 adrenergic receptor agonist, phenylephrine (PE), to constrict isolated rat thoracic aorta was determined using experimental design A.

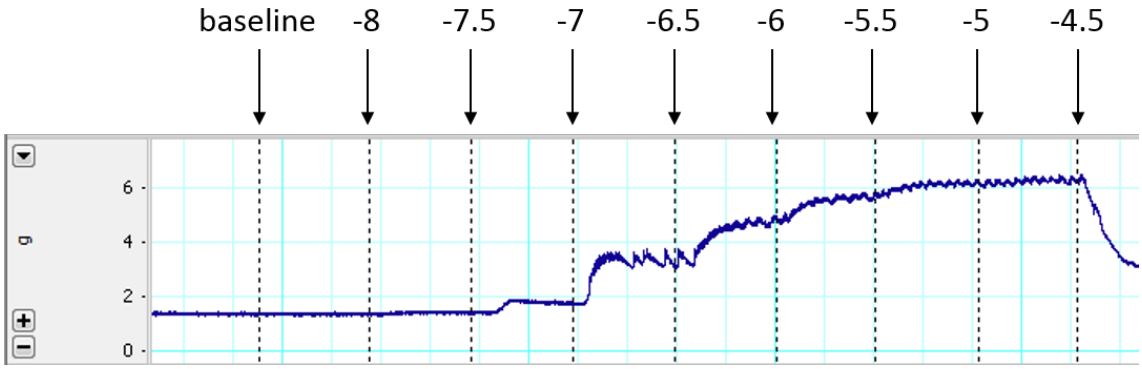

Figure 5.5: Myograph recording (in ChartLab) showing the constriction of rat thoracic aorta segments by phenylephrine. Segments of rat thoracic aorta cleaned of surrounding tissue were mounted on a wire myograph in physiological salt solution (PSS). Functional integrity was confirmed with a contractile response to KPSS, before baseline tension was restored with washes of fresh PSS. The segments were then constricted with cumulative concentrations of phenylephrine (10 nM – 30 µM).

PE concentration-dependently constricted rat thoracic aorta segments (Figure 5.5). To determine whether this could be reversed, the concentration required to evoke 80% of the maximum response (EC_{80}) was calculated for each segment individually. From baseline tension, segments were constricted with the calculated EC_{80} and allowed to reach a stable response. Segments were then incubated with or without the vasodilator, acetylcholine (ACh) and any change in tension measured and recorded (Figure 5.6).

ACh binds to muscarinic acetylcholine receptors (mAChR) on the endothelium, increasing intracellular calcium concentration which activates endothelial nitric oxide synthase (eNOS). The resulting nitric oxide (NO) is released from the endothelial cell and in adjacent smooth muscle cells (SMC) it activates soluble guanylyl cyclase, which converts guanosine triphosphate (GTP) to cyclic guanosine monophosphate (cGMP). cGMP activates protein kinase G (PKG), which promotes the relaxation of vessels.

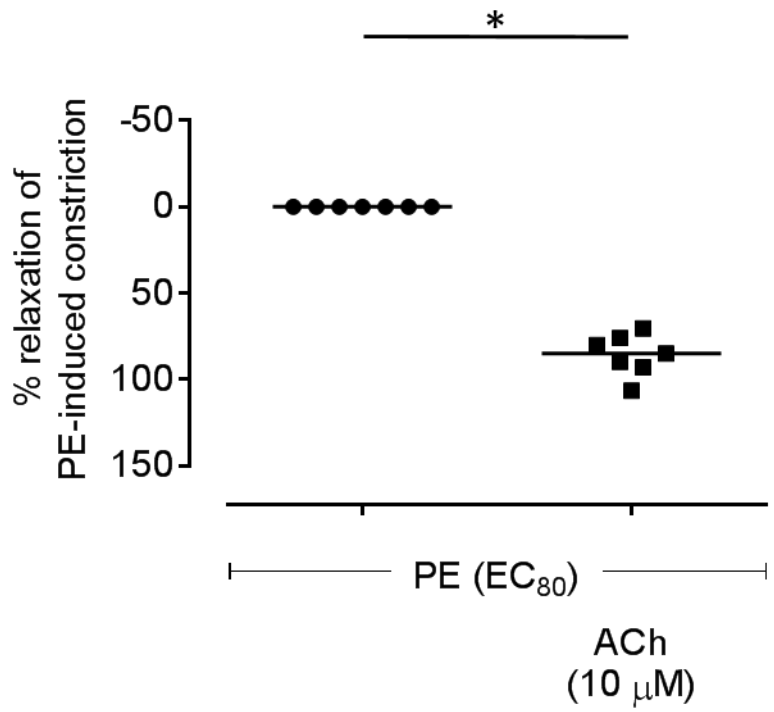

Figure 5.6: Acetylcholine (ACh)-induced relaxation of phenylephrine (PE)-constricted rat thoracic aorta. Using experimental design A, segments of rat thoracic aorta mounted on a wire myograph were constricted with a concentration of PE calculated to induce 80% of the maximum constriction and left to obtain a plateau. ACh (10 μM) was then added to the segments and any relaxation recorded as a percentage of the PE-induced constriction. Statistical analysis indicated that ACh significantly relaxes PE-constricted rat aorta segments (n=7, mean ± SEM, p<0.05 Wilcoxon matched-pairs signed rank test).

In Figure 5.6, the PE-induced plateau at the level obtained just prior to the addition of ACh has been normalised to zero, and the relaxation induced following the addition of ACh is expressed as percent relaxation in relation to the plateau. ACh (10 μM) significantly ($p<0.05$) reversed the PE-induced pre-constriction, relaxing the vessels by approximately 85%.

5.3.2 The effect of resolvins on agonist-induced pre-constriction of rat aorta

The ability of resolvins to relax rat thoracic aorta segments pre-constricted with a sub-maximal concentration (EC_{80}) of PE was investigated. As in the experiment described in Figure 5.6, segments were constricted with the EC_{80} of PE and allowed to plateau. The segments were then incubated with or without RvD1, RvD2 or RvE1 (100 nM) and any change in tension recorded over 10 minutes (Figure 5.7) (experimental design A).

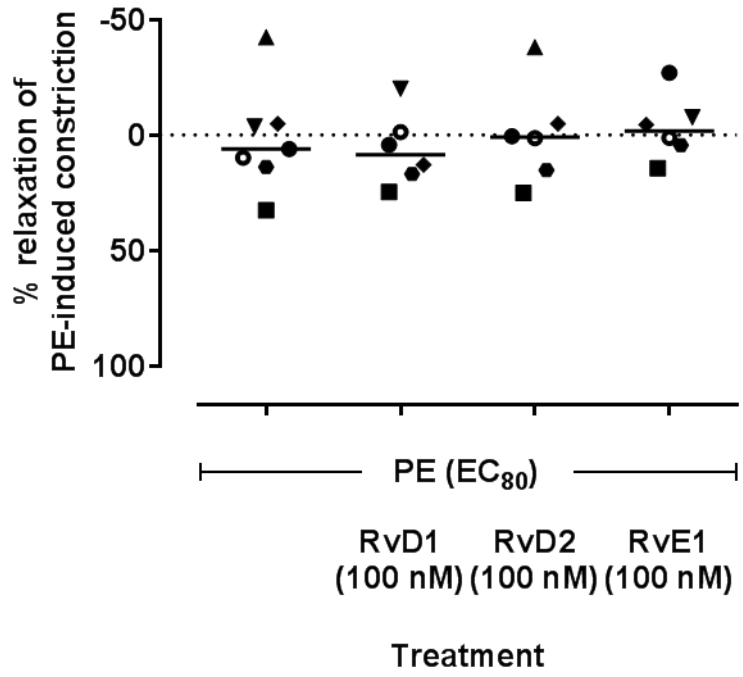

Figure 5.7: Effect of resolvins (Rv) on phenylephrine (PE)-constricted rat thoracic aorta segments. Using experimental design A, a full PE cumulative concentration-response curve was carried out on each segment and the concentration required to evoke 80% of the maximum constriction calculated (EC_{80}). After washing, segments were constricted with the EC_{80} and once a stable response was achieved, segments were incubated with or without RvD1, RvD2 and RvE1 (100 nM). Any change in tension was measured over 10 minutes. The data indicate that RvD1, RvD2 and RvE1 do not significantly relax PE-constricted rat aorta segments when compared with control (n=6/7, mean ± SEM, p=ns, Kruskal-Wallis test with Dunn's multiple comparisons).

Statistical analysis indicates that the three commercially-available resolvins, RvD1, RvD2 or RvE1 at 100 nM do not significantly relax (p=ns) PE-constricted rat thoracic aorta segments (Figure 5.7).

To determine whether these resolvins are capable of relaxing segments constricted with a different agonist, rat thoracic aorta segments mounted on a wire myograph were incubated with 100 nM of U46619, a stable thromboxane mimetic.

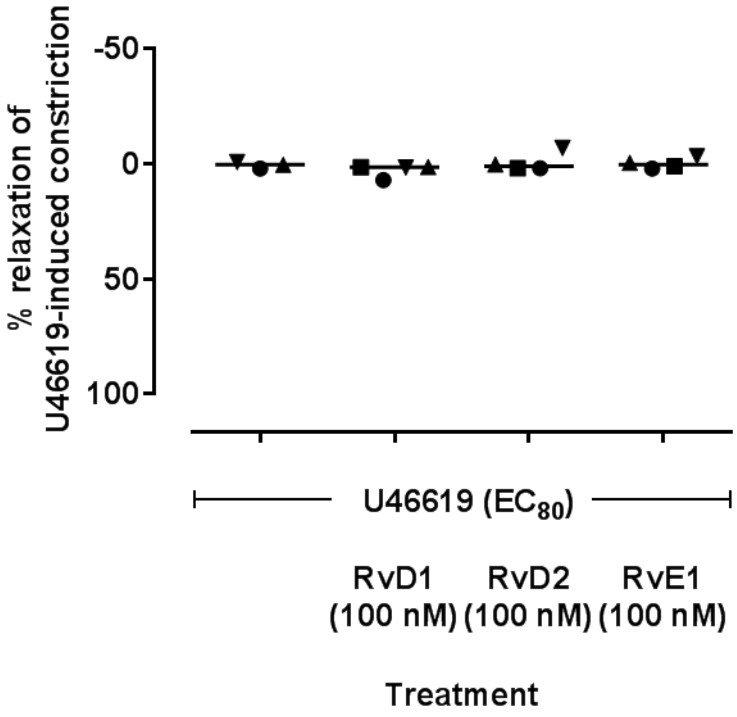

Figure 5.8: Effect of resolvins (Rv) on rat thoracic aorta segments constricted with the stable thromboxane A_2 mimetic, U46619. Functionally-viable segments were constricted with 100 nM U46619 and allowed to plateau. Segments were then incubated with or without RvD1, RvD2 or RvE1 (100 nM) and tension recorded for 10 minutes (experimental design A). The resolvins were unable to significantly relax the U46619-preconstricted rat thoracic aorta segments (n=3-4, mean ± SEM, p=ns, Kruskal-Wallis test with Dunn's multiple comparisons).

Figure 5.8 shows that resolvins D1, D2 and E1 do not relax U46619-constricted segments of rat thoracic aorta (n=3-4, p=ns). Together, the data in Figure 5.7 and Figure 5.8 indicate that these resolvins do not relax rat artery segments submaximally constricted with an agonist mimicking a contractile lipid (U46619) or one mimicking the alpha-adrenergic actions of (nor)adrenaline.

5.3.3 Effect of resolvins on LTD_4-induced pre-constriction of human pulmonary arteries

The ability of resolvins to relax LTD_4-induced constriction of HPA was assessed using experimental design A (section 5.2.1).

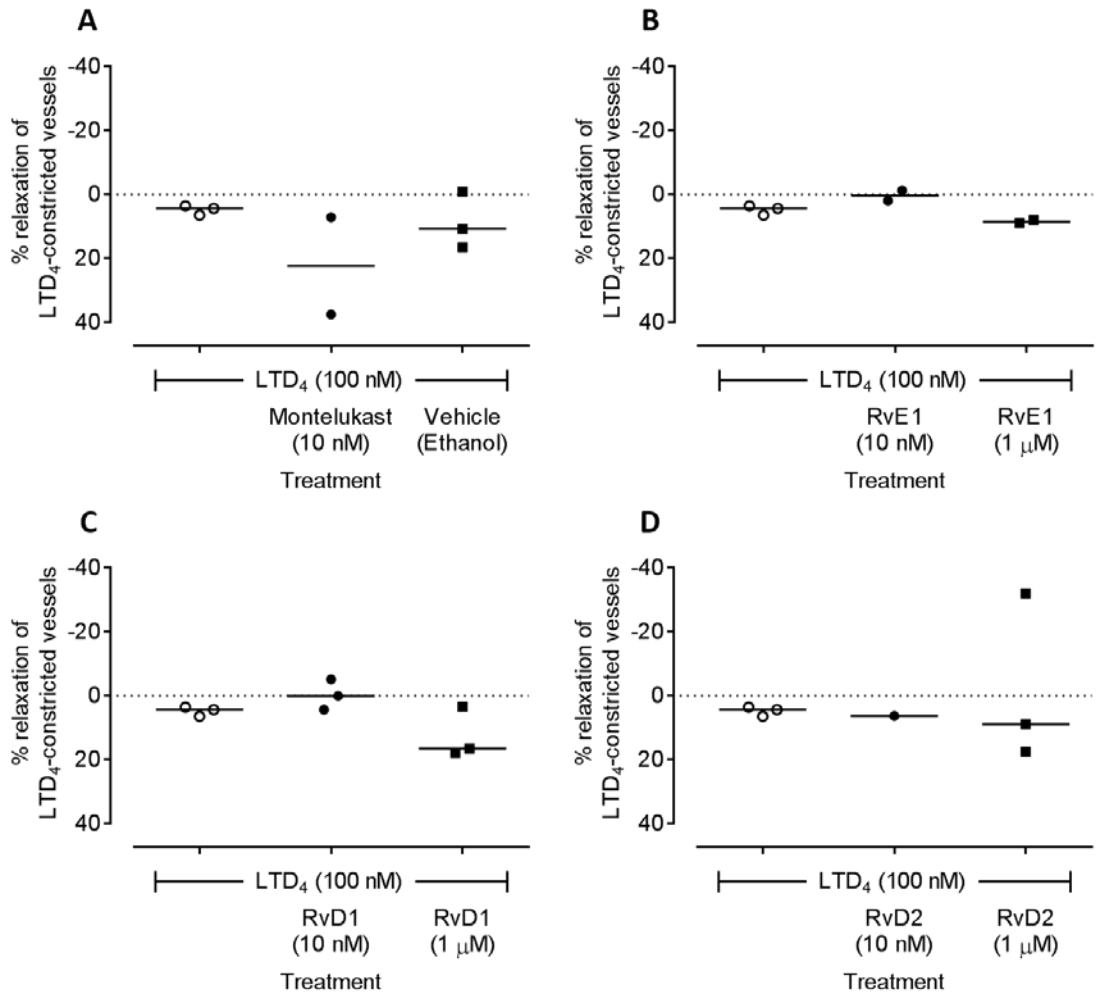

Figure 5.9: Ability of resolvins and other reagents to reverse leukotriene D_4 (LTD_4)–induced pre-constriction of human pulmonary artery (HPA). Segments were constricted with a submaximal concentration of LTD_4 (100 nM) and allowed to plateau (experimental design A). (A) Montelukast at 10 nM induced modest relaxation of LTD_4-constricted HPA (n=2). Whilst the vehicle (ethanol)-treated segments relaxed by approximately 8.8%, this was not significantly different from HPA not receiving any treatment. (B) Resolvin E1 at either 10 nM (n=2) or 1 μM (n=2) did not induce relaxation of the LTD_4-constricted HPA. (C) Resolvin D1 at 10 nM (n=3) or 1 μM (n=3) also did not significantly relax the HPA. (D) Resolvin D2 had no effect at either 10 nM (n=1) or 1 μM (n=3).

In the experiment shown in Figure 5.9 the ability of RvE1, RvD1 and RvD2 to relax HPA was assessed by first pre-constricting the artery segments with LTD_4 (100 nM), and then exposing the segments to the resolvin and measuring its effect over a 10 minute period. In addition, treatment with the $CysLT_1$ antagonist montelukast (10 nM) was used as a positive control. However, when compared with baseline, the resolvins (10 nM or 1 μM) did not induce significant relaxation, whilst montelukast (10 nM, n=2) only modestly relaxed LTD_4 pre-constricted HPA.

5.3.4 Effect of resolvins on agonist-induced constriction of human pulmonary artery segments constricted with cumulative concentration-response curves (CCRC) in series

In the experiment shown below (experimental design B), segments of HPA were constricted with cumulative concentrations of the stable thromboxane A_2 mimetic U46619, before being washed with PSS and then incubated for 1 hour with or without resolvin. At the end of the incubation period, the segments were constricted cumulatively with U46619 for a second time in the in continued presence or absence of the resolvin.

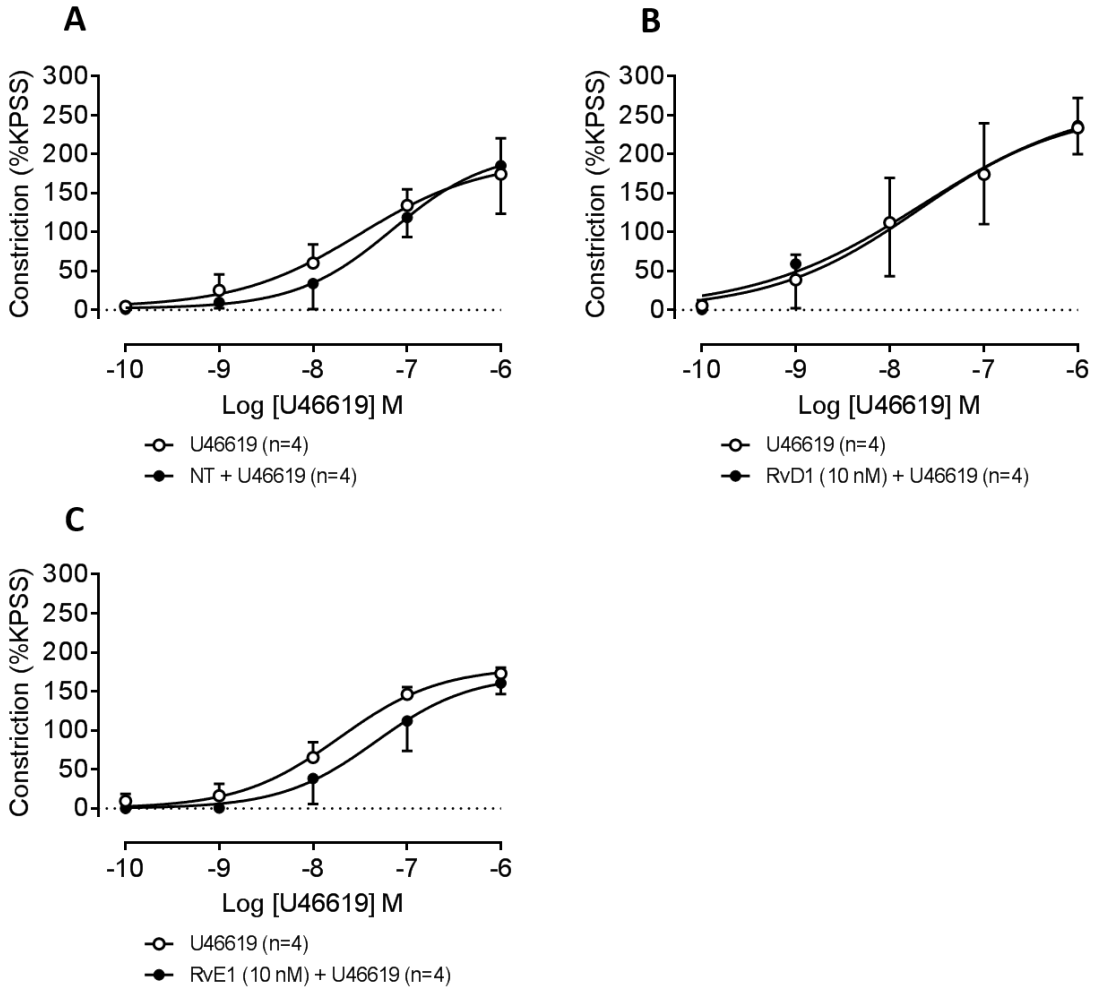

Figure 5.10: Effects of resolvins (Rv) D1 and E1 on U46619-induced constriction of human pulmonary artery (HPA) segments (using experimental design B). HPA segments were constricted with cumulative concentrations of U46619, washed with PSS to restore baseline tension before being incubated with or without RvD1 (10 nM) or RvE1 (10 nM) for 1 hour. Segments were subsequently constricted cumulatively with U44619 for a second time in the continued presence or absence of resolvin. (A) Serial treatment of HPA segments in the absence of Rv did not affect the ability of U46619 to induce constriction (n=4, mean ± SEM, p=ns). (B) Following incubation with RvD1 (10 nM) for 1 hour, the contractile response of HPA segments to U46619 was unchanged (n=4, mean ± SEM, p=ns). (C) A 1 hour incubation of HPA segments with RvE1 (10 nM) produced only a trend for inhibition (n=4, mean ± SEM, p=0.07).

The constriction of isolated segments of artery with consecutive cumulative concentration-response curves (CCRC) separated by an incubation with/without resolvin allows the investigator to first obtain the baseline response to the contractile agonist, and then examine how the response to the agonist changes following the incubation with the molecule of interest, in this case resolvins. However, as observed in chapter 4, this experimental design relies on tissue responsiveness to the agonist not spontaneously changing over time or as a consequence of repeated exposure to the agonist. Experiments to control for this can be carried out (experimental design C) and are described later in the chapter.

In the experiment above, the segments of isolated HPA do not appear to be affected by repeated exposure to the agonist, since the response to U46619 does not significantly differ following a 'no-treatment' incubation (Figure 5.10A). There was also no significant difference between the constriction of segments following their incubation with either RvD1 (Figure 5.10B) or RvE1 (Figure 5.10C).

Similar experiments were carried out to determine the effect of resolvins on leukotriene D_4 (LTD_4)-induced constriction of HPA. Segments were mounted on a wire myograph and constricted with increasing concentrations of LTD_4 before being washed and then incubated for 1 hour with or without RvD1 or RvE1. At the end of the 1 hour incubation, segments were immediately constricted with a second LTD_4 CCRC (Figure 5.11).

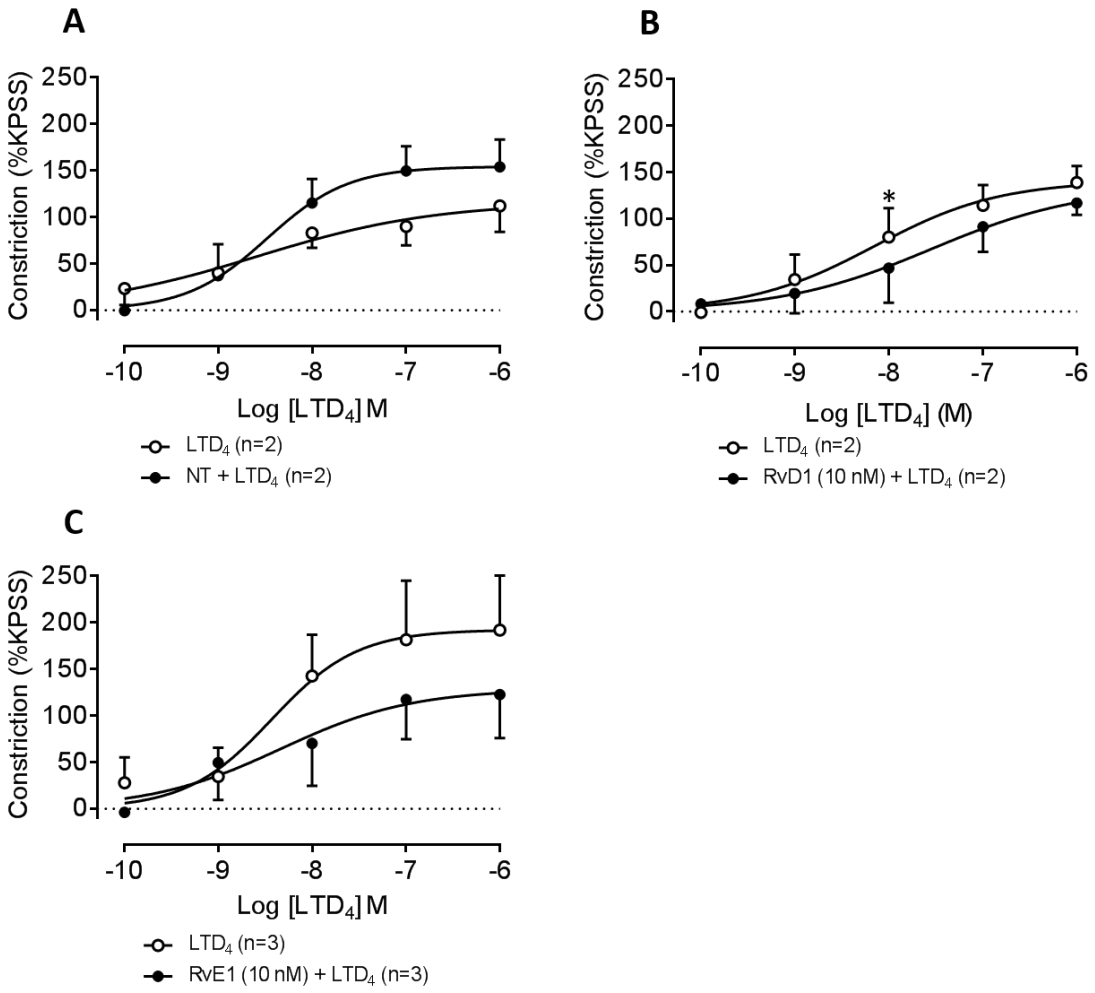

*Figure 5.11: The ability of resolvins (Rv) D1 and E1 to modulate LTD_4-induced constriction of human pulmonary arteries (HPA) (using experimental design B). (A) Segments incubated with PSS alone (no treatment) appeared to have an increased response to LTD_4 after the incubation, when compared to their response to LTD_4 prior to the incubation (n=2, mean ± SEM). (B) Following incubation of HPA segments with RvD1 (10 nM, 1 hour) the response to LTD_4 was not significantly reduced overall compared to the cumulative concentration-response curve performed prior to the incubation (n=3, mean ± SEM, p=ns), but multiple comparison testing indicates that the response is significantly lower at 10 nM LTD_4 ($p<0.05$). (C) The response of HPA segments to increasing concentrations of LTD_4 was not significantly modulated by incubation with RvE1 (10 nM, 1 hour) (n=3, mean ± SEM, p=ns). Multiple comparisons: * $p<0.05$ LTD_4 vs NT/Rv + LTD_4.*

The data in Figure 5.11 investigating whether or not resolvin D1 or E1 can modulate LTD_4-induced constriction suggest, as observed in chapter 4, that responsiveness to some agonists, particularly LTD_4, may change with repeated exposures separated by washouts. In Figure 5.11A, the segments are constricted with cumulative concentrations of LTD_4, washed to restore baseline tension and incubated in PSS in the absence of any treatment for 1 hour, before then being constricted with the same cumulative concentrations of LTD_4. Constriction of the segment to LTD_4 appears to increase during the second exposure to

LTD_4, indicating that the response to this agonist is not reproducible when repeated in the same segment. In both Figure 5.11B and 5.18C, the LTD_4 responses after resolvin incubation are lower than during the first CCRC. Whilst a repeated measures two-way ANOVA suggests that this reduction in response to LTD_4 is not significant, it suggests that an inhibitory effect of the resolvins may be masked by the baseline hyperresponsiveness induced by LTD_4 alone (Figure 5.11A).

To take this into account it is possible to group together the initial responses to LTD_4 from all of the segments as this part of the experiment is identical for all segments so that there is now a combined *n* of 7. From there, the response to LTD_4 in the first CCRC from all experiments (n=7) can be compared to the response LTD_4 in the second CCRC following each treatment (n=2-3) (Figure 5.12).

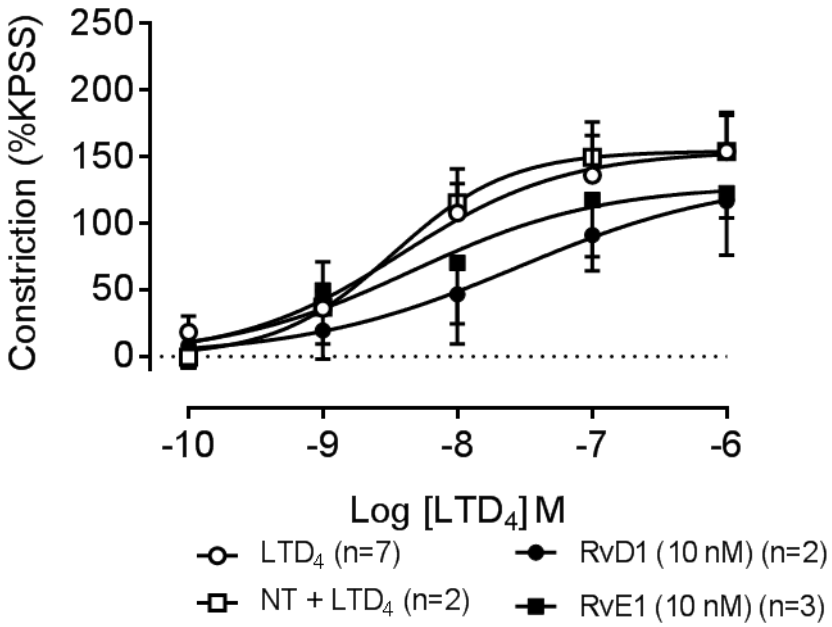

Figure 5.12: Effect of resolvins on LTD_4-induced constriction of human pulmonary artery (HPA) segments. Functionally-viable segments of HPA were constricted with increasing concentrations of LTD_4 (n=7). Baseline tension was restored to all segments. For one hour, two of the segments were incubated without resolvin, two of the segments with RvD1 (10 nM) and three of the segments with RvE1 (10 nM). Each segment was then constricted again with cumulatice concentrations of LTD_4, still in the absence or presence of resolvin. Having combined this data onto one graph, the results now suggest that there is no difference between the initial LTD_4 curve (n=7) and the LTD_4 curve following a 'no treatment' incubation (n=2), whilst both RvD1 (n=2) and RvE1 (n=3) appear to be reducing LTD_4-induced constriction of the HPA.

By pooling the LTD_4 cumulative concentration-response curve from all segments carried out prior to the incubation and thus placing all treatments on one graph, it is

possible to take into account the changing response to LTD_4 after a 'no treatment' incubation. In Figure 5.12, the pooled data suggest that there is no difference between the LTD_4 cumulative concentration-response curve (CCRC) prior to the incubation, and the LTD_4 CCRC following an incubation with PSS alone. In contrast, incubation with either RvD1 (10 nM) or RvE1 (10 nM) for 1 hour appears to dampen LTD_4-induced constriction of HPA when compared with the LTD_4 CCRC carried out prior to the incubation, even when the data are pooled and thus unpaired, although low experimental numbers may have precluded statistical significance.

5.3.5 The effect of resolvin E1 (RvE1) pre-treatment on U46619-induced constriction of rat thoracic aorta

A reoccurring problem throughout the early experiments of the overall project was a changing baseline to known contractile agonists, in particular the pro-contractile lipids LTD_4 and U46619. A new experimental design was adopted (design C – see section 5.2.3) to address this problem and avoid generating false positive or negative results.

To determine whether resolvin pre-treatment may modulate agonist-induced constriction (using experimental approach C), segments of rat thoracic aorta were incubated in DMEM-F12 (+ 10% NCS) with or without RvE1. A range of concentrations of RvE1 were tested – 0.1 nM, 1 nM, 10 nM, 100 nM and 300 nM. The segments were incubated in a culture plate for 1 or 24 hours in an incubator at 37◦C and 5% CO_2.

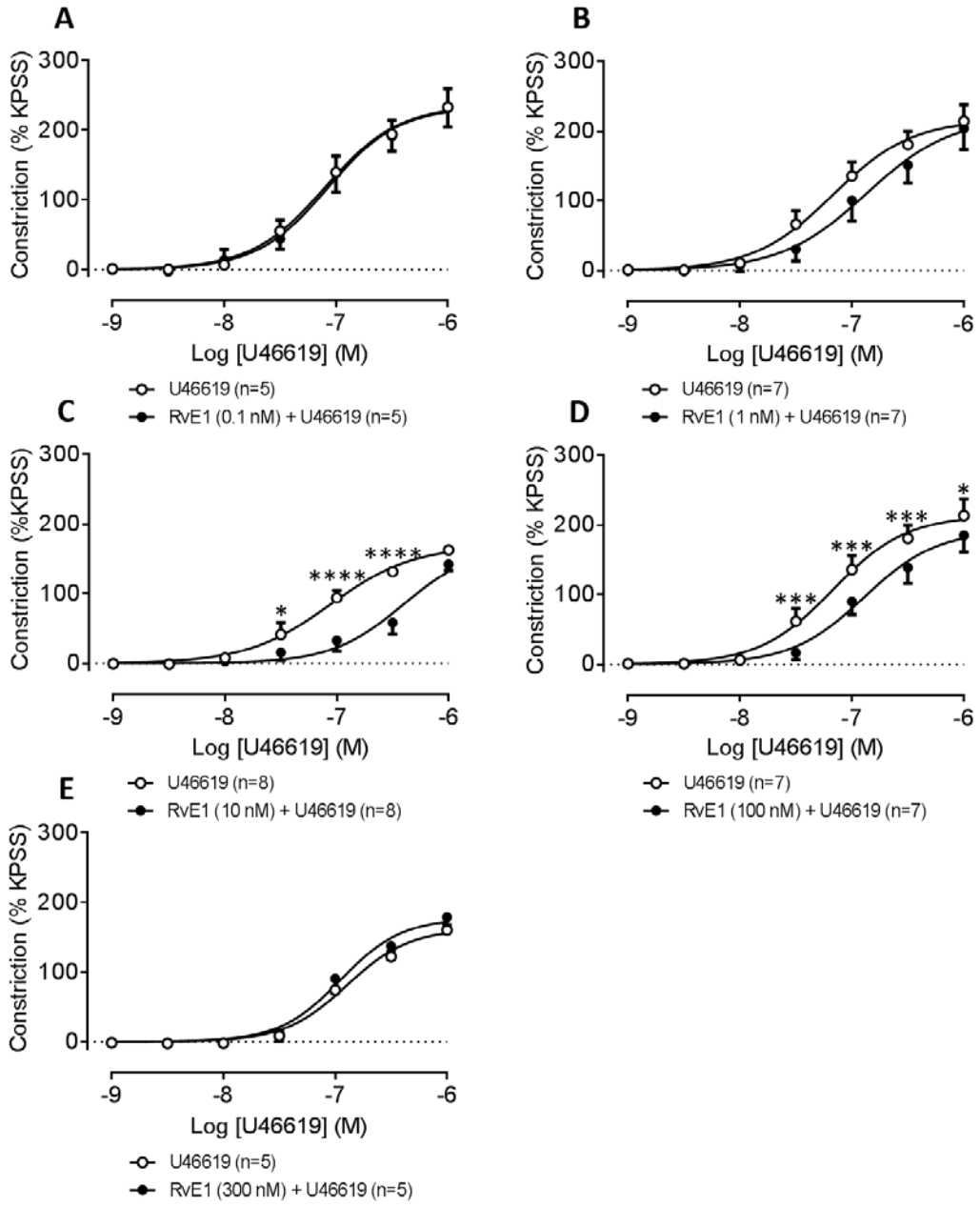

*Figure 5.13: The effect of resolvin E1 (RvE1) pre-treatment on U46619-induced constriction of rat thoracic aorta segments. Using experimental design C, segments were placed into the individual wells of a culture plate with DMEM-F12 with RvE1 at 0, 0.1, 1, 10, 100 or 300 nM for 1 hour. Following incubation, the segments were mounted on the wire myograph in physiological salt solution (PSS) and then assessed for functional integrity with KPSS. The segments were washed with PSS to restore baseline tension before being constricted with cumulative concentrations of the thromboxane A_2 mimetic U46619. Pre-treatment with RvE1 at (A) 0.1 nM (n=5) or (B) 1 nM had no significant effect on U46619-induced constriction compared with control (n=7, mean ± SEM, p=ns). (C) Incubation of segments with RvE1 (10 nM) significantly inhibited U46619-induced constriction (n=8, mean ± SEM, p<0.0001). (D) Pre-treatment with RvE1 (100 nM) caused a strong trend for inhibition of U46619-induced constriction (n=7, mean ± SEM, p=0.05). Sidak's multiple comparisons test suggests that inhibition by 100nM RvE1 is significant at all U46619 concentrations above 30 nM. (E) Segments pre-treated with RvE1 (300 nM) did not respond significantly differently to U46619-induced constriction when compared with control. Multiple comparisons: * p<0.05 U46619 vs RvE1 + U46619, *** p<0.001 U46619 vs RvE1 + U46619, **** p<0.0001 U46619 vs RvE1 + U46619.*

The results in Figure 5.13 suggest that pre-treatment of rat thoracic aorta segments with RvE1 for 1 hour significantly impairs their contractile response to U46619. The inhibitory effect of RvE1 appears to follow a bell-shaped concentration curve, with 10 nM of RvE1 causing the most effective inhibition of U46619-induced constriction, and declining at lower and higher concentrations (Figure 5.14).

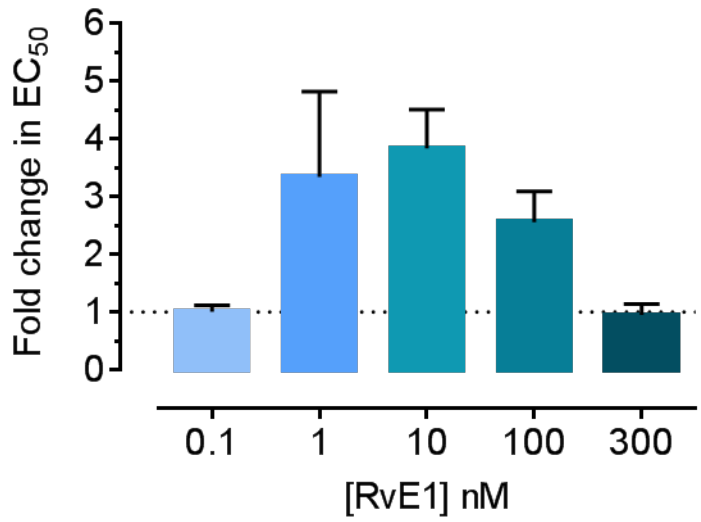

Figure 5.14: The fold change in EC_{50} for U46619-induced constriction of rat aorta after 1 hour pre-treatment with a range of concentrations of RvE1. The EC_{50} of each cumulative concentration-response curve (CCRC) was individually calculated, and the ratio between the EC_{50}'s of the CCRC carried out on control segments and the EC_{50}'s of the CCRC carried out on RvE1 pre-treated segments was calculated. Pre-treatment with RvE1 at 10 nM induced the biggest fold increase in EC_{50}, whilst pre-treatment with 1 or 100 nM induced a slightly smaller change in EC_{50}. Neither the lowest (0.1 nM) nor the highest (300 nM) concentration of RvE1 tested caused any clear change in the EC_{50}, suggesting that the inhibitory effect of RvE1 is bell-shaped.

Statistical analysis suggests that the EC_{50} (concentration of agonist required to evoke 50% of the maximum response) from the control U46619 cumulative concentration-response curve (CCRC) is significantly different to the EC_{50} of the paired RvE1 treated U46619 CCRC (Table 5-1).

[RvE1] nM	Ratio	t test p value
0.1	1.01	0.28
1	3.34	0.09
10	3.84	0.004
100	2.56	0.02
300	0.95	0.96

Table 5-1: Comparing EC_{50}'s between control and RvE1 pre-treated rat thoracic aorta segments. The EC_{50} (concentration of agonist required to evoke 50% of the maximum response) of the control and RvE1 pre-treated segments were calculated, and their differences determined. A paired, two-way Student's t-test indicates that treatment with RvE1 at 10 nM (n=8, p=0.004) or 100 nM (n=7, p<0.05) significantly shifts the EC_{50} to the right, meaning that significantly more U46619 is required in the presence of RvE1 in order to evoke half of the maximal contractile response.

To determine whether a longer treatment with RvE1 would have a different effect on U46619-induced constriction, segments were incubated with RvE1 in culture plates, as described in the experiment above, but for 24 hours instead of 1 hour.

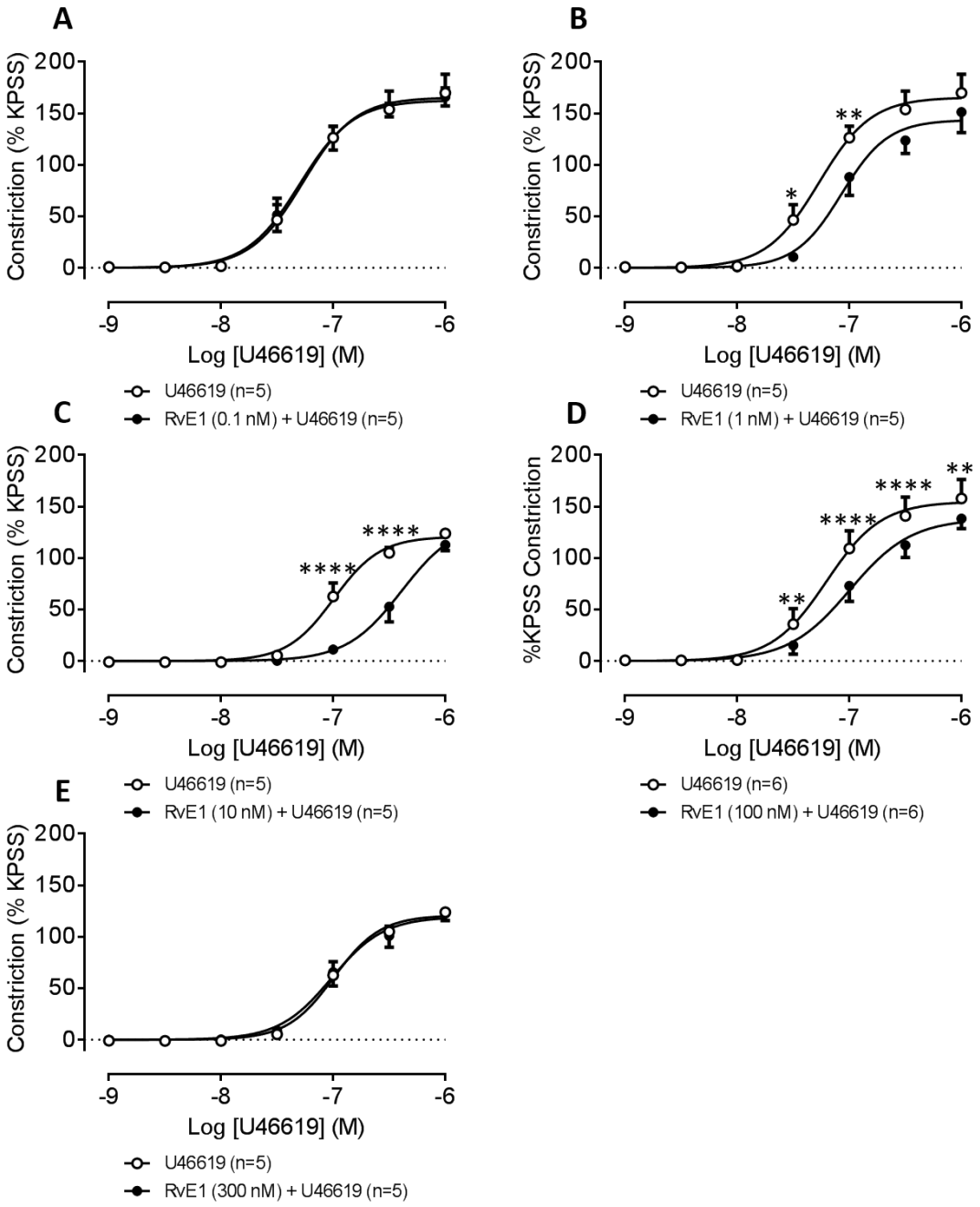

*Figure 5.15: The effect of resolvin E1 (RvE1) pre-treatment on U46619-induced constriction of rat thoracic aorta segments, as assessed by experimental design C. (A) Pre-treatment for 24 hours with RvE1 at 0.1 nM had no significant effect on U46619-induced constriction of rat aorta segments (n=5, mean ± SEM, p=ns). (B) Overall, treatment with RvE1 at 1 nM did not significantly modulate U46619-induced constriction, but, Sidak's multiple comparisons test indicated that RvE1 (1 nM) did significantly impair constriction when U46619 was used at 30 nM and 100 nM concentrations (n=5, mean ± SEM, p=ns). (C) Pre-treatment with 10 nM RvE1 for 24 hours resulted in the significant inhibition of U46619-induced constriction (n=5, mean ± SEM, p<0.05), with multiple comparison testing indicating that the difference is biggest at 100 and 300 nM U46619. (D) Pre-treatment with 100 nM RvE1 had a similar effect on U46619-induced constriction as 10 nM RvE1, significantly shifting the curve rightward (n=6, mean ± SEM, p<0.05). (E) Pre-treatment with the highest concentration of RvE1 tested, 300 nM, had no significant effect on U46619-induced constriction. Multiple comparisons: * p<0.05 U46619 vs RvE1 + U46619, ** p<0.01 U46619 vs RvE1 + U46619, **** p<0.0001 U46619 vs RvE1 + U46619.*

The pre-treatment of rat thoracic aorta segments with RvE1 for 24 hours mediated a similar effect as pre-treating for just 1 hour. To quantify the effect, the fold change in EC_{50} after 24 hours pre-treatment was calculated for each pair of segments – one in the absence of RvE1 and one in the presence of RvE1, and is shown in Figure 5.16.

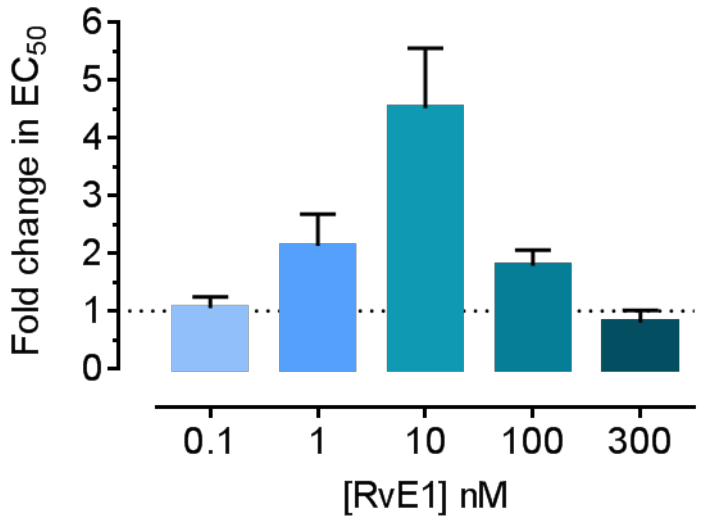

Figure 5.16: The fold change in EC_{50} for U46619-induced constriction of rat aorta after 24 hour pre-treatment with a range of concentrations of RvE1.

The data in Figure 5.16 demonstrate a clear bell-shaped inhibition curve for RvE1 on U46619-induced constriction. The fold change in EC_{50} was calculated for each pair (control matched with an RvE1 pre-treated segment) of segments, and the mean fold change in EC_{50} plotted. Pre-treatment with 10 nM RvE1 induced a 4.5-fold increase in EC_{50}, whilst the inhibitory effect declined at lower and higher RvE1 concentrations. The results of paired Student's t-tests are shown in Table 5-2.

[RvE1] nM	Fold change	Student's t-test p value
0.1	1.05	0.86
1	2.13	0.12
10	4.52	0.03
100	1.78	0.03
300	0.80	0.39

Table 5-2: Fold change in EC_{50} of U46619 following pre-treatment with RvE1 for 24 hours. Pre-treatment of rat thoracic aorta segments with RvE1 at both 10 and 100 nM caused a significant change in EC_{50} ($p<0.05$), but treatment with 0.1, 1 or 300 nM RvE1 did not had no significant effect.

5.3.6 The effect of a resolvin E1 (RvE1) pre-treatment on phenylephrine-induced constriction of rat aorta

It was pertinent to investigate whether this inhibitory effect of RvE1 is specific to thromboxane (U46619)-induced constriction, or whether it can also dampen the constriction of vessels induced by other agonists. Here, the ability of RvE1 (10 nM) to inhibit PE-induced constriction of rat aorta was determined using experimental design C.

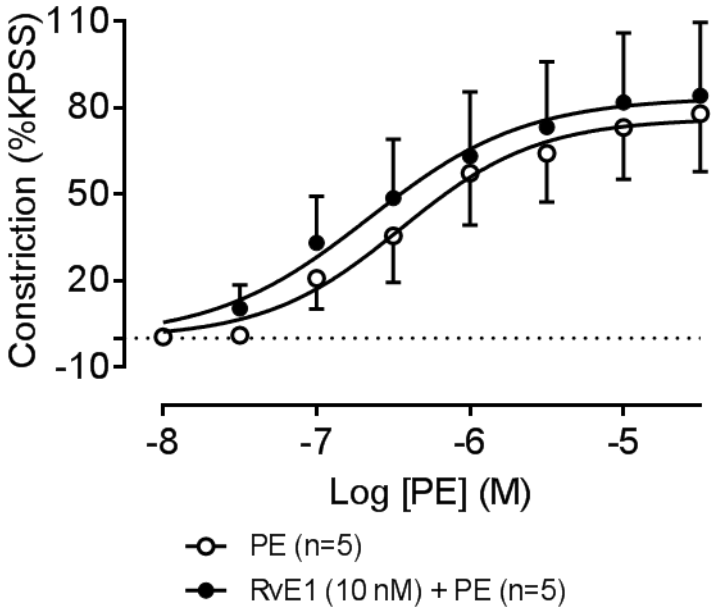

Figure 5.17: The effect of a 1 hour pre-treatment with RvE1 (10 nM) on phenylephrine (PE)-induced constriction of rat thoracic aorta. The ability of RvE1 to modulate PE-induced constriction was assessed using experimental design C. The data indicate that RvE1 (10 nM) mediates no significant effect on PE-induced constriction of rat aorta segments in vitro (n=5, mean ± SEM, p=ns).

The data in Figure 5.17 suggests that the pre-treatment of rat thoracic aorta segments with RvE1 at 10 nM for 1 hour does not significantly affect the ability of PE to mediate constriction.

5.3.7 Effect of pre-treatment (1 hour) with D series resolvins RvD1 and RvD2 on U46619-induced constriction of rat aorta

Having shown that pre-treatment with EPA-derived resolvin E1 can modulate U46619-induced constriction of isolated rat aorta segments, it was important to determine whether members of the D series resolvin family, derived from DHA, are also capable of mediating such effects. Segments of rat thoracic aorta were incubated with/without RvD1 (Figure 5.18) or RvD2 (Figure 5.19) for 1 hour at one of three concentrations – 1, 10 or 100 nM. These concentrations were chosen based on the results with RvE1 (Figure 5.13), and since much evidence suggests that the resolvins are bioactive in the nanomolar range.

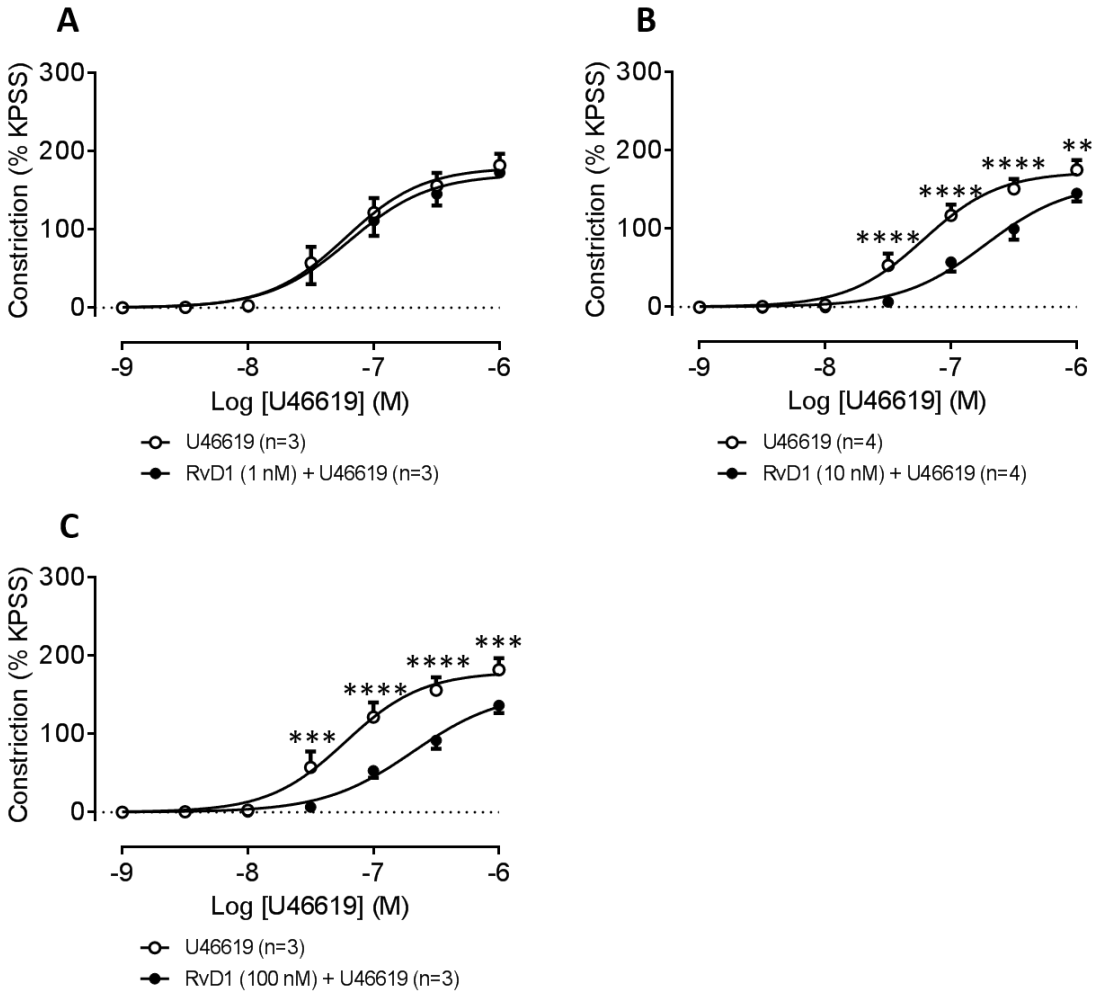

*Figure 5.18: The effect of pre-treating rat thoracic aorta segments with RvD1 for 1 hour on U46619-induced constriction. Segments were incubated with or without RvD1 for 1 hour, and mounted on a wire myograph where they were assessed for functional integrity. Segments were then constricted with increasing concentrations of U46619. (A) Pre-treatment of segments with RvD1 at 1 nM had no significant effect on U46619-induced constriction. In contrast, pre-treatment with RvD1 at (B) 10 nM (n=4, mean ± SEM, p<0.01) or (C) 100 nM (n=3, mean ± SEM, p<0.05) significantly inhibited U46619-induced constriction. Multiple comparisons: ** p<0.01 U46619 vs RvD1 + U46619, *** p<0.001 U46619 vs RvD1 + U46619, **** p<0.0001 U46619 vs RvD1 + U46619.*

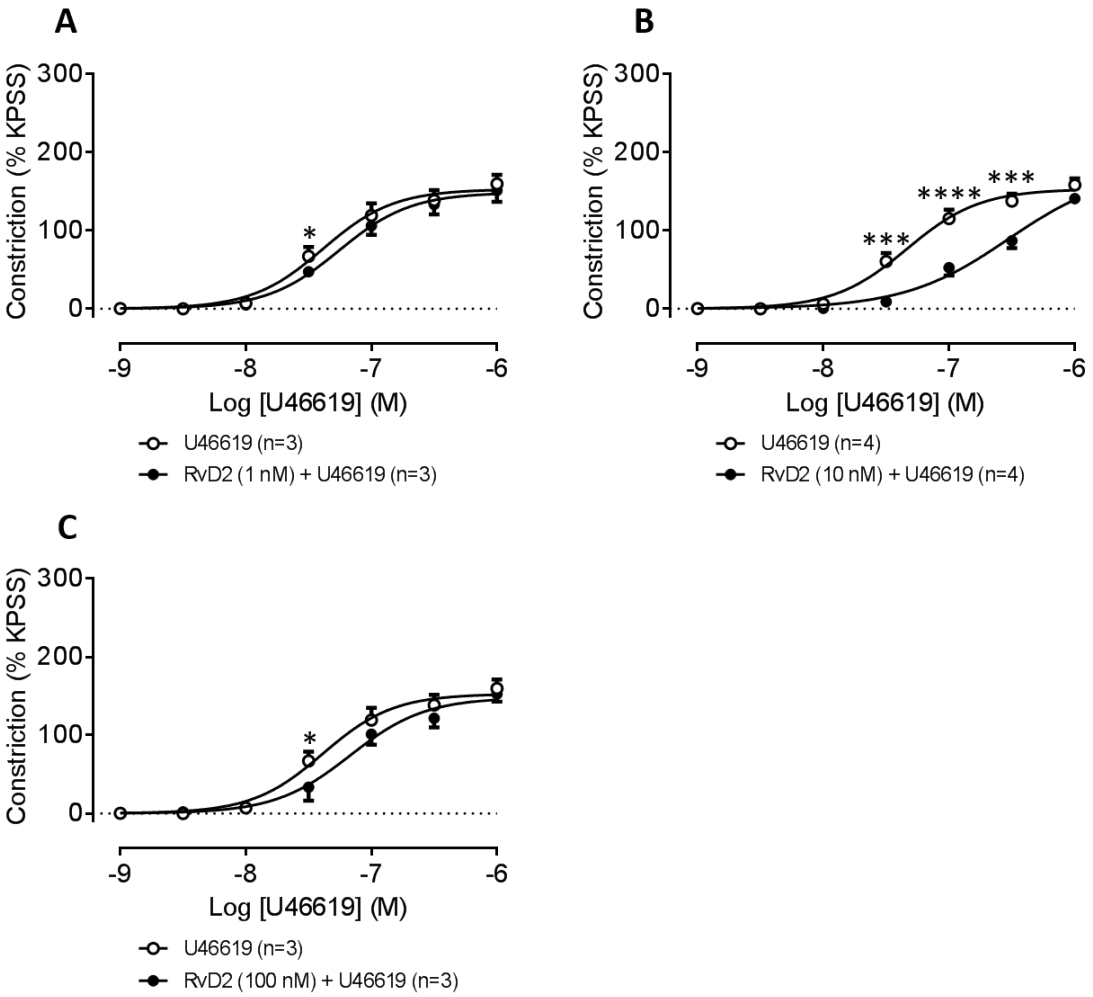

*Figure 5.19: Effect of pre-treating rat thoracic aorta segments with RvD2 for 1 hour on U46619-induced constriction. Segments were incubated with or without RvD2 for 1 hour, mounted on a wire myograph and constricted with cumulative concentrations of the stable thromboxane mimetic, U46619. The pre-treatment of vessels for 1 hour with (A) 1 nM RvD2 or (n=3, mean ± SEM, $p<0.05$) (B) 10 nM RvD2 (n=4, mean ± SEM, $p<0.05$) significantly inhibited U46619-induced constriction. (C) Those segments of rat thoracic aorta pre-treated with 100 nM RvD2 did not overall respond significantly differently to those segments incubated in media alone, although multiple comparison testing suggesting that at 30 nM U46619, the response to U46619 is lower in those segments pre-treated with RvD2. Multiple comparisons: * $p<0.05$ U46619 vs RvD2 + U46619, *** $p<0.001$ U46619 vs RvD2 + U46619, **** $p<0.0001$ U46619 vs RvD2 + U46619.*

The data in Figure 5.18 and Figure 5.19 demonstrate that pre-treatment for 1 hour with either RvD1 or RvD2 significantly inhibited U46619-induced constriction of rat thoracic aorta. As with RvE1 pre-treatment, the inhibitory effect of the D series resolvins is dependent on the concentration used, with moderate concentrations having the maximal effect, and inhibition declining at lower and higher concentrations.

5.3.8 Effect of resolvin E1 pre-treatment (1 hour) on U46619-induced constriction of human pulmonary artery

Having shown that RvE1 can concentration-dependently inhibit U46619-induced constriction of rat thoracic aorta segments, it was of interest to determine whether or not these findings are also apparent in human arteries.

Human pulmonary arteries (HPA) were isolated from lung tissue samples donated by patients undergoing thoracic surgery. The HPA were cleaned of surrounding tissue and incubated in DMEM-F12 with RvE1 for 1 hour at 37◦C/5% CO_2. A number of concentrations of RvE1 were investigated – 0, 0.1, 1, 10, 100 and 300 nM. Following the incubation, the segments were carefully mounted on to a wire myograph in PSS and a baseline tension of 1.5g was set. Functional integrity was confirmed as a positive response to KPSS, after which the segments were washed with PSS to restore baseline tension. Finally, the segments were constricted with cumulative concentrations of the stable thromboxane mimetic, U46619 (Figure 5.20).

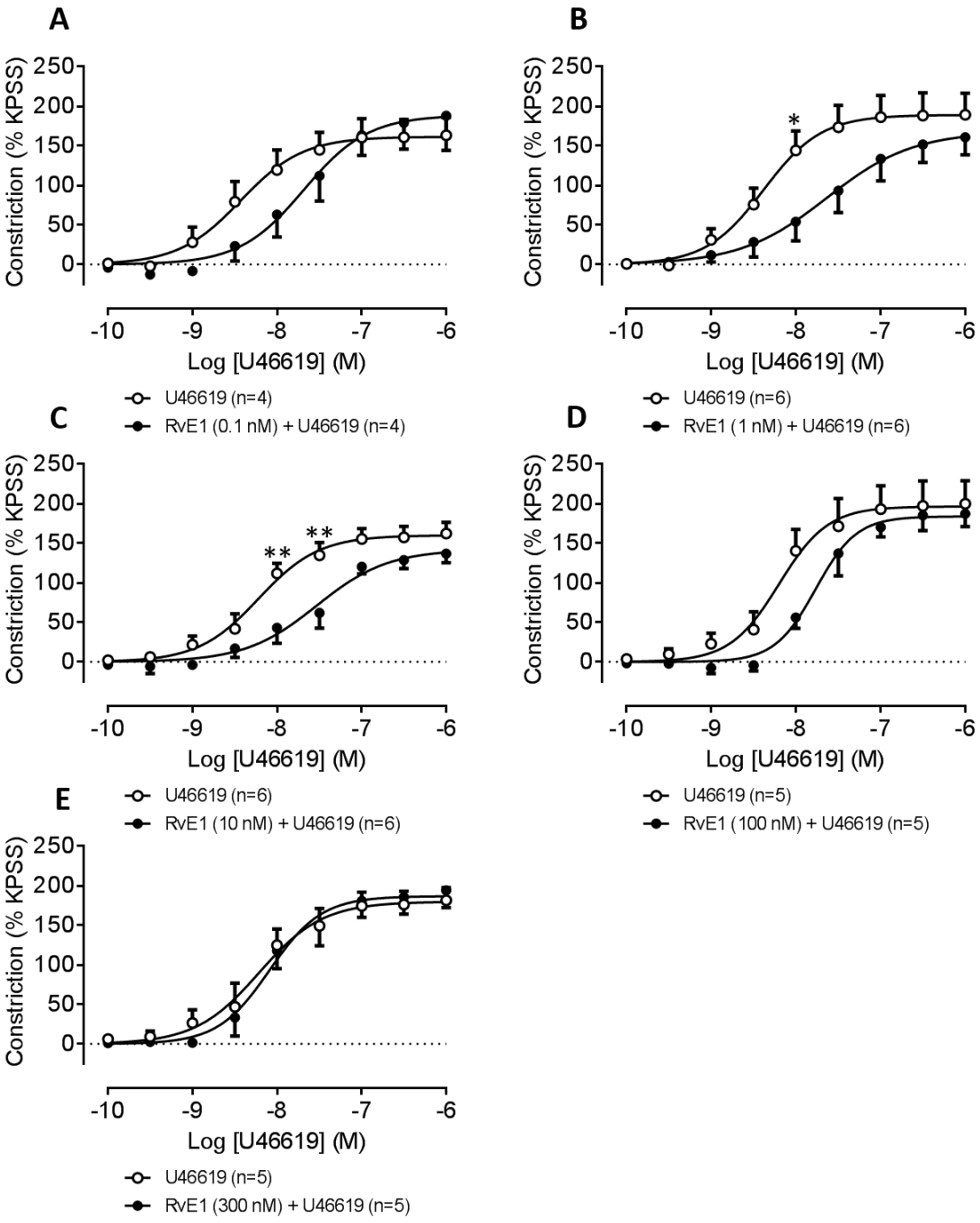

*Figure 5.20: Effect of RvE1 pre-treatment (1 hour) on U46619-induced constriction of segments of human pulmonary artery (HPA). Segments were incubated for 1 hour with or without a range of concentrations of RvE1 (0.1, 1, 10, 100, 300 nM), mounted on a wire myograph and constricted with cumulative concentrations of U46619 (experimental design C). (A) Pre-treatment of segments with 0.1 nM RvE1 had no significant effect on U46619-induced constriction (n=4, mean ± SEM, p=ns). (B) Pre-treatment with 1 nM RvE1 significantly inhibited the contractile response to U46619 (n=6, mean ± SEM, p=0.0003). (C) Pre-treatment with 10 nM RvE1 significantly inhibited U46619-induced constriction, particularly at 10 and 30 nM of U46619 (n=6, mean ± SEM, p<0.0001). (D) Pre-treatment with 100 nM RvE1 significantly inhibited U46619-induced constriction (n=5, mean ± SEM, p<0.05). (E) Segments pre-treated with 300 nM RvE1 did not constrict significantly differently to U46619 when compared with control (n=5, mean ± SEM, p=ns). Multiple comparisons: * p<0.05 U46619 vs RvE1 + U46619, ** p<0.01 U46619 vs RvE1 + U46619, ordinary two-way ANOVA (not repeated measures) with Sidak's multiple comparisons test.*

The data in Figure 5.20 suggest that RvE1 has a similar inhibitory effect on U46619-induced constriction in human pulmonary arteries as it does in rat thoracic aorta. Following a 1 hour incubation with RvE1 at a range of concentrations, it is evident that 10 nM RvE1 was most effective overall at inhibiting U46619-induced constriction in HPA (n=6, $p<0.0001$). This concentration of RvE1 was also the most effective in rat thoracic aorta. Yet, as shown Figure 5.20, RvE1 at just 1 nM also mediates significant inhibition of U46619-induced constriction in HPA (n=6, $p=0.0003$), causing a rightward shift in EC_{50} that is approximately 5.5-fold. Ordinary two-way ANOVA, and not repeated measures ANOVA was carried out since the initial experiments were carried out with a U46619 CCRC from 1 nM – 1 µM, but this was then extended to 0.1 nM – 1 µM.

5.5 Results – expression of receptors for pro-resolving mediators in human pulmonary arteries

Aim 3b (section 1.9) was to quantify the immunoexpression of the putative SPM receptors ChemR23, GPR32 and ALX in human pulmonary arteries and to localise the receptors with markers for smooth muscle and other cell-types.

5.5.1 Visualising smooth muscle and endothelium in human pulmonary artery by immunofluorescent confocal microscopy

α-Smooth muscle actin (α-SMA) is a cytoskeletal protein strongly expressed in smooth muscle cells. Von Willebrand factor (vWF) is a glycoprotein involved in haemostasis and is considered a marker of endothelial cells. The expression of α-SMA and vWF in sections of human pulmonary artery was investigated using immunofluorescent antibodies and confocal microscopy (as described in section 2.8.4). Figure 5.21 shows that α-SMA (red stain) was expressed in a thick layer of arterial smooth muscle beneath the single layer of endothelial cells (stained green for vWF) lining the lumen. Cell nuclei were stained blue with DAPI.

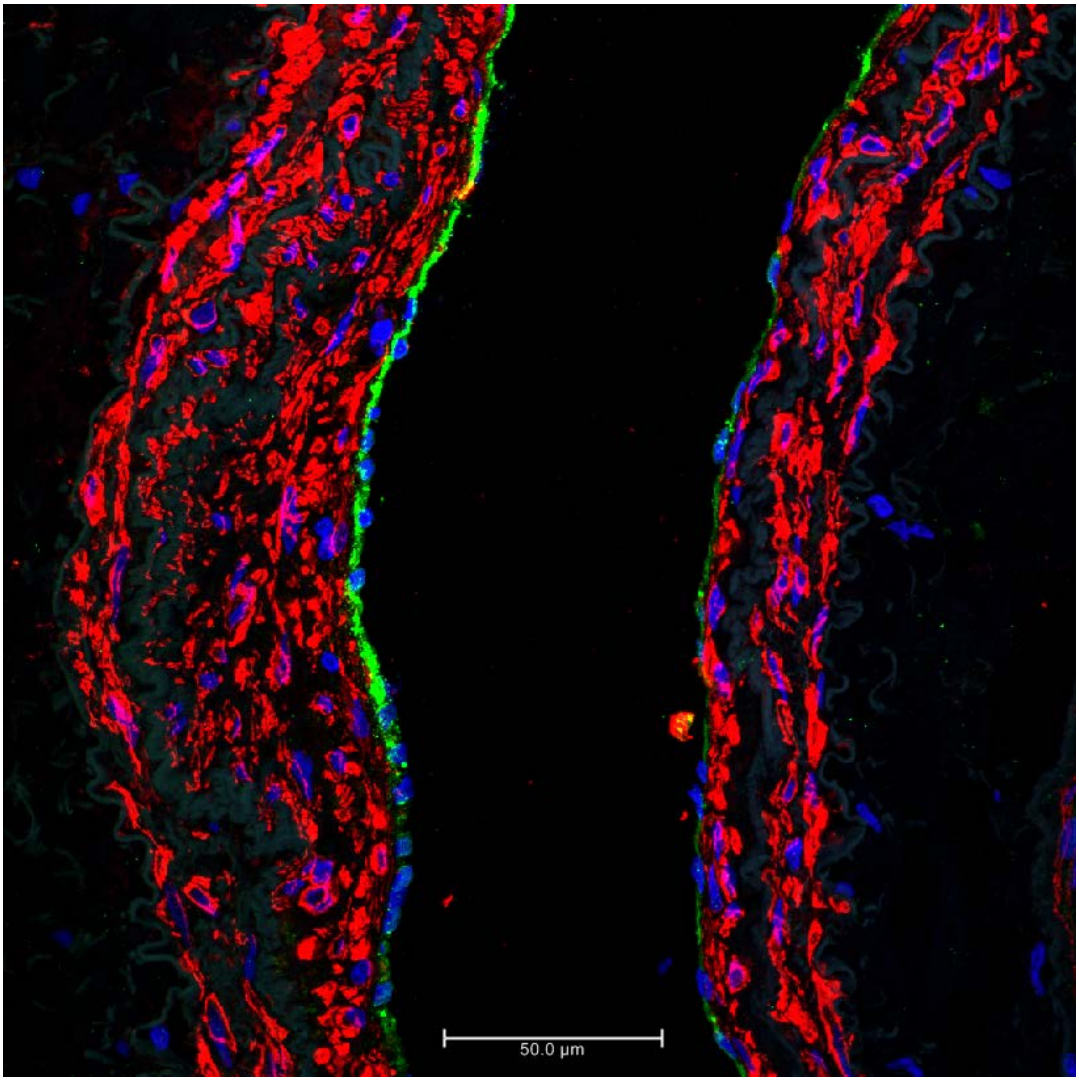

Figure 5.21: Expression of α-smooth muscle actin (α-SMA) and von Willebrand factor (vWF) in sections of human pulmonary artery, as visualised by immunofluorescent confocal microscopy. The thick layers of arterial smooth muscle stain red for α-SMA and are situated beneath to the endothelial cell layer, which stains green for vWF and lines the lumen. The cell nuclei stained with DAPI appear blue. Scale bar = 50 µm.

5.5.2 Investigating the expression of putative pro-resolving receptors in human pulmonary artery by immunohistochemistry

As described in chapter 1, resolvins may act at common receptors shared with other lipid families (e.g. BLT1 receptor shared by LTB_4 and RvE1), or at one or more orphan GPCRs putatively identified as mediating the effects of the different specialised pro-resolving mediators (SPM), including ChemR23, GPR32, and ALX.

The natural ligand for ChemR23 is the chemotactic peptide chemerin. More recently, resolvin E1 has been shown to be an agonist at ChemR23 receptors, mediating pro-resolution actions such as inhibiting PMN infiltration in mice with zymosan A-induced

peritonitis (Arita et al. 2007). The orphan receptor GPR32 is now known to be activated by three different DHA-derived resolvins – RvD1, RvD3 and RvD5 – as well as by lipoxin A_4. The ALX receptor, formally known as the formyl-peptide receptor (FPR)2 or formyl-peptide receptor-like 1 (FPRL1), is activated by LXA_4 and also by RvD1 (Krishnamoorthy et al. 2010). Despite the multiple agonists at each pro-resolving receptor, identifying their tissue sites and intensity of expression in HPA may help identify the receptor(s) responsible for mediating the physiological actions of the resolvins investigated in this chapter. As described in section 2.8, HPA sections in paraffin wax were stained with rabbit primary antibodies for ALX, ChemR23 or GPR32 (Figure 5.22) and visualised with biotinylated secondary antibodies linked to avidin-biotin peroxidase complex, with AEC (red) as the chromogen (section 2.8).

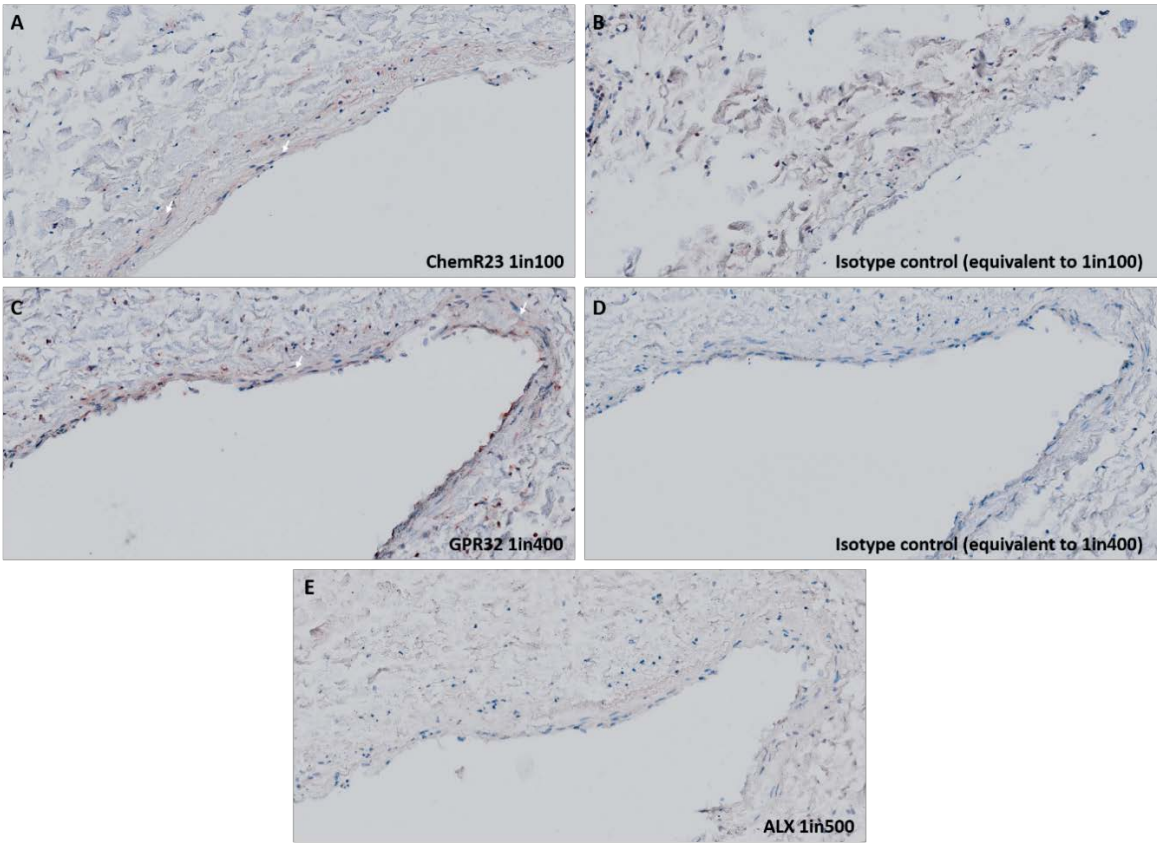

Figure 5.22: Expression of the pro-resolving receptors ChemR23, GPR32 and ALX in human pulmonary artery (HPA) as determined by immunohistochemistry (n=1). After fixation and embedding in paraffin wax, HPA sections were treated with rabbit primary antibodies for the receptors or with isotype controls, as described in the Methods (section 2.9). Avidin-biotin-peroxidase amplification in conjunction with the AEC chromogen (red) was used to visualise the receptors (section 2.9.5), whilst Mayer's haematoxylin (blue) was the nuclear stain. (A) ChemR23 (a receptor for RvE1) appears to be positively expressed in the vascular smooth muscle layers (white arrows), compared to its isotype control (B). (C) GPR32 (a receptor for RvD1) appears to be strongly expressed in vascular endothelium, as well as in the smooth muscle layers (white arrows), compared to its isotype control in (D). (E) The lipoxin A_4 receptor ALX (which is also a receptor RvD1) does not appear to be expressed strongly in HPA.

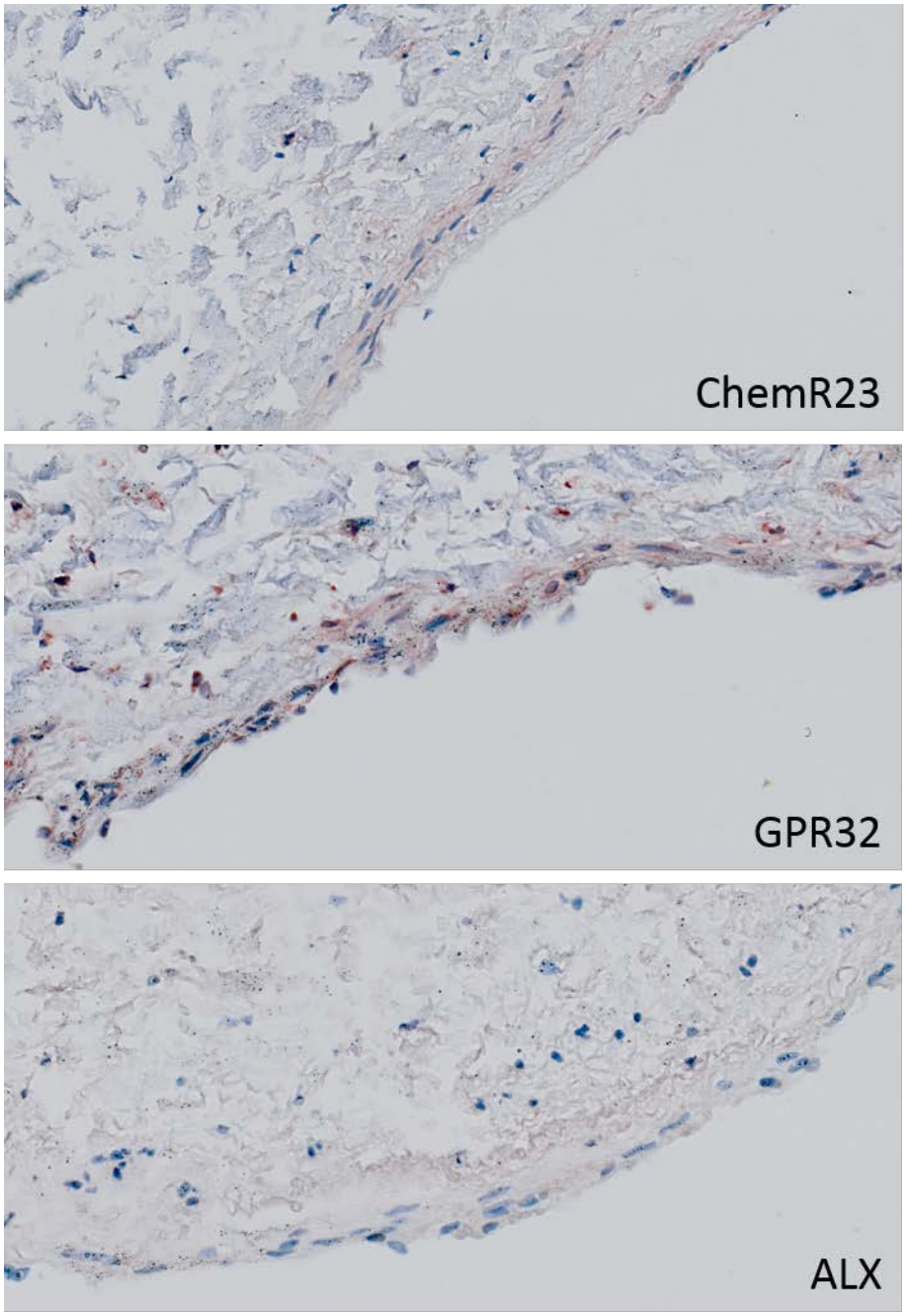

Figure 5.23: Magnified view of immunohistochemistry staining for pro-resolving G protein-coupled receptors, ChemR23, GPR32 and ALX, in human pulmonary artery tissue as described in the previous figure.

Figure 5.22 and Figure 5.23 suggest that both GPR32 and ChemR23 are expressed in the smooth muscle of human pulmonary arteries, consistent with the possibility they directly mediate the inhibitory effects of resolvins D1 and E1 respectively, as seen in the myography experiments. It is possible that the GPR32 receptor immuno-expressed on vascular endothelium may have a role in the secondary release of vasoactive mediators, although exploring this possibility requires studies in endothelium-denuded HPA.

5.6 Summary of Results

The experiments described in this chapter explored (a) the effects of resolvins D1, D2 and E1 on the contractility of rat thoracic aorta and human pulmonary arteries, and (b) the immunoexpression of pro-resolving receptors ChemR23, GPR32 and ALX in human arteries, as outlined in Aim 3b (see section 1.9). The main findings were:

- Using experimental design A, resolvins D1, D2 and E1 (100 nM) did not reverse pre-constrictions of rat thoracic aorta segments induced by either PE or U46619, nor did they reverse LTD_4-induced constriction of human pulmonary arteries, although the latter could be partly reversed by the $CysLT_1$ receptor antagonist montelukast.
- Using experimental design B:
    - Pre-treatment for 1 hour with resolvins D1 or E1 (10 nM) did not inhibit U46619-induced constriction of human pulmonary arteries.
    - Studies with LTD_4 in human pulmonary artery were complicated by low numbers of experiments and possible changes in baseline responsiveness, but pre-treatment with resolvin D1 or E1 (10 nM) produced non-significant trends for reduced contractility.
- Using experimental design C:
    - In rat thoracic aorta, pre-treatment with RvE1 for 1 hour did not inhibit constriction induced by PE, but it significantly inhibited constriction induced by U46619. The inhibition followed a bell-shaped curve over a range of RvE1 concentrations (0.1 to 300 nM) with maximal inhibition at 10 nM. A similar bell-shaped inhibition curve was seen with RvE1 pre-treatment for 24 hours.
    - Constriction of rat aorta induced by U46619 was also significantly inhibited by 1 hour pre-treatment with RvD1 or RvD2, with bell-shaped inhibition curves maximal at about 10 nM.
    - In human pulmonary arteries, RvE1 pre-treatment for 1 hour significantly inhibited U46619-induced constriction, again with a bell-shaped curve but with maximal inhibition achieved at concentrations approaching 1 nM.
- The pro-resolving receptors GPR32 (bound by RvD1) and ChemR23 (bound by RvE1) were expressed within the layers of vascular smooth muscle (expressing α-smooth muscle actin) in human pulmonary arteries, with GPR32 also present in the vascular endothelium (expressing von Willebrand factor). The ALX receptor was poorly expressed and not well-localised.

5.7 Discussion

This chapter attempted the twin objectives of Aim 3, namely to use wire myography to explore the ability of resolvins to modulate the contractility of rat and human arteries constricted with phenylephrine (PE) or with the lipid mediators thromboxane A_2 and leukotriene D_4, and to use immunofluorescence confocal microscopy and immunohistochemistry to quantify the expression of receptors for RvD1 (GPR32 and ALX) and RvE1 (ChemR23) in human pulmonary artery and to localise them to smooth muscle and/or vascular endothelium.

The myography experiments in blood vessels used the three experimental designs (A, B and C) discussed in the airway myography experiments in chapter 4. In **experimental design A** (section 5.3.1, figures 5.1 and 5.2), a single concentration of resolvin was added to vessels pre-constricted with a known contractile agonist to determine whether the resolvin can reverse or enhance the constriction. This design is sensitive as a resolvin effect is readily visible against the stable plateau of pre-constriction, but with the disadvantage that the response has to be rapid enough to occur within a short period (10 minutes). In **experimental design B** (section 5.2.2, Figure 5.3) a cumulative concentration-response curve was established to the agonist, and after a washout the cumulative concentration-response curve was repeated following resolvin pre-treatment (1 hour, and in its continued presence during the second agonist exposure), or with no resolvin. This 'series' design means that resolvin activity with a slower onset can be investigated, and it enables comparisons of the responses with and without the resolvin on the same vessel segment. However, the possibility of a 'hangover' effect (such as tachyphylaxis or hyperreactivity) from the first agonist exposure persisting into the second exposure led to the use in some experiments of **design C** (section 5.2.3) in which the control and resolvin treatments were applied simultaneously and in parallel to pairs of adjacent segments from the same vessels which were subsequently mounted in separate myograph chambers.

Initial characterisation of rat thoracic aorta by myography not only confirmed their functional viability with KPSS, but also confirmed that they constrict as expected in a concentration-dependent manner to the alpha-1 adrenoceptor agonist PE, showing that the vessels can respond to a GPCR-dependent contractile agonist (Figure 5.5). Furthermore they were completely relaxed by acetylcholine (ACh) (Figure 5.6), which relaxes vascular smooth muscle by secondary release of NO from endothelial cells, mediated by muscarinic

receptors; this 'physiological antagonism' of PE by ACh provides a positive control for exploring the physiological relaxant effects of resolvins in this model.

The initial experiments in blood vessels with resolvins used experimental design A to determine whether they can reverse (or enhance) pre-existing constrictions. At 100 nM, resolvins D1, D2 and E1 did not reverse (or enhance) pre-constriction of rat thoracic aorta induced by PE (Figure 5.7) or U-46619 (Figure 5.8), or pre-constriction of human pulmonary arteries (HPA) induced by LTD_4 (Figure 5.9). In a limited number of experiments montelukast partially blocked LTD_4-induced pre-constriction of HPA; this demonstrates the expected control response to pharmacological (competitive) antagonism of the $CysLT_1$ receptors on vascular smooth muscle cells. These controls, together with the sensitivity of experimental design A, provide clear evidence that these resolvins (at 100 nM concentration) cannot acutely relax rat and human arteries.

This initial result is somewhat surprising as topical application of RvD2 applied to the ears of mice (100 ng per ear) generated the vasodilator nitric oxide (NO) (Spite et al. 2009). NO was released significantly above control levels by 10 minutes, and this increased further by 30 minutes, indicating that NO is produced in response to RvD2 within the time frame of the experiments shown in Figure 5.7 and Figure 5.8. Thus, were RvD2 capable of inducing relaxation via NO production in rat aorta then it should have been seen in these experiments. In addition, RvD2, even at a much lower concentration (1 nM) than that used in the current experiment (100 nM) can generate both NO and prostacyclin (PGI_2, another potent vasodilator) in human umbilical vein endothelial cells (HUVECs) in culture (Spite et al. 2009). As noted, acetylcholine was able to relax rat aorta in the current study and this depends on NO generation from intact endothelium, so RvD2 at 100 nM should have been able to do the same.

A putative receptor for RvD2 has recently been identified. Orphan receptor GPR18 was shown to mediate pro-resolving actions of RvD2 in leukocytes, such as inhibiting the recruitment of PMN and enhancing the efferocytosis of apoptotic neutrophils (Chiang et al. 2015). This receptor is also responsible for mediating the actions of endogenous lipid N-arachidonoyl glycine, which has previously been shown to induce relaxation in rat mesenteric arteries in a manner that was partly dependent on NO, but principally dependent on the activation of big conductance calcium-activated potassium channels (BK_{Ca}) (Parmar and Ho 2010). Many molecules (N-acyl amino acids) closely related to N-arachidonoyl glycine are also capable of mediating vasodilatation often through the activation of TRPV1 channels (Zygmunt et al. 1999), but experiments by Parmar and

colleagues suggest that N-arachidonoyl glycine-dependent vasorelaxation is independent of TRPV1 channels. Given the proposed involvement of TRPV1 channels in vasodilatation induced by N-acyl amino acids and the finding that MaR1 potently inhibits capsaicin-induced TRPV1 currents (Serhan et al. 2012), it would be interesting to determine any vasomodulatory effect of the maresins in future work.

Experimental design B enabled slower-onset activity of resolvins to take effect after pre-treatment of human pulmonary arteries for 1 hour followed by constriction with U46619 (Figure 5.10) or LTD_4 (Figure 5.11). Untreated HPA were similarly constricted and compared with constriction to the agonists before resolvin pre-treatment; this allows monitoring of baseline responsiveness, which was stable in the HPA constricted with U46619, but RvD1 and RvE1 did not affect HPA contractility to the thromboxane mimetic. The situation was more complex however with LTD_4; the small number of experiments (n=2-3) precludes proper analysis but there was a tendency of baseline responsiveness to LTD_4 to increase in the absence of resolvin treatment (Figure 5.11A). Intriguingly, this is the opposite of the *decreased* responsiveness of human bronchioles to LTD_4 reported in chapter 4 (Figure 4.15). This baseline shift may have masked an even greater relaxant effect of resolvin pre-treatment, but despite this both RvD1 (Figure 5.11B) and RvE1 (Figure 5.11C) showed a visible trend to reduce LTD_4 constrictions. This is more evident in the pooled data shown in Figure 5.12, in which the *initial* concentration-response curves in segments subsequently stimulated with or without resolvin were pooled to provide a baseline of n=7 for the experiment. In this analysis, the second LTD_4 concentration-response curve was not different from the first and the apparent trends for RvD1 and RvE1 to inhibit contractility are seen more clearly, although they remain non-significant (Figure 5.12). Further experiments with HPA segments are a high priority to enhance statistical power sufficiently to enable the confirmation or refutation of these early indications of a potentially important finding, which could indicate an endogenous role or novel therapeutic approach for resolvins in limiting pulmonary arterial hypertension, or even systemic hypertension, produced by pro-inflammatory insults to the vasculature.

As with the airway experiments reported in chapter 4, experimental design C was also used in blood vessels to compare adjacent segments of rat thoracic aorta simultaneously in parallel in separate myograph chambers. In addition, to allow a longer pre-treatment with resolvin (for 24 hours) as well as the usual 1 hour pre-treatment, segments of rat aorta or HPA were placed in a 24-well plate with or without a range of RvE1 concentrations and cultured in a cell incubator for 1 or 24 hours, before mounting on

the myograph for constriction with cumulative U46619 concentrations in the absence of resolvin. These experiments provided consistent findings with strong statistical significance that resolvin E1 inhibits constriction of rat thoracic aorta induced by U46619 (Figure 5.13), but not by PE (Figure 5.17), that this inhibitory action is also apparent after 24 hours of pre-treatment (Figure 5.15), that it is shared by RvD1 and RvD2 (Figure 5.18 and Figure 5.19), and that RvE1 has a similar but possibly more potent inhibitory effect on U46619-induced constriction in human pulmonary artery (Figure 5.20). This inhibitory effect of resolvins on U46619-induced constriction of both rat and human arteries is the first evidence that resolvins can modulate the contractility of smooth muscle acutely (with only 1 hour exposure). A range of physiologically-plausible concentrations was tested and consistently identified that inhibition followed a bell-shaped response curve, peaking at 1-10 nM, but disappearing completely at 300 nM. Ironically, this was the concentration used by Hiram and colleagues, who failed to show an inhibitory effect of RvD1 or RvE1 on U46619-induced constriction of HPA (Hiram et al. 2014, 2015), a result that thereby confirms our positive data at lower resolvin concentrations (Figures 5.14 and 5.16). A resolvin concentration of 300 nM could also be argued to be supraphysiological, as resolvins have been assayed only at picomolar to low nanomolar concentrations in human blood (Colas et al. 2014) and urine (Sasaki et al. 2015).

Hiram and colleagues go on to show that 300 nM RvD1 or RvE1 can inhibit the ability of the vasoconstrictor peptide endothelin to enhance the responsiveness of HPA to U46619 (Hiram et al. 2014, 2015). Again, the biological relevance of such a high resolvin concentration can be questioned, but at 300 nM the resolvins modulated the expression and phosphorylation of contractile proteins including CPI-17 and myosin binding subunit (MYPT). The authors did not test whether these signalling mechanisms also operate at lower resolvin concentrations within the bioactive range. There is substantial evidence to suggest that bell-shaped activity curves are characteristic of resolvins and other SPMs and that their activity peaks in the low nanomolar concentrations (Spite et al. 2009, Oh et al. 2011, Jones et al. 2012, Rogerio et al. 2012).

An explanation of the bell shape of the resolvin inhibition curves may lie in the use of intact vessel segments in the present study. The endothelium contributes significantly to vascular tone, acting as a source of vasodilators including NO and prostacyclin, and vasoconstrictors such as ET-1. Resolvins are promiscuous lipids, typically able to act at more than one receptor to mediate different effects. Thus, it is possible that resolvins act on different receptors on the endothelium and the smooth muscle, to produce an inhibitory

effect at low nanomolar concentrations that is overcome by a constrictor effect at higher concentrations, either of which could involve the generation of secondary mediators. An involvement of endothelial mediators could be defined by comparing resolvin actions in endothelium-denuded and endothelium-intact vessels.

RvE1 is a full agonist at ChemR23, a GPCR that is also activated by the chemoattractant protein chemerin (Figure 1.8). Chemerin-9 concentration-dependently constricts rat aorta segments and enhances constriction produced by submaximal concentrations of PE, prostaglandin $F_{2\alpha}$ or potassium chloride (Watts et al. 2013). These findings suggest that ChemR23, a receptor bound by both lipids and peptides, can mediate differential effects on the vasculature depending on the nature of the agonist. Indeed, there is growing evidence to suggest that biased agonism is important in the activation of ALX receptors, another pro-resolving receptor for both lipid and peptide ligands (see section 1.7.2).

The inhibitory effect of RvE1 on U46619-induced constriction, but not on constriction induced by PE (Figure 5.17), suggests that it may require specific interaction with thromboxane TP receptors, or with signalling pathways specific for TP receptors. Given that in experimental design C, RvE1 was only present during pre-treatment in the 24-well plate and not within the myograph chamber during U46619 constriction, it seems unlikely that the effect of RvE1 can depend on direct and reversible antagonism of the TP receptor, although irreversible binding cannot be ruled out. However, ligand binding studies in HEK293 cells showed that RvE1 does not compete for the TP receptor (Dona et al. 2008), indicating a probable action instead on intracellular signalling.

Existing evidence indicates that resolvins can modulate the phosphorylation status of receptors, including GPCRs. Activation of GPR32 receptors by RvD1 inhibited histamine-mediated calcium mobilisation and mucin secretion in conjunctival goblet cells, and this inhibitory effect was abolished by either a protein kinase C (PKC) inhibitor or an inhibitor of beta-adrenergic receptor kinase/G-protein coupled receptor kinase 2 (βARK/GRK2) (Li et al. 2013). Both RvE1 and aspirin-triggered LXA_4 inhibit phosphorylation of PDGF receptors, thereby inhibiting migration of VSMC (Ho et al. 2010). Thus, it is possible that RvE1, RvD1 and RvD2 similarly reduce TP receptor activation in rat and human arteries.

The inhibitory effect of RvE1 on U46619-induced constriction of rat aorta (Figure 5.13, Figure 5.14, Figure 5.15 and Figure 5.16) was also shared by RvD1 and RvD2; these resolvins are not thought to act on ChemR23 receptors but their receptors may

share signalling pathways with ChemR23. Growing interest in the SPM field has increased the availability of pharmacological tools for deciphering receptor involvement in the actions of pro-resolving mediator. The WRW4 peptide (Trp-Arg-Trp-Trp-Trp-Trp-NH_2) and Boc-2 peptide (Boc-Phe-Leu-Phe-Leu-Phe), both of which are commercially available, antagonise the ALX receptor for LXA_4 and RvD1, whilst ChemoCentryx have developed a ChemR23 receptor antagonist (CCX832). In future work, these antagonists could be used to identify the receptors that underlie the inhibitory effects of RvE1 and RvD1 on U46619-induced vascular constriction.

The involvement of a given receptor in the resolvin inhibitory effects described in this chapter requires the expression of relevant receptors. Immunohistochemistry for ChemR23, GPR32 and ALX receptors in HPA showed that both ChemR23 and GPR32 are expressed in the smooth muscle, with GPR32 expressed at particularly high levels, and also being present in vascular endothelium (Figure 5.22). In contrast, the ALX receptor was expressed more weakly and was more widespread throughout the tissue. This suggests that the inhibitory effects of RvE1 and RvD1 might be mediated via ChemR23 and GPR32 respectively. The orphan receptor GPR18 was recently shown capable of mediating the pro-resolving effects of RvD2 including enhancing the phagocytosis of apoptotic cells and bacteria, actions that were reduced in GPR18 knockout mice (Chiang et al. 2015). Because of the long association of this receptor with the cannabinoid N-arachidonyl glycine, an antibody for this receptor is available and has been used to identify it immunohistochemically in various tissues including endothelial cells (Wilhelmsen et al. 2014). Furthermore, a GPR18 receptor antagonist is commercially available which could be used to explore the possible involvement of GPR18 in the RvD2-induced inhibition of U46619-induced constriction seen here in rat thoracic aorta segments.

In summary, this study demonstrated that resolvins can acutely inhibit contractions of rat and human arteries induced by agonists of lipid mediator GPCRs, namely TP receptors (U46619) and possibly $CysLT_1$ receptors (LTD_4) – U46619 and LTD_4. The mechanisms behind this effect will be the subject of future work, although the presence of relevant SPM receptors has been demonstrated in human pulmonary arteries, both in this thesis and in published work (Hiram et al. 2014, 2015). Novel SPM mediators are being identified and the pharmacological tools needed to identify their roles in vascular contractility are increasingly becoming available. They may form the basis of novel therapeutic approaches to moderate both the altered vascular reactivity and the inflammatory processes that are implicated in pulmonary and systemic hypertension.

Chapter 6: Final Discussion

6.1 Conclusions

The aims of this project were to investigate whether airway and vascular smooth muscle contractility can be modulated by key members of novel families of specialised pro-resolving lipid mediators (SPMs), including resolvins and protectins derived from the omega-3 polyunsaturated fatty acids (PUFA) eicosapentaenoic acid (EPA) and docosahexaenoic acid (DHA), and lipoxins derived from the omega-6 PUFA arachidonate. The wide range of actions of SPMs in suppressing inflammatory leukocyte function and promoting resolution of inflammation have been intensively researched, but before this project there was no published research investigating these lipids for their ability to modulate smooth muscle contraction. Changes in smooth muscle contractility underlie the vascular events in inflammation and also contribute to morbidity in chronic inflammatory conditions such as bronchial asthma.

Three principal techniques were applied to rat and human cells and tissues in the project – collagen lattice contraction assays, wire myography and immunostaining.

Collagen lattice assays are a model of collagen remodelling in resolution and wound healing, and were adapted to compare smooth muscle cells from human bronchioles (HBSMC) and umbilical arteries (HUASMC) with human lung fibroblasts (HLF); the latter are well characterised in this model and respond strongly to growth factors including TGFβ and PDGF. Collagen lattice assays are a productive technique as a culture flask of several million cells provides sufficient material to explore a number of stimuli and SPMs over a range of culture times and concentrations in a single 24-well plate. Two results stood out from the collagen lattice studies reported in chapter 3. Firstly, the SPMs investigated did not alter the background rate of cell-mediated contraction of lattices, but RvE1, a resolvin derived from EPA, abolished the ability of PDGF-AB to enhance the contraction of lattices populated with HBSMC, bringing the rate of contraction completely back to background levels. Secondly, PDX, an isomer of the DHA derivative protectin D1, inhibited PDGF-AB-induced contraction of both HBSMC and HLF lattices, although to a lesser extent than RvE1. There has been no previous research investigating the effects of protectins on smooth muscle cells or fibroblasts, making the research here especially novel, and SPM in general have only very recently been investigated in HLF-populated collagen lattices (see below - (Roach et al. 2015)).

RvE1 impairs the phosphorylation of PDGF receptors in vascular smooth muscle cells, resulting in inactivation of the PDGF receptor (Ho et al. 2010). This suggests a

mechanism for RvE1-mediated inhibition of PDGF-AB-induced lattice contraction, and it would be worthwhile to investigate PDGF receptor phosphorylation in the HBSMC investigated in chapter 3. Receptors have yet to be identified for the protectins, but RvE1 activates ChemR23 receptors with downstream kinase/phosphatase signalling. The ChemR23 receptor antagonist (CCX832) produced by ChemoCentryx will be a useful tool for understanding the involvement of this receptor in RvE1-treated collagen lattices and also in myography experiments in rat and human airways and arteries. A study by Roach and colleagues investigating the effect of LXA_4 on both constitutive and TGFβ1-induced contraction of HLMF-populated collagen lattices demonstrated that pre-treatment with LXA_4 (10 nM) for 24 hours in serum free medium significantly reduced contraction of the lattices, reduced α-SMA expression and stress fibre formation, and inhibited collagen secretion (Roach et al. 2015), suggesting that LXA_4 is able to attenuate pro-fibrotic activity in these cells. In addition, LXA_4 and RvD2 have both been shown to decrease TGFβ1-induced migration and closure in a scratch assay, and inhibit TGF-β1-induced fibroblast proliferation (Herrera et al. 2015). Thus, in agreement with this recently published work, the findings in chapter 3 provide further evidence that SPMs can inhibit contraction of cell-populated collagen lattices, and therefore may be important in novel therapeutic approaches to chronic inflammation, delayed wound healing and fibrosis.

The second technique, which was used in the bulk of experiments in airways (chapter 4) and arteries (chapter 5), was wire myography. Myography is an established physiological and pharmacological technique to measure contractility in airways, blood vessels and gut, but it has been used here to study segments of small bronchioles as the site of inflammation and bronchoconstriction in asthma, and also arteries from small laboratory animals that would otherwise be too small for conventional organ-bath myography. Dissection and mounting of such small specimens on the wire myograph requires practice and is a laborious process, contributing significantly to the workload of this project, but the value of myography lies in its examination of the integrated function of intact airways and vessels, rather than isolated cells or tissues of a single smooth muscle phenotype. While lung tissue from rats was readily available, lung samples from human patients undergoing resection surgery are a more sporadic resource. As many of these donors were elderly smokers with COPD, their bronchial segments could be fragile and the majority (61%) showed poor functional responses to KPSS (Table 2-1) and to contractile agonists in the myograph. In contrast, 97% of human pulmonary arteries isolated and mounted on the wire myograph displayed good contractile responses to KPSS (Table 2-1).

As discussed in chapter 4 (section 4.7) and chapter 5 (section 5.7), three experimental designs were used for myography, each with its own strengths and weaknesses. The 'reversal' by resolvins of pre-existing contraction in airways and arteries (design A) is a sensitive way to detect acute effects, while design B assesses longer-term effects in the same segments in series, providing strong statistical power to detect changes, but it is prey to potential 'hangover' effects, such as were seen with reactivity to LTD_4 in this thesis and as described by others (Lei et al. 2011). Design C precludes this problem by comparing segments in separate myograph chambers, but introduces some extra variability because it compares different segments tested in parallel. Nevertheless, by using adjacent segments from the same bronchiole of each animal, inter-segment variation was minimised and paired statistical analyses could still be used to maximise statistical power. In all myography experiments, normalising constriction to the KPSS response for each segment also minimised variation in segment size, because the KPSS response gives a reliable indication of the maximum calcium-dependent contractile response. Other appropriate controls were used where feasible, including receptor-specific drug antagonists (such as atropine and montelukast in airways) or physiological controls (such as salbutamol in airways and acetylcholine in blood vessels) to confirm the functional ability of mounted segments to contract and/or relax in the myography model.

Together, experimental designs A, B and C provided novel information on resolvin actions on smooth muscle contractility. Overall, bronchioles from rat and human lung constricted with carbachol or the thromboxane mimetic U-46619 were relatively unresponsive to resolvins (chapter 4). Promising early results indicating that resolvins profoundly inhibit LTD_4-induced bronchiolar contraction (Figure 4.12) were undermined by changes in baseline responsiveness to the LTD_4, but experiments with design C suggested that RvD1 may indeed inhibit contraction in the subset of rat bronchioles that were responsive to LTD_4 (Figure 4.13); it is clearly impossible to detect a relaxation by resolvin of those rat bronchioles that were unresponsive to LTD_4. The experiment using design A in human bronchioles showed little effect of RvD1, RvD2 or RvE1 on LTD_4-induced contraction (Figure 4.16), but this was in tissue from only a single donor, whose airways may have been relatively unresponsive to LTD_4. Furthermore the resolvins were tested at a single concentration of 100 nM later shown in blood vessels to be much less than optimal on their bell-shaped curves. It is therefore important to extend the human bronchiole studies with experimental design A using lower resolvin concentrations in more subjects.

More striking results were seen in the blood vessel studies in chapter 5. Resolvins E1, D1 and D2 significantly inhibited constriction of rat thoracic aorta induced by U46619 (Figure 5.13, Figure 5.14, Figure 5.15, Figure 5.16, Figure 5.18 and Figure 5.19), and RvE1 similarly inhibited U46619-induced constrictions of human pulmonary arteries (Figure 5.20). These findings are summarised in the schematic shown below in Figure 6.1. It is a priority to extend the RvE1 studies in human arteries to include RvD1 and RvD2, and also to test them against other agonists such as LTD_4. Nevertheless the evidence in both rat and human arteries was that maximal inhibition by resolvins occurred at low nanomolar concentrations (1-10 nM) similar to those demonstrated for resolvin actions in leukocytes, and tailing off at higher (supraphysiological) concentrations. Intriguingly, a non-significant trend in the same direction had been seen in rat bronchioles, with RvE1 appearing to normalise U46619-induced constriction (Figure 4.11), suggesting some commonality between bronchioles and arteries in their responses to RvE1. The bell-shaped inhibition curves showed the value of examining resolvin concentration-response relationships, as the highest concentrations of RvD1 and RvE1 (300 nM) had no direct effect on U46619-induced contraction of HPA or human bronchioles in this project or in other studies (Hiram et al. 2014, 2015, Khaddaj-Mallat et al. 2015). Resolvins used in this project at 1-10 nM directly prevented smooth muscle contraction to a TP-dependent contractile agonist, while the other studies showed only that very high resolvin concentrations inhibit the 'priming' effect of cytokines and other mediators, including endothelin-1, TNF, IL-6 and IL-13, on smooth muscle reactivity. It remains to be seen whether such resolvin concentrations ever occur *in vivo*.

The possibility that resolvins may modulate contraction induced by omega-6 derived lipid mediators (TxA_2, LTD_4) by acting at the same receptors was of particular interest in this project, because of the evidence that some eicosanoid receptors, such as BLT1, may bind both an omega-6 lipid and an SPM, with potentially different consequences for each agonist. The inhibitory effect of RvE1 on vascular contraction appeared to be selective for thromboxane receptors activated by U46619 as it was not apparent against the alpha-1 adrenoceptor agonist phenylephrine (a catecholamine not a lipid). This may suggest a selective effect targeting lipid receptor signalling, although a wider range of non-lipid contractile agonists such as angiotensin II or endothelin-1 should be investigated as well as more lipid agonists to delineate the extent of this selectivity. It is nevertheless supported by the non-significant trends seen with the other lipid agonist investigated, LTD_4. Contractions to LTD_4 presented significant problems of tachyphylaxis, but in both rat

bronchioles (Figure 4.12) and human pulmonary arteries (Figure 5.11 and Figure 5.12) they were non-significantly inhibited by resolvins.

In summary, given that resolvins and other SPMs have established roles in the resolution of inflammation by virtue of their actions on leukocytes, the proof in this project that members of these families also (a) completely inhibit contraction by PDGF of collagen lattices populated by human bronchial smooth muscle cells, (b) may inhibit bronchiolar smooth muscle contraction stimulated by the potent bronchoconstrictor leukotriene D_4, and (c) potently inhibit constriction of rat and human arteries stimulated via thromboxane receptors, together represent substantial novel insights into the potential roles of SPMs in health and disease. A recent review described an exciting future terrain of novel therapeutic approaches based on SPMs and their synthetic analogues (Serhan, Chiang, and Dalli 2015). Indeed, a stable analogue of RvE1 (RX 10045; Auven Therapeutics) is currently in clinical trials for treating inflammation in dry eye disease and the development of further analogues of resolution mediators is increasingly becoming reality (Takano et al. 1998, Fredman et al. 2015, Orr et al. 2015).

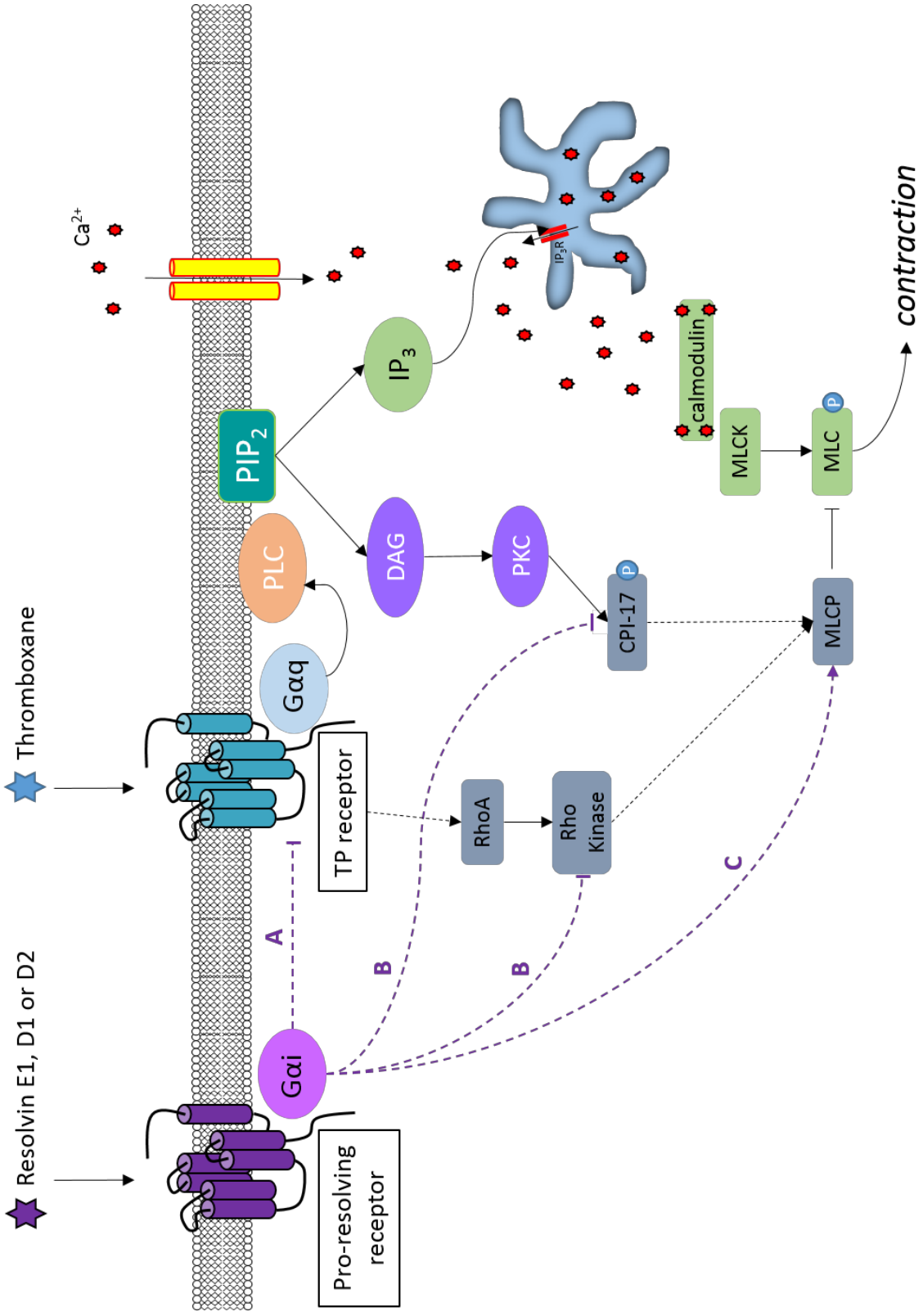
Ca2+
IP3R
IP3
PIP2
PLC
DAG
PKC
calmodulin
MLCK
MLC
P
contraction
Thromboxane
Gαq
TP receptor
RhoA
Rho Kinase
CPI-17
P
MLCP
A
B
B
C
Resolvin E1, D1 or D2
Gαi
Pro-resolving receptor

Figure 6.1: Summary schematic illustrating the major findings of this thesis, and the potential mechanisms behind these findings. Pre-treatment with resolvin E1, D1 or D2 (10 nM) for 1 hour was found to inhibit thromboxane (U4661)-induced constriction of rat aorta segments. Early evidence using human pulmonary arteries suggests that the same is true of resolvin E1 in this tissue, but pre-treatment with resolvins D1 and D2 are yet to be investigated. Given that the resolvins were not present in the myography chamber at the same time as the U46619 compound, it is unlikely that the resolvins are competing for the thromboxane receptor (TP), which is in agreement with previously published radioligand data which indicates that resolvin E1 does not compete for the TP receptor in HEK293 cells (Dona et al., 2009). As such, it is proposed that the resolvins are acting via pro-resolving receptors to mediate changes in the sensitivity of the contractile machinary. Immunohistochemistry evidence located in chapter 5 of this thesis suggests that both ChemR23 and GPR32 are expressed in the smooth muscle layer of human pulmonary arteries, whilst GPR32 is also strongly expressed in the endothelial layer. In the schematic, A, B and C illustrate putative mechanisms by which the pro-resolving receptors could be mediating this inhibitory effect. In A, direct 'cross-talk' between the pro-resolving receptor and the thromboxane receptor could result in reduced intracellular signalling of the calcium dependent pathway from the TP receptor, resulting in reduced contraction. In B, inhibition of proteins that contribute to calcium-independent contraction could result in reduced constriction. Lastly in C, it is possible that signalling from the pro-resolving receptors may enhance myosin-light chain phosphatase (MLCP) activity directly, resulting in increased phosphorylation of the myosin light chain and thus reduced contractile activity.

6.2 Strengths and limitations of the thesis

There are a number of strengths to the protocols and techniques used in this thesis, as well as some limitations. The use of human tissue and cells throughout this thesis is a major strength; the intact vessels and arteries used on the wire myograph constitute a bioassay which provides an insight into smooth muscle contractility as a functional and physiological readout. In addition, the lattice contraction assay permits the embedding of a wide range and choice of cells, and in this thesis primary human cells were utilised throughout.

In chapters 4 and 5, where wire myography predominates, there is a clear and logical progression through different experimental designs that address unexpected problems and ultimately overcome these problems. There is also extensive validation of the lattice contraction assay in chapter 3; however, the optimal conditions determined for HLF-populated lattices were then used when carrying out experiments populated by the two types of smooth muscle cells. It would have been better to optimise the conditions for lattices populated by each cells type individually to ensure the best possible assay performance.

In chapter 3, each SPM was assessed at only as single concentration (10 nM). Given the bell-shaped responses shown in some of the experiments in chapter 5 as well as previously published findings, it may have been better to test a wider range of concentrations of SPMs, sacrificing some of the other permutations such as two different growth factors and four SPMs. That said, it is a strength of some of the experiments carried out in chapter 5 that a range of concentrations of SPMs were assessed for their ability to modulate constriction in intact vessels, and that in doing so, concentration-dependent effects were identified.

In general, there are low repeats on a few of experimental datasets shown in each of the chapters, but particularly those in chapters 4 and 5. Often such low numbers are likely precluding statistical significance and so it is of interest to increase the experimentals numbers in these experiments in order to understand whether this is true or not.

6.3 Future work

There are results in each of the chapters in this thesis which are promising and warrant further work in order to fully understand their importance. Experiments with the lattice contraction assay showed that RvE1 can inhibit PDGF-AB-induced contraction of HBSMC-populated lattices, which builds on findings from the Conte group that treatment of VSMC with RvE1 inhibits PDGF-induced migration and PDGF receptor inactivation (Ho et al. 2010). It would therefore be important to determine whether the ChemR23 receptor is expressed in HBSMC – and indeed whether it is absent from HLF and HUASMC which could explain the lack of effect of RvE1 in these cells. In addition, the phosphorylation status of the PDGF receptor in HBSMC could be determined to understand whether this mechanism maybe also be important in the inhibitory actions seen here. Li et al (2013) suggest that cross-talk exists between the pro-resolving receptor, GPR32, and the histamine receptor, H1, in conjunctival goblet cells, whereby GPR32 mediates phosphorylation of the H1 receptor, and they were shown to be co-localised. It would be interesting to explore whether the PDGF receptor and the ChemR23 receptor co-localise in HBSMC. Additionally, preliminary work shown below in Figure 6.2 demonstrates that contraction of collagen lattices populated with HUASMC can be enhanced by known smooth muscle agonists including histamine. Given the work by Li et al (2013) described above which suggests that cross-talk exists between the receptors GPR32 and H1, it would be interesting to see if cross-talk is also applicable in VSMC.

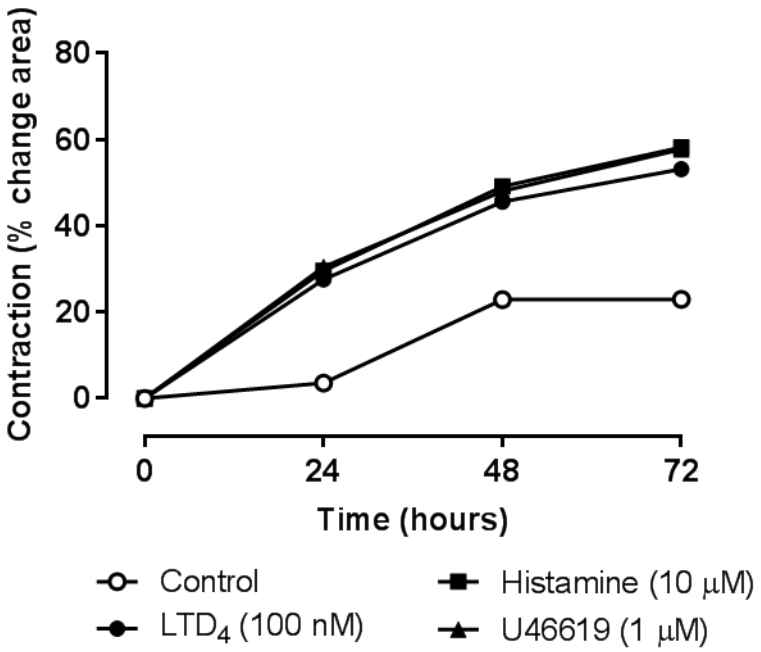

Figure 6.2: Effect of smooth muscle contractile agonists on collagen lattices populated by human umbilical artery smooth muscle cells (HUASMC) (n=1). Collagen lattices populated with HUASMC were floated in Petri dishes containing DMEM (0.5% NCS) and left unstimulated (control) or exposed to either leukotriene D_4 (LTD_4) (100 nM), histamine (10 μM) or stable thromboxane mimetic U46619 (1 μM). Contraction was measured every 24 hours over a 72 hour period. All agonists tested enhanced contraction of the HUASMC-populated collagen lattices in a time-dependent manner.

There are a number of experiments in chapter 4 which require increased repeats in order to be completely satisfied that there is no modulatory effect of the resolvins, including those shown in Figure 4.9 and Figure 4.16. However, there are also findings that warrant further work to fully elucidate the promising inhibitory effect of some of these SPMs. The preliminary data using experimental design C showed that pre-treatment of rat bronchioles with RvD1 (10 nM) reduced LTD_4-induced constriction compared with untreated segments (Figure 4.13), and this difference was significant with a paired student's T-test ($p<0.05$, $n=4$). This experiment requires further repeats to ensure that the RvD1 inhibitory effect is true, and should be extended to human bronchiole segments and human pulmonary arteries. If the results are translated using human tissue then it would be important to assess the ability of other resolvins (E1 and D2), possibly at a range of concentrations, to modulate LTD_4-induced constriction, and then to discern the receptors involved using commercially available antagonists or blocking antibodies.

These antagonists and antibodies could also shed light on the mechanism behind the stand-out results from chapter 5, that is, the ability of resolvins E1, D1 and D2 to inhibit

U46619-induced constriction of rat and human arteries using experimental design C. In addition, further immunohistochemistry experiments are required in order to confirm pro-resolving receptor expression in arteries from other patient samples. This could also be extended to determine receptor expression in rat and human bronchiole segments, where the expression of GPR32 and ALX is of particular interest given the preliminary data suggesting an ability of RvD1 to inhibit LTD_4-induced constriction. In HPA, determining the localisation of the TP receptor could provide insight into potential intracellular cross-talk between the TP receptor and pro-resolving receptors.

In summary there are many exciting future paths that this project could take which would build on the data shown in each of the three results chapters. This future work is important to fully understand the role that SPM may play in modulating the contractility of smooth muscle.

References

Aalkjær, C., Boedtkjer, D., and Matchkov, V., 2011. Vasomotion – what is currently thought? *Acta Physiol*, **202** (3), 253–269.

Abdulnour, R. E., Dalli, J., Colby, J. K. et al, 2014. Maresin 1 biosynthesis during platelet–neutrophil interactions is organ-protective. *PNAS*, **111** (46), 16526–16531.

Adatia, I., Barrow, S. E., Stratton, P. D. et al, 1993. Thromboxane A2 and prostacyclin biosynthesis in children and adolescents with pulmonary vascular disease. *Circulation*, **88** (5), 2117–2122.

Al-Muhsen, S., Johnson, J. R., and Hamid, Q., 2011. Remodeling in asthma. *J Allergy Clin Immunol*, **128** (3), 451–62.

Archer, S. L., Weir, E. K., and Wilkins, M. R., 2010. Basic science of pulmonary arterial hypertension for clinicians: new concepts and experimental therapies. *Circulation*, **121** (18), 2045–2066.

Ariel, A., Li, P. L., Wang, W. et al, 2005. The docosatriene protectin D1 is produced by TH2 skewing and promotes human T cell apoptosis via lipid raft clustering. *J Biol Chem*, **280** (52), 43079–43086.

Arif, S. A. and Poon, H., 2011. Tadalafil: a long-acting phosphodiesterase-5 inhibitor for the treatment of pulmonary arterial hypertension. *Clin Ther*, **33** (8), 993–1004.

Arita, M., Bianchini, F., Aliberti, J. et al, 2005. Stereochemical assignment, antiinflammatory properties, and receptor for the omega-3 lipid mediator resolvin E1. *J Exp Med*, **201** (5), 713–722.

Arita, M., Ohira, T., Sun, Y. P. et al, 2007. Resolvin E1 selectively interacts with leukotriene B4 receptor BLT1 and ChemR23 to regulate inflammation. *J Immunol*, **178** (6), 3912–3917.

Arora, P. D., Narani, N., and McCulloch, C. A. G., 1999. The compliance of collagen gels regulates transforming growth factor-β induction of α-smooth muscle actin in fibroblasts. *Am J Pathol*, **154** (3), 871–882.

Badr, K. F., DeBoer, D. K., Schwartzberg, M., and Serhan, C. N., 1989. Lipoxin A4 antagonizes cellular and in vivo actions of leukotriene D4 in rat glomerular mesangial cells: evidence for competition at a common receptor. *PNAS*, **86** (9), 3438–3442.

Balas, L., Guichardant, M., Durand, T., and Lagarde, M., 2014. Confusion between protectin D1 (PD1) and its isomer protectin DX (PDX). An overview on the dihydroxy-docosatrienes described to date. *Biochimie*, **99**, 1-7.

Barst, R. J., Rubin, L. J., Long, W. A. et al., 1996. A comparison of continuous intravenous epoprostenol (prostacyclin) with conventional therapy for primary pulmonary hypertension. The Primary Pulmonary Hypertension Study Group. *N Engl J Med*, **334** (5), 296–301.

Bartho, L. and Benko, R., 2013. Should antihistamines be re-considered as antiasthmatic drugs as adjuvants to anti-leukotrienes? *Eur J Pharmacol*, **701** (1-3), 181–4.

Bell, E., Ivarsson, B., and Merrill, C., 1979. Production of a tissue-like structure by contraction of collagen lattices by human fibroblasts of different proliferative potential in vitro. *PNAS*, **76** (3), 1274–1278.

Bena, S., Brancaleone, V., Wang, J. M., Perretti, M., and Flower, R. J., 2012. Annexin A1 interaction with the FPR2/ALX receptor: Identification of distinct domains and downstream associated signaling. *J Biol Chem*, **287** (29), 24690–24697.

Berair, R., Saunders, R., and Brightling, C., 2013. Origins of increased airway smooth muscle mass in asthma. *BMC Med*, **11** (1), 1741–7015.

Bossé, Y., 2012. Asthmatic airway hyperresponsiveness: the ants in the tree. *Trends Mol Med*, **18** (11), 627–633.

Bossé, Y., Riesenfeld, E. P., Paré, P. D., and Irvin, C. G., 2010. It's not all smooth muscle: non-smooth-muscle elements in control of resistance to airflow. *Annu Rev Physiol*, **72** (1), 437–462.

Boxall, C., Holgate, S. T., and Davies, D. E., 2006. The contribution of transforming growth factor-β and epidermal growth factor signalling to airway remodelling in chronic asthma. *Eur Respir J*, **27** (1), 208–229.

Bozinovski, S., Hutchinson, A., Thompson, M. et al, 2008. Serum amyloid A is a biomarker of acute exacerbations of chronic obstructive pulmonary disease. *Am J Respir Crit Care Med*, **177** (3), 269–278.

Bozinovski, S., Uddin, M., Vlahos, R. et al, 2012. Serum amyloid A opposes lipoxin A_4 to mediate glucocorticoid refractory lung inflammation in chronic obstructive pulmonary disease. *PNAS*, **109** (3), 935–40.

Brink, C., Dahlén, S. E., Drazen, J. et al, 2003. International Union of Pharmacology XXXVII. Nomenclature for leukotriene and lipoxin receptors. *Pharmacol Rev*, **55** (1), 195–227.

Brinkmann, V., Reichard, U., Goosmann, C. et al, 2004. Neutrophil extracellular traps kill bacteria. *Science*, **303** (5663), 1532–1535.

Buckley, C. D., Gilroy, D. W., and Serhan, C. N., 2014. Proresolving lipid mediators and mechanisms in the resolution of acute inflammation. *Immunity*, **40** (3), 315–327.

Cazzola, M., Page, C. P., Calzetta, L., and Matera, M. G., 2012. Pharmacology and therapeutics of bronchodilators. *Pharmacol Rev*, **64** (3), 450–504.

Cazzola, M., Rogliani, P., Segreti, A., and Matera, M. G., 2012. An update on bronchodilators in Phase I and II clinical trials. *Expert Opin Investig Drugs*, **21** (10).

Chan, C. P., Lan, W. H., Chang, M. C. et al, 2005. Effects of TGF-betas on the growth, collagen synthesis and collagen lattice contraction of human dental pulp fibroblasts in vitro. *Arch Oral Biol*, **50** (5), 469–79.

Chatterjee, A., Sharma, A., Chen, M., Toy, R., Mottola, G., and Conte, M. S., 2014. The pro-resolving lipid mediator maresin 1 (MaR1) attenuates inflammatory signaling pathways in vascular smooth muscle and endothelial cells. *PloS One*, **9** (11), e113480.

Chen, J., Shetty, S., Zhang, P. et al, 2014. Aspirin-triggered resolvin D1 down-regulates inflammatory responses and protects against endotoxin-induced acute kidney injury. *Toxicol Appl Pharmacol*, **277** (2), 118–123.

Chen, P., Fenet, B., Michaud, S. et al, 2009. Full characterization of PDX, a neuroprotectin/protectin D1 isomer, which inhibits blood platelet aggregation. *FEBS Letters*, **583** (21), 3478–3484.

Chen, P., Véricel, E., Lagarde, M., and Guichardant, M., 2011. Poxytrins, a class of oxygenated products from polyunsaturated fatty acids, potently inhibit blood platelet aggregation. *FASEB J*, **25** (1), 382–388.

Chiang, N., Arita, M., and Serhan, C. N., 2005. Anti-inflammatory circuitry: Lipoxin, aspirin-triggered lipoxins and their receptor ALX. *Prostaglandins Leukot Essent Fatty Acids*, **73** (3-4), 163-177.

Chiang, N., Dalli, J., Colas, R. A., and Serhan, C. N., 2015. Identification of resolvin D2 receptor mediating resolution of infections and organ protection. *J Exp Med*, **212** (8), 1203-1217.

Chiang, N., Fredman, G., Bäckhed, F. et al, 2012. Infection regulates pro-resolving mediators that lower antibiotic requirements. *Nature*, **484** (7395), 524–528.

Chiba, Y., Matsusue, K., and Misawa, M., 2010. RhoA, a possible target for treatment of airway hyperresponsiveness in bronchial asthma. *J Pharmacol Sci*, **114** (3), 239–247.

Choi, M. E., Ding, Y., and Kim, S. Il, 2012. TGF-β signaling via TAK1 pathway: Role in kidney fibrosis. *Semin Nephrol*, **32** (3), 244–252.

Christie, P., Spur, B., and Lee, T., 1992. The effects of lipoxin A4 on airway responses in asthmatic subjects. *Am Rev Respir Dis*, **145** (6), 1281–1284.

Christman, B. W., McPherson, C. D., Newman, J. H. et al, 1992. An imbalance between the excretion of thromboxane and prostacyclin metabolites in pulmonary hypertension. *N Engl J Med*, **327** (2), 70–75.

Churchman, A. T. and Siow, R. C. M., 2009. Isolation, culture and characterisation of vascular smooth muscle cells. *Methods Mol Biol*, **467** (4), 127–138.

Ciana, P., Fumagalli, M., Trincavelli, M. et al, 2006. The orphan receptor GPR17 identified as a new dual uracil nucleotides/cysteinyl-leukotrienes receptor. *EMBO J*, **25** (19), 4615–4627.

Clària, J. and Serhan, C. N., 1995. Aspirin triggers previously undescribed bioactive eicosanoids by human endothelial cell-leukocyte interactions. *PNAS*, **92** (21), 9475–9479.

Clark, R. A. F., Folkvord, J. M., Hart, C. E., Murray, M. J., and McPherson, J. M., 1989. Platelet isoforms of platelet-derived growth factor stimulate fibroblasts to contract collagen matrices. *J Clin Invest*, **84** (3), 1036–1040.

Colas, R. A, Shinohara, M., Dalli, J., Chiang, N., and Serhan, C. N., 2014. Identification and signature profiles for pro-resolving and inflammatory lipid mediators in human tissue. *Am J Physiol Cell Physiol*, **307** (1), C39–C54.

Coleman, R. A., Humphrey, P. P., Kennedy, I., Levy, G. P., and Lumley, P., 1981. Comparison of the actions of U-46619, a prostaglandin H2-analogue, with those of prostaglandin H2 and thromboxane A2 on some isolated smooth muscle preparations. *Br J Pharmacol*, **73** (3), 773–778.

Coleman, R. A. and Sheldrick, R. L., 1989. Prostanoid-induced contraction of human bronchial smooth muscle is mediated by TP-receptors. *Br J Pharmacol*, **96** (3), 688–692.

Console-Bram, L., Brailoiu, E., Brailoiu, G. C., Sharir, H., and Abood, M. E., 2014. Activation of GPR18 by cannabinoid compounds: A tale of biased agonism. *Br J Pharmacol*, **171** (16), 3908–3917.

Cooray, S. N., Gobbetti, T., Montero-Melendez, T. et al, 2013. Ligand-specific conformational change of the G-protein-coupled receptor ALX/FPR2 determines proresolving functional responses. *PNAS*, **110** (45), 18232–7.

Croasdell, A., Thatcher, T. H., Kottmann, R. M. et al, 2015. Resolvins attenuate inflammation and promote resolution in cigarette smoke-exposed human macrophages. Am J *Physiol Lung Cell Mol Physiol*, **309** (8) L888-901.

Curry, J. J., 1946. The action of histamine on the respiratory tract in normal and asthmatic subjects. *J Clin Invest*, **25** (6), 785–791.

Dahlén, S. E., Hansson, G., Hedqvist, P., Björck, T., Granström, E., and Dahlén, B., 1983. Allergen challenge of lung tissue from asthmatics elicits bronchial contraction that correlates with the release of leukotrienes C4, D4, and E4. *PNAS*, **80** (6), 1712–1716.

Dahlén, S., Hedqvist, P., Hammarström, S., and Samuelsson, B., 1980. Leukotrienes are potent constrictors of human bronchi. *Nature*, **288** (5790), 484–486.

Dalli, J., Chiang, N., and Serhan, C. N., 2015. Elucidation of novel 13-series resolvins that increase with atorvastatin and clear infections. *Nat Med*, **21** (9), 1071–1075.

Dalli, J., Colas, R. A., and Serhan, C. N., 2013. Novel n-3 immunoresolvents: structures and actions. *Sci Rep*, **3** (1940), 1–13.

Dalli, J., Winkler, J. W., Colas, R. A. et al, 2013. Resolvin D3 and aspirin-triggered resolvin D3 are potent immunoresolvents. *Chem Biol*, **20** (2), 188–201.

Dalli, J., Zhu, M., Vlasenko, N. A et al, 2013. The novel 13S,14S-epoxy-maresin is converted by human macrophages to maresin 1 (MaR1), inhibits leukotriene A4 hydrolase (LTA4H), and shifts macrophage phenotype. *FASEB J*, **27** (7), 2573–2583.

Dallon, J. C. and Ehrlich, H. P., 2010. Differences in the mechanism of collagen lattice contraction by myofibroblasts and smooth muscle cells. *J Cell Biochem*, **111** (2), 362–369.

Daniele, S., Trincavelli, M. L., Gabelloni, P. et al, 2011. Agonist-induced desensitization/resensitization of human G protein-coupled receptor 17: a functional cross-talk between purinergic and cysteinyl-leukotriene ligands. *J Pharmacol Exp Ther*, **338** (2), 559–567.

Dartt, D. A., Hodges, R. R., Li, D., Shatos, M. A., Lashkari, K., and Serhan, C. N., 2011. Conjunctival goblet cell secretion stimulated by leukotrienes is reduced by resolvins D1 and E1 to promote resolution of inflammation. *J Immunol*, **186** (7), 4455–4466.

Davenport, A. P., Kuc, R. E., Maguire, J. J., and Harland, S. P., 1995. ETA receptors predominate in the human vasculature and mediate constriction. *J Cardiovasc Pharmacol*, **26** (Suppl 3), S265-S267.

Davenport, A. P., Alexander, S. P. H., Sharman, J. L. et al, 2013. International Union of Basic and Clinical Pharmacology. LXXXVIII. G protein-coupled receptor list: recommendations for new pairings with cognate ligands. *Pharmacol Rev*, **65** (3), 967–986.

Davies, D. E., Wicks, J., Powell, R. M., Puddicombe, S. M., and Holgate, S. T., 2003. Airway remodeling in asthma: new insights. *J Allergy Clin Immunol*, **111** (2), 215–225.

Deng, B., Wang, C.-W., Arnardottir, H. H. et al, 2014. Maresin biosynthesis and identification of maresin 2, a new anti-inflammatory and pro-resolving mediator from human macrophages. *PloS One*, **9** (7), 1–9.

Department of Health, 2012. An outcomes strategy for COPD and asthma: NHS companion document. www.dh.gov.uk/publications.

Devchand, P. R., Keller, H., Peters, J. M., Vazquez, M., Gonzalez, F. J., and Wahli, W., 1996. The PPARalpha-leukotriene B4 pathway to inflammation control. *Nature*, **384** (6604), 39–43.

Dimopoulos, G. J., Semba, S., Kitazawa, K., Eto, M., and Kitazawa, T., 2007. Ca2-dependent rapid Ca2 sensitization of contraction in arterial smooth muscle. *Circ Res*, **100** (1), 121–129.

Dingemanse, J., Sidharta, P. N., Maddrey, W. C., Rubin, L. J., and Mickail, H., 2014. Efficacy, safety and clinical pharmacology of macitentan in comparison to other endothelin receptor antagonists in the treatment of pulmonary arterial hypertension. *Expert Opin Drug Saf*, **13** (3), 391–405.

Dona, M., Fredman, G., Schwab, J. M. et al, 2008. Resolvin E1, an EPA-derived mediator in whole blood, selectively counterregulates leukocytes and platelets. *Blood*, **112** (3), 848–855.

Eickelberg, O. and Morty, R. E., 2007. Transforming growth factor beta/bone morphogenic protein signaling in pulmonary arterial hypertension: remodeling revisited. *Trends Cardiovasc Med*, **17** (8), 263–9.

Enderby, C. Y., Soukup, M., Al Omari, M., Zeiger, T., and Burger, C., 2014. Transition from intravenous or subcutaneous prostacyclin therapy to inhaled treprostinil in patients with pulmonary arterial hypertension: a retrospective case series. *J Clin Pharm Ther*, **39** (5), 496-500.

Eto, M., 2009. Regulation of cellular protein phosphatase-1 (PP1) by phosphorylation of the CPI-17 family, C-kinase-activated PP1 Inhibitors. *J Biol Chem*, **284** (51), 35273-35277.

Fang, Q., Ma, Y., Wang, J., Michalski, J., Rennard, S. I., and Liu, X., 2013. PGE(2) desensitizes β-agonist effect on human lung fibroblast-mediated collagen gel contraction through upregulating PDE4. *Mediators Inflamm*, **2013** (145197), 1-9.

Farber, H. W. and Loscalzo, J., 2004. Pulmonary arterial hypertension. *N Engl J Med*, **351** (16), 1655–1665.

Fiore, S., Maddox, J. F., Perez, H. D., and Serhan, C. N., 1994. Identification of a human cDNA encoding a functional high affinity lipoxin A4 receptor. *J Exp Med*, **180** (1), 253–260.

Foudi, N., Kotelevets, L., Louedec, L. et al, 2008. Vasorelaxation induced by prostaglandin E2 in human pulmonary vein: role of the EP4 receptor subtype. *Br J Pharmacol*, **154** (8), 1631–1639.

Fredman, G., Kamaly, N., Spolitu, S. et al, 2015. Targeted nanoparticles containing the proresolving peptide Ac2-26 protect against advanced atherosclerosis in hypercholesterolemic mice. *Sci Transl Med*, **7** (275), 275ra20.

Fredman, G., Oh, S. F., Ayilavarapu, S., Hasturk, H., Serhan, C. N., and Van Dyke, T. E., 2011. Impaired phagocytosis in localized aggressive periodontitis: rescue by Resolvin E1. *PloS One*, **6** (9), e24422.

Fredman, G., Ozcan, L., Spolitu, S. et al, 2014. Resolvin D1 limits 5-lipoxygenase nuclear localization and leukotriene B4 synthesis by inhibiting a calcium-activated kinase pathway. *PNAS*, **111** (40), 14530–14535.

Fredman, G. and Serhan, C., 2011. Specialized proresolving mediator targets for RvE1 and RvD1 in peripheral blood and mechanisms of resolution. *Biochem J*, **437** (2) 185-197.

Van Ganse, E., Kaufman, L., Derde, M. P., Yernault, J. C., Delaunois, L., and Vincken, W., 1997. Effects of antihistamines in adult asthma: a meta-analysis of clinical trials. *Eur Respir J*, **10** (10), 2216–2224.

Giaid, A. and Saleh, D., 1995. Reduced expression of endothelial nitric oxide synthase in the lungs of patients with pulmonary hypertension. *N Engl J Med*, **333** (4), 214–212.

Giaid, A., Yanagisawa, M., Langleben, D. et al, 1993. Expression of endothelin-1 in the lungs of patients with pulmonary hypertension. *N Engl J Med*, **328** (24), 1732–1739.

Grainge, C. L., Lau, L. C. K., Ward, J. A. et al, 2011. Effect of bronchoconstriction on airway remodeling in asthma. *N Engl J Med*, **364** (21), 2006–2015.

Gronert, K., Martinsson-Niskanen, T., Ravasi, S., Chiang, N., and Serhan, C. N., 2001. Selectivity of recombinant human leukotriene D(4), leukotriene B(4), and lipoxin A(4) receptors with aspirin-triggered 15-epi-LXA(4) and regulation of vascular and inflammatory responses. *Am J Pathol*, **158** (1), 3–9.

Gryglewski, R. J., 2008. Prostacyclin among prostanoids. *Pharmacol Rep*, **60** (1), 3–11.

Haworth, O., Cernadas, M., Yang, R., Serhan, C., and Levy, B., 2008. Resolvin E1 regulates interleukin 23, interferon-gamma and lipoxin A4 to promote the resolution of allergic airway inflammation. *Nat Immunol*, **9** (8) 873-879.

Heldin, C.-H., Eriksson, U., and Ostman, A., 2002. New members of the platelet-derived growth factor family of mitogens. *Arch Biochem Biophys*, **398** (2), 284–90.

Herrera, B. S., Kantarci, A., Zarrough, A., Hasturk, H., Leung, K. P., and Van Dyke, T. E., 2015. LXA4 actions direct fibroblast function and wound closure. *Biochem Biophysl Res Commun*, **464** (4), 1072–7.

Hiram, R., Rizcallah, E., Marouan, S. et al, 2015. Resolvin E1 normalizes contractility, Ca2+ sensitivity and smooth muscle cell migration rate in TNF-α- and IL-6-pretreated Human Pulmonary Arteries. *Am J Physiol Lung Cell Mol Physiol*, **309** (8), L776-788.

Hiram, R., Rizcallah, E., Sirois, C. et al, 2014. Resolvin D1 reverses reactivity and Ca2+ sensitivity induced by ET-1, TNF-α, and IL-6 in the human pulmonary artery. *Am J Physiol Heart Circ Physiol*, **307** (11), H1547–H1558.

Ho, K. J., Spite, M., Owens, C. D. et al, 2010. Aspirin-triggered lipoxin and resolvin E1 modulate vascular smooth muscle phenotype and correlate with peripheral atherosclerosis. *Am J Pathol*, **177** (4), 2116–2123.

Hong, S., Gronert, K., Devchand, P. R., Moussignac, R.-L. L., and Serhan, C. N., 2003. Novel docosatrienes and 17S-resolvins generated from docosahexaenoic acid in murine brain, human blood, and glial cells. Autacoids in anti-inflammation. *J Biol Chem*, **278** (17), 14677–14687.

Horie, M., Saito, A., Yamauchi, Y. et al, 2014. Histamine induces human lung fibroblast-mediated collagen gel contraction via histamine H1 receptor. *Exp Lung Res*, **40** (5), 222–236.

Hsiao, H. M., Sapinoro, R. E., Thatcher, T. H. et al, 2013. A novel anti-inflammatory and pro-resolving role for resolvin D1 in acute cigarette smoke-induced lung inflammation. *PLoS One*, **8** (3), 1–15.

Hsiao, H.-M., Thatcher, T. H., Levy, E. P. et al, 2014. Resolvin D1 attenuates polyinosinic-polycytidylic acid-induced inflammatory signaling in human airway epithelial cells via TAK1. *J Immunol*, **193** (10), 4980–4987.

Humbert, M., Sitbon, O., and Simonneau, G., 2004. Treatment of pulmonary arterial hypertension. *N Engl J Med*, **351** (14), 1425–1436.

Hyytiäinen, M., Penttinen, C., and Keski-Oja, J., 2004. Latent TGF-beta binding proteins: extracellular matrix association and roles in TGF-beta activation. *Crit Rev Clin Lab Sci*, **41** (3), 233–264.

Isobe, Y., Arita, M., Matsueda, S. et al, 2012. Identification and structure determination of novel anti-inflammatory mediator resolvin E3, 17,18-dihydroxyeicosapentaenoic acid. *J Biol Chem*, **287** (13), 10525–10534.

Jacques, C. A., Spur, B. W., Crea, A. E., and Lee, T. H., 1988. The contractile activities of lipoxin A4 and lipoxin B4 for guinea-pig airway tissues. *Br J Pharmacol*, **95** (2), 562–568.

Jiang, X. and Jing, Z.-C., 2013. Epidemiology of pulmonary arterial hypertension. *Curr Hypertens Rep*, **15** (6), 638–649.

Johnston, S. L., Freezer, N. J., Ritter, W., O'Toole, S., and Howarth, P. H., 1995. Prostaglandin D2-induced bronchoconstriction is mediated only in part by the thromboxane prostanoid receptor. *Eur Respir J*, **8** (3), 411–415.

Jones, C. N., Dalli, J., Dimisko, L., Wong, E., Serhan, C. N., and Irimia, D., 2012. Microfluidic chambers for monitoring leukocyte trafficking and humanized nano-proresolving medicines interactions. *PNAS*, **109** (50), 20560–5.

Kanaoka, Y., Maekawa, A., and Austen, K. F., 2013. Identification of GPR99 protein as a potential third cysteinyl leukotriene receptor with a preference for leukotriene E4 ligand. *J Biol Chem*, **288** (16), 10967–10972.

Kane, G. C., Maradit-Kremers, H., Slusser, J. P., Scott, C. G., Frantz, R. P., and McGoon, M. D., 2011. Integration of clinical and hemodynamic parameters in the prediction of long-term survival in patients with pulmonary arterial hypertension. *Chest*, **139** (6), 1285–1293.

Kazani, S., Planaguma, A., Ono, E. et al, 2013. Exhaled breath condensate eicosanoid levels associate with asthma and its severity. *J Allergy Clin Immunol*, **132** (3), 547–553.

El Kebir, D., Gjorstrup, P., and Filep, J., 2012. Resolvin E1 promotes phagocytosis-induced neutrophil apoptosis and accelerates resolution of pulmonary inflammation. *PNAS*, **109** (37), 14983–14988.

Khaddaj-Mallat, R., Sirois, C., Sirois, M., Rizcallah, E., Morin, C., and Rousseau, É., 2015. Reversal of IL-13-induced inflammation and Ca2+ sensitivity by resolvin and MAG-DHA in association with ASA in human bronchi. *Prostaglandins Other Lipid Mediat*, [Epub ahead of print].

Kim, S. Il, Kwak, J. H., Na, H.-J., Kim, J. K., Ding, Y., and Choi, M. E., 2009. Transforming growth factor-β (TGF-β1) activates TAK1 via TAB1-mediated

autophosphorylation, independent of TGF-β receptor kinase activity in mesangial cells. *J Biol Chem*, **284** (33), 22285–22296.

Kingman, M., Ruggiero, R., and Torres, F., 2009. Ambrisentan, an endothelin receptor type A-selective endothelin receptor antagonist, for the treatment of pulmonary arterial hypertension. *Expert Opin Pharmacother*, **10** (11), 1847–1858.

Kitamura, N., Kaminuma, O., Kobayashi, N., and Mori, A., 2008. A contraction assay system using established human bronchial smooth muscle cells. *Int Arch Allergy Immunol*, **146** (Suppl 1), 36–39.

Kitamura, N., Kaminuma, O., Ohtomo, T. et al, 2009. Evaluation of cysteinyl leukotriene-induced contraction of human cultured bronchial smooth muscle cells. *Int Arch Allergy Immunol*, **149** (Suppl 1), 83–86.

Kobayashi, T., Liu, X., Kim, H. J. et al, 2005. TGF-beta1 and serum both stimulate contraction but differentially affect apoptosis in 3D collagen gels. *Respir Res*, **6** (141).

Kohno, M., Hasegawa, H., Inoue, A. et al, 2006. Identification of N-arachidonylglycine as the endogenous ligand for orphan G-protein-coupled receptor GPR18. *Biochem Biophys Res Commun*, **347** (3), 827–32.

Kohyama, T., Liu, X., Wen, F. Q. et al, 2002. PDE4 inhibitors attenuate fibroblast chemotaxis and contraction of native collagen gels. *Am J Respir Cell Mol Biol*, **26** (6), 694–701.

Kondo, S., Kagami, S., Urushihara, M. et al, 2004. Transforming growth factor-beta1 stimulates collagen matrix remodeling through increased adhesive and contractive potential by human renal fibroblasts. *Biochim Biophys Acta*, **1693** (2), 91–100.

Krishnamoorthy, S., Recchiuti, A., Chiang, N. et al, 2010. Resolvin D1 binds human phagocytes with evidence for proresolving receptors. *PNAS*, **107** (4), 1660–1665.

Kuzuya, M., Cheng, X. W., Sasaki, T., Tamaya-Mori, N., and Akihisa Iguchi, M., 2004. Pitavastatin , a 3-hydroxy-3-methylglutaryl-coenzyme A reductase inhibitor, blocks vascular smooth muscle cell. *J Cardiovasc Pharmacol*, **43** (6), 808–814.

Labat, C., Ortiz, J. L., Norel, X. et al, 1992. A second cysteinyl leukotriene receptor in human lung. *J Pharmacol Exp Ther*, **263** (2), 800–805.

Lee, T. H., Austen, K. F., Corey, E. J., and Drazen, J. M., 1984. Leukotriene E4-induced airway hyperresponsiveness of guinea pig tracheal smooth muscle to histamine and evidence for three separate sulfidopeptide leukotriene receptors. *PNAS*, **81** (15), 4922–4925.

Lefer, A. M., Stahl, G. L., Lefer, D. J. et al, 1988. Lipoxins A4 and B4: comparison of icosanoids having bronchoconstrictor and vasodilator actions but lacking platelet aggregatory activity. *PNAS*, **85** (21), 8340–8344.

Lei, Y., Cao, Y., Zhang, Y., Edvinsson, L., and Xu, C. B., 2011. Enhanced airway smooth muscle cell thromboxane receptor signaling via activation of JNK MAPK and extracellular calcium influx. *Eur J Pharmacol*, **650** (2-3), 629–638.

Leuchte, H. H., Baezner, C., Baumgartner, R. A. et al, 2008. Inhalation of vasoactive intestinal peptide in pulmonary hypertension. *Eur Respir J*, **32** (5), 1289–1294.

Levy, B. D., Bonnans, C., Silverman, E. S. et al, 2005. Diminished lipoxin biosynthesis in severe asthma. *Am J Respir Crit Care Med*, **172** (7), 824–830.

Levy, B. D., Clish, C. B., Schmidt, B., Gronert, K., and Serhan, C. N., 2001. Lipid mediator class switching during acute inflammation: signals in resolution. *Nat Immunol*, **2** (7), 612–619.

Levy, B. D., Kohli, P., Gotlinger, K. et al, 2007. Protectin D1 Is generated in asthma and dampens airway inflammation and hyperresponsiveness. *J Immunol*, **178** (1), 496–502.

Li, D., Hodges, R. R., Jiao, J. et al, 2013. Resolvin D1 and aspirin-triggered resolvin D1 regulate histamine-stimulated conjunctival goblet cell secretion. *Mucosal Immunol*, **6** (6), 1–12.

Li, N., He, J., Schwartz, C. E., Gjorstrup, P., and Bazan, H. E. P., 2010. Resolvin E1 improves tear production and decreases inflammation in a dry eye mouse model. *J Ocul Pharmacol Ther*, **26** (5), 431–439.

Lin, N., Cai, R., Niu, Y., Shen, B., Xu, J., Cheng, Y., 2012. Inhibition of angiotensin II-induced contraction of human airway smooth muscle cells by angiotensin-(1-7) via downregulation of the RhoA/ROCK2 signaling pathway. *Int J Mol Med*, **30** (4), 811–818.

Maguire, J. J. and Davenport, A. P., 1995. ETA receptor-mediated constrictor responses to endothelin peptides in human blood vessels in vitro. *Br J Pharmacol*, **115** (1), 191–197.

Marcheselli, V. L., Hong, S., Lukiw, W. J. et al, 2003. Novel docosanoids inhibit brain ischemia-reperfusion-mediated leukocyte infiltration and pro-inflammatory gene expression. *J Biol Chem*, **278** (44), 43807–43817.

Marcheselli, V. L., Mukherjee, P. K., Arita, M. et al, 2010. Neuroprotectin D1/protectin D1 stereoselective and specific binding with human retinal pigment epithelial cells and neutrophils. *Prostaglandins Leukot Essent Fatty Acids*, **82** (1), 27–34.

Maron, B. A. and Leopold, J. A., 2014. The role of the renin-angiotensin-aldosterone system in the pathobiology of pulmonary arterial hypertension (2013 Grover Conference series), *Pulm Circ*, **4** (2), 200–210.

Martin, J. G., Duguet, A., and Eidelman, D. H., 2000. The contribution of airway smooth muscle to airway narrowing and airway hyperresponsiveness in disease. *Eur Respir J*, **16** (2), 349–354.

Martin, P., 1997. Wound healing--aiming for perfect skin regeneration. *Science*, **276** (5309), 75–81.

Matsumoto, H., Moir, L. M., Oliver, B. G. G. et al, 2007. Comparison of gel contraction mediated by airway smooth muscle cells from patients with and without asthma. *Thorax*, **62** (10), 848–854.

McGoon, M. D., Frost, A. E., Oudiz, R. J. et al, 2009. Ambrisentan therapy in patients with pulmonary arterial hypertension who discontinued bosentan or sitaxsentan due to liver function test abnormalities. *Chest*, **135** (1), 122–129.

McMahon, B., Mitchell, D., Shattock, R., Martin, F., Brady, H. R., and Godson, C., 2002. Lipoxin, leukotriene, and PDGF receptors cross-talk to regulate mesangial cell proliferation. *FASEB J*, **16** (13), 1817–1819.

McMahon, B., Stenson, C., McPhillips, F., Fanning, A., Brady, H. R., and Godson, C., 2000. Lipoxin A4 antagonizes the mitogenic effects of leukotriene D4 in human renal mesangial cells. Differential activation of MAP kinases through distinct receptors. *J Biol Chem*, **275** (36), 27566–27575.

Merched, A. J., Ko, K., Gotlinger, K. H., Serhan, C. N., and Chan, L., 2008. Atherosclerosis: evidence for impairment of resolution of vascular inflammation governed by specific lipid mediators. *FASEB J*, **22** (10), 3595–3606.

Mitzner, W., 2004. Airway smooth muscle: the appendix of the lung. *Am J Respir Crit Care Med*, **169** (7), 787–790.

Miyahara, T., Runge, S., Chatterjee, A. et al, 2013. D-series resolvin attenuates vascular smooth muscle cell activation and neointimal hyperplasia following vascular injury. *FASEB J*, **27** (6), 1–13.

Moos, M. P. W., Mewburn, J. D., Kan, F. W. K. et al, 2008. Cysteinyl leukotriene 2 receptor-mediated vascular permeability via transendothelial vesicle transport. *FASEB J*, **22** (12), 4352–4362.

Moulin, V., Castilloux, G., Jean, A., Garrel, D. R., Auger, F. A., and Germain, L., 1996. In vitro models to study wound healing fibroblasts. *Burns*, **22** (5), 359–362.

Mubarak, K. K., 2010. A review of prostaglandin analogs in the management of patients with pulmonary arterial hypertension. *Respir Med*, **104** (1) 9-21.

Mukherjee, P. K., Marcheselli, V. L., Serhan, C. N., and Bazan, N. G., 2004. Neuroprotectin D1: a docosahexaenoic acid-derived docosatriene protects human retinal pigment epithelial cells from oxidative stress. *PNAS*, **101** (22), 8491–8496.

Mustafa, M., Zarrough, A., Bolstad, A. I. et al, 2013. Resolvin D1 protects periodontal ligament. *Am J Physiol Cell Physiol*, **305** (6), C673–9.

Narala, V. R., Adapala, R. K., Suresh, M. V, Brock, T. G., Peters-Golden, M., and Reddy, R. C., 2010. Leukotriene B4 is a physiologically relevant endogenous peroxisome proliferator-activated receptor-alpha agonist. *J Biol Chem*, **285** (29), 22067–22074.

Nathan, C. and Ding, A., 2010. Nonresolving Inflammation. *Cell*, **140** (6) 871-882.

Norel, X., Walch, L., Gascard, J.-P., DeMontpreville, V., and Brink, C., 2004. Prostacyclin release and receptor activation: differential control of human pulmonary venous and arterial tone. *Br J Pharmacol*, **142** (4), 788–796.

Norel, X., Walch, L., Labat, C., Gascard, J. P., Dulmet, E., and Brink, C., 1999. Prostanoid receptors involved in the relaxation of human bronchial preparations. *Br J Pharmacol*, **126** (4), 867–872.

O'Byrne, P. M. and Inman, M. D., 2003. Airway hyperresponsiveness. *Chest*, **123** (3 Suppl), 411S–416S.

Oh, S. F., Dona, M., Fredman, G., Krishnamoorthy, S., Irimia, D., and Serhan, C. N., 2012. Resolvin E2 formation and impact in inflammation resolution. *J Immunol*, **188** (9), 4527–34.

Oh, S. F., Pillai, P. S., Recchiuti, A., Yang, R., and Serhan, C. N., 2011. Pro-resolving actions and stereoselective biosynthesis of 18S E-series resolvins in human leukocytes and murine inflammation. *J Clin Invest*, **121** (2), 569–581.

Opitz, C. F. and Rubin, L. J., 2009. Acute vasodilator testing in idiopathic pulmonary arterial hypertension: must we take NO for the answer? *Eur Respir J*, **33** (6), 1247–1249.

Orr, S. K., Colas, R. A., Dalli, J., Chiang, N., and Serhan, C. N., 2015. Proresolving actions of a new resolvin D1 analog mimetic qualifies as an immunoresolvent. *Am J Physiol Lung Cell Mol Physiol*, **308** (9), L904–11.

Ortiz, J. L., Labat, C., Norel, X., Gorenne, I., Verley, J., and Brink, C., 1992. Histamine receptors on human isolated pulmonary arterial muscle preparations: effects of endothelial cell removal and nitric oxide inhibitors. *J Pharmacol Exp Ther*, **260** (2), 762–767.

De Paiva, C. S., Schwartz, C. E., Gjörstrup, P., and Pflugfelder, S. C., 2012. Resolvin E1 (RX-10001) reduces corneal epithelial barrier disruption and protects against goblet cell loss in a murine model of dry eye. *Cornea*, **31** (11), 1299–1303.

Parmar, N. and Ho, W. S. V., 2010. N-arachidonoyl glycine, an endogenous lipid that acts as a vasorelaxant via nitric oxide and large conductance calcium-activated potassium channels. *Br J Pharmacol*, **160** (3), 594–603.

Paruchuri, S., Tashimo, H., Feng, C. et al, 2009. Leukotriene E4-induced pulmonary inflammation is mediated by the P2Y12 receptor. *J Exp Med*, **206** (11), 2543–2555.

Pascual, R. M. and Peters, S. P., 2005. Airway remodeling contributes to the progressive loss of lung function in asthma: an overview. *J Allergy Clin Immunol*, **116** (3), 477–86.

Pelaia, G., Renda, T., Gallelli, L. et al, 2008. Molecular mechanisms underlying airway smooth muscle contraction and proliferation: Implications for asthma. *Respir Med*, **102** (8), 1173–1181.

Perretti, M., Becherucci, C., Mugridge, K. G., Solito, E., Silvestri, S., and Parente, L., 1991. A novel anti-inflammatory peptide from human lipocortin 5. *Br J Pharmacol*, **103** (2), 1327–1332.

Perretti, M., Chiang, N., La, M. et al, 2002. Endogenous lipid- and peptide-derived anti-inflammatory pathways generated with glucocorticoid and aspirin treatment activate the lipoxin A4 receptor. *Nat Med*, **8** (11), 1296–1302.

Perretti, M., Christian, H., Wheller, S. K. et al, 2000. Annexin I is stored within gelatinase granules of human neutrophil and mobilized on the cell surface upon adhesion but not phagocytosis. *Cell Biol Int*, **24** (3), 163–174.

Petkov, V., Mosgoeller, W., Ziesche, R. et al, 2003. Vasoactive intestinal peptide as a new drug for treatment of primary pulmonary hypertension. *J Clin Invest*, **111** (9), 1339–1346.

Pike, K. C., Davis, S.A., Collins, S.A. et al, 2014 Prenatal development is linked to bronchial reactivity: epidemiological and animal model evidence. *Sci Rep*, **4** (4705) 1-7.

Planagumà, A., Kazani, S., Marigowda, G. et al, 2008. Airway lipoxin A4 generation and lipoxin A4 receptor expression are decreased in severe asthma. *Am J Respir Crit Care Med*, **178** (6), 574–582.

Prüss, H., Rosche, B., Sullivan, A. B. et al, 2013. Proresolution lipid mediators in multiple sclerosis - differential, disease severity-dependent synthesis - a clinical pilot trial. *PLoS One*, **8** (2), 1–5.

Puetz, S., Lubomirov, L. T., and Pfitzer, G., 2009. Regulation of smooth muscle contraction by small GTPases. *Physiology*, **24** (79), 342–356.

Pulido, T., Adzerikho, I., Channick, R. N. et al, 2013. Macitentan and morbidity and mortality in pulmonary arterial hypertension. *N Engl J Med*, **369** (9) 809-818.

Qu, X., Zhang, X., Yao, J., Song, J., Nikolic-Paterson, D. J., and Li, J., 2012. Resolvins E1 and D1 inhibit interstitial fibrosis in the obstructed kidney via inhibition of local fibroblast proliferation. *J Pathol*, **228** (4), 506–519.

Recchiuti, A., 2013. Resolvin D1 and its GPCRs in resolution circuits of inflammation. *Prostaglandins Other Lipid Mediat*, **107**, 64–76.

Redden, R. a and Doolin, E. J., 2006. Complementary roles of microtubules and microfilaments in the lung fibroblast-mediated contraction of collagen gels: Dynamics and the influence of cell density. *In Vitro Cell Dev Biol Anim*, **42** (3-4), 70–74.

Roach, K. M., Feghali-Bostwick, C. a., Amrani, Y., and Bradding, P., 2015. Lipoxin A4 attenuates constitutive and TGF- 1-dependent profibrotic activity in human lung myofibroblasts. *J Immunol*, **195** (6) 2852-2860.

Rogerio, A. P., Haworth, O., Croze, R. et al, 2012. Resolvin D1 and aspirin-triggered resolvin D1 promote resolution of allergic airways responses. *J Immunol*, **189** (4), 1983–91.

Rubin, L. J., 2012. Endothelin receptor antagonists for the treatment of pulmonary artery hypertension. *Life Sci*, **91** (13-14), 517–521.

Said, S. I., Galie, N., Palazzini, M., and Manes, A., 2012. Correspondence: Vasoactive intestinal peptide in pulmonary arterial hypertension. *Am J Respir Crit Care Med*, **185** (7), 786.

Said, S. I., Hamidi, S. A., and Gonzalez Bosc, L., 2010. Asthma and pulmonary arterial hypertension: do they share a key mechanism of pathogenesis? *Eur Respir J*, **35** (4), 730–734.

Sakao, S., Tatsumi, K., and Voelkel, N. F., 2009. Endothelial cells and pulmonary arterial hypertension: apoptosis, proliferation, interaction and transdifferentiation. *Respir Res*, **10** (1), 95.

Sasaki, A., Fukuda, H., Shiida, N. et al, 2015. Determination of ω-6 and ω-3 PUFA metabolites in human urine samples using UPLC/MS/MS. *Anal Bioanal Chem*, **407** (6), 1625–1639.

Schild, H., 1951. Reactions of isolated human asthmatic lung and bronchial tissue to a specific antigen histamine release and muscular contraction. *The Lancet*, **258** (6679), 376–382.

Seehase, S., Schlepütz, M., Switalla, S. et al, 2011. Bronchoconstriction in nonhuman primates: a species comparison. *J Appl Physiol*, **111** (3), 791–8.

Seow, C. Y. and Fredberg, J. J., 2001. Signal transduction in smooth muscle: historical perspective on airway smooth muscle: the saga of a frustrated cell. *J Appl Physiol*, **91** (2), 938–952.

Serhan, C. N. and Chiang, N., 2013. Resolution phase lipid mediators of inflammation: agonists of resolution. *Curr Opin Pharmacol*, **13** (4), 632–640.

Serhan, C. N., Chiang, N., and Dalli, J., 2015. The resolution code of acute inflammation: Novel pro-resolving lipid mediators in resolution. *Semin Immunol*, **27** (3), 200–215.

Serhan, C. N., Chiang, N., Dalli, J., and Levy, B. D., 2014. Lipid mediators in the resolution of inflammation. *Cold Spring Harb Perspect Biol*, **7** (2) a016311.

Serhan, C. N., Clish, C. B., Brannon, J., Colgan, S. P., Chiang, N., and Gronert, K., 2000. Novel functional sets of lipid-derived mediators with antiinflammatory actions generated from omega-3 fatty acids via cyclooxygenase 2–nonsteroidal antiinflammatory drugs and transcellular processing. *J Exp Med*, **192** (8), 1197–1204.

Serhan, C. N., Dalli, J., Colas, R. A., Winkler, J. W., and Chiang, N., 2015. Protectins and maresins: New pro-resolving families of mediators in acute inflammation and resolution bioactive metabolome. *Biochim Biophys Acta*, **1851** (4), 397–413.

Serhan, C. N., Dalli, J., Karamnov, S. et al, 2012. Macrophage proresolving mediator maresin 1 stimulates tissue regeneration and controls pain. *FASEB J*, **26** (4) 1755-1765.

Serhan, C. N., Gotlinger, K., Hong, S. et al, 2006. Anti-inflammatory actions of neuroprotectin D1/protectin D1 and its natural stereoisomers: assignments of dihydroxy-containing docosatrienes. *J Immunol*, **176** (3), 1848–1859.

Serhan, C. N., Hamberg, M., and Samuelsson, B., 1984a. Trihydroxytetraenes: a novel series of compounds formed from arachidonic acid in human leukocytes. *Biochem Biophys Res Commun*, **118** (3), 943–949.

Serhan, C. N., Hamberg, M., and Samuelsson, B., 1984b. Lipoxins: novel series of biologically active compounds formed from arachidonic acid in human leukocytes. *PNAS*, **81** (17), 5335–5339.

Serhan, C. N., Hong, S., Gronert, K. et al, 2002. Resolvins: a family of bioactive products of omega-3 fatty acid transformation circuits initiated by aspirin treatment that counter proinflammation signals. *J Exp Med*, **196** (8), 1025–1037.

Serhan, C. N. and Savill, J., 2005. Resolution of inflammation: the beginning programs the end. *Nat Immunol*, **6** (12), 1191–1197.

Serhan, C. N., Yang, R., Martinod, K. et al, 2009. Maresins: novel macrophage mediators with potent antiinflammatory and proresolving actions. *J Exp Med*, **206** (1), 15–23.

Shapiro, S., Traiger, G., Hill, W., Zhang, L., and Doran, A. K., 2013. Safety, tolerability, and efficacy of overnight switching from sildenafil to tadalafil in patients with pulmonary arterial hypertension. *Cardiovasc Ther*, **31** (5), 274–279.

Simonneau, G., Robbins, I. M., Beghetti, M. et al, 2009. Updated clinical classification of pulmonary hypertension. *J Am Coll Cardiol*, **54** (1), S43–54.

Sirois, P., Roy, S., Tétrault, J. P., Borgeat, P., Picard, S., and Corey, E. J., 1981. Pharmacological activity of leukotrienes A4, B4, C4 and D4 on selected guinea-pig, rat, rabbit and human smooth muscles. *Prostaglandins Med*, **7** (4), 327–340.

Spite, M., Norling, L. V, Summers, L. et al, 2009. Resolvin D2 is a potent regulator of leukocytes and controls microbial sepsis. *Nature*, **461** (7268).

Stramer, B. M., Mori, R., and Martin, P., 2007. The inflammation-fibrosis link? A Jekyll and Hyde role for blood cells during wound repair. *J Invest Dermatol*, **127** (5), 1009–1017.

Tabas, I. and Glass, C. K., 2013. Anti-inflammatory therapy in chronic disease: challenges and opportunities. *Science*, **339** (6116), 166–172.

Takano, T., Clish, C. B., Gronert, K., Petasis, N., and Serhan, C. N., 1998. Neutrophil-mediated changes in vascular permeability are inhibited by topical application of aspirin-triggered 15-epi-lipoxin A4 and novel lipoxin B4 stable analogues. *J Clin Invest*, **101** (4), 819–826.

Takano, T., Fiore, S., Maddox, J., and Brady, H., 1997. Aspirin-triggered 15-epi-lipoxin A4 (LXA4) and LXA4 stable analogues are potent inhibitors of acute inflammation: evidence for anti-inflammatory receptors. *J Exp Med*, **185** (9), 1693–1704.

Takatsuki, S., Rosenzweig, E. B., Zuckerman, W., Brady, D., Calderbank, M., and Ivy, D. D., 2013. Clinical safety, pharmacokinetics, and efficacy of ambrisentan therapy in children with pulmonary arterial hypertension. *Pediatr Pulmonol*, **48** (1), 27–34.

Tilley, S. L., Hartney, J. M., Erikson, C. J. et al, 2003. Receptors and pathways mediating the effects of prostaglandin E2 on airway tone. *Am J Physiol Lung Cell Mol Physiol*, **284** (4), L599–L606.

Tingström, A, Heldin, C. H., Rubin, K., 1992. Regulation of fibroblast-mediated collagen gel contraction by platelet-derived growth factor, interleukin-1 alpha and transforming growth factor-beta 1. *J Cell Science*, **102** (Pt 2) 315–322.

Tjonahen, E., Oh, S., Siegelman, J. et al, 2006. Resolvin E2: identification and anti-inflammatory actions: pivotal role of human 5-lipoxygenase in resolvin E series biosynthesis. *Chem Biol*, **13** (11), 1193–1202.

Touyz, R. M., 2003. The role of angiotensin II in regulating vascular structural and functional changes in hypertension. *Curr Hypertens Rep*, **5** (2), 155–164.

Trow, T. K. and Taichman, D. B., 2009. Endothelin receptor blockade in the management of pulmonary arterial hypertension: selective and dual antagonism. *Respir Med*, **103** (7), 951–962.

Tuder, R. M., Cool, C. D., Geraci, M. W. et al, 1999. Prostacyclin synthase expression is decreased in lungs from patients with severe pulmonary hypertension. A*m J Respir Crit Care Med*, **159** (6), 1925–1932.

Vachier, I., Bonnans, C., Chavis, C. et al, 2005. Severe asthma is associated with a loss of LX4, an endogenous anti-inflammatory compound. *J Allergy Clin Immunol*, **115** (1), 55–60.

Vago, J. P., Nogueira, C. R. C., Tavares, L. P. et al, 2012. Annexin A1 modulates natural and glucocorticoid-induced resolution of inflammation by enhancing neutrophil apoptosis. *J Leukoc Biol*, **92** (2), 249–258.

Viola, J. and Soehnlein, O., 2015. Atherosclerosis – A matter of unresolved inflammation. *Semin Immunol*, **27** (3) 184–193.

Walch, L., Norel, X., Bäck, M., Gascard, J.-P., Dahlén, S.-E., and Brink, C., 2002. Pharmacological evidence for a novel cysteinyl-leukotriene receptor subtype in human pulmonary artery smooth muscle. *Br J Pharmacol*, **137** (8), 1339–1345.

Wan, M., Godson, C., Guiry, P. J., Agerberth, B., and Haeggström, J. Z., 2011. Leukotriene B4/antimicrobial peptide LL-37 proinflammatory circuits are mediated by BLT1 and FPR2/ALX and are counterregulated by lipoxin A4 and resolvin E1. *FASEB J*, **25** (5), 1697–1705.

Wan, M., Sabirsh, A., Wetterholm, A., Agerberth, B., and Haeggström, J. Z., 2007. Leukotriene B4 triggers release of the cathelicidin LL-37 from human neutrophils: novel lipid-peptide interactions in innate immune responses. *FASEB J*, **21** (11), 2897–2905.

Wang, X., Zhu, M., Hjorth, E. et al, 2015. Resolution of inflammation is altered in Alzheimer's disease. *Alzheimers Dement*, **11** (1) 40-50.

Watts, S. W., Dorrance, A. M., Penfold, M. E. et al, 2013. Chemerin connects fat to arterial contraction. *Arterioscler Thromb Vasc Biol*, **33** (6), 1320–1328.

Webb, R. C., 2003. Smooth muscle contraction and relaxation. *Adv Physiol Educ*, **27** (1-4), 201–206.

Wenzel, S. E., 2012. Asthma phenotypes: the evolution from clinical to molecular approaches. *Nat Med*, **18** (5), 716–725.

Wenzel, S. E., 2013. Complex phenotypes in asthma: current definitions. *Pulm Pharmacol Ther*, **26** (6), 710–715.

Westergren-Thorsson, G., Larsen, K. et al, 2010. Pathological airway remodelling in inflammation. *Clin Respir J*, **4** (Suppl 1), 1–8.

Wilhelmsen, K., Khakpour, S., Tran, A. et al, 2014. The endocannabinoid/endovanilloid N-arachidonoyl dopamine (NADA) and synthetic cannabinoid WIN55,212-2 abate the inflammatory activation of human endothelial cells. *J Biol Chem*, **289** (19), 13079–13100.

Wittamer, V., Grégoire, F., Robberecht, P., Vassart, G., Communi, D., and Parmentier, M., 2004. The C-terminal nonapeptide of mature chemerin activates the chemerin receptor with low nanomolar potency. *J Biol Chem*, **279** (11), 9956–9962.

Woodward, D. F., Jones, R. L., and Narumiya, S., 2011. International union of basic and clinical pharmacology. LXXXIII: classification of prostanoid receptors, updating 15 years of progress. *Pharmacol Rev*, **63** (3), 471–538.

Wu, D., Lee, D., and Sung, Y. K., 2011. Prospect of vasoactive intestinal peptide therapy for COPD/PAH and asthma: a review. *Respir Res*, **12** (45), 1–8.

Xu, Z. C., Zhang, Q., and Li, H., 2013. Human hair follicle stem cell differentiation into contractile smooth muscle cells is induced by transforming growth factor-beta1 and platelet-derived growth factor BB. *Mol Med Rep*, **8** (6) 1715-1721.

Yang, T. and Du, Y., 2012. Distinct roles of central and peripheral prostaglandin E2 and EP subtypes in blood pressure regulation. *Am J Hypertens*, **25** (10), 1042–1049.

Ye, R. D., Boulay, F., Wang, J. M. et al, 2009. International Union of Basic and Clinical Pharmacology. LXXIII. Nomenclature for the formyl peptide receptor (FPR) family. *Pharmacol Rev*, **61** (2), 119–161.

Yildiz, F. and Group, on behalf of the A. I. T. S., 2014. Importance of inhaler device use status in the control of asthma in adults: the asthma inhaler treatment study. *Respir Care*, **59** (2), 223–230.

Yin, H., Chu, A., Li, W. et al, 2009. Lipid G protein-coupled receptor ligand identification using beta-arrestin PathHunter assay. *J Biol Chem*, **284** (18), 12328–12338.

Yokomizo, T., Izumi, T., Chang, K., Takuwa, Y., and Shimizu, T., 1997. A G-protein-coupled receptor for leukotriene B4 that mediates chemotaxis. *Nature*, **387** (6633), 620–624.

Zhang, F., Yang, H., Pan, Z. et al, 2010. Dependence of resolvin-induced increases in corneal epithelial cell migration on EGF receptor transactivation. *Invest Ophthalmol Vis Sci*, **51** (11), 5601–5609.

Zygmunt, P. M., Petersson, J., Andersson, D. A. et al, 1999. Vanilloid receptors on sensory nerves mediate the vasodilator action of anandamide. *Nature*, **400** (6743), 452–457.